Roar Nålsund

Railway Ballast Characteristics, Selection Criterion and Performance

NTNU – Trondheim
Norwegian University of
Science and Technology

Roar Nålsund

Railway Ballast Characteristics, Selection Criterion and Performance

Thesis for the degree of Philosophiae Doctor

Trondheim, September 2014

Norwegian University of Science and Technology
Faculty of Engineering Science and Technology
Department of Civil and Transport Engineering

NTNU – Trondheim
Norwegian University of
Science and Technology

ABSTRACT

This work is a comprehensive investigation to find to what extent simple laboratory tests e.g. Los Angeles abrasion and micro-Deval might be suitable for predicting real railway ballast performance with respect to deformation and degradation. A number of tests to measure essential properties of ballast aggregate have been performed in addition to advanced material testing. Large cyclic triaxial loading test and full scale railway track model test were employed to simulate the effects of train loading and tamping, and to study settlement, stiffness and degradation of a range of ballast materials. The testing programme included both wet and dry testing conditions. All the rock types tested were mainly composed of combinations of principal rock-forming silicate minerals. They represent all together a wide variety of igneous, metamorphic and consolidated/metamorphosed sedimentary rocks mainly fine to very fine grained.

Mechanical properties
Change in the ballast grading proved to affect the ballast breakage development over time. However, the abrasion property expressed by the micro-Deval value did not show any association with the degradation of ballast under repeated load testing. Simulation of repeated tamping seemed to be the main source of ballast breakage.

Most rocks showed high frost resistance after long term impact, but samples with high content of amphibole were less frost resistant. The rocks' mechanical strength in terms of the Los Angeles abrasion or micro-Deval value did not show any correlation with either the amount of micro-cracks or the rocks' average mineral grain size. A new method to measure the amount of micro-cracks based on luminescence measurements was developed. It is suggested that micro-cracks represent open channels for water to penetrate into the aggregate, which was confirmed by good correlation between water absorption and the amount of micro-cracks.

Moisture had generally a negative effect on rocks' mechanical strength according to Los Angeles abrasion and Point Load strength results. On the other hand, dry and wet triaxial tests with cyclic loadings did not confirm this effect. Neither did mineral grain size distribution show any correlation with mechanical strength, but the range of coefficient of conformity ($Cu = D_{60}/D_{10}$) was probably too narrow to obtain a reliable conclusion. A new method to quantify the mineral grain size distribution was developed under these test series.

Functional properties
Both resilient modulus of the ballast layer and the stiffness of the track were governed by the materials' grading curve and specific density. A possible relation between the amount of micro-cracks in the aggregate and resilient modulus as well as ballast breakage is suggested. The permanent vertical strain during repeated load testing was affected by both the micro-Deval value, the grading curve of the ballast and the aggregate's content of soft minerals.

Improvements of test methods
The Los Angeles abrasion test distinguished clearly between the superior quality material and the very poor material. The Los Angeles abrasion value is, however, a poor parameter to indicate how the intermediate material will behave in service regarding ballast breakage.

This study proposes to improve the ranking of ballast materials by introducing two additional methods. One which is able to measure some rocks' ability to recover mechanical strength after repeated crushing, and one which measures the production of fines (0/0.125 mm) during crushing.

Saturation of ballast material before micro-Deval testing did not have any significant effect on degradation. Neither did the use of 1 % sodium-chloride solution have any effect.

Roar Nålsund

ACKNOWLEDGEMENTS

Roar Nålsund

THE COMMITTEE FOR APPRAISAL OF THIS THESIS COMPRISED THE FOLLOWING MEMBERS:

Professor António Gomes Correia,
Department of Civil Engineering,
University of Minho, Braga, Portugal.

PhD Lillian Uthus Mathisen, Veidekke AS, Trondheim.

Associate Professor, Helge Mork,
Department of Civil and Transport Engineering,
Faculty of Engineering Science and Technology,
Norwegian University of Science and Technology, (Administrator).

ADVISORS DURING THIS STUDY HAVE BEEN:

Dr.Ing. Ivar Horvli, Norwegian Public Roads Administration, Molde

Adjunct Professor Børge Johannes Wigum,
Department of Geology and Mineral Resources Engineering,
Faculty of Engineering Science and Technology,
Norwegian University of Science and Technology.

Professor Inge Hoff,
Department of Civil and Transport Engineering,
Faculty of Engineering Science and Technology,
Norwegian University of Science and Technology.

LIST OF ABBREVIATIONS

COV	Coefficient of variation
Cu	Coefficient of uniformity
D_{50}	Average mineral grain size (area based)
MD	Micro-Deval test (abrasion)
LAA	Los Angeles abrasion test (crushing)
PLI	Point Load Index Is_{50mm} (tensile strength)
R^2	Regression coefficient
STI	Surface Texture Index (roughness)
XRD	X-ray diffraction test

TABLE OF CONTENTS

1. INTRODUCTION

1.1 Background

Freight tonnage, traffic speeds and frequency of trains has been steadily increasing over time worldwide. These changes in traffic characteristics have led to increased wear and shorter lifetime for all track components in superstructure and substructure (Figure 1.1).

Although the substructure components have a major influence on the cost of track maintenance (Selig & Waters, 1994), less attention has been given to the substructure compared with components in the superstructure.. Deterioration of the track geometry is recognized as being the main source of the need for track maintenance, and settlement in the ballast layer contributes the most to this deterioration (Selig 1998). This study has investigated railway ballast characteristics, selection and performance.
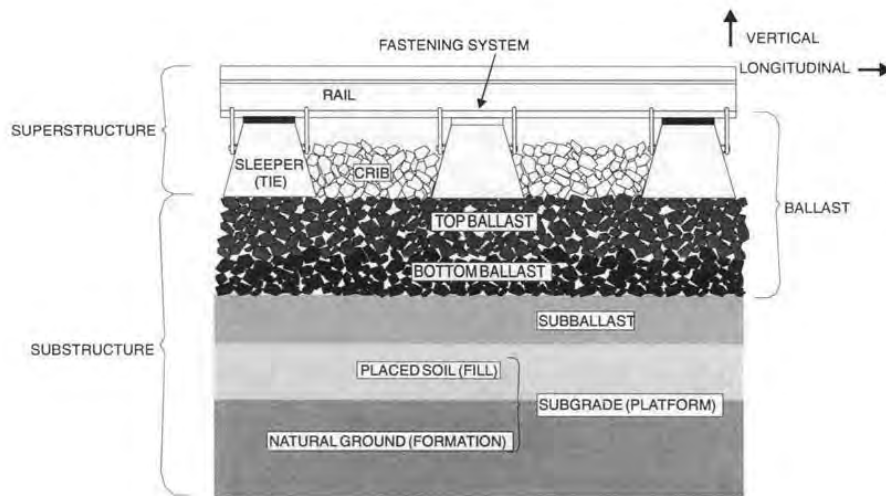
Figure 1.1. Track layout of a typical ballasted track- side view (Selig & Waters 1994).

The ballast layer is therefore a key component of the conventional track structure. Its importance has grown with increasing axle loads and train speeds. New ballast is normally a narrow-graded material (i.e. contains a limited range of particle sizes) consisting of a large amount of open pore space and a permeable structure. Under repeated sleeper loading, railway ballast undergoes unrecoverable vertical deformations due to ballast densification, aggregate degradation, and lateral spread of ballast beneath the sleepers (Raymond and Bathurst 1987).

A very important function for all track components, from rail via sleeper and ballast down to subballast, is to distribute wheel load and contact pressure gradually to successive reduced levels from interface to interface down to the subgrade (embankment or natural ground), see Figure 1.2. The purpose is to avoid ballast breakage, permanent settlements and in worst-case failure in bearing capacity. The figure also shows that the wheel load of 100 kN is distributed with 60 % to the sleeper under the wheel and remaining 40 % to the two neighboring sleepers with about 20 % of each.

Two other very important functions of the ballast layer are firstly to retain the track in its required position by withstanding vertical, lateral and longitudinal forces applied to the sleepers, and secondly provide drainage of water falling in the track and from snow melt.
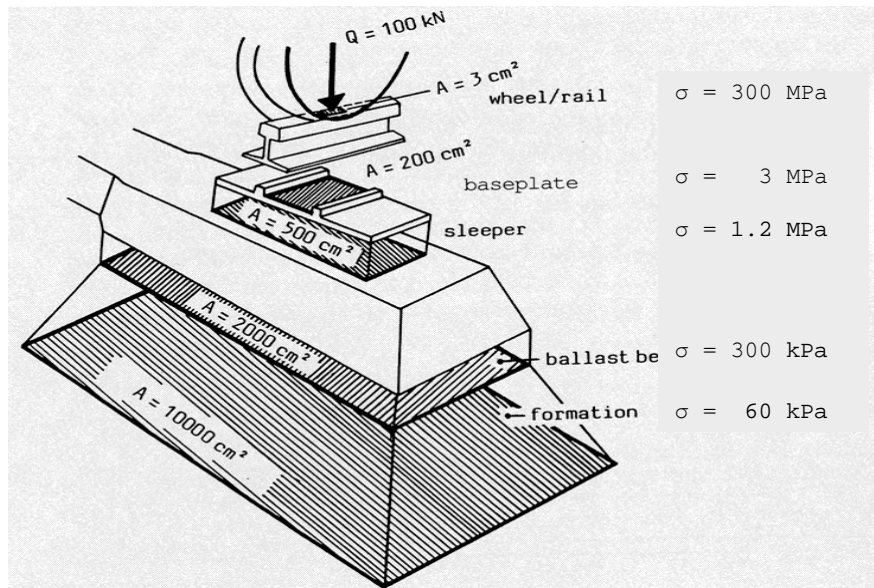
Figure 1.2. Example of pressure distribution from wheel/rail interface down to ballast/subballast interface (modified after Esveld 1989/ Führer 1978).

Under traffic loading, the stresses applied to the ballast are sufficient to cause both significant strain in the ballast and ballast particle breakage. This effect causes track settlement and therefore the track geometry will need to be restored by tamping. Every tamping implies loosening of ballast material which has to be compacted by the subsequent rail traffic. The compaction causes additional particle crushing including production of fines. Therefore, repeated tamping is the main source of ballast degradation (Selig and Waters 1994). This maintenance cycle will normally lead to loss of strength and stiffness in the ballast when fine material generated from ballast breakdown reaches a critical level and when the water fails to drain properly from the ballast. At this stage, the track needs to be maintained either by ballast cleaning or ballast renewal. Hence, it is important to use good quality ballast material in order to increase elapsed time between each tamping which will increase ballast life on the track (elapsed time between each ballast-cleaning).

Raymond et al (1983) reported that a large number of serious accidents occur through carriage derailments. Many such accidents may be due to the poor quality of ballast stones. Fouling of ballast (Figure 1.3) is a main source of loss of track geometry partly from degradation of aggregates. Much effort and cost are spent on maintaining correct track alignment and Raymond et al. (1983) suggests a correlation between substructure performance and derailment. Another cause of loss of track geometry is originating from the railway track construction period where segregation of new ballast material, due to handling all the way from production site to ballast bed, leads to great deviations from expected gradation which again results in non-uniformly or differentially settlements after primary compaction (Knutson and Thompson 1978; Selig and Roner 1987) along a short length of track. These can cause track twist which tends to be permanent despite repeated future tamping actions. Any improvement in the understanding of track behaviour which results in even a modest decrease in either track maintenance cost or derailment frequency will produce immediate and substantial financial benefits to the railways.

Figure 1.3. Fouled ballast on Stavne-Leangen Line near Trondheim.

In most countries the requirements for ballast materials is expressed by limit values for the Los Angeles abrasion test and the micro-Deval test. However, several researchers (e.g. Bosserman 1981; Wright 1983; Selig & Boucher 1990) have shown that these conventional mechanical tests for ballast, gave conflicting results and often failed to represent actual field performance, e.g. they were able to predict neither track permanent settlement nor ballast layer stiffness as well as particle breakage. They did not tell anything about the potential to produce fines (West et al. 1970) or recover strength by repeated crushing (Heikkila 1991). Furthermore, these tests involve revolving particles in a cylinder or drum to measure degradation. Hudec (1983) stated that these tests "…*have no difficulty in distinguishing between the superior quality material and the very poor material. They cannot, however, indicate with any certainty how the intermediate material will behave in service. Some tests such as Los Angeles abrasion (ASTC-131 and C-535) have little relationship to aggregate requirements or performance. The results indicate, rather, how easily the material will crush in a ball mill*". The particle mechanics here would not appear to be the same as those beneath the sleeper in a railway track during traffic loading. Despite these shortcomings, these mechanical tests are still considered as the best and most important indicators of ballast performance in service.

Regarding Norwegian conditions, most of the Norwegian railway ballast specifications currently in use have been copied from other countries some fifty years ago, and investment in railway research has been quite limited. Since around 2000, an ongoing project in Norway aims to build about 400 km with double track railway lines in the southeastern part of the country in Norway's most densely populated area. The new lines are designed for 250 km/h (passenger train) and will probably result in increased capacity for freight traffic as well. This will lead to more and heavier loads to the track, which will inevitably give a more rapid degradation of the ballast material (Raymond and Bathurst 1987) and an increase in loss of track geometry. This can to some extent be avoided by revising and optimizing the Norwegian ballast specifications regarding reduced breakage, less permanent settlements and more efficient tamping (longer alignment duration). In

addition, test analyses currently in use for assessing railway ballast materials have never been adapted to Norwegian rocks and climate. The most important ballast properties regarding lowering future maintenance costs are high resistance to crushing, low production of fines and least possible permanent vertical settlements during compaction. Results from the current mechanical test methods do not always take this into account. Therefore, in order to reduce the maintenance costs caused by the above mentioned problems, a better understanding of the behaviour of ballast during heavy rail traffic is required.

1.2   Objectives and aims

The objectives of the present thesis are:

    a) Evaluate whether simple standard laboratory tests are suited for selecting and ranging aggregate ballast materials for railway track, by studying railway ballast behaviour for typical Norwegian-quarried rocks under heavy railway traffic.

    b) Examine whether there is potential to reduce ballast breakage by a more optimal material selection and thus reduce the costs of railway track maintenance work.

and, consequently:

    c) Evaluate whether Norwegian technical specifications and requirements should be improved

The following tasks and investigations are required to achieve these objectives:

1. Verify whether today's ballast testing methods (i.e. Los Angeles abrasion and micro-Deval) can give results reflecting the field performance (large scale cyclic triaxial test and full scale rail track model test) of different ballast materials (different rock types).

2. Study possible laboratory procedure improvements for the Los Angeles abrasion test and the micro-Deval test.

3. Design and build a full scale rail track model test apparatus for simulating field loading conditions.

4. Identify rock properties affecting ballast breakage and the production of fines (particles less than 0.125 mm).

5. Study possible tradeoff between rock characteristics and ballast behaviour.

6. Investigate whether the ballast gradation is related to the rate of degradation and resilient properties.

7. Study the effect of frost weathering.

8. Study the production of fines from selected rock types during train loading.

1.3   Structure of the thesis

This thesis consists of seven chapters and four papers. The main contributions of the scientific work are presented in the papers. The chapters are mainly extracts from the papers but also some additional investigations not being presented there. The chapters in this way tie all the results from the individual papers together and give a total overview of the whole project.

1.3.1 Main chapters

Chapter 1 gives the background for this study.

Chapter 2 gives an overview of the test methods used with references to European standards and the modifications done with some of the methods.

Chapter 3 gives an overview of the full laboratory test programme.

Chapter 4 summarizes the findings from the laboratory testing performed. Data reported in papers are briefly mentioned here, and data not presented in the papers are shown in more detail.

Chapter 5 presents the conclusions.

Chapter 6 gives recommendations on how the findings can be used to improve ballast performance.

Chapter 7 is an identification of research needs based on this work..

1.3.2 Papers

Paper I:

Nålsund, R. (2010). **Effect of grading on degradation of crushed-rock railway ballast and on permanent axial deformation.**

Presented at Transportation Research Board's 89th Annual Meeting, Washington DC, in 2010. Published in the journal Transportation Research Record 2154: 149-155.

The paper was written by the author of the thesis alone. The author has also performed all the planning and organising of the laboratory tests and conducted all the data processing.

Paper II:

Nålsund, R. and Jensen, V. (2011). **Classification of micro-cracks, luminescence measurement, water absorption and frost resistance in Norwegian produced railway ballast.**

Proceedings of the 13th Euroseminar on Microscopy Applied to Building Materials. Ljubljana, Slovenia, pp.10.

The main author wrote most of the paper and planned and organised all the laboratory tests. The co-author Viggo Jensen (Norwegian Concrete and Aggregate Laboratory/NBTL) contributed strongly to the main idea of this paper, discussed the findings and gave valuable advice for the interpretation.

Paper III:

Nålsund, R., Tutumluer, E. and Horvli, I. (2013). **Degradation of railway ballast through large scale triaxial and full scale rail track model tests - Comparison with mechanical laboratory tests.**

Proceedings of the 9th International Conference on the Bearing Capacity of Roads, Railways and Airfields. Trondheim, Norway, pp.13.

This paper was written by the author of the thesis alone. He also planned and organised all the laboratory tests and conducted all the data processing. Co-authors were Erol Tutumluer and Ivar Horvli. Erol Tutumluer contributed with the three dimensional image analyses on the materials using the University of Illinois' Aggregate Image Analyzer

(UIAIA), as well as giving valuable advice for the interpretation. Ivar Horvli, who was the main supervisor at NTNU, contributed during discussions on interpretation.

Paper IV:

Nålsund, R. and Jensen, V. (2013). **Influence of mineral grain size, grain size distribution and micro-cracks on rocks' mechanical strength**.

Proceedings of the 14th Euro-seminar on Microscopy Applied to Building Materials. Helsingør, Denmark, pp.13.

This paper was written by the author of the thesis alone. Co-author Viggo Jensen (NBTL) contributed with micro-cracks information (luminescence measurements), advice and discussions on interpretation. The main author did all the microscopic grain size measurements of the thin sections.

2.   TEST METHODS

2.1   Selection of test methods

A number of tests for characterization of technical and functional properties for railway ballast are performed. In addition a number of analyses describing several geological properties (textural properties) of interest for mechanical strength and ballast performance under cyclic loading have been performed (Table 2.1).

Table 2.1. Test methods used to measure the aggregates' durability and geological properties.

Properties	Test method	Test type
Mechanical properties	Los Angeles (dry and wet)	Impact and some abrasion
	Micro-Deval (wet and NaCl))	Abrasion
	Point Load (dry and wet)	Tensile strength
	Freeze-Thaw (wet)	Frost resistance
Functional properties	Triaxial loading(dry and wet)	Cyclic loading
	Full scale railway track model (dry)	Cyclic loading
Geological properties / textural properties	Water absorption	Porosity
	Specific density	Weight per solid volume unit
	Microscopy	Micro-cracks
	Microscopy	Mineral grain size distribution
	Microscopy	Mineral distribution
	Microscopy	Mineral grain size
	Image analysis	Surface texture
	X-Ray Diffraction	Semi-quantitative mineral identification and distribution
	Coulter	Sieve analysis (fines)

The mechanical tests such as Los Angeles abrasion and micro-Deval are required according to Norwegian specifications for railway ballast. The Point Load test was chosen because it is suitable to study the impact of water on rocks' mechanical strength. It is also a widely used method internationally and links the results of this project to a wide range of literature within the field of Rock Mechanics. The Freeze-Thaw test is necessary to simulate climate impact in countries with cold winters.

The triaxial test and full scale railway track model test were used to simulate actual ballast field performance in order to assess the reliability compared to using simple laboratory tests (e.g. Los Angeles abrasion and micro-Deval tests).

Rocks' (geological) intrinsic properties as micro-cracks, mineral grain size and content of soft minerals, affect the ballast's mechanical strength and have to be investigated and quantified. Otherwise they will appear as unknown variables and complicate every attempt to reveal correlations between different properties. Hence, the quantification of the geological properties is very important work in this context.

Some tests are conducted under dry conditions, others are performed wet. In this study dry test means that test materials were air dried at room temperature before testing (no oven-drying). Wet test means that the materials were soaked in water for at least 7 days prior to test

2.2 Sample conditioning

2.2.1 Soaking duration

Experiments performed by Broch (1974) with the Point Load test (see Chapter 2.3.3) on drilled cores measuring tensile strength revealed that most specimens lost mechanical strength when they absorbed water. He also found that the loss of mechanical strength was dependent on the water content in the rock. Norwegian railway lines run through regions with a humid climate. Thus it is reasonable also to test ballast materials under conditions when they are at the weakest.
Figure 2.1 shows how the tensile strength is dependent on the water content, and that the strength decreases with increasing amount of water. The reduction rate is largest within the range of 0 to 25 % water content. It can also be seen that the loss of strength is much smaller from 75 to 100 %. Hence, for practical reasons the soaking period can be terminated when the water content reaches minimum75 %.
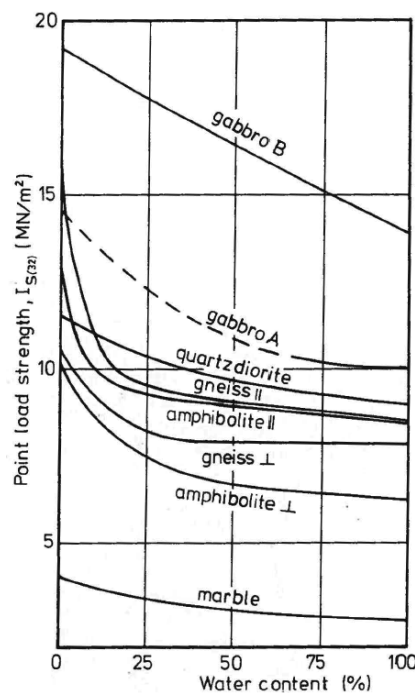
Figure 2.1 Point load strength index ($I_{S(32)}$) as a function of the water content in rock cores (Broch 1974).

Sufficient time to achieve 100 % water saturation will vary from rock to rock and can in some cases take as long time as weeks. Absorption experiments with drilled rock cores in this study showed that 75 % water saturation was achieved for all samples after 24 hours (test period 21 days) as seen in Figure 2.2. With reference to the previous paragraph the water storage time for wet Point Load test could be set to 24 hours.
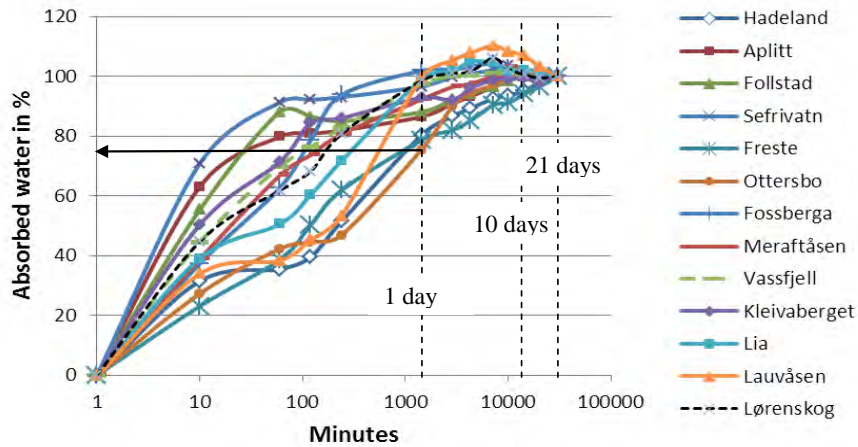
Figure 2.2 Percent absorbed water as a function of time (soaked in water) for drilled cores. Weighing conducted after 10 min, 1h, 2h, 4h, 1d, 2d, 3d, 5d, 7d, 10d, 14d and 21days. Arrow marks 75 % absorption.

However, a trial series with Los Angeles tests performed wet (Chapter 4.1.2) revealed that one test sample (Vassfjell meta-gabbro) out of a series of 19 different rocks showed an exceptional drop in mechanical strength when the exposure time in water was extended from 24 hours to 7 days. Due to this experience it was decided that the soaking time in general should be extended to 7 days. An additional test with the meta-gabbro aggregate was also conducted to verify whether the first result was reliable (Table 2.2) which it proved to be.

Table 2.2. Los Angeles abrasion values for different pre-treatment of test materials. Test fraction 31.5/50 mm.

Rock type	Standard test. (no water)	Wet test. Stored in water 24 hours	Wet test. Stored in water 7 days
Vassfjell meta-gabbro	13.3	14.4	24.1 and 22.6

2.2.2 Air-drying of samples

As part of the preparation work standards for laboratory analyses sometimes require drying of test material at high temperature after washing. NS EN 1097-2 (Los Angeles abrasion test) says: "*Wash each fraction separately (.....) and dry them to constant mass*". This means normally that the material is subjected to oven-drying temperature of 100-110 ^{o}C. However, some types of rocks are temperature sensitive and achieve increased mechanical strength by heating. Research done by Simpson and Fergus (1968) on diabase showed that the compressive strength did not change between drying temperature from 27 to 110 ^{o}C, but rose to higher strength after further heating (190 and 345 ^{o}C) as displayed in Figure 2.3. Another study performed by Obert et al. (1946) on drilled cores from six different rocks (marble, limestone, granite, slate and 2 sandstones) dokumented an average increase in compressive strength on 6 % when drying temperatur rose from room temperature (14 days) to 100 ^{o}C (7 days). Lowest and highest increase obtained were 1 % and 18 % respectively. Storage in water for 7 days led to an average decrease in compressive

strength of 12 % (-4 to -20 %). This experience shows that oven-drying of test specimens can change the rocks' original mechanical strength.
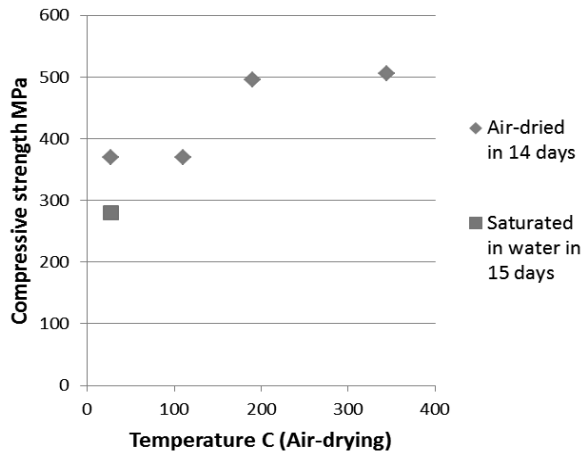
Figure 2.3 **Compressive strength of rock cores (diabas) increases with increasing drying temperature (27, 110, 190, and 345 ⁰C). Modified after Simpson and Fergus (1968).**

Hence, in this project test sample materials prepeared for dry state testing (the Los Angeles abrasion test, the Point Load test, the cyclic triaxial test and the full scale rail track model test) were all dried at room temperature. But this procedure requires that the storage time is longer than one day. An investigation conducted by Broch (1974) showed that necessary drying time to obtain 0 % water content is minimum one month (Figure 2.4).
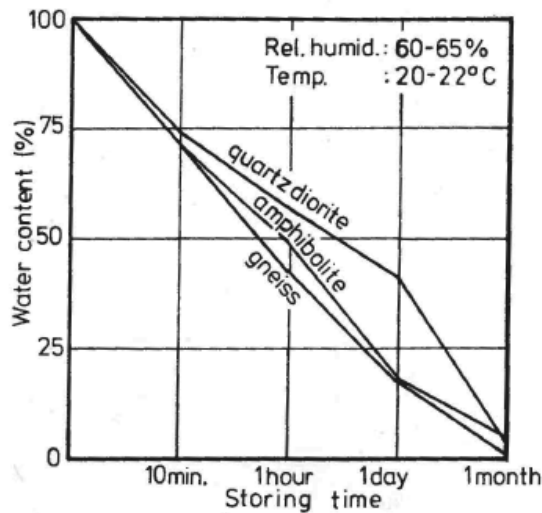
Figure 2.4 **Water content in rock cores as a function of storing time in a laboratory environment with relative humidity of 60-65 % and temperature of 20-22 ⁰C (Broch 1974).**

10

2.3   Mechanical strength

2.3.1 Los Angeles test (dry and wet state)

The classic test for measuring resistance to mechanical breakdown of aggregate is the Los Angeles abrasion test developed in 1916 (Woolf 1937), the most universally used aggregate qualification test throughout the world (Meininger 1994). The test was adopted by the Norwegian National Railway Administration in the 1950's to assess mechanical strength of railway ballast materials. In this study the test has been run according to both NS-EN 1097-2 (fraction 10/14 mm / road materials) and NS-EN 13450 (fraction 31.5 /50 mm / railway materials) which both are performed dry. Figure 2.5 shows the steel drum used for both fractions. The inside diameter is 71 cm and the drum rotates around the horizontal axis. The sample amount for fraction 10/14 mm is 5000 g. It is exposed to 500 revolutions together with 11 steel balls (charges). The corresponding data for fraction 31.5/50 mm is 10000 g, 1000 revolutions and 12 steel balls. A steel shelf within the drum, mounted parallel to the axis, lifts and drops the ballast sample. The tumbling action and the impacts from the charges cause the more brittle particles to shatter, in addition to surface wear and abrasion as the particles rub against one another and against the steel charges.

Figure 2.5   The Los Angeles abrasion test drum without cover used for both fraction 10/14 and 31.5/50 mm. Interior diameter is 71 cm.

To reveal how the samples' mechanical strength respond on water, a modified procedure with 3 litres of water added to the drum when testing fraction 31.5/50 mm was performed. Wet state also included that the material was soaked in water for 7 days before test. Wet test of fraction 10/14 mm was not included in this investigation. After the test the crushed material was washed and sieved through a 1.6 mm sieve. The dry weight of the material passing the sieve relative to the total weight expresses the Los Angeles abrasion value. According to standard procedure only one analysis is required per each material.

Repeatability
Investigations of repeatability of the Los Angeles abrasion test showed that the standard deviation and coefficient of variation (COV) are low which indicated that the test repeatability is good.

Cuelho et al. (2007) examined 20 gravel aggregates according to ASTM C131-06 (maximum particle size less than 37.5 mm and sample weight 5000 g) and found that the average COV was 5.8 % with a variation range between 0.9 and 15.6 % as shown in Figure 2.6. Three or more (up to fifteen) repeated tests were conducted for the Los Angeles abrasion test, and average LAA value was 27.3 %.
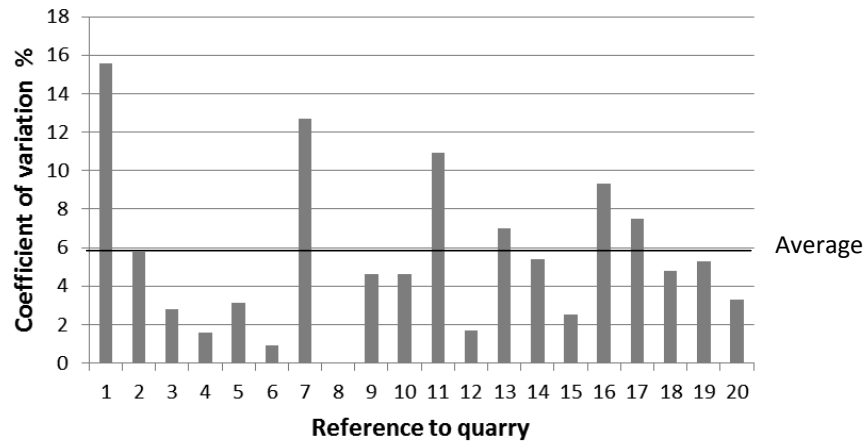
Figure 2.6 Coefficient of variation (COV) for Los Angeles abrasion values (modified after Cuelho et al. 2007).

Cuelho's (2007) single-lab repeatability study also indicated that the COV value varied a lot from source to source (e.g. no.1, 7 and 11). This indicates that some materials in a scientific context should have been tested twice to achieve sufficient accuracy, but it is difficult to reveal which material that needs this handling due to lack of knowledge about what rock properties that cause this variation in test results. This PhD project has used only one test (replica) to determine the Los Angeles value to an aggregate material.

2.3.2 *Micro-Deval test*

The micro-Deval test is run wet (standard procedure) and measures the aggregates' resistance to wear which means that the particles are forced to rub against another in a rotating steel cylinder. The test was adopted by the Norwegian National Railway Administration in 2008 to assess mechanical strength of railway ballast materials together with the Los Angeles test. In this study the micro-Deval test has been performed according to both EN-NS 1097-1 on 10/14 mm (road materials) and EN-NS 13450 on 31.5/50 mm (railway materials), see Table 2.3. The coarse fraction uses a cylinder with length 400 mm (Figure 2.7), and the finer fraction uses a cylinder with length 154 mm. The inside diameter is 20 cm for both.

Table 2.3. Micro-Deval test specifications

Test fraction	Sample weight kg	No. of revolutions	Water added ltr	Weight of steel balls kg	No. of test parallels
10/14 mm	0.5	12000	2.5	5	2
31.5/50 mm	10.0	14000	2.0	None	2

Test sample is not soaked in water prior to the test even though this is a wet test. After the test the aggregate is sieved on a 1.6 mm sieve. The amount of dry material passing the sieve expresses the micro-Deval value in percent of the sample's total weight (calculated as average of two analyses).

Figure 2.7   The micro-Deval test cylinder for fraction 31.5/50 mm ballast.

Strength reduction due to freeze-thaw cycling

Finishing the frost resistance test (Chapters 4.1.4), the micro-Deval test was applied on remaining test samples to investigate whether 150 freeze-thaw cycles had any influence on the mechanical strength (Chapter 4.1.5). In order to achieve sufficient material the micro-Deval test had to be modified and test fraction was expanded from 10/14 mm to 8/16 mm. There was only sufficient material for one parallel test instead of two (standard).

Testing change in the micro-Deval procedure

As mentioned above the micro-Deval test uses dry material despite the fact that this is a wet test. To investigate whether a wet pre-treatment of test sample could affect the mechanical strength, two sets of tests were performed. The first used materials (31.5/50 mm) soaked in pure water for seven days in advance, another set of tests used materials (31.5/50 mm) stored in salt water for 7 days (1 % NaCl). Water added to the drum had equivalent salinity.

2.3.3 Point Load test (dry and wet state)

Point Load test was conducted on drilled rock cores with diameter 50 mm. The test is measuring tension strength and a principle drawing is shown in Figure 2.8. The records were provided by a hydraulic machine with automatic load control (constant load application rate). All samples were supposed to have isotropic mechanical properties after a visual inspection, and the load direction was always placed perpendicular to indications of foliation plane, if any. Dry procedure means that test material was air dried in room temperature (no oven-drying) prior to test for at least one month. Wet procedure means that test specimens were soaked in water for 7 days before testing without use of vacuum in order to copy field conditions. Vacuum is normally used to obtain maximum water content.

Handling procedure of drilled cores immediately after completed drilling in terms of storage in water or air-drying before future measurements (e.g. water absorption and Point Load strength) can affect the result (Broch 1979). In this study all core samples were allowed to dry in room temperature before further test measurements. An alternative handling procedure was not discussed. Use of vacuum was not a part of the wet procedure with the purpose of increasing the water absorption.
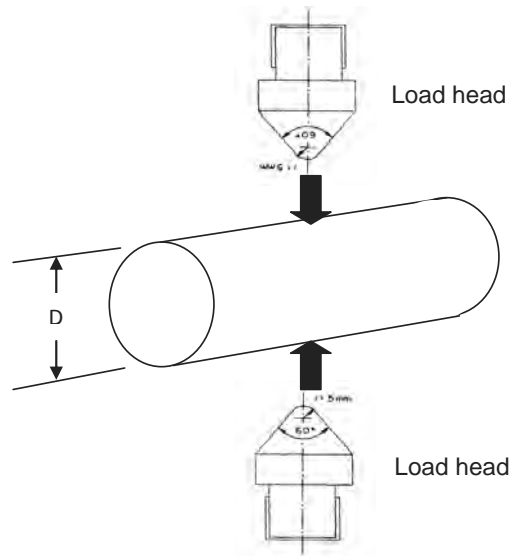
Figure 2.8   Point Load test on drilled cores from rocks. Diameter D was 50 mm.

Number of parallel measurements

Tests on rocks which normally are a heterogeneous material require a large number of single measurements to achieve representative average values. It generally applies that the more parallel tests, the better result. Broch (1979) investigated three sandstones each with around 40 parallel tests and observed that the average value began to stabilize at about 12 measurements. He suggested that minimum number of tests should be 12 or higher. Two examples of equivalent data from this study are shown in Figure 2.9. Number of measurements are 15 and 16. Low extreme values occur because cracks and other weakness planes not representative for the rock are loaded. Hadeland has two and Lauvåsen has one extreme value. These outliers were deleted from the data set when calculating average values. The total number of measurements before deleting varied from 14 to 18.
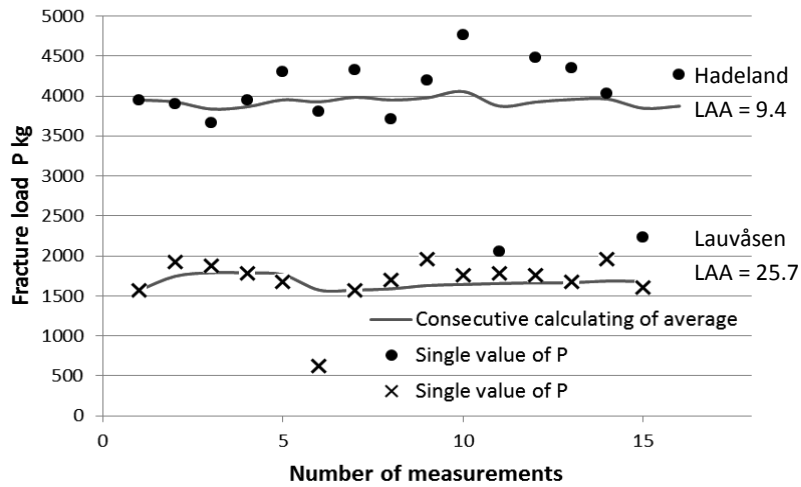
Figure 2.9   Example of calculation of aritmetic value of fracture load P for two rocks as a function of number of measurements. Core diameter D was 50 mm. LAA values relate to fraction 31.5-50 mm.

2.3.4 Frost resistance (freeze-thaw cycling)

Freeze-thaw cycling test has been performed according to both EN-NS 1367-1 (water) and EN-NS 1367-6 (1 % NaCl solution) with following modifications:

(a) Testing on one parallel instead of three,

(b) The sample weight was reduced to1 kg instead of 2 kg and stored in a metallic cylinder filled with water, and

(c) 150 freeze-thaw cycles instead of 10.

This change in procedure ((a) and (b)) was chosen due to limitations in both freezing space and freezing capacity. The aim of increasing the number of cycles (c) from 10 to 150 (=days) was firstly that it should be significant longer than the standard test in order to investigate whether a long term impact could reveal an increase in weathering rate. Secondly it should examine if frost impact had any influence on the particles' intrinsic mechanical strength relevant for railway ballast in cold climate. It was also interesting to examine if the long term weathering progress is linear, accelerating or asymptotic.

The test fraction 8/16 mm (according to the standard test procedure) was manufactured from original rail ballast (unused 31.5/63 mm) by means of laboratory crushing and sieving. The temperature range was +8 ^{0}C to -18 ^{0}C. Measurements of material change (loss of weight) were conducted after every 10, 20, 30, 60, 90, 120 and 150 days.

Sodium chloride concentration

The freeze-thaw test with NaCl solution was conducted according to standard specification which says 1 % NaCl. However, an investigation by Verbech and Klieger (1957) on frost resistance for 25 rocks with test fraction 4.5/19.5 mm, ten freezing cycles (ten times 24 hours) and four different NaCl concentrations (0, 3, 5 and 8 %) found that the strongest impact from NaCl occurred with concentrations between about 2 and 6 % as shown in Figure 2.10.
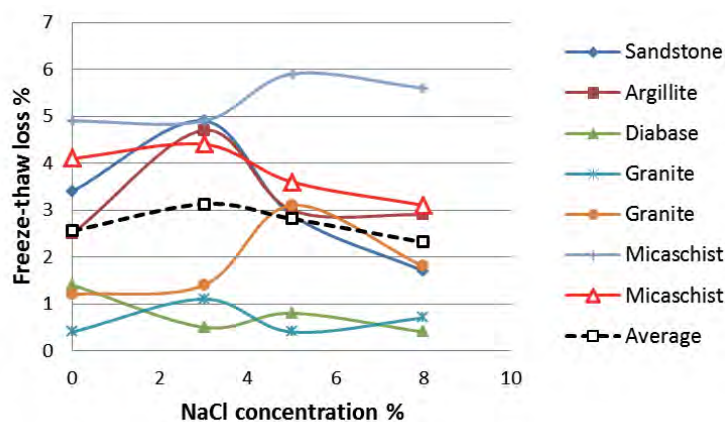
Figure 2.10   Correlation between sodium chloride concentration and freeze-thaw degradation (weight loss), modified after Verbech and Klieger 1957.

Only seven out of 25 rock samples, assumed to be most relevant compared with Scandinavian conditions, are displayed in the diagram together with average values (dotted line). The remaining 18 rocks which had very poor resistance to freezing were skipped. It can be seen that the NaCl concentration with maximum impact varies from rock to rock with a maximum average value around 3 % sodium chloride. Some rocks respond on low concentrations of sodium chloride, others at higher concentrations.

2.4   Textural properties

2.4.1 Water absorption

The water absorption test was conducted in accordance with EN-NS1097-6 on two different fractions, 8/16 mm (used in the freeze-thaw test) , and 40/50 mm (Annex B.2.3 Rail ballast; each sample included 10 pieces), and in addition on drilled cores (6 pieces) with diameter 50 mm with ends sawed-off. Core length varied from 139 to 204 mm. To get close to field conditions, vacuum was not used. Vacuum is usually recommended in order to increase water absorption. The duration of soaking was 24 hours for both fraction 8/16 mm and 40/50 mm, for drilled cores 10 days, and even more for some samples (see Figures 4.40 and 4.41). The defined geometrical surface gives the possibility to measure water absorption with a high level of accuracy.

2.4.2 Mineral distribution

The mineral composition was analyzed utilizing both modal analysis and X-ray diffraction. The modal analyses were performed by examination of thin sections in an optical microscope by means of point counting using a symmetrical point grid. Number of points calculated was 363 for each thin section, and the mineral distribution was expressed as frequencies. The mineral composition was also determined with X-ray diffraction analysis. In order to make a reliable sample selection, the test materials were sampled from production of fines after Los Angeles abrasion tests where the test sample size is 10 kg supposed to represent a fair average of the ballast material. Particles passing sieve 0.125 mm were used in XRD analysis.

2.4.3 Micro-cracks

In general, all igneous and metamorphic rocks contain varying amounts of very small flaws or fissures. These micro-cracks are important for the mechanical and physical properties of aggregates because they cause mechanically weak planar discontinuities which may develop to penetrative fractures under stress, and the strength properties can change very significantly. Micro-cracks also represent channels for ingress of water into the aggregate. Standard procedure on quantifying the amount of micro-cracks in rocks does not exist. Image analysis of thin sections impregnated with a fluorescent agent is an established and very useful technique for determining the occurrence and quantification of micro-cracks (e.g. mm/mm^2). The method can have problems with fine grained rocks especially when the mineral grains are smaller than the thickness of the thin section (25 μm) and where cracks may appear on several levels over each other. Image analysis may also have problems quantifying distinct micro-cracks in combination with more massive-porosity cracking and "holes" as observed in most of the aggregate samples in this study (Figure 2.11). Therefore a new measurement method was developed and used in this thesis, namely luminescence measurement (Paper II). The term "luminescence" has been used because transmitted light intensity has been measured (Lux) in fluorescent light by use of UV filters in the microscope. The measurements represent an indirect quantification of the amount of micro-cracks and porosities in the aggregates.

Polarized light	Fluorescent light
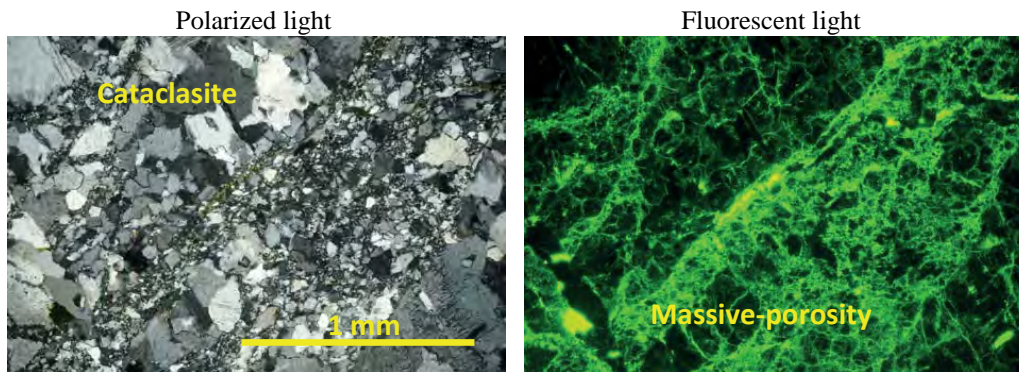
Figure 2.11   Micro images of thin section (Aplitt cataclasite) with massive porosity.

2.4.4 Specific density and particle shape

Rocks' specific density was measured according to NS-EN 1097-6 and particle shape according to NS-EN 933-4.

2.4.5 Particle surface texture

The coarse aggregates morphological or shape properties such as angularity and surface texture have been recognized to be critical factors affecting the performances of ballast materials (Thom and Brown 1989). The terms are explained in Figure 2.12. Particle surface roughness or surface micro relief was quantified at the University of Illinois at Urbana Campaign, USA, utilizing a three-dimensional image analyzing technique named University of Illinois Aggregate Image Analyzer (UIAIA). The roughness is expressed by the Surface Texture Index, and the technique is further described in Rao et al. (2003).
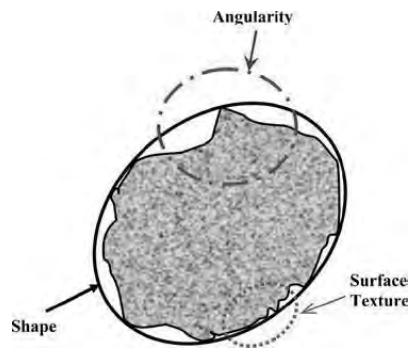
Figure 2.12   Key morphological properties of an aggregate particle. (Pan and Tutumluer 2005).

2.4.6 Mineral grain size distribution

The mineral grain size frequency was calculated based on examination of thin sections with optical microscopy where each mineral "diameter" was manually measured as cumulated intercept lengths along a set of parallel equidistant lines. The grain size was calculated by transforming measured diameter D (chord length) to a corresponding grain cross-section area (circle area with $A = \pi*(D/2)^2$). Based on these data, a mineral grain size distribution curve was constructed similar to the distribution curve commonly used among engineering geologists for describing aggregates for building purposes (Paper III).

2.5   Ballast performance

The aim of the cyclic loading triaxial testing programme was to measure the functional properties of the ballast in terms of ballast breakage, resilient modulus and permanent strain using the following procedures:

2.5.1 Cyclic triaxial test with fixed single-graded curve and constant confining pressure, both dry and wet condition (Paper III)

The quarried ballast material was washed, sieved, air dried and blended to a fixed predetermined grading curve. The specimens were built of five equal layers in a cylindrical steel mould. Each layer was compacted in a dry state for 30 sec using a vibrating plate compactor equipped with two vibrating motors. A maximum centripetal force of 12 kN and 48 Hz was used. A change in specific density and grading as well, will influence the ballast bulk density and finely the sample's height. Each test specimen should have a height of approximately 600 mm at the beginning of the loading test. In order to obtain this a certain amount of material was added. After compaction the specimen was dressed with an inner rubber membrane while a hydraulic piston pushed the sample out of the steel cylinder.

Suction was used under this process in order to keep the specimen standing. After demoulding the specimen was placed in the triaxial rig, and the outer rubber membrane was mounted and instrumented with four LVDTs for axial and radial strain monitoring. Then the specimen was moistened by adding water through the drainage system from the bottom pedestal and then drained

18

immediately. As described above, the single-graded railway ballast specimens were subjected to long term cyclic loading to simulate railway traffic. All triaxial tests were performed in drained condition with a maximum dynamic axial stress of 250 kPa corresponding to about 250 kN axle load given a stiff foundation, and a cyclic rate of 5 Hz. The static confining (air) pressure was 60 kPa for all samples. The triaxial cell apparatus with specimen is shown in Figure 2.13.
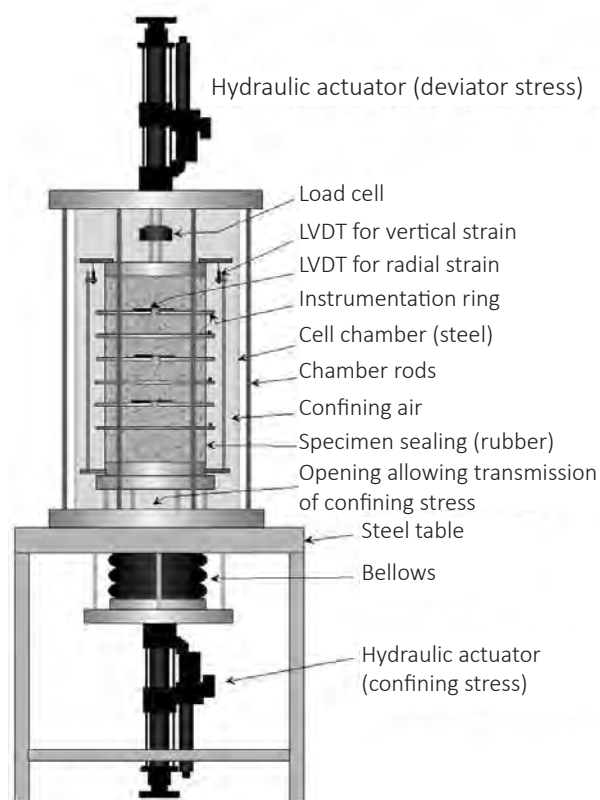
Figure 2.13 The triaxial cell apparatus with specimen, cables not shown (Skoglund 2002).

A complete test was made up of four test repetitions, step 1 through 4.. To simulate the tamping operation in situ (loosening the ballast followed by compaction) the loading (step 1) was stopped after 1 million cycles. The test specimen was than dismantled, re-compacted with the same material as used in step 1 and loaded with another 1 million load applications (step 2).

This loading procedure was followed by two additional similar steps (no.3 and no.4) until a total of 4 million dynamic loads or approximately 100 million gross tons. After each dismantling and before rebuilding, the tested ballast was sieved to remove breakage material (0 / 22.4 mm). This material was collected and weighed at the end of the test to find the total amount of breakage after 4 million load applications (inclusive tamping). This loss of material in the specimen was not compensated with new material. Thus a lower sample height (and lower sample density) was accepted throughout the test.

Estimation of lateral confining pressure
To choose a suitable value for the lateral confining pressure in the ballast layer is not an easy task. It is generally difficult to measure horizontal stress with pressure cells because railway ballast is

normally a coarse material with few particles in contact with the cell area (Shenton 1975). Greater axial stresses near the surface tend to cause significant breakage of ballast just beneath the sleepers (Indraratna et al. 1998, Lim 2004). Lim (2004) developed a box test for ballast to simulate the effects of train loading and tamping on a simulated sleeper, and to study settlement, stiffness and degradation of a range of ballasts. He found that, for tests in which no simulated tamping was performed, the degradation occurred mainly directly beneath the sleeper and was most evident in the upper-most 10 cm of the layer. The horizontal support in the ballast layer due to train load is in general low due to the fact that the ballast has limited width perpendicular to the rail. The confining pressure is never uniform with the depth of the track (Indraratna et al. 1998). Suiker (2002) suggested that the range 10 to 90 kPa covers in-situ conditions, while Raymond and Davis (1998) concluded that the lateral confining stress is unlikely to exceed 140 kPa. Selig and Alva-Hurtado (1982) estimated confining pressure to range between 21 to 83 kPa, although the method of obtaining these values was not disclosed.

In this study 60 kPa was chosen as the value for static confining pressure in the triaxial tests. This is according to Indraratna et al. (2005) a stress level that causes the least breakage on the ballast materials (Figure 2.14).
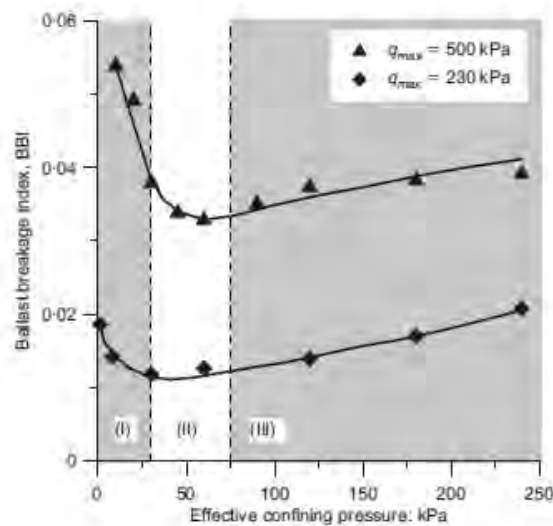
Figure 2.14 Effect of confining pressure on particle degradation at different deviatoric stress levels (Indraratna et al. 2005).

The diagram shows that the ballast degradation depends on the size of the confining pressure and has an optimum point around 30 kPa at 230 kPa deviatoric stress and increases to about 60 kPa at deviatoric stress of 500 kPa together with a significant increase in ballast breakage. It is likely to assume that the level of breakage is affected by the ballast material's mechanical strength.

Preliminary tests in this study were conducted with cyclic confining pressure but it was difficult to find a rubber membrane that could survive more than 1 million cycles. Since the materials have large pores the movemenst of membrane also become large. This membrane had to be repaired by sealing rather frequently, and this delayed the progress of the test series. Consequently, the test procedure was changed from cyclic to constant confining pressure.

Compaction forces and test load magnitude selection

Traditional sleeper-ballast contact pressure calculation utilizes a single axle load with the assumption that it acts over multiple sleepers due to rail stiffness. The load is distributed to at least three sleepers which is demonstrated in Figure 2.15 (Selig and Waters 1994). The drawing shows the rails deflection profile (exaggerated) and relative size of vertical stress distribution at rail seat, top of ballast and top of subballast.
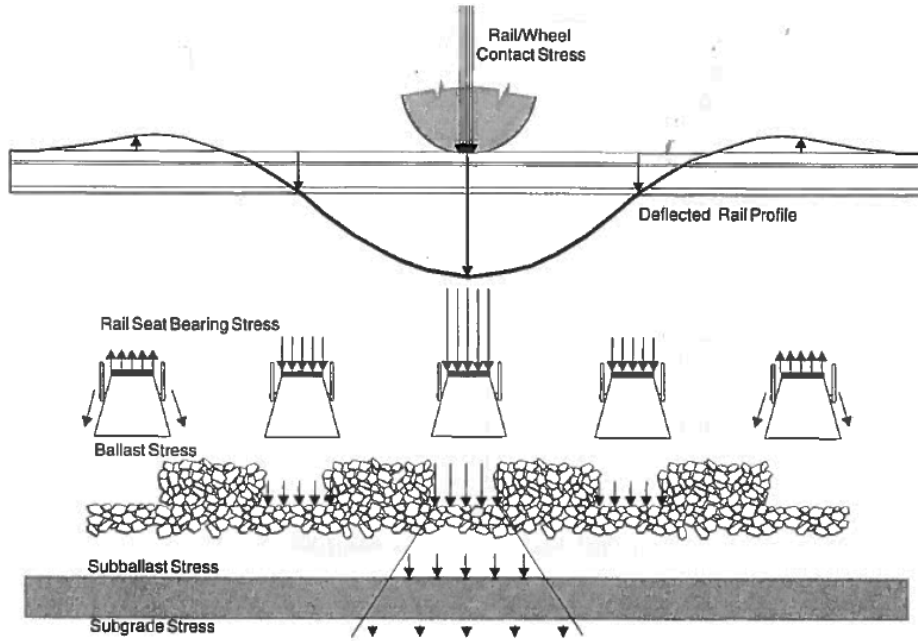
Figure 2.15   Typical wheel load and stress distribution into the track structure (Selig and Waters 1994).

Selig suggests that the sleeper just below the train wheel is loaded with more than 50 % of the wheel load. Each of the two neighbouring sleepers is loaded with half of the remaining wheel load. A quantification of the per cent distribution is displayed in Figure 1.2 where the distribution 20-60-20 is used in the stress calculation. 60 % of the wheel load is given to the principal sleeper. Shenton (1975) have used the distribution 25-50-25 shown in Figure 2.16. Half of the axle load P goes to each wheel and is transmitted to the rail seat as

$$(P \text{ kN} / 2) * 0.5 = P/4 \text{ kN.}$$

50 % of the wheel load to the main sleeper is selected to be used in this study. In Norway, the static design load (axle load limitation) is 22.5 tons, but 25 tons were used in the triaxial and full scale tests to take account for future load increase. The pressure in the interface between sleeper and ballast layer when the interface area is 0.247 m^2 is

$$(250 \text{ kN/4}) / 0.247 \text{m}^2 = 253 \text{ kN/m}^2 = 253 \text{ kPa.}$$

21

This agrees with the calculated value for pressure on ballast in both Figure 1.2 and Figure 2.16. Others as Lichtberger (2003) has used 70 % to the principal sleeper, and Profillidis (2006) proposes the distribution 7-23-40-23-7 based on stress measurements and modelling (Table 2.4)

Table 2.4. Wheel load distribution

Year	Auther	Load P	Interface sleeper/ballast	Stress P/Area	Distribution factor	UIC
1975	Shenton	100 kN			0.50	
1989	Esveld	100 kN	2000 cm^2	30 N/cm^2	0.60	54 kg
2003	Lichtberger	125 kN	2380 cm^2	37 N/cm^2	0.70	
2006	Profillidis	10 t	2000 cm^2	2 kp/cm^2	0.40	

It must be noted that the load distribution regarding the sleepers (e.g. 25-50-25) is affected by the dimension of the rail (54 kg/rail-meter or 60 kg/rail-meter).
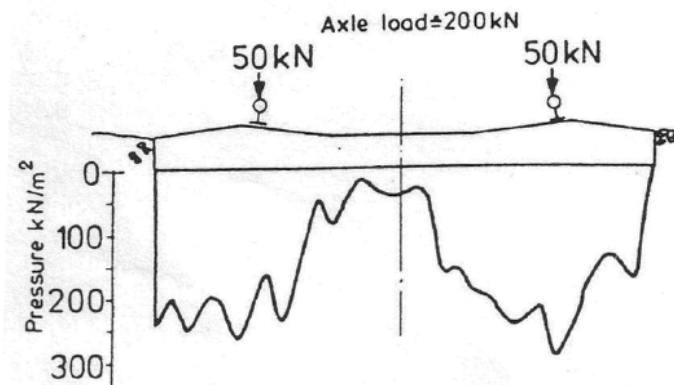
Figure 2.16   Distribution of vertical stress at the sleeper-ballast interface (Shenton 1975).

In the cyclic triaxial tests each vertically applied load cycle was returned to almost full unloading (5 kN) to avoid stroke on ballast from the loading plate.

Number of test repetitions
Each sample was tested through four steps (step 1 through step 4 in the triaxial test rig). It was expected that the stress condition in the sample could vary a lot from test to test due to changes in number of contact points (number of ballast particles) at interface between loading plate and the sample. This will probably affect the transfer of stress and, consequently, influence important properties like strain and breakage. Three steps could have been sufficient, but four was chosen to improve the reliability of the measurements with respect to resilient modulus, ballast breakage, and perhaps reveal a possible trend for the resilient modulus over time.

The number of aggregate particles at the top and the bottom of the sample (Figure 2.17) in contact with the loading plate will change randomly from step 1 through step 4.

Figure 2.17   Preparation of a test specimen.

The transformation of the stress from the top to the bottom of one sample will be different from step to step. Consequently, the contact stress between the aggregate particles and the ability to particle edge wear or breakage will also change and thus the recorded amount of ballast breakage will vary.

Frequency selection

The aim for this test was partly to subject the ballast to real field track conditions with a train speed of 80 km/h and maximum axle load (here: 250 kN) to take into account the impact from heavy freight traffic. The axle load limitation for trains in Norway is 225 kN, but new lines will be designed for 250 kN. A frequency of 5 Hz was chosen for two reasons. Firstly, we wanted to use as high frequency as possible to save time in the laboratory. Necessary time to finish 1 million loadings with 5 Hz is 56 hours or scarcely 2.5 working days. Secondly, the hydraulic actuator available for this study could not provide higher frequency than 5 Hz under maximum loading of 125 kN corresponding to 250 kN train axle load. Triaxial test with 5 Hz as loading frequency corresponds to different speeds depending on varying wheelbase. A common wheelbase of 1.8 meter (Figure 2.18) and 5 Hz is equal to 32 km/h (1.8 * 5 Hz * 3.6 = 32 km/h). Ideally, train speed should have been 80 km/h similar to 12 Hz. For wagons with 2 axles the shortest distance between the axles can be around 5 meter which corresponds to a train speed of 90 km/h.
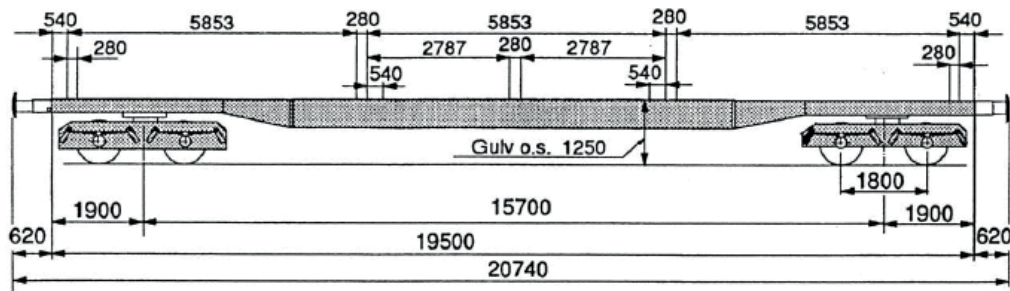
Figure 2.18   Container carriage with four axles (bogie), measures in millimetre (Norwegian Railway Company 2000).

23

Using a lower frequency than 12 Hz should not, according to Shenton (1975), have any effect on the test result. He investigated the permanent vertical strain at different loading frequencies and found that the ballast strain was independent of the frequency (Figure 2.19). Unfortunately, additionally studies of frequency and accompanying ballast degradation have not been found in the literature.
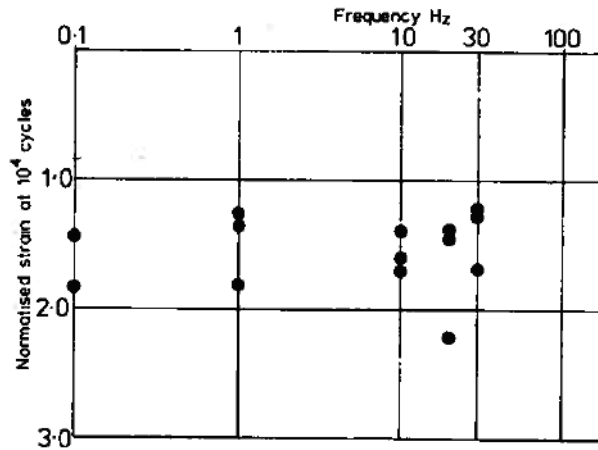
Figure 2.19   The permanent axial strain produced by 10^4 load cycles is plotted against loading frequency (Shenton 1975).

To reduce the amount of scatter in the diagram, Shenton normalised the permanent axial strain measurements by dividing the strain at 10^4 load cycles by the strain produced by the first 8 cycles since the test machine did not always achieve full axial stress for the first 1 or 2 cycles.

Wet state

It is well known that saturation of water usually has a negative effect on rocks' mechanical strength (e.g. Kessler et al. 1940, Broch and Franklin 1972). Hence, it was considered as relevant to run triaxial tests under wet conditions to study ballast durability. The triaxial testing procedure was first performed dry with 4 million cycles followed by another 4 million cycles under wet conditions, totally 8 million cycles in each series. The procedure for the wet condition testing is the same as for the dry testing except that test material was stored in water for seven days before and immersed in water during the test. The voids between the stone particles in the upper 4 cm of the prepared test specimen were not filled with water during the cyclic loading (Figure 2.20). This was to avoid pore water pressure problems due to the sample's elastic behaviour (reduced effective *stress*).
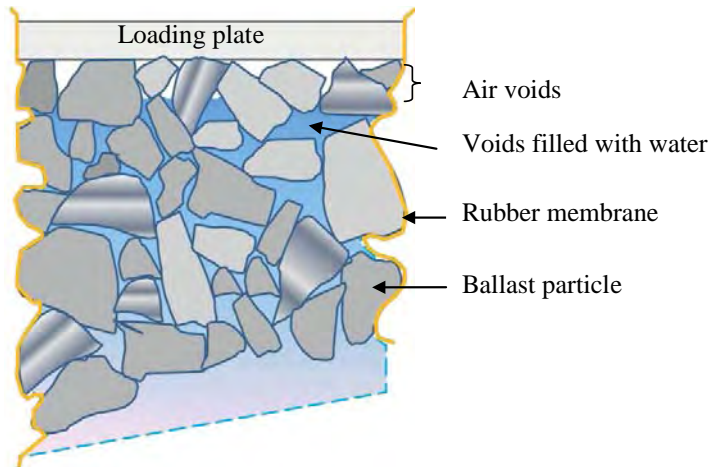
Figure 2.20   Upper section of a wet triaxial test specimen ready for loading, almost completely filled with water.

2.5.2 Cyclic triaxial tests with stepwise finer single-graded curve and constant confining pressure and only dry condition (Paper I)

This experiment was conducted in exactly the same way as the other cyclic triaxial tests as described in Chapter 2.5.1 except for use of three different gradings as shown in Figure 3.1 tagged Arema 4, E_{fine} and E_{coarse}. Test procedure and equipment were the same.

2.5.3 Cyclic loading full scale rail track model test (Paper III)

The general test setup is shown on Figure 2.21. A 300 mm thick layer of crushed rock ballast was confined within a rigid test box 3 m long by 1.5 m wide with plywood bulkheads supported with wood bars, and steel bars in the corners (Figure 2.22).
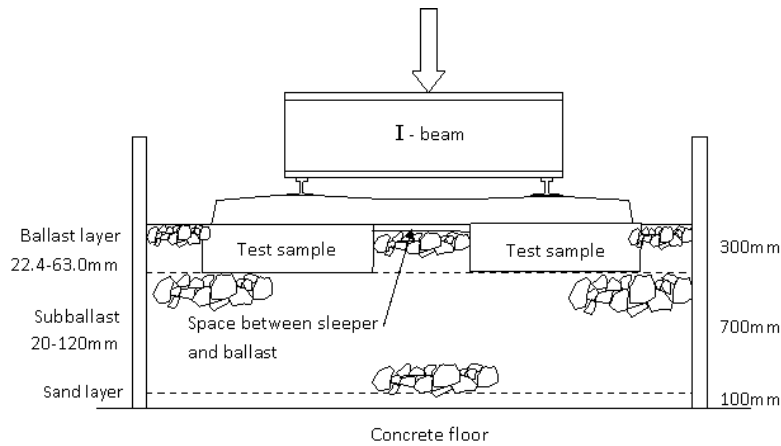
Figure 2.21   Cross-section of the full scale rail track model test setup.

The ballast support was made of a 700 mm thick layer of 20/120 mm crushed rock material (Vassfjell meta-gabbro) overlaying 100 mm of sand resting on a concrete floor. The materials in the two support layers were not changed during the whole tests series.

Two ballast samples, each of 240 kg, from the same rock source were subsequently placed within the ballast layer under each end of the middle sleeper (Figure 2.21). A supporting steel frame with width 400 mm by length 1000 mm was used preliminary to getting the samples in place and with the right shape. A concrete sleeper 2400 mm long by 260 mm wide by 200 mm deep (at rail seat) was placed in the middle of the test box directly on the ballast floor. Two other sleepers were placed on each side with 500 mm spacing to simulate typical track structure but not loaded during the tests. To achieve an easier test performance, no ballast was placed in the cradle between the sleepers.

To separate the test sample from the surrounding ballast and to avoid loss of degradation fines, the material was wrapped in a geotextile. Having backfilled the surrounding ballast material and removed the steel frame, the area was aligned by hand and compacted with a small vibrating device with ten passages for each sample.

According to Raymond (1977a, p.21) the vertical displacement is not uniform across the tie. The settlements under the rails are greater than those under the middle of the sleeper. This leads to a center binding phenomenon, which in turn results in a chance of error with respect to the size of the interface between sleeper and ballast. To counteract this phenomenon, some ballast material under the center of the sleeper was taken away to allow no settlement in the area between the two ballast test samples. The area of interface between sleeper and ballast was 260 mm by 950 mm. In accordance with the triaxial test procedure the maximum dynamic load on each end of the sleeper was about 62.5 kN corresponding to an axle load of 250 kN. The cyclic loading rate was 5 Hz and the specimens were subjected to totally 4 mill loadings interrupted after each 1 mill to perform a "tamping operation". After having temporarily moved the hydraulic jack, the I-bar and the sleeper, the samples were penetrated with a crowbar simulating "in situ" tamping. This was performed on ten different points to loosen the ballast with the intention to re-orientate each aggregate particle.

Repeated load between 5 kN to 125 kN was performed by a computer-controlled closed-loop electrohydraulic actuator working on a I-beam that distributed 62.5 kN to each of the rail seats for a duration equivalent to about 100 million gross tons (MGTs) of axle loading in track. The equivalent axle tonnage was calculated by summing the number of load repetitions and multiplied by twice the applied load (25 tons axle load * $4*10^6$ loadings = 100 million tons).

Figure 2.22   Full scale rail track model test equipment for cyclic loading simulating train traffic and tamping.

3   LABORATORY TEST PROGRAMME

3.1   Test materials

The selection of crushed rock samples was made in order to represent a wide variation in the mechanical properties, i.e. Los Angeles value. Most samples are taken from quarries supporting The National Railway Administration (Jernbaneverket) with railway ballast (strong enough for construction purposes), including one of Norway's strongest rocks. All the tested rock types are composed of combinations of principal rock-forming silicate minerals with few exceptions. They make up a wide variety of igneous rocks, metamorphic rocks and consolidated/metamorphosed sedimentary rocks. Most rocks are fine to very fine grained. A list of rock samples is presented in Table 3.1.

Representative rock samples were collected from across the country and sampled from stockpiles inside the quarries (commercial products). A couple of tests (water absorption and Point Load strength) are performed on drilled cores provided from rock boulders collected in the same quarries that supplied this investigation with crushed materials.

Table 3.1. Aggregate deposits with geologic names, rock characteristics and mechanical properties.

Deposit no. 08115-	Quarry and rock name(s)	Specific density	Average mineral grain size D_{50} (µm) *)	Grain size distribution curve (Cu) **)	Los Angeles 10/14 m dry	Los Angeles 31/50 m dry	Los Angeles 31/50 m wet	Micro-Deval 10/14 mm	Micro-Deval 31.5/50 mm	Point Load Index Is50 dry	Point Load Index Is50 wet
1	**Steinkjer**: meta-sandstone; meta-greywacke; quartzite	2.71	138 /2	4.4	20.9	16.9	14.1	6.0	4.8	-	--
2	**Meraftåsen**: greenstone	2.95	88 /1	5.1	17.5	12.4	18.3	13.6	11.2	6.7	6.7
3	**Lauvåsen**: meta-greywacke; argillite	2.77	119 /1	7.1	19.2	25.7	26.7	24.0	15.7	6.9	4.5
4	**Vassfjell**: meta-gabbro; cataclasite	3.08	333 /2	3.8	14.4	13.3	23.4	8.4	8.7	9.6	3.4
6	**Aplitt**: cataclasite; crushed breccia; granite	2.67	487 /2	3.7	21.3	21.4	20.7	3.7	3.4	6.2	6.6
7	**Ottersbo**; mylonite; cataclasite	2.79	252 /1	7.9	12.0	9.4	11.9	3.8	3.3	8.6	10.4
9	**Hello**: marble	2.73	254 /2	5.2	25.7	32.4	37.3	20.1	16.0	--	--
10	**Lia**: Greenstone; meta-gabbro, basalt	3.02	60 /1	4.8	14.3	10.8	16.5	8.1	7.9	16.3	10.5
11	**Lørenskog**: mylonite; gneiss; gabbro	2.91	203 /1	2.7	20.3	12.8	16.3	9.1	6.0	11.6	8.2
12	**Freste**: monzonite	2.73	3815 /1	3.1	22.5	21.8	21.0	6.2	6.6	11.3	11.1
13	**Helgeland**: syenite; monzonite; gneiss	2.78	1320 /1	4.0	30.3	27.6	29.0	10.9	9.9	--	--
14	**Lillehammer**: sandstone; siltstone; greywacke	2.70	--	--	15.8	13.8	--.	8.0	4.8	--	--
15	**Hadeland**: porphyric trachyte	2.64	123 /1	4.1	15.4	9.4	10.4	2.5	1.9	15.8	14.

No.	Quarry										
16	**Velde**: granite	2.66	1050 /1	2.9	27.0	15.4	17.9	6.8	4.9	--	--
17	**Norstone Tau**: mylonite; cataclasite	2.77	--	--	13.0	10.2	--	6.8	6.0	--	--
19	**Hellvik**: anorthosite	2.73	--	--	14.9	13.7	--	5.9	5.7	--	--
20	**Ramsland**: anorthosite	2.71	3351 /1	3.5	19.7	18.7	17.4	4.9	4.8	--	--
21	**Fossberga**: greywacke	2.71	200 /2	3.7	15.7	13.7	19.9	5.7	4.8	8.8	5.5
22	**Hello quarry**: greenstone; schist; slate	3.00	123 /3	2.9	16.8	17.5	19.8	8.0	7.8	--	--
23	**Rombak**: quartz biotite gneiss; schist	2.78	180 /1	3.3	18.1	13.7	20.2	11.9	9.5	--	--
24	**Kleivaberget**: sandstone	2.63	268 /1	2.7	--	21.0	18.7	--	--	14.3	13.3
26	**Sefrivatn**: granite; granitic gneiss;	2.67	263 /1	3.2	24.9	24.4	19.3	5.4	4.6	9.0	7.2
27	**Follstad**: quartz diorite; tonalite; trondhjemite	--	--	--	--	--	--	--	--	7.7	6.3
28	**Beiarn** marble	--.	--	--	--	--	--	--	--	--	--
29	**Beiarn** amphibole schist	--	--	--	--	--	--	--	--	--	--

1) Corrected with French factor 1.75. Digit after slash represents number of investigated thin sections which the calculation of average mineral grain size is based on.
D_{50} is based on the mineral grain's area

2) Coefficient of uniformity $Cu = D_{60}/D_{10}$ (slope of mineral grain size distribution curve)

Table 3.2. Aggregate deposits with mineral composition based on X-Ray Diffraction (XRD).

Deposit no. 08115-	Quarry	Quartz	Plagioclas feldspar	Alkali feldspar	Biotite	Muscovite	Amphibole	Pyroxen	Epidote	Chlorite	Carbonate	Particle size (mm)
1	Steinkjer	48	18	15		18						0.1-1.5
2	Meraftåsen	5	32	5		6	8		9	29	6	0.01-0.2
3	Lauvåsen	14	23	3		26				25	9	0.05-0.5
4	Vassfjell	1	18	6			41		12	18	4	0.1-5
6	Aplitt	54	15	29						2		0.05-2.5
7	Ottersbo	38	34	8			1		9	10		0.01-0.1
9	Hello marble	3	3			10				2	82	0.05-0.3
10	Lia	5	34	5			30			24	2	0.1-0.5
11	Lørenskog	28	48	6	4		14					0.05-1
12	Freste	7	59	23			7			2	1	7-10
13	Helgeland	8	29	27		27	9					0.3-10
14	Lillehammer	47	12	19		14				8		0.1-2
15	Hadeland	12	54	30			1	3				0.01-5
16	Velde	28	14	40	7	8				2	1	0.2-7
17	Norstone Tau	29	30	4		17				20	3	0.2-3
19	Hellvik	1	80		3		4	8			1	1-8
20	Ramsland	2	83			9				3	3	3-8
21	Fossberga	37	35	10		15				2	1	0.1-2
22	Hello quarry	15	29				42		6	8		0.1-2
23	Rombak	46	21	2	10	17				3	1	0.01-0.4

28

24	Kleivaberget	46	7	20		19	2			6	0.2-1.5
26	Sefrivatn	24	42	27	2		2		2	1	0.1-0.5
28	Beiarn *)	4			2	3		2		87	0.1-2.0
29	Beiarn **)	10	11		5		68				0.05-0.5

*) Modal composition. Opaque 2 %

**) Modal composition. Opaque 4 %, Quartz/feldspar 21 % (difficult to distinguish)

3.1.1 Challenge of achieving representative rock samples

The samples from the different quarries were assumed to be homogeneous and representative within each source. Even with a strong focus on random and representative sampling, it was hard to avoid differences between samples from the same source. This was clearly demonstrated during the microscopic inspection of thin sections to provide texture characteristics. With the aim to reveal a possible geological variation in the deposit, rock fragments that "looked" different were selected for further investigation. Between one and five thin sections from each deposit were fabricated with three as an average to cover "all" variations.

3.2 Functional properties

Table 3.3 provides an overview of which analyses that each material has been subjected to.

Table 3.3. Conducted analyses in addition to those mentioned in Table 3.1.

Deposit no. 08115-	Quarry name	Absorption 1)		Drilled cores, diameter 50mm	Shape 31.5/50 mm 2)	Particle surface texture 31.5/50	Triaxial test dry	Triaxial test wet	Full scale rail track model test	Frost resistance test	LAA test after 60 freeze-thaw	MD test after 150 freeze-thaw	Coulter (fines from LAA test)	Coulter (fines from Full scaletest)	X-Ray Diffraction (mineral distribution)	Micro-cracks (Luminescence)	Petrographic examination
		8/16 mm	40/50 mm														
1	Steinkjer	x	x		20.4	x	x	x	x	x	x	x	x	x	x	x	x
2	Meraftåsen	x	x	x	7.1	x	x	x	x	x	x	x	x	x	x	x	x
3	Lauvåsen	x	x	x	13.5	x	x	x	x	x	x	x	x	x	x	x	x
4	Vassfjell	x	x	x	7.3	x	x	x	x	x	x	x	x	x	x	x	x
6	Aplitt	x	x	x	13.4	x	x	x	x	x	x	x	x	x	x	x	x
7	Ottersbo	x	x	x	17.3					x		x	x		x	x	x
9	Hello marble	x	x		21.2					x		x			x	x	x
10	Lia	x	x	x	7.4					x		x	x		x	x	x
11	Lørenskog	x	x	x	14.7	x	x	x	x	x	x	x	x	x	x	x	x
12	Freste	x	x	x	13.9	x	x	x	x	x	x	x	x	x	x	x	x
13	Helgeland	x	x		8.8					x		x			x	x	x
14	Lillehammer		x												x	x	x
15	Hadeland	x	x	x	14.0					x	x	x	x		x	x	x
16	Velde	x	x		8.9					x		x			x	x	x
17	Norstone Tau		x												x	x	x

No	Name				Value											
19	Hellvik		x									x		x	x	x
20	Ramsland	x	x		5.7					x	x	x		x	x	x
21	Fossberga	x	x	x						x	x	x	x	x	x	x
22	Hello quarry	x	x							x	x	x	x	x	x	x
23	Rombak	x	x		11.7	x	x		x	x	x	x	x	x	x	x	x
24	Kleivaberget			x	18.5									x	x	x
26	Sefrivatn	x	x	x	11.2	x	x	x	x	x		x	x	x	x	x
27	Follstad			x												
28	Beiarn marble	x								x						x
29	Beiarn amphibole schist	x								x						x

1) Measured values are listed in Paper II.
2) Rod-shaped

3.2.1 Large scale cyclic loading triaxial test

The main objective was to measure ballast breakage, elastic properties and vertical permanent deformation.

Fixed grading curve and constant confining pressure (Paper III)
The test series involved nine different rock types subjected to two different test conditions, 4 times 1 million cycles with dry materials (tamping simulation) and 4 times 1 million cycles with wet materials (simulation of climate and tamping operation). Each material was tested 4 times in order to improve the reliability and to observe changes over time. Final results from ballast breakage, resilient modulus and permanent deformation are presented as an average of these four tests. Sample preparation for the wet testing consisted in storage in water at room temperature for 7 days ahead of the test and the sample immersed in water during test performance. One exception from this procedure was the sample from Rombak mica schist which was only analysed in dry state. The grading curve used was E medium shown in Figure 3.1.

Variable grading curve with constant confining pressure (Paper I)
To compare the effect of ballast grading on degradation, resilient modulus and vertical permanent deflection, three different grading curves were used. Those are two gradings representing extremities within the Norwegian limit curves according to EN13450 and Arema no.4 (Arema envelope) as seen in Figure 3.1.
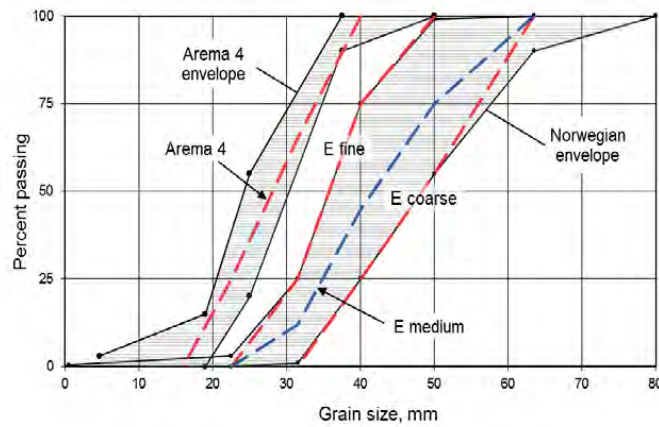
Figure 3.1. Ballast grading curves employed in the large scale triaxial tests and the full scale rail track model test.

These tests involved only one rock type, namely Steinkjer meta-sandstone and only dry materials. Like the triaxial test with fixed grading curve, each material was tested 4 times in order to obtain more reliable values (lower the standard deviation) and reduce the scattering in comparison diagrams. Applied load was similar to an axle load of 25 tons.

3.2.2 Full scale cyclic loading rail track model test (dry state, Paper III)

The test series involved nine different rock types suited for ballast materials with the objective of measuring ballast breakage under approximately in situ rail track stress conditions. To arrange for comparisons, the rock types used are identical with those used in the triaxial test with fixed grading curve. The grading curve in this test was also the same, tagged as E medium in Figure 3.1. The materials were tested 4 times each interrupted by a "tamping" operation after every 1 million loadings until 4 million in total. Applied load on each end of the sleeper was similar to an axle load of 25 tons. Wet state was not conducted due to practical problems with adding water.

3.2.3 Freeze-thaw resistance test (Paper II)

20 different types of quarried aggregates, most of them suitable as ballast material, were tested for frost resistance in a 150 freeze-thaw cycles test (duration of five month) including two rock types with expected low resistance documented from field experience. The tests were performed with both water and 1 % NaCl solution. The fraction used was 8/16 mm.

Remaining mechanical strength after 150 freeze-thaw cycles
To inquire whether the freeze-thaw process had caused any damage in terms of rock's mechanical strength or not, micro-Deval tests on fraction 10/14 mm were run on the residual material. Standard procedure requires two parallel tests but it was sufficient material to only one parallel due to weight loss during the foregoing freeze-thaw test.

3.3   Mechanical properties

3.3.1 The effect of pre-treatment of test samples (micro-Deval test)

The micro-Deval method is already standardized as a wet test to take into account rocks' loss of mechanical strength in general when they get wet. In an attempt to improve the reliability of the test, two test series were performed where materials from 18 quarries were tested for abrasion resistance with the following change in the standard procedure:

(a) test samples were stored in water for 7 days in advance, and
(b) test samples were stored in 1 % NaCl solution before testing. The drum was also added NaCl with the same resolution.

3.3.2 Loss of mechanical strength due to freeze-thaw impact

Ballast strength loss after long term freeze-thaw impact
The long term freeze-thaw test opened the possibility of examining whether Norwegian aggregates loose mechanical strength due to frost impact in wet climate in addition to weathering. Since the freeze-thaw test was performed on fraction 8/16 mm, the control of the strength was done with the micro-Deval test

Ballast strength loss after 60 freeze-thaw cycles (Los Angeles abrasion)
Los Angeles abrasion tests have been carried out on railway ballast materials subjected to 60 freeze-thaw cycles (soaked in water). Duration of one cycle was 24 hours (standard performance for this thesis). Temperature range was between +8 ^{o}C and -18 ^{o}C.

3.3.3 Micro-cracks (Paper II)

Measurements of the amount of micro-cracks in rocks were carried out using a newly developed method described in Paper II. 71 thin sections were examined distributed on 22 different rock samples.

4. SUMMARY OF FINDINGS

Test results that are described in the attached papers, are only summarized in this chapter. Unpublished results are mentioned in more details.

4.1 Functional properties.

4.1.1 *Resilient modulus of ballast material under triaxial testing*

Triaxial testing with cyclic loading of nine different rock types with the aim to document ballast breakage (Paper III) also provided information about the materials' elastic properties. Resilient modulus is defined as the repeated deviator stress divided by the recoverable portion of the axial strain (Monismith et al. 1967). Calculation of the resilient modulus value was based on measured recoverable axial strain at the end of each test (after each 1 million loadings).

The investigation revealed that the elastic properties varied a great deal from rock to rock. Analysis results are shown in Figure 4.1. The average values vary from 308 to 613 MPa (factor of two between highest and lowest value) and are listed in Table 4.1.

Table 4.1. Resilient modulus (MPa) of ballast materials in dry and wet state.

	Lørenskog	Vassfjell	Freste	Meraftåsen	Lauvåsen	Aplitt	Rombak	Steinkjer	Sefrivatn
Step 1 (dry state)	616	568	534	514	436	371	356	301	282
Step 2	627	566	506	481	492	384	389	313	289
Step 3	630	623	548	466	536	393	381	324	398
Step 4	579	530	519	493	451	386	347	326	260
Average dry resilient modulus MPa	**613**	**572**	**527**	**488**	**479**	**384**	**368**	**316**	**308**
Standard deviation	20.3	33.2	15.8	17.6	38.9	8.0	17.3	10.0	53.5
Coefficient of variation	3.3	5.8	3.0	3.6	8.1	2.1	4.7	3.2	17.4
Step 1 (wet state)	-	457	485	463	419	343	-	321	313
Step 2	524	485	476	454	407	352	-	335	320
Step 3	573	455	-	436	408	356	-	295	305
Step 4	540	-	487	453	394	376	-	299	308
Average wet resilient modulus MPa	**546**	**466**	**483**	**452**	**407**	**357**	**-**	**313**	**312**
Standard deviation	20.4	13.7	4.8	9.8	8.9	12.0	-	16.3	5.7
Change in resilient modulus from dry to wet state (%)	÷ 10.9	÷18.5	÷ 8.3	÷ 7.4	÷ 15.0	÷ 7.0	-	÷ 1.3	1.3
Coefficient of variation	3.7	2.9	1.0	2.2	2.2	3.4	-	5.2	1.8

It was expected that the histogram could suggest a trend for decreasing resilient modulus with increasing step number based on considerations about change in sample bulk density (Paper I). However, no such trend appeared, probably due to too few number of tests. It can further be observed that single values of resilient modulus showed a relative deviation of up to about 11 % (Lauvåsen) from the mean value and for Sefrivatn even more.
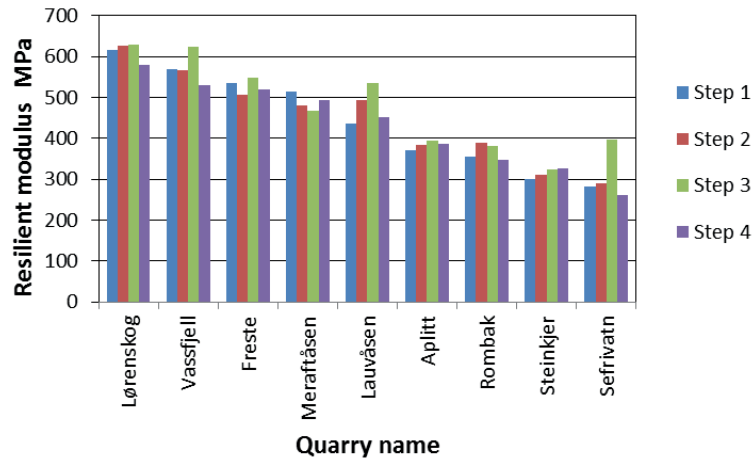
Figure 4.1 Elastic properties (dry state) to nine different rock types. Number of loadings are 1 million for each step.

The only rock property that showed significant correlation with ballast's resilient modulus found in this investigation, was rock specific density as shown in Figure 4.2. The modulus increases with increasing specific density. The regression coefficient R^2 is 0.55, but increases to 0.75 when the aggregate from Freste monzonite is considered as an outlier in this context (medium-grained) and removed. The other samples in the diagram are fine grained and in that collection Freste may perform in a different way.
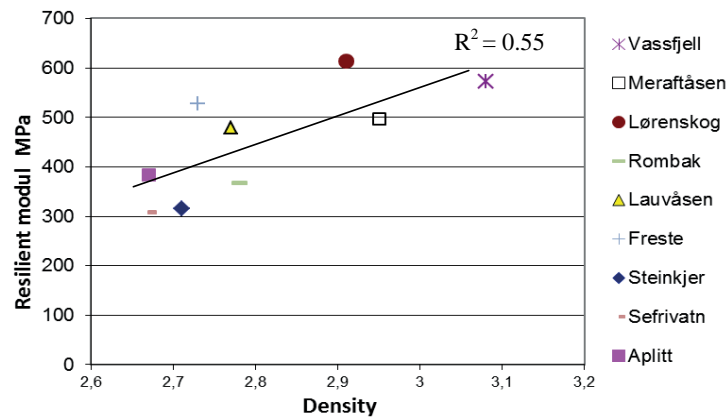
Figure 4.2 Relationship between ballast elastic property and rock density

There is of course a possibility that the resilient modulus is affected by other rock properties in addition to the specific density. In Figure 4.2 it is seen that the aggregate from Lørenskog obtained

the highest value of all samples (613 MPa) although it did not have the highest specific density. From the microscopic investigation it is observed that Lørenskog has the lowest amount of micro-cracks of all the samples tested. It is obvious to suggest that, to some extent, the less fractured the rock is, the higher is the resistence to deflection.

The knowledge that the ballast's resilient modulus varies from rock type to rock type provides the ability to design tracks with required stiffness (Chapter 6. Fields of applications). This is interesting because the stiffness of the track affects both driving costs and track geometry maintenance costs (Lopez Pita et al. 2004). Owners of rolling stock will benefit from that new tracks are built with optimum stiffness.

Wet testing

Wet testing involved that voids in the triaxial test sample were filled with water during the test and that the test material was immersed in water for 7 days before sample compaction and cyclic loading. The relation between dry and wet resilient modulus is shown in Figure 4.3. Most of the selected rocks increased their elastic properties when submerged in water (less stiff). The loss in resilient modulus were up to 18 % (Vassfjell meta-gabbro) compared with dry values. But two rocks, namely Sefrivatn (granitic gneiss) and Steinkjer (meta- sandstone (granitic composition)), did not change their elastic properties. They are mainly composed of the minerals quartz and feldspar. No explanations are available to account for this performance.
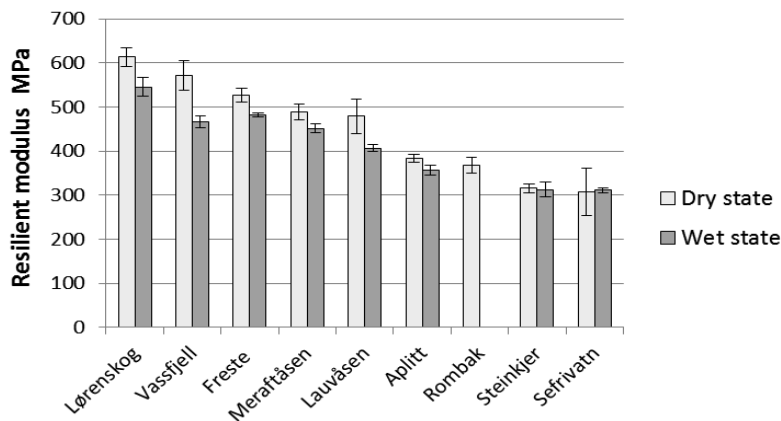
Figure 4.3   Resilient modulus of cyclic triaxial tests in dry and wet state (average of four tests). One standard deviation (+ / -) is added to the columns.

Resilient modulus affected by change in ballast grading

The effect of ballast grading on resilient modulus was investigated on only one type of rock (Steinkjer meta-sandstone) and three uniformly graded materials labeled E_{coarse}, E_{fine} and Arema 4 as shown in Figure 3.1. The nominal size was 31.5/63 mm, 22.4/50 mm and 16/40 mm respectively and only dry materials were used. Broad-graded materials was not a part of this study. Paper I suggests that the ballast's resilient modulus correlates with the gradation (Figure 4.4). The histogram shows that the modulus decreases with decreasing D_{50} (particle grain size). The standard deviation was 18.4 for E_{coarse}, 9.6 for E_{fine} and 4.0 for Arema 4, and Coefficient of variation (COV) was 5.73 %, 3.05 % and 1.43 % respectively.
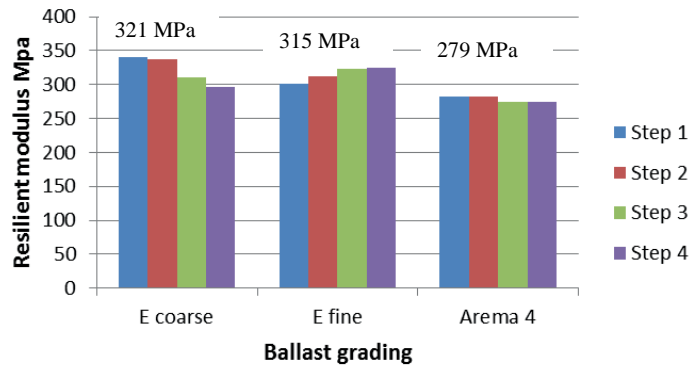
Figure 4.4   Variation of resilient modulus from cyclic triaxial testing with ballast grading. The rock type was Steinkjer meta-sandstone.

The variation with grading seems to have minor effect on resilient modulus. The investigated rock, Steinkjer meta-sandstone, is a rather strong rock. However, others and weaker materials may perform with larger differences (Raymond 1977b). Thom and Brown (1988) examined a uniformly graded and a well graded aggregate of dolomitic limestone with similar maximum particle size (10 mm), and found that the former with higher D_{50} had slightly larger resilient modulus. This also agrees with Heydinger et al. (1996) which tested crushed limestone, natural stone and slag and five different gradings. Their testing indicated that the resilient modulus of aggregates varied significantly depending on the type of material and varied less significantly depending on material gradation and moisture condition. There seems to be a general rule that resilient modulus of ballast increases with increasing D_{50}. This was also the conclusion from a field test reported by Bosserman (1981) as shown in Figure 4.5.
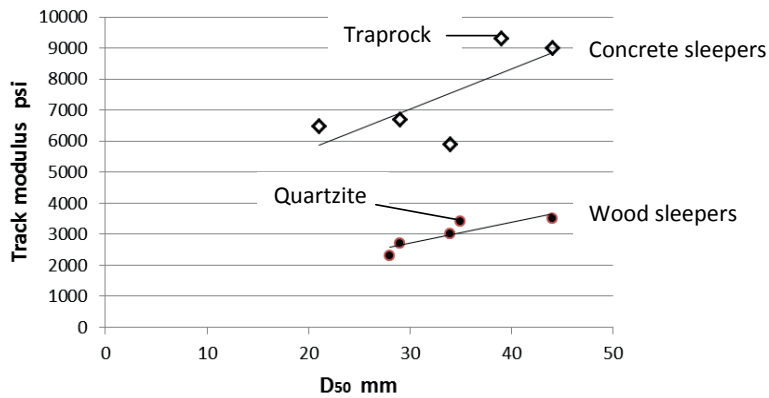
Figure 4.5   Variation in track modulus with ballast particle size. Regression coeffisient R^2 for concrete sleepers is 0.55 and for wood sleepers 0.77. Test materials are different types of granite with two exceptions. 1 psi = 6.89 kPa. Modified after Bosserman 1981.

The diagram shows that use of concrete sleepers obtained higher modulus values than wooden sleepers. Note that there is a mix of different rocks in the diagram which usually results in increased data scattering according to Figure 4.2. Resilient modulus correlates with rocks' specific

density. 8 out of 10 data points in Figure 4.5 refer to variants of granite which all have similar specific density values (about 2.65 kg/dm^3) Traprock is a gabbro with normally significant higher specific density compared with granite and may perform with a higher modulus. Replacing the traprock with granite, the corresponding track modulus would have decreased and the regression coefficient would probably have increased.

4.1.2 *Effect of water on rocks' mechanical strength*

Water has generally a negative effect on rocks' mechanical strength (Kessler et al 1940, West et al. 1970), and the influence of water on the strength of rocks may be considerable (Broch 1979). The strength reduction has been documented in this study utilizing both Los Angeles Abrasion test and Point Load test (Figure 4.6 and 4.7). The last test was added to the project to create a link to the field of rock mechanics where the Point Load test is very common and widespread. This knowledge about strength reduction has obviously not been taken into consideration owing to the fact that the LAA test cannot yet provide a standardized wet procedure.

Los Angeles abrasion test

The Los Angeles abrasion test has been conducted in both dry and wet stage on fraction 31.5/50 mm. The laboratory results are shown in Figure 4.6 and can be divided into three groups: (a) some rocks increased their resistance to crushing in contact with water, (b) some rocks decreased their strength when they absorbed water and (c) others performed unaffected. A common feature for several specimens within group (a) is that they mainly constitute the minerals quartz and feldspar (granitic composition), some of them contain a high amount of the mineral quartz (here: 40-60 %) and some have a high amount of the mineral feldspar (up to 80 %).
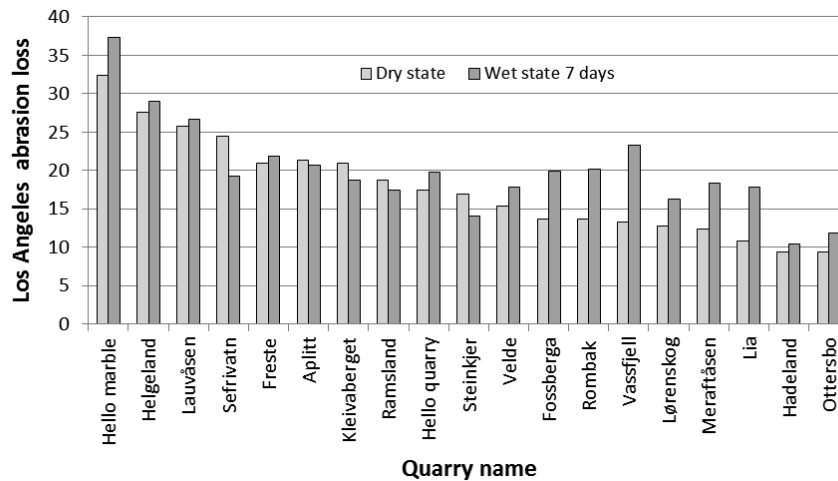
Figure 4.6 Los Angeles abrasion test results conducted on fraction 31.5/50 mm in both dry and wet state.

The three test samples with highest loss of strength (group (b)) have in part a high amount of the mineral amphibole. There are indications that perhaps other and still unknown properties are affecting the result. The significant loss of strength to Fossberga (greywacke) and Rombak (mica-gneiss) despite a mineral content of 82 and 67 % with quartz + feldspar can have been governed by their content of mica (15 and 27 % respectively).

Water's effect on mechanical strength regarding the Los Angeles abrasion test is summarized in Figure 4.6. Loss of strength due to water absorption, results in higher Los Angeles abrasion values and these rocks are displayed in Figure 4.7 with relative values (%) higher than 100 %. Vice versa for rocks that increase strength in contact with water. Red line marks no change in mechanical strength (100 %). The blue lines mark one standard deviation (+ / -). As mentioned in Chapter 2.3.1 under Repeatability the size of standard deviation and corresponding coefficient of variation for the Los Angeles abrasion test were not mapped in this study. But an average value of 5.8 % provided by Cuelho et al. (2007) and based on results from 20 rocks is used in the diagram below as a substitute.
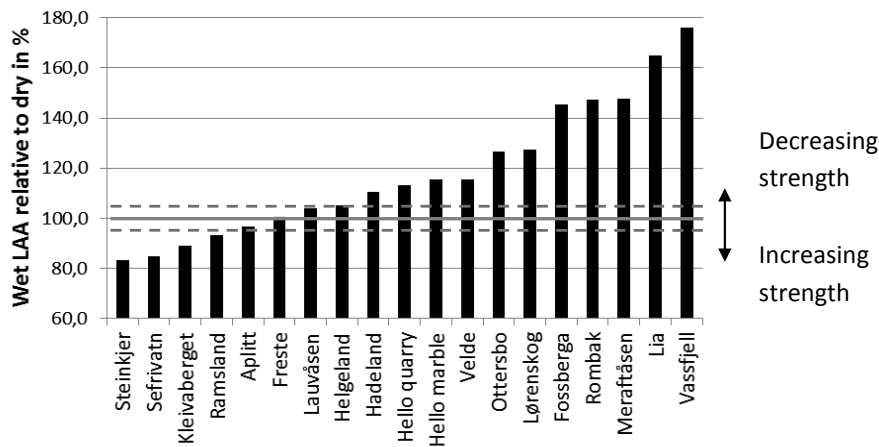
Figure 4.7 Los Angeles abrasion values (31.5/50 mm) of water saturated rocks in per cent of the strength (LAA) of air-dried rocks. Dotted lines suggest one standard deviation (average).

This means that rocks like Aplitt, Freste Lauvåsen and Helgeland are most probably unaffected regarding strength. Cuelho et al. (2007) also demonstrated that the diffence in standard deviation between to rocks can be significant (e.g. 0.9 % and 15.6 %). Thus, this gives reason to believe that use of average value can lead to incorrect conclusions. An investigation of the repeatability of the Los Angeles abrasion test would have provided this study knowledge of a possible correlation between repeatability and rock properties such as mineral grain size, mineral content and sample fraction due to less scattering in the correlation diagrams.

It should be emphasized that the result in Figure 4.7 are partly ruled by the mineral content. The three rocks with the largest strength improvement (Steinkjer, Sefrivatn and Kleivaberget) constitute mainly a combination of the minerals quartz and feldspar and consequently low values for specific density (around 2.65). The three rocks with the largest loss of strength are those with the highest specific density (around 3.00) which normally means high content of dark minerals, e.g amphibole.

Point Load test

Results from the Point Load test performed on 13 different rocks show principally the same
tendency obtained with the LAA test that most rocks lose mechanical strength when they are in
contact with water while a few others increase in strength (Figure 4.8).
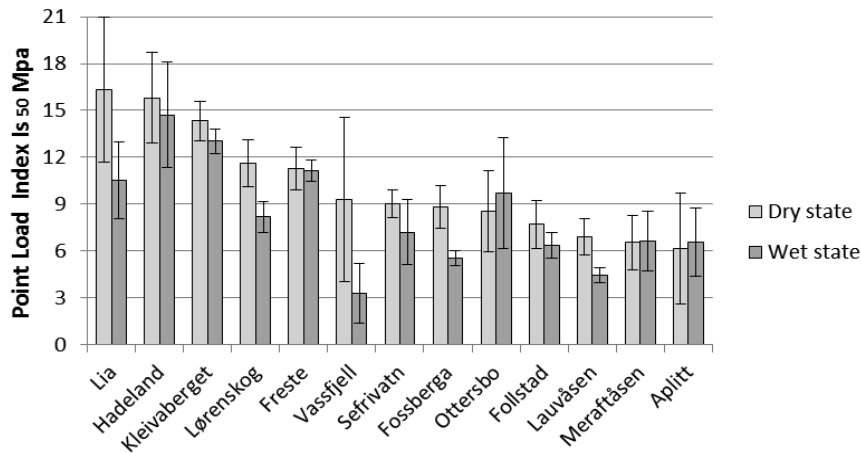
**Figure 4.8   Histogram of Point Load test results from both dry and wet state with one
standard deviation added.**

However, the effect of water is more clearly negative for the Point Load test (Figure 4.9). Only
one sample (Ottersbo) out of thirteen can show an increase in strength. Vassfjell (meta-gabbro)
and Lia (greenstone) with high content of amphibole are those two samples that have the highest
loss of strength from both Los Angeles abrasion and Point Load tests. Other samples with similar
reaction are Lørenskog (gneiss/gabbro) and Fossberga (greywacke) which suggest that the loss of
strength can be caused by one or several other properties than mineralogy. On the other hand
samples with granitic composition like Sefrivatn (granitic gneiss) and Kleivaberget (sandstone)
with increasing strength as regards LAA, show an unexpected decrease in PLI. This phenomenon
seems to be quite complicated and cause and effect are not fully understood.
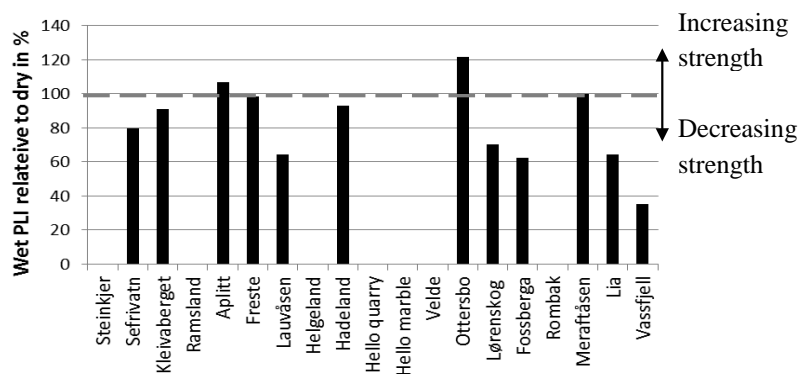
**Figure 4.9   Point Load Index (Is_{50}) or tensile strength for water saturated rocks in per cent
of the strength of air dried rocks. Drilled core diameter was 50 mm.**

That amphibole could have a negative influence on the strength of water saturated rocks has been mentioned earlier in the literature. When keeping fine grained, "non-porous" rocks as a separate group, Broch (1979) pointed out that the strength reduction increases with increasing amount of dark minerals (mica, amphibole and pyroxene) measured with the Point Load test.

It is interesting to combine the two data sets from Los Angeles abrasion loss and Point Load Index because the Point Load test can be performed during field work. Is the Point Load test able to predict the mechanical strength? Results from dry tests did not show any correlation. Using data from wet tests a fair relation occurs as seen in Figure 4.10. The regression coefficient is not high, only 0.53, but if we disregard the two outliers Freste (medium grained monzonite) and Kleivaberget (sandstone), the correlation looks much more attractive with R^2 like 0.83. The Point Load test is a fast and uncomplicated method, and the field version of the Point Load test apparatus can be used to predict a reliable LAA value in an early stage of a field investigation.
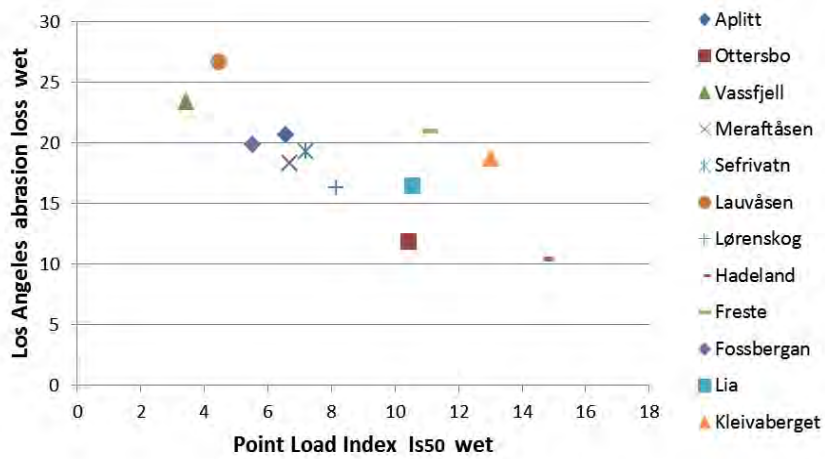
Figure 4.10   Correlation between Los Angeles abrasion 31.5/50 mm and Point Load Index, both wet state.

The two diagrams in Figure 4.11 are an attempt at finding a relation between mechanical strength and rock texture. Neither Los Angeles abrasion test nor Point Load test can show signs of any association with the content of soft minerals. However, few of the data points exceeded about 25 % soft minerals and the conclusion is uncertain. On the other hand, it is possible that an amount of soft minerals less 25 % do not have any visible negative effect on mechanical strength probably because a possible influence is overruled by the impact from one or several other unidentified rock texture properties.
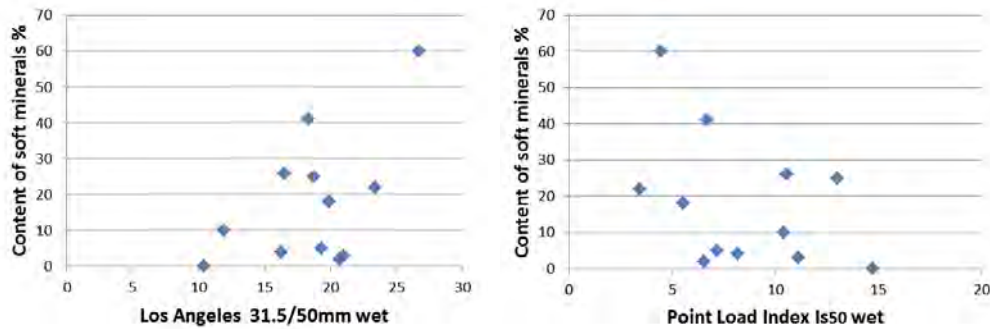
Figure 4.11   Relation between rocks' content of soft minerals and mechanical strength (wet state). Left: Los Angeles 31.5/50 mm wet. Right: Point Load Index Is$_{50}$ wet.

Cyclic triaxial testing

Moisture has in general a negative influence on rocks' mechanical strength (Kessler et al. 1940, West et al. 1970, Broch 1974). Los Angeles Abrasion test and Point Load test results in this study (Figure 4.7 and 4.9) supports these investigations. Consequently, it seems reasonable to believe that triaxial testing with wet material should act in the same manner, i.e. an increase in ballast breakage from dry to wet procedure. Amount of breakage material (0/22.4 mm) from both dry and wet conditions is shown in Figure 4.12 and on accumulated basis in Figure 4.13. It is the same material that has been tested eight times from test 1 through test 8.
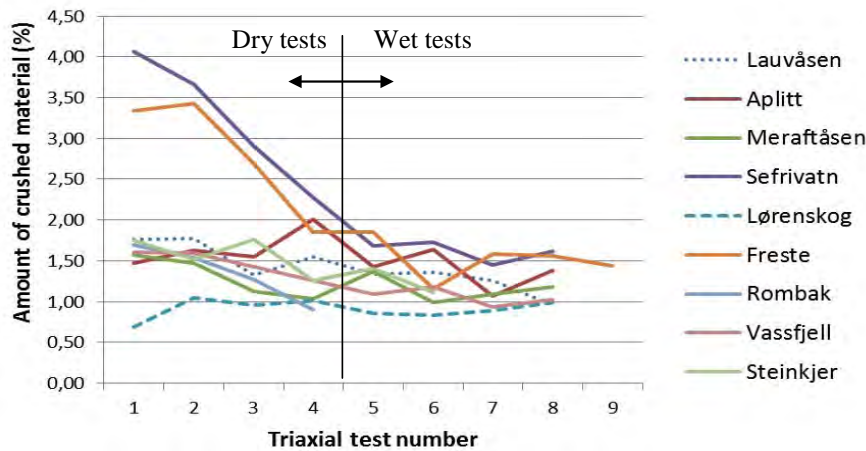
Figure 4.12   Amount of crushed material 0/22.4 mm after each triaxial test. The test fraction at the beginning of each test was 22.4/63.0 mm. Number 1 to 4 represent dry state, and 5 to 8 represent wet state. Mica gneiss from Rombak was tested only in dry state.

The diagram shows there is no sign of an increase in ballast deterioration after test number 4. This means that water did not have any negative effect. However, there is rather a slight decrease in breakage as seen in Figure 4.13 where some of the curves are making a bend (change in crushing rate) after test number 4. This result was quite unexpected and there is no explanation of the phenomenon. It is hard to explain why water more and less reduces rocks' mechanical strength, and even more difficult to explain why no reaction occurred in this case. It is interesting to

41

mention that Los Angeles abrasion and Point load tests were carried out on fresh materials, i.e. unused, while the wet triaxial tests were conducted on used materials (subjected to 4 million loadings in advance).
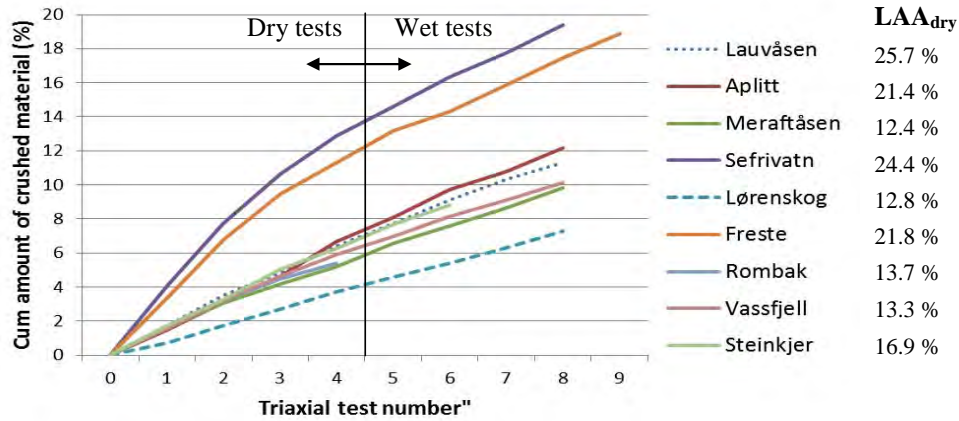
Figure 4.13 Cumulative amounts of crushed material 0/22.4 mm after 8 triaxial tests. Freste was tested 9 times. Test number 1 to 4 represents dry state, and number 5 to 8 represents wet state. Mica gneiss from Rombak was tested only under dry conditions. All rocks are fine to very fine grained except Freste.

4.1.3 Effect of rock type on ballast's performance

Number of rocks included in this study is too small to draw any clear conclusions regarding rock type and the ballast's performance, but some correlations seem to appear. Rocks (but not all) that have granitic mineral composition (consisting of about 30 % quartz and 60 % feldspar), or contain a high amount of the mineral quartz (here: 40-60 %), or contain a high amount of the mineral feldspar (around 80 %) appear to:

1. Improve or keep strength when moistened (according to LAA test), see Figure 4.7.
2. Be among those with highest frost resistance, see Figure 4.14.

For all rocks in this study, there is a fair correlation between rocks' specific density and resilient modulus (Figure 4.2).

4.1.4 Freeze-thaw resistance test with both water and 1 % NaCl solution

The Norwegian specifications for railway ballast materials do not require documentation on frost resistance. Due to lack of relevant experience it is assumed that rocks approved for construction purposes have sufficient resistance to weathering. The Norwegian standard test for measuring frost resistance on rocks recommends use of water. Test results (blue bars (left twin) in Figure 4.14) show that this is a low impact test. It has no difficulty in distinguishing between the superior quality material and the very poor material (marble (reference) and amphibole schist (reference)). It cannot, however, indicate with any certainty how the intermediate material will behave. Replacing water with 1 % NaCl solution the test is transformed to an effective decision tool that is able to divide rocks with lower frost resistance from excellent rocks.
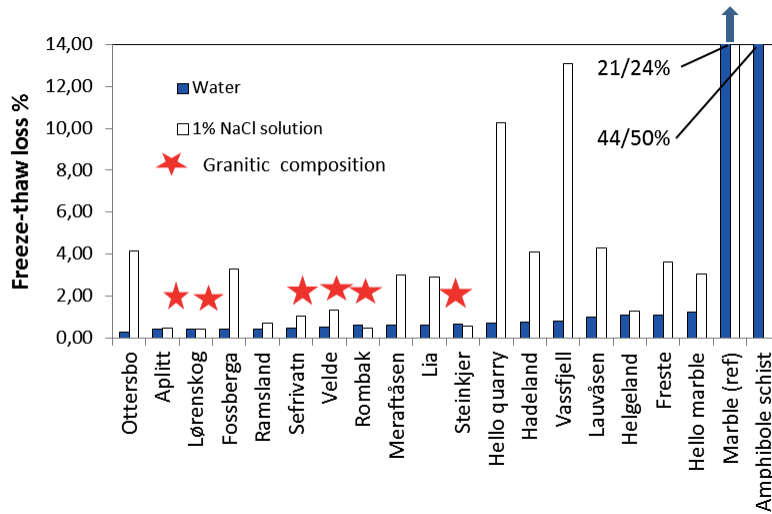
Figure 4.14   Freeze-thaw results for 20 different rock types (fraction 8/16 mm) after 150 freeze-thaw cycles. Carbonate rock and amphibole schist are samples with documented low frost resistance from field experience and used here for comparison.

Slope of the weathering curve.

Regarding the water procedure, the slope of the long term curve of crumbling for both strong and weak materials makes a significant change to a lower rate at around 20 - 30 cycles (Figure 4.15 and 4.17). This suggests that the test conclusion in terms of ranking can be different compared with the standardized 10 cycles test. For the strong materials, it has no consequences owing to the fact that the weathering rate is far below the Norwegian requirement. The situation is quite different for the NaCl procedure where the weathering rate is both higher and approximately linear throughout the test. However, the ranking of the materials (Figure 4.16) are not settled before after approximate 60 cycles.
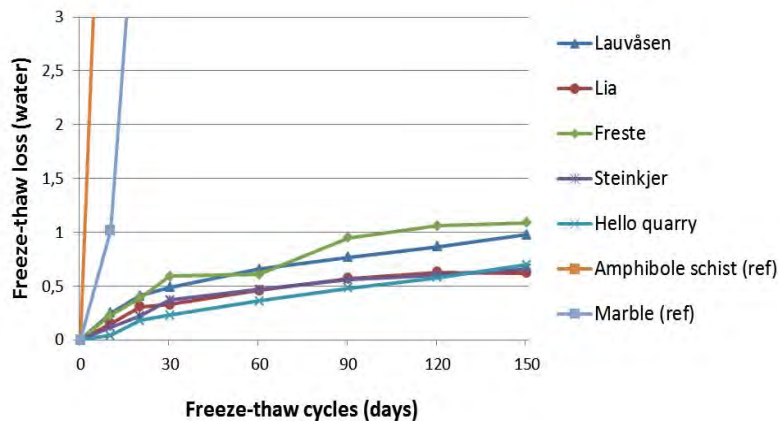
Figure 4.15   Example of long term recording of frost resistance of Norwegian rocks (water). Freeze-thaw loss in % of dry weight. Fraction 8/16 mm and 1 kg sample weight.

43
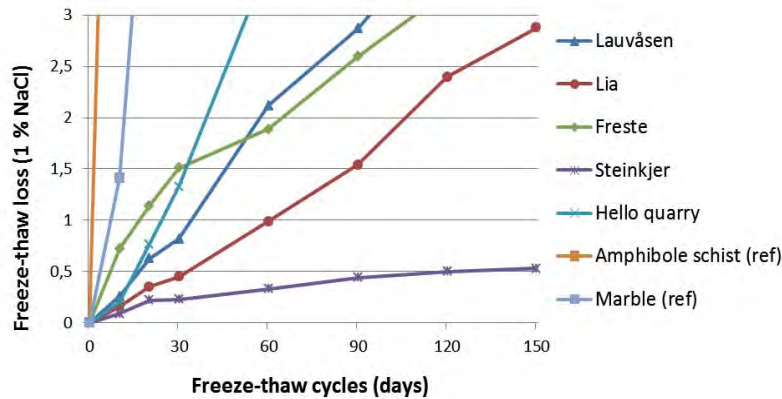
Figure 4.16   Example of long term recording of frost resistance in 1 % NaCl solution. Freeze-thaw loss in % of dry weight. Fraction 8/16 mm and 1 kg sample weight.
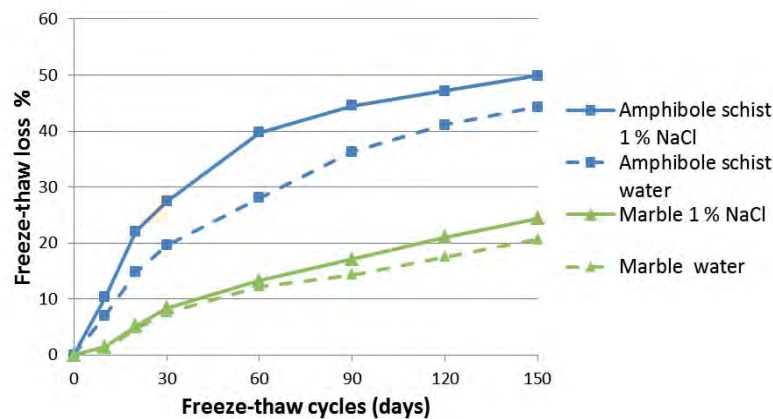
Figure 4.17   Long term weathering curves for two rocks with confirmed low frost resistance (the reference rocks from Beiarn, Nordland county).

Comparing the two tests, two interesting relations appear for the weak materials tested (Figure 4.17). Firstly, the NaCl procedure is still the most severe test, but the difference between them is small. Secondly, the degradation rate makes a change around 20–30 cycles which means that the measurement at 10 cycles cannot predict the amount of long term weathering. According to Norwegian requirements (1 % weight loss after 10 cycles) the marble would have barely passed even though it shows a significant frost weathering.

Impact from mineralogy on freeze-thaw resistance
The study of 20 rocks' freeze-thaw resistance (Figure 4.14 and Paper II) has some interesting results that coincide with the former comparison between LAA and Point Load test. Use of NaCl solution seems to be a significantly more hash procedure compared with water. All eighteen samples (reference samples not included) would have passed the Norwegian requirements to freeze-thaw resistance. Eight out of twenty different rock types are almost unaffected by the freeze-thaw cycling process. Most of them consisted of quartz and feldspar or classified as granite.

Some of them were identical with those samples which increased their strength when saturated with water (LAA test). Further eight samples exhibited a slight reaction on NaCl (only 3-4 % weight loss). A significant amount of weight loss was obtained for Hello quarry and Vassfjell with 42 % and 41 % content of amphibole respectively.

Finally, the two reference samples which consisted of carbonate rock and amphibole schist, demonstrated frost resistance complying with field experience. The latter consisted of 68 % amphibole. We can here observe a possible interesting trend regarding the content of amphibole: With 30 % amphibole, Lia obtained a slight reaction (3 % weight loss), Hello quarry and Vassfjell with about 40 % amphibole registered 10 % and 13 % weight loss respectively, and the reference rock with 68 % amphibole recorded 50 % weight loss. A suggestion to a conclusion is that the frost resistance decreases with increasing content of amphibole when the amount exceeds around 30 %.

4.1.5 Remaining mechanical strength after freeze-thaw test trial

Micro-Deval 10/14 mm

Most Norwegian rocks suitable for construction purposes do not show any or very small weathering caused by freeze-thaw processes, but do they maintain their mechanical strength after 150 freeze-thaw cycles? The histogram in Figure 4.18 contains the results from the micro-Deval tests and shows that most rocks kept their mechanical strength after the frost impact with 1 % NaCl. Only Fossberga and Lauvåsen (meta-greywacke), Meraftåsen (greenstone) and Hello (marble) did not maintain their strength. On the other hand, no rocks but one were affected from frost impact when tested with water (Hello marble). It is important to consider a NaCl test procedure when wear in a salt environment is a concern. Limited amount of relevant materials after the freeze test (original 2 kg of fraction 8/16 mm) resulted in a deviation from standard procedure. Only one parallel test could be performed instead of two and fraction used was 8/16 mm. However, the reference MD value was conducted according to standard procedure.
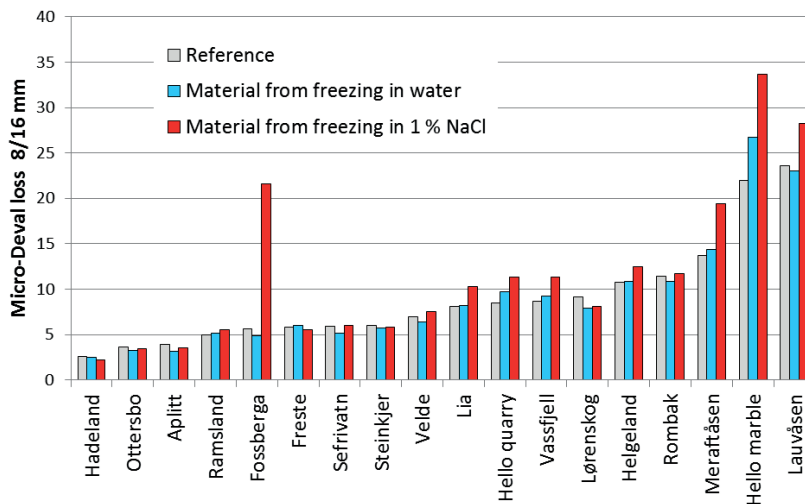
Figure 4.18   Micro-Deval test run on aggregates (8/16 mm) after subjected to 150 freeze-thaw cycles.

45

Los Angeles 31.5/50mm

It was impossible to run LAA test on material from the freeze-thaw test with 150 freezing cycles since the LAA test requires a test portion of 5 kg. As a substitute, new material of fraction 31.5/50 mm was subjected to 60 freeze-thaw cycles as an additional test and a possible reduction in mechanical strength due to freezing was controlled afterwards with the LAA test (dry state).. The results are shown in Figure 4.19.
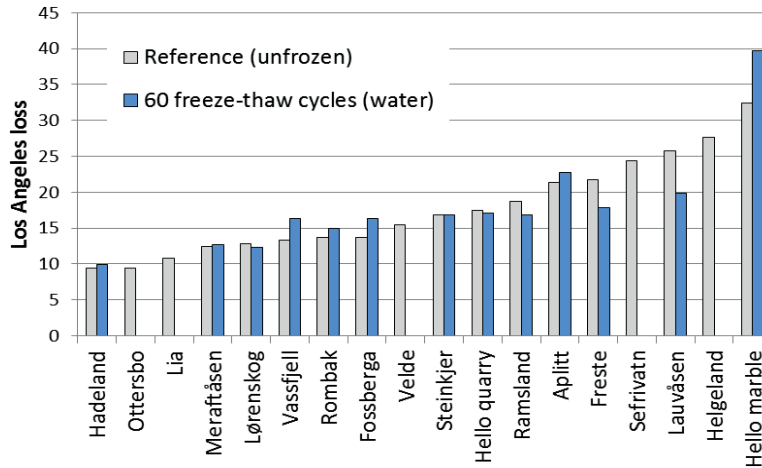
Figure 4.19   Los Angeles abrasion test run on aggregates (31.5/50 mm) after subjected to 60 freeze-thaw cycles.

The results are difficult to interpret. Some materials are unaffected, some have recovered strength (lower LAA values, Freste and Lauvåsen), and some (Vassfjell, Rombak and Fossberga) have possibly lost strength. Concerning the latter, the increase in LAA value is so small that it can represent only a natural variation. This emphasizes how important it is to know the coefficient of variation for each type of aggregate which was not documented in this study. The number of freezing cycles was limited to 60 (two months) due to lack of time. An increment to 150 cycles could have enhanced any weakening reaction and separated them clearly from those without any reaction. Freezing time was a question of capacity.

Figure 4.20   Thawing phase of the test. Test material was soaked in water during both freezing and thawing.

A modification of this freeze-thaw test would have speeded up the process. If the free water in the tray (Figure 4.20) had been removed before freezing, the capacity could have been doubled or even more. Another benefit is that this simulation of winter conditions (storage in water) is closer to the real situation in the railway track than without.

4.1.6 Relation between micro-Deval test and ballast field performance

The micro-Deval method is utilized to assess the hardness of ballast materials. Very little is known about which factors determine a rock's resistance to abrasion and to what extent this value correlates with ballast field performance. The Norwegian railway ballast specification requires that ballast materials shall meet the requirements according to both micro-Deval and Los Angeles abrasion test. But the reliability of the analyses has been questioned (Lynch 1978, Chrismer 1986). Studies in Canada three decades ago (Klassen et al. 1987) showed that the results of LAA tests correlated poorly with field performance. They observed that rocks often demonstrated a tradeoff between hardness and toughness where a material that performs well according to an abrasion test (Mill Abrasion) may fall apart in the LAA test, and vice versa. To handle this problem, they combined the two tests in the following equation as a measure of quality.

$$Abrasion\ Number = LAA\ value + 5 * MA$$

The equation says that the abrasion property (MA) is five times more important than the resistance to crushing (LAA) in terms of ranking ballast materials. The interesting question is if this experience can be transferred directly to the Nordic countries, and the answer is probably no. Norway has certainly similar climate but the range of rock types available for construction purposes are somewhat different, and the potential for rock weathering is much higher in for instance Canada (Rogers 2010).
Norwegian Railway Administration adopted the micro-Deval method in 2008 with the objective to avoid application of soft rocks as ballast material. It was assumed (but not documented) that rocks with high abrasion values would cause increased production of fines and contribute to more rapid degradation of track geometry during traffic loading. By means of a method study and a comprehensive documentation of textural and functional properties to about twenty rocks, this study has tried to investigate in what degree the results of micro-Deval tests correlate with ballast performance.

4.1.7 Influence of rocks' textural properties on micro-Deval value

The correlation between micro-Deval value and eight different texture properties are shown in Figure 4.21. The eight properties are mineral grain size, water absorption, specific density, micro-cracks, particle's angularity, particle's surface roughness, soft and hard minerals. It is essential to emphasize that the following results are based on a very narrow range of rock types characterized with crystalline rocks, mostly fine grained, non-foliated and contained with mostly hard minerals.

As seen in diagram (a) and (b), neither average mineral grain size nor water absorption appear to correlate with abrasion resistance (MD value). In diagram a) the MD values vary from 2 through 16 without any significant change in mineral grain size. Diagram c) shows that there is a slight but not strong correlation between the rock properties abrasion and specific density. The R^2 value is very low (0.15) but the two data points at the top can be regarded as outliers. Lauvåsen meta-greywacke and Hello marble contains 60 and 94 % soft minerals respectively and do not belong to the "hard rock group". R^2 without these two samples rises to 0.51. Increasing specific density means increasing amount of dark minerals (e.g. pyroxene and amphibole) in the rock. This can be interpreted as that resistance to abrasion decreases when the content of dark minerals increases.

47
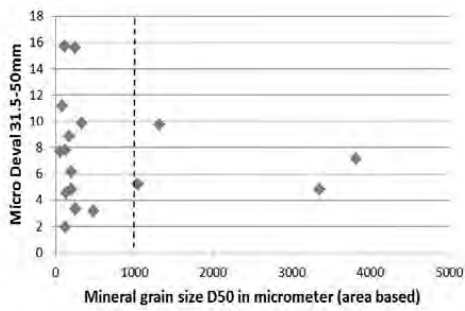
a). Mineral grain size
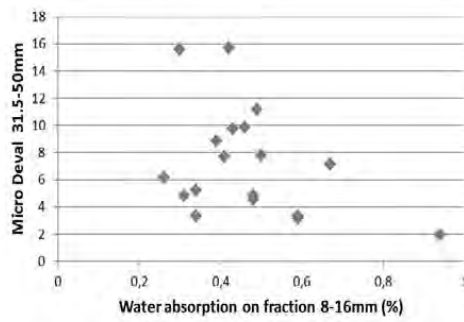
b). Water absorption
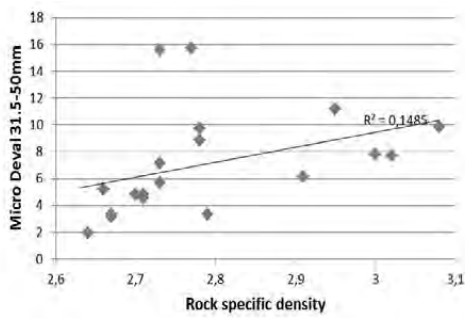
c). Specific density
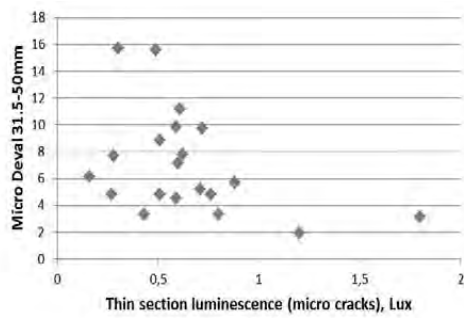
d). Micro-cracks (luminescence)
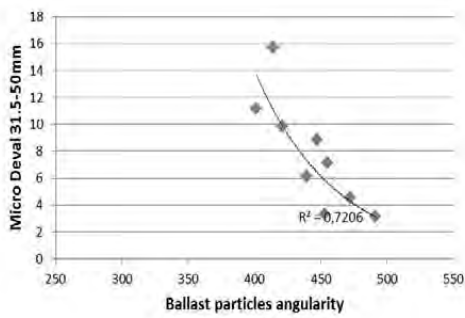
e). Angularity of ballast particles
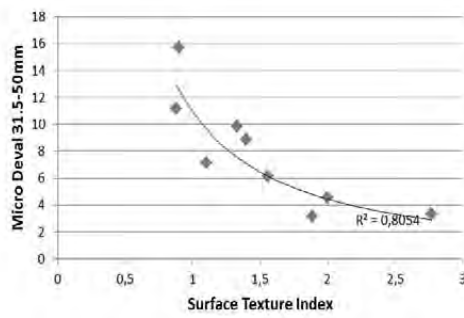
f). Particle surface roughness
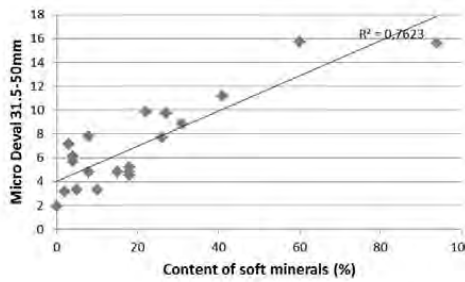
g). Soft minerals (mica, chlorite and carbonate)
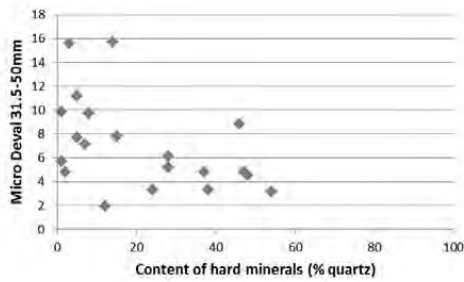
h). Content of quartz

Figure 4.21   Some rocks' texture properties that might affect the resistance to abrasion (micro-Deval value).

Micro-cracks make access channels for ingress of water into the aggregate (Nålsund et al. 2011) and are naturally linked to water absorption. It is natural to believe that the more cracks at the ballast particle surface the easier it is to break off micro pieces which contribute to an increasing MD value. But this is obviously not the situation as seen in diagram d). There is no correlation between content of micro-cracks and the MD value when the water absorption value is less than 1 %.

Particle angularity and surface texture seem to be two aspects of the same case as displayed in diagram e) and f). The terms are explained in Figure 2.12.
The range of angularity values vary with a factor of 1.25 from lowest to highest value, while the range of Surface Texture Index vary with a factor of 3. STI is therefore better to use than Angularity when correlations with other properties are concerned. An R^2 value of 0.80 suggests a rather strong correlation with abrasion resistance. This means that the surface roughness more than anything else governs the growth of MD value. But there is no explanation of which factors govern the growth of surface roughness.
Finally, diagram g) and h) show the effect of mineralogy. As can be seen in g), the content of soft minerals has a fair correlation with abrasion resistance, but it looks like the amount must exceed about 20 % before it has any influence on the strength. Quartz is known as the hardest rock-forming mineral we have, and diagram h) shows a poor correlation, but suggests that quartz might have a positive effect when the content exceeds approximately 20 %.

4.1.8 Effect of grading on ballast performance (Paper I)

Ballast breakage

Effect of grading on ballast breakage was only investigated on one type of rock, Steinkjer meta-sandstone, by means of triaxial testing. The micro-Deval value is very low (4.8 %) and an LAA value of 16.9 % (test fraction 31.5/50 mm for both) represents a medium strong ballast material compared with Norwegian requirements. Three different and uniformly graded grain size distribution curves were used as shown in Figure 3.1 and Table 4.2.

Table 4.2. Three different grading curves were used.

Grading	16/22.4 mm	22.4/31.5 mm	31.5/40 mm	40/50 mm	50/63 mm
Arema 4	25	40	35	-	-
E fine	-	25	50	25	-
E coarse	-	-	25	30	45

The triaxial testing simulated a maximum axle load of 250 kN and subjected the ballast sample to 4 million cyclic loadings divided into four equal sections. The ballast breakage was recorded after each section. This means fraction 0/16 for Arema 4, fraction 0/22.4 mm for E fine and fraction 0/31.5 mm for E coarse. Each grading was tested four times to reduce scattering in the results, to improve the measurements' accuracy. The procedure was supposed to simulate tamping as a repeated maintenance operation.

Two "groups" of breakage performance have been identified, rocks that increase their mechanical strength after each loading sequence (recovering strength due to repeated compaction) and those who do not show any change in mechanical strength. This phenomenon is discussed elsewhere (Figure 4.12). The findings show that ballast breakage decreases when the ballast's average grain size decreases. Arema 4 obtain less crushing than E coarse, but the differences are small.

The hypothesis is that the breakage is almost independent of grading for the strongest rocks but gets more pronounced for the weaker rocks. This is based on an investigation of Raymond (1977b) who tested different ballast gradings from uniformly to broadly graded (Figure 4.22). He wanted to see the effect of change in grading but the diagram also shows that the effect is more pronounced with mechanically weak materials.
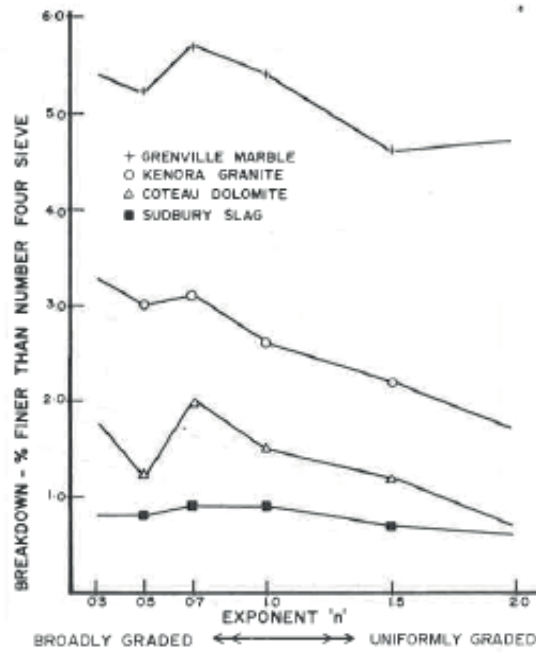
Figure 4.22   Variation in ballast breakage with gradation and with mechanical strength (Raymond 1977b). Number four sieve has 4.75 mm openings.

The ballast breakage is associated with the sample's bulk density and decreases with increasing bulk density, as shown in Figure 4.23. The measures are taken after each preconditioning (compaction in the steel mould) but before the cyclic loading sequence. The abnormal value of Ecoarse in step 2 was discussed in Paper I.
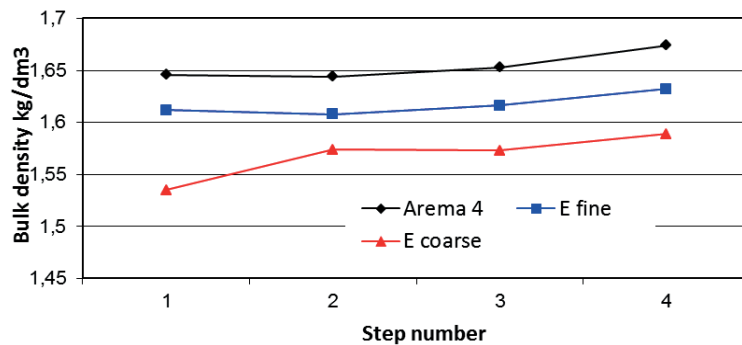
Figure 4.23   Change in specimens' bulk density from step 1 to step 4 (from cyclic triaxial testing in Paper I).

A possible conclusion can be that weak materials benefit most from an optimization of the grading curve towards finer average grain size if ballast breakage is concerned. More research needs to be done before we can throw light on this part of the ballast performance.

Vertical permanent strain in ballast layer

The effect of grading on vertical strain in ballast layer was only investigated on one type of rock, Steinkjer meta-sandstone, by means of cyclic triaxial loading. Accumulated permanent strain during each step of one million loadings and with three different gradings are shown in detail in Figure 4.24 and with average values in Figure 4.25. Maximum strain at the end of each loading sequence varies apparently randomly from sequence to sequence without showing any trend towards higher or lower values for maximum strain (Figure 4.24). This diagram shows the necessity of repeating the test four times to increase the accuracy of the measurements.
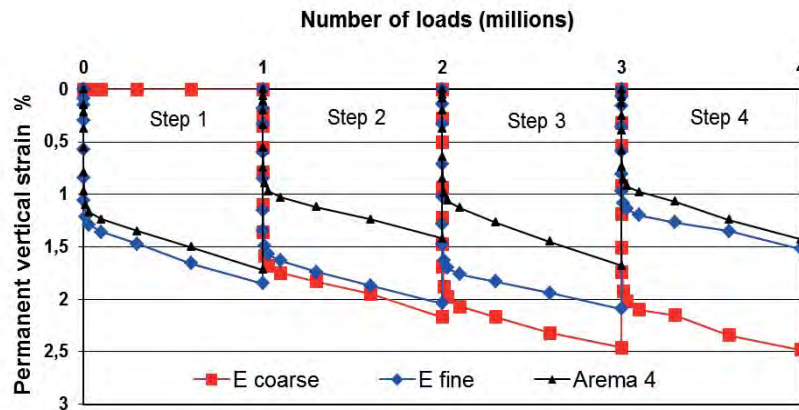
Figure 4.24   Vertical permanent strain against number of loads. Each of the three different gradings (Ecoarse, etc) was tested through four steps and totally subjected to 4 million load applications. Data from step 1 for grading Ecoarse was unintentionally not recorded.

The correlation between ballast gradation and permanent vertical strain is quite clear as displayed in Figure 4.25. The strain increases with increasing average grain size (or decreasing bulk density). The tested rock has a medium mechanical strength according to Norwegian ballast requirements. As suggested by Raymond (1977b) in Figure 4.22 rocks that are either stronger or weaker than Steinkjer meta-sandstone can behave in another way with less or more pronounced differences in permanent strain. This is not investigated in this study. The author knows of no such work on permanent strain in ballast layer.
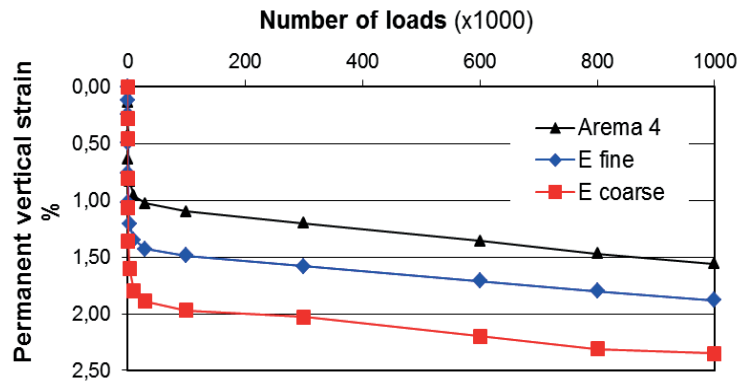
Figure 4.25. **Permanent vertical strain against number of loads. Each curve represents the average of four steps, totally 4 x 1 million loadings (average of three steps for grading Ecoarse).**

Resilient modulus of ballast layer

The correlation between ballast gradation and resilient modulus of ballast layer is mentioned in Chapter 4.1.1 and Figure 4.4.

4.1.9 Prediction of railway ballast performance from mechanical tests

Correlation between Los Angeles abrasion test and ballast breakage in triaxial and full scale model testing (Paper III)

Paper III aimed to describe how reliable the LAA test can range between strong and weak ballast materials in terms of in service performance. According to Hudec (1983) "*The LAA test has no difficulty in distinguishing between the superior quality material and the very poor material. They cannot, however, indicate with any certainty how the intermediate material will behave in service. LAA test has little relationship to aggregate requirements or performance. The results indicate, rather, how easily the material will crush in a ball mill*". The results displayed in Figure 4.26 correspond with Hudec's (1983) findings regarding the intermediate materials. The LAA$_{31.5/50 \text{ mm}}$ test (dry state) has for example given the materials Lørenskog, Meraftåsen, Rombak and Vassfjell similar assessment. This is in contrast to the rating given by the full scale model test which says that Lørenskog is three times more durable than Vassfjell (amount of crushed material: Lørenskog 0.44 %, Meraftåsen 0.78 %, Rombak 0.94 % and Vassfjell 1.22 %).
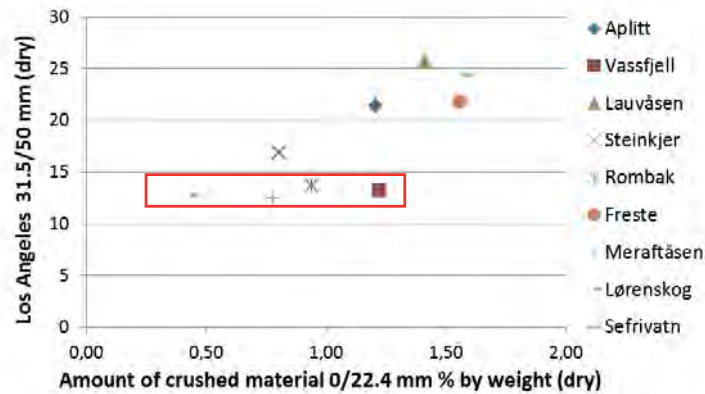
Figure 4.26   Total amount of crushed material from full scale model test (4x1 million loadings and dry state) related to mechanical strength (LAA dry). R^2 =0.64.

If we replace the results from LAA$_{31.5/50 \text{ mm}}$ dry with LAA$_{31.5/50 \text{ mm}}$ wet, the situation changes apparently in a positiv direction as shown in Figure 4.27 where Lørenskog is still the best and Vassfjell is number four according to LAA value. But this can be a random improvement. All the four materials mentioned got weaker (higher LAA values) by going from dry to wet state. If the four rocks had been of granitic composition, they would probably have achieved similar or lower LAA values (strength improvement). The conclusion is likely that the Los Angeles abrasion test does not distinguish intermediate ballast materials in a reliable way as implied by Hudec (1983).
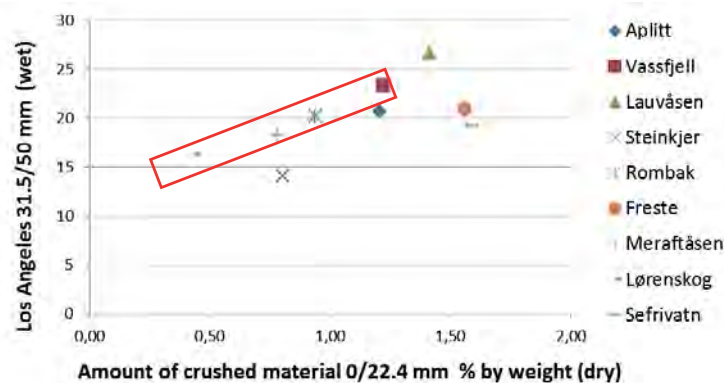
Figure 4.27   Total amount of crushed material from full scale model test (4x1 million loadings (dry state) related to mechanical strength (LAA$_{31.5/50 \text{ m}}$wet). R^2=0.41.

These two tests (triaxial and full scale) use different mechanisms to quantify the relative durability of an aggregate. It is supposed that the full scale model test simulates the field stresses in the ballast layer in the most correct way, and, therefore, gives the most reliable relative rating of ballast aggregates. The degradation process inside the ball mill is supposed to consist of both particle crushing from stroke (steel balls) and abrasion from contact between aggregate particles. In the full scale model test, the traffic loading applied stresses in railway ballast which were sufficient to cause ballast particle breakage. Any possible abrasion effect is supposed to be of secondary importance or absent. This may explain why these two tests do not correlate well.

Figure 4.28 shows a comparison between Los Angeles abrasion loss (31.5/50 mm) and total amount of crushed material fraction 0/22.4 mm from the triaxial testing (both dry state) of ballast aggregate. It was expected that increasing LAA values should result in increasing amount of ballast breakage (0/22.4 mm). This was only partly ashieved. The four points in the black frame represent almost equal amount of crushed material from the triaxial testing independent of the corresponding LAA values that vary from 13.3 % to 25.7 %. The fraction used is 31.5/50 mm. The diagram suggests that the correlation between the LAA value and the ballast breakage from cyclic triaxial testing is poor. A relation that probably disturbs the situation is that aggregates that recover mechanical strength due to repeated crushing (Freste and Sefrivatn) are mixed together with rock types that do not recover mechanical strength.
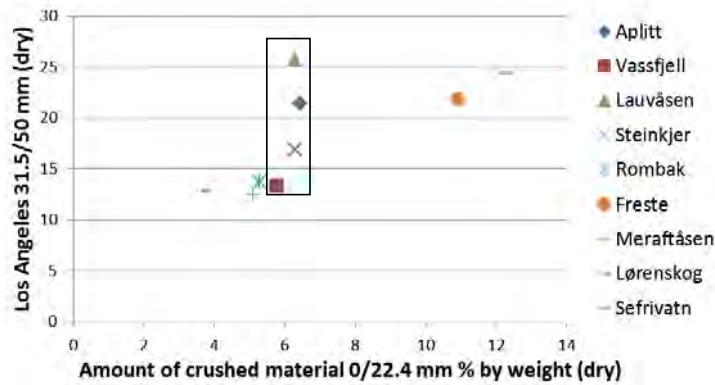
Figure 4.28   Total amount of crushed material from triaxial testing (4x1 million loadings) (dry state) related to mechanical strength (LAA$_{31.5/50 \text{ mm}}$dry). R^2=0.77.

If we replace the LAA values tied to fraction 31.5/50 mm with values from fraction 10/14 mm the correlation improves dramatically (Figure 4.29) from poor to very good if we ignore the "outlier" from Lørenskog. Why does this happen? A possible explanation is that abrasion contributes partly to the degradation under Los Angeles abrasion test on fraction 31.5/50 mm (Erichsen et al. 2011). The degradation under Los Angeles abrasion test on fraction 10/14 mm comes mainly from crushing similar with the degradation process under cyclic triaxial testing.
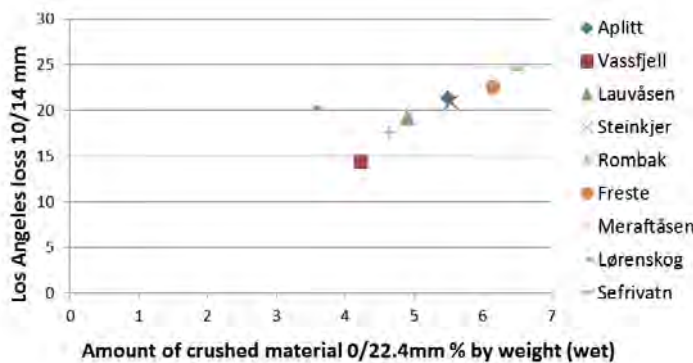
Figure 4.29   LAA values (10/14 mm dry) plotted against ballast breakage (0/22.4 mm) from triaxial tests performed in wet state (4 million loadings). R^2= 0.53, without Lørenskog 0.97.

Correlation between Los Angeles abrasion test and vertical permanent strain in ballast layer (Paper III)

It is reasonable to believe that ballast settlement and ballast breakage due to train loads are connected with each other. The stresses in railway ballast are sufficient to cause both significant strain and ballast particle breakage. The weaker the ballast is, the more crushing due to train traffic. The relation between LAA values and permanent vertical deformations in ballast layer due to train traffic   (triaxial test measurements) is shown in Figure 4.30. According to this investigation, it is evident that there is no correlation between ballast resistance to crushing and permanent vertical strain in the ballast layer.
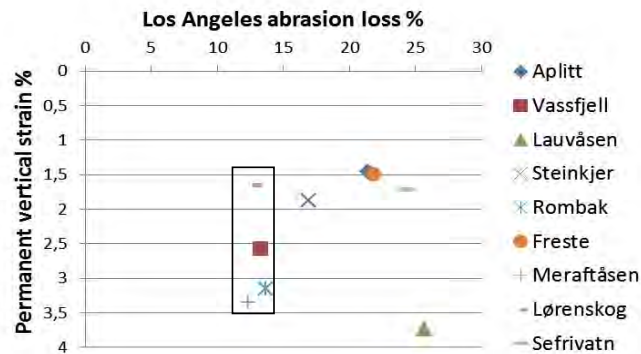
Figure 4.30   Variation of permanent vertical strain in ballast layer from triaxial cyclic loading with dry LAA value (31.5/50 mm)

Five aggregates with little strain between 1.5 and 2.0 have great variation in LAA values from 13 to 24. On the other hand the same five have very low MD values between 6.6 and 3.4. The four LAA values within the frame are all close to 13, but the MD values increases gradually with increasing permanent vertical strain (from 6.0 (Lørenskog) to 11.2 (Meraftåsen)). This suggests that the strain is governed by abrasion properties and not by crushing properties. See also Figure 4.32.

The lack of correlation between LAA and permanent vertical strain in this study does not say that the expected correlation does not exist. It is possible that the correlation can be revealed under altered test conditions. The pre-compaction of the triaxial test specimen before the cyclic loading sequence, was probably just too tough for the material. Most of the settlement and more than half of the total crushing appeared during this part of the work. However, it was unsuitable to transfer most of the strain (and particle breakage) from the compaction steel mould by reducing the compacting energy and over to the triaxial cell due to limited measuring range of the LVDT equipment.

Correlation between micro-Deval test and ballast breakage in triaxial and full scale model testing

A very interesting question is to what extent the micro-Deval result has any influence on ballast degradation, or does it have any relevance at all to ballast performance prediction? Figure 4.31 shows the results of ballast breakage from cyclic loading of triaxial testing and full scale model testing of nine different ballast materials. None of the two test trials can reveal any correlation between micro-Deval results and ballast breakage due to traffic loading.

The two "outliers" in the triaxial diagram, Freste monzonite with 11 % degradation and Sefrivatn granitic gneiss with 13 % degradation, stands out from the other regarding resistance to fragmentation.
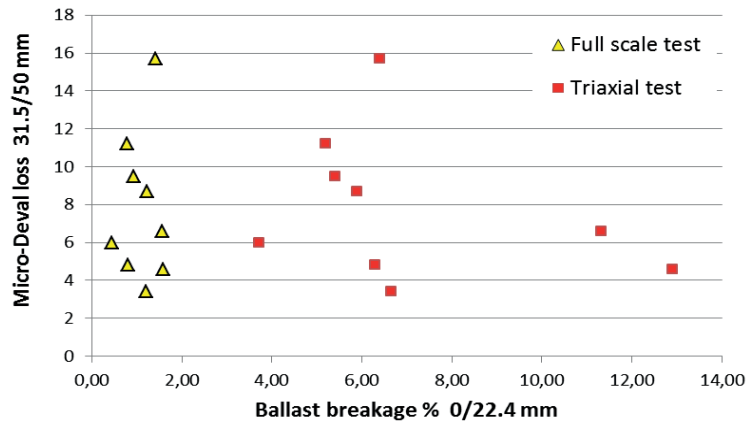
Figure 4.31   Correlation between micro-Deval and ballast breakage after both triaxial testing (dry/red) and after full scale model test (dry/yellow).

They had the highest LAA value but recovered strength after each pre-compaction (crushing) of test sample as opposed to the other rock materials.

The amount of ballast breakage in the two diagrams is quite different. The range between lowest and highest value constitutes a factor of three to four in both diagrams, but the degradation after the triaxial tests is about five to six times greater compared with the full scale tests. This is not due to different impact from the loading in the two trial test series. They both subjected the test materials to the same maximum axle load of 25 tons. A strong pre-compaction by means of a vibrating weight of 30 kg for 30 seconds of the triaxial test specimen is probably the main reason for the differences in degradation (Paper III). The compaction energy should be significantly reduced so that the ballast breakage is on the same level as that from full scale test/ field performance.

Correlation between micro-Deval and vertical permanent strain in ballast layer
The relation between micro-Deval values and permanent vertical deformations in ballast layer due to train traffic (i.e. triaxial test measurements) is shown in Figure 4.32. The correlation is fair with a regression coefficient on 0.83.
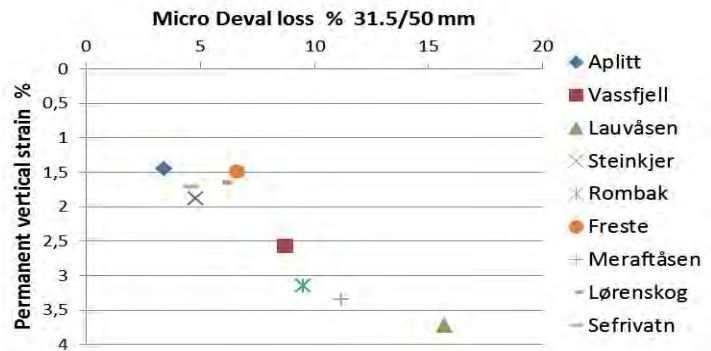
Figure 4.32   Permanent vertical strain from triaxial tests (dry) compared with micro-Deval results. Regression coefficient R^2 is 0.83. R^2 is 0.88 without Freste which can be an outlier (medium grained)

With reference to Figure 4.32, an exceptional correlation (in a petrological context) occurs in Figure 4.33 when we replace the parameter micro-Deval value with the rocks' content of soft minerals (i.e. total amount of mica, chlorite and carbonate).The data set has a regression coefficient of 0.95. In this context Steinkjer meta-sandstone can act as an "outlier". It contains 18 % fine grained mica (muscovite) with random orientation and perform better than expected. The hypothesis is that mica affects neither the mechanical strength nor the ballast performance when the mica has a random orientation within certain limitations. It is also possible that the XRD test has overestimated the volume of mica due to the mica's foliated shape. On the other hand, Rombak mica schist/granitic gneiss constitute 27 % mica (biotite and muscovite) but do not perform "abnormal". With high degree of probability and based on these data, it is possible to predict the ballast's relatively permanent vertical strain when the content of soft minerals is known through petrographic examination.
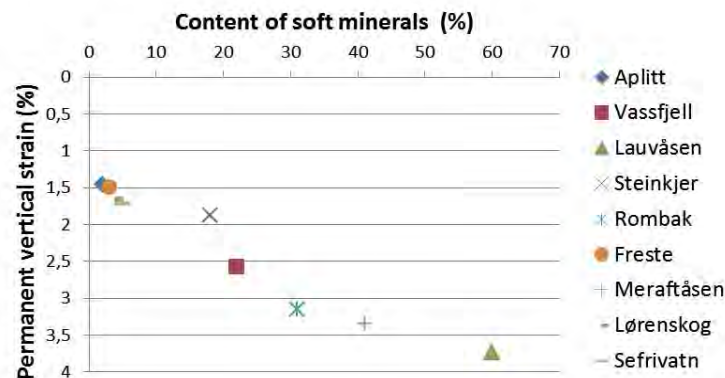
Figure 4.33 Permanent vertical strain from triaxial tests (dry) compared with rocks' content of soft minerals (mica, chlorite and carbonate). Regression coefficient (R^2) is 0.95.

Another aspect of the diagram in Figure 4.33 is that it gives information on the question of whether the rocks' resistance to fragmentation has any influence on track settlement due to train traffic. It is rational to imagine that ballast breakage is closely related to ballast settlement, the more fragmentation, the more vertical deformation. The data points start with 1.5 % strain which is governed by the sample preparation (Paper III). Three out of four samples with least strain are the same three materials that have the least resistance to fragmentation. (Aplitt with LAA 21, Freste with LAA 21 and Sefrivatn with LAA 24; Norwegian limitation for approved says less than 24). On the other hand Lørenskog (LAA 12) and Lauvåsen (LAA 25) performed as expected. This suggests that the rocks' content of soft minerals is the main factor affecting permanent strain, and that resistance to fragmentation has a secondary role.

4.1.10 *Correlation between triaxial test and full scale rail track model test with respect to ballast breakage*

In this study, ballast materials' resistance to crushing have been measured in three different ways: Los Angeles abrasion test, triaxial cyclic loading test, and full scale rail track model test. The first simulates the impact from train traffic by turning stones against both each other and against steel balls in a tumbling drum. The stress condition in the drum is far from the real situation in situ. The correlation between Los Angeles abrasion and the other two test methods is discussed in Chapter 4.1.9. The last two methods simulate the in service stress conditions under the railway sleepers in a more reliable way. The full scale test is supposed to provide the most reliable measurements

because applied vertical stiffness and confining pressure are close to the field conditions. The correlation between the two tests (both dry state) is shown in Figure 4.34.
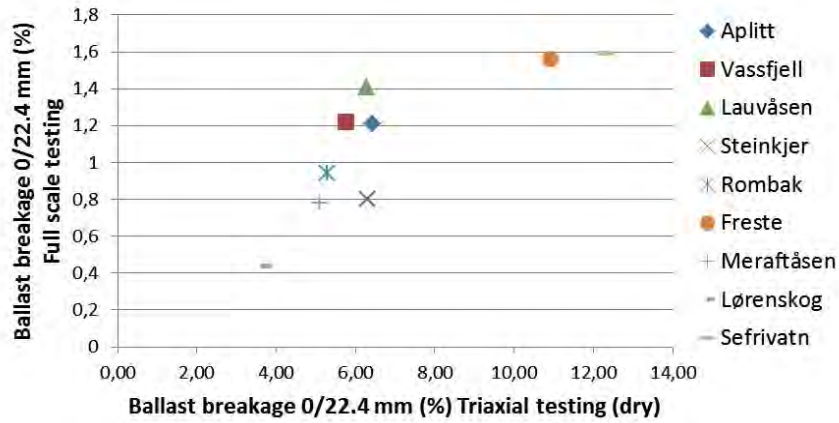
Figure 4.34   Comparison between cyclic triaxial testing and full scale rail track model testing in terms of ballast breakage (0/22.4 mm). Original grading 22.4/63 mm.

The full scale test divide better between good and poor aggregates in terms of larger range from 0.4 to 1.6 %. The range from the triaxial testing is narrower and goes from 3.8 to 6.4 % if we ignore Freste and Sefrivatn. They may act as a separate group (recover strength due to repeated crushing). This can again be a consequence of the strong pre-compaction of the triaxial test specimens. This phenomenon is absent as for the full scale test. The diagram indicates that the full scale test gives results that we can rely on.

It should be more interesting to measure the amount of fines than fraction 0/22.4 mm because they contribute more to water capillarity and rataining of water than coarser materials. When we allow the amount of fines represents the ballast breakage from the triaxial and full scale testing as displayed in Figure 4.35, it appears that the triaxial test perform better than the full scale test (larger range of data). This is opposite result compared with the information in Figure 4.34. On the other hand, the full scale test is able to sort out Lauvåsen (high amount of fines).
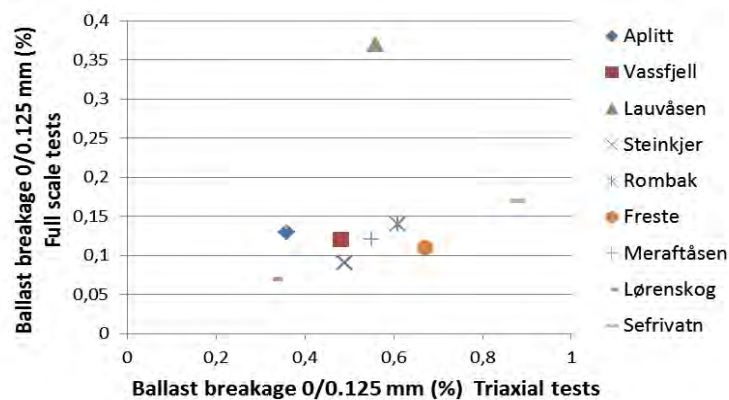
Figure 4.35   Comparison between triaxial testing and full scale model railway track test in terms of ballast breakage (0/0.125 mm). Original grading 22.4/63 mm.

4.1.11 Production of fines

The ballast's resistance to crushing is expressed by the Los Angeles abrasion value which is based on sieving of the degraded material on sieve 1.6 mm after testing. The material below 1.6 mm is not a matter. Production of fines is a core question regarding ballast performance. A study carried out by West et al. (1970) on evaluating of tests for degradation of base course aggregates (roads), compared production of fines against Los Angeles abrasion loss and found that rocks with similar LAA values produced different amount of fines as marked with a rectangle in the Figure 4.36. The variation is less pronounced for the stronger rocks than for weaker rocks.
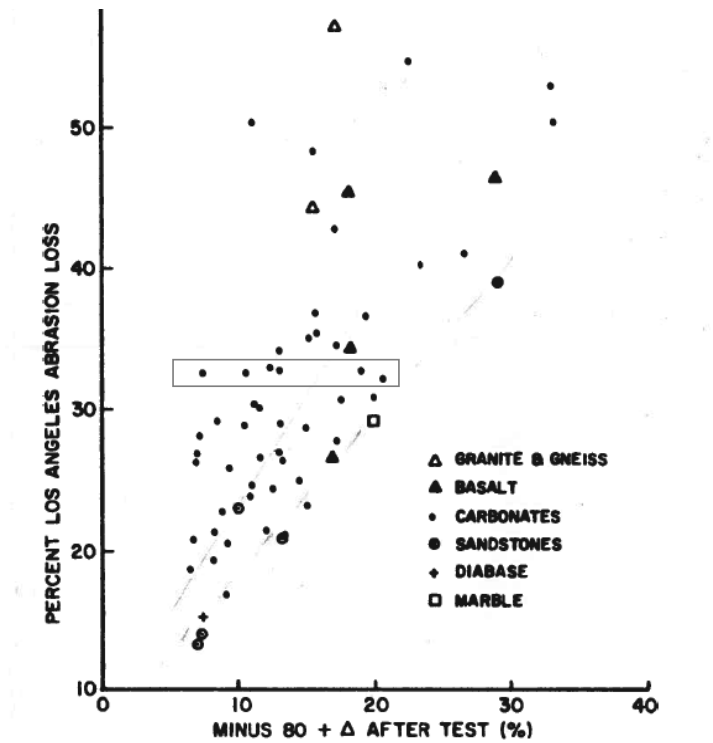
Figure 4.36   Production of fines versus Los Angeles abrasion loss for several rock types. Sieved on sieve no. 80 (0.178 mm). Modified after West et al. 1970.

In a study conducted by Bjerga (2011) the same relation was investigated with 10 rocks including some of the rocks from this study (Vassfjell, Lørenskog, Rombak, Freste and Sefrivatn).The fine fraction studied was 0/0.02 mm. Her findings in Figure 4.37 agreed with the results from West et al. (1970).

59
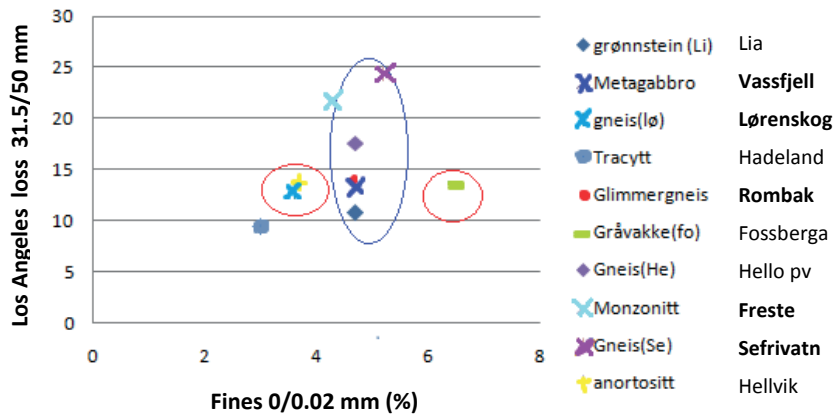
Figure 4.37   Production of fines during Los Angeles abrasion tests versus LAA value for several rock types. Tested fraction was 31.5/50 mm. Modified after Bjerga (2011).

Fossberga greywacke (red circle right) produced almost twice as much fines than Lørenskog gneiss (red arrow left) despite of that they are similar in mechanical strength. On the other side, Sefrivatn gneiss (top oval) produced about equal amount of fines compared with Lia greenstone (bottom oval) even though Sefrivatn had more than twice as high Los Angeles abrasion loss. The question is if this means that Sefrivatn is equal to Lia regarding ballast performance? One answer is that Lia is still the best, but Sefrivatn can perform better than its reputation.

Measuring the production of fines should be a part of the laboratory work when ballast materials are to be selected because it can increase the reliability. It remains to control that the degradation product from the Los Angeles abrasion test is able to predict the production of fines from ballast in service. Fines with diameter less than 0.063 mm contribute more to the frost susceptibility than fines with diameter less than 0.125 mm but the latter is easier and faster to document in the laboratory. Figure 4.38 suggests that there is a fair correlation between the amount of fines with diameter less than 0.125 mm and the amount of fines with diameter less than 0.040 mm.
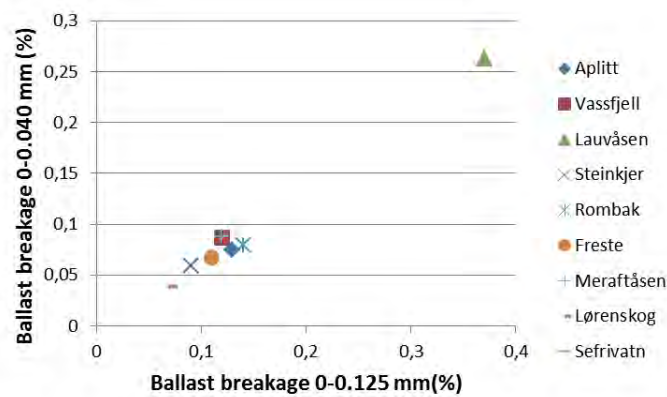
Figure 4.38   Ballast breakage from full scale railway track model test. Original grading 22.4/63 mm. Correlation between fraction 0/0.040 mm and 0/0.125 mm. $R^2 = 0.985$

4.2   Supplementary findings

4.2.1 Relationship between the intrinsic properties of rock material and the ballast's mechanical strength (Paper II and IV)

Water absorption

Measurements of water absorption were performed on the basis of the hypothesis that absorption correlates with both resistance to crushing and frost resistance. Micro-cracks filled with water were supposed to give a hydraulic burst effect when subjected to a blow from another aggregate particle or steel ball (Los Angeles abrasion machine) with crack extension as result. Micro-cracks with water that freezes were also supposed to give a burst effect with subsequent crack extension. As a consequence, water absorption measurements could be able to predict aggregates' mechanical strength.

Figure 4.39 shows the correlation between water absorption and the content of micro-cracks expressed as luminescence (explained in Paper II). It is likely to believe that micro-cracks make access channels for ingress of water into the aggregate. The amount increases with increasing occurrence of cracks.
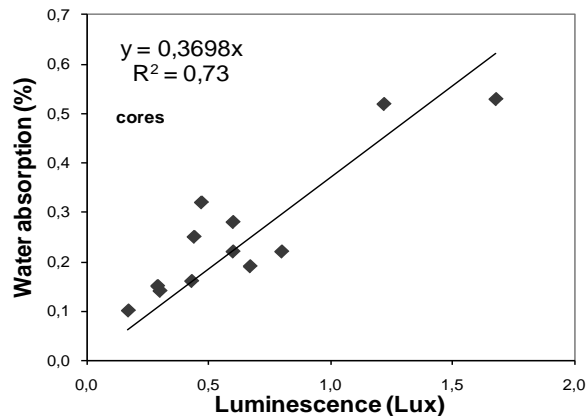
Figure 4.39   A graphic plot between luminescence and water absorption from drilled cores.

 Water absorption tests on fraction 8/16 mm, 40/50 mm and drilled cores revealed that the result also depends on type of fraction. The amount of absorbed water decreases with increasing particle size (reduced surface area pr. weight unit). Average of measurements on 11 samples gave the following result: fraction 8/16 mm 0.51 % water absorption, fraction 40/50 mm 0.31 % and drilled cores 0.27 %. With reference to regression analysis (R^2), the accuracy increased from 0.42 for fraction 8/16 mm via 0.53 (40/50 mm) to 0.73 for drilled cores (Figure 4.39). In general, measurements on drilled cores showed that necessary time to complete water saturation varied a lot. Some samples completed absorption at 24 hours, some at 5 to 7 days, and two extreme samples did not complete at 10 months (Figures 4.40 and 4.41). These results are valid for aggregates with water absorption less than about 1 % (based on 8/16 mm fraction)
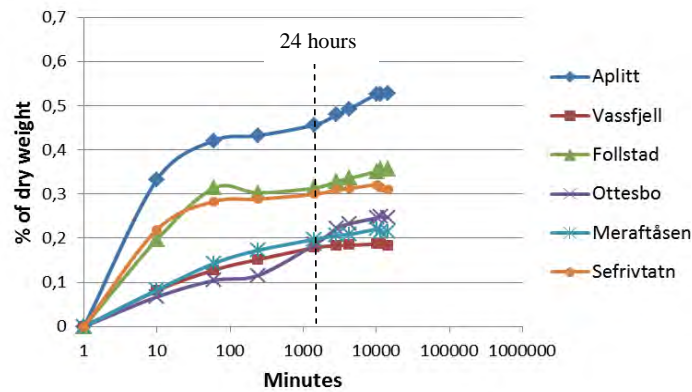
Figure 4.40   Absorption of water on drilled cores. No vacuum used. Test finished after 10 days (Bjerga 2011).
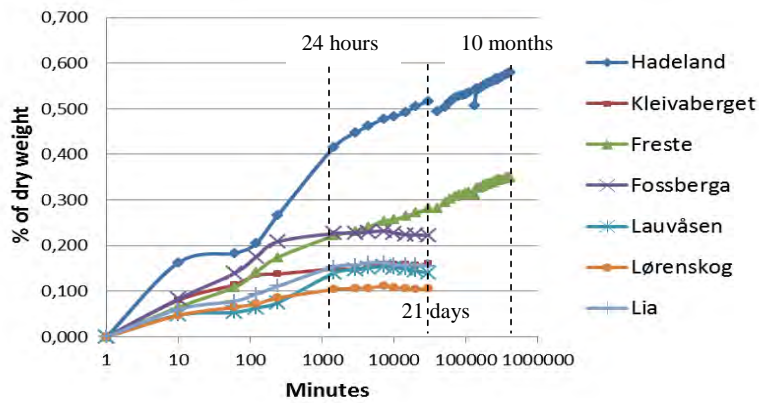
Figure 4.41   Absorption of water on drilled cores. No vacuum used.

According to Figure 4.42, no correlation seemed to occur between mechanical strength and rocks' absorption value. Several samples with absorption around 0.1-0.2 % have corresponding LAA values from 9 to 26 %. This is inconsistent with the hypothesis mentioned above. Neither does the micro-Deval test shows any correlation with absorption as displayed in Figure 4.21.b. This suggests that other intrinsic properties than absorption or the amount of micro-cracks affect the mechanical strength when the absorption value is less than about 0.5 % for drilled cores or less than approximately 1 % for fraction 8/16 mm.
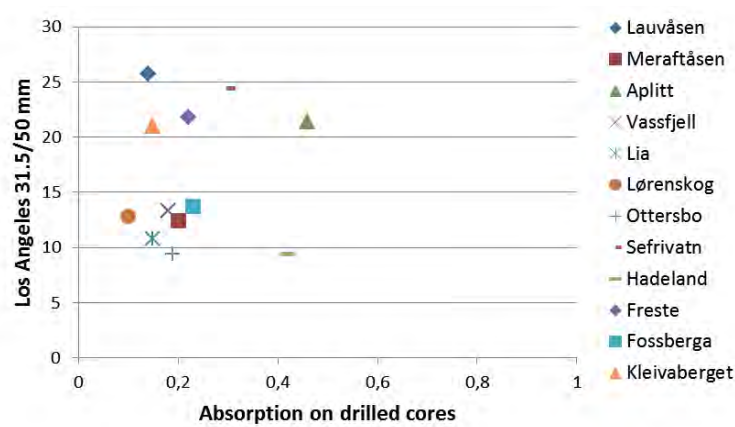
Figure 4.42 Correlation between dry Los Angeles abrasion loss $_{31.5/50\,m}$ test and water absorption (24h) for drilled cores.

Frost resistance

In this study frost resistance seems to be marginally affected by the rocks' intrinsic properties provided that the absorption is less than 0.5 % (fraction 40/50 mm). The only one that displayed a negative effect was where there was an increase in the content of the mineral amphibole (more than 30 % is suggested) which gave rise to a minor reduction in frost resistance when subjected to salt water (Figure 4.14) but still approved according to Norwegian requirements. On the other hand, rocks composed of almost entirely of the minerals quartz and feldspar ("granitic composition") were generally almost completely unaffected by frost impact after 150 freeze-thaw cycles.

Mineral content

To quantify any relationship between mineral composition and rocks' mechanical strength was not a topic in this study. But one correlation was accidently encountered. It appears that content of soft minerals affects the results from the micro-Deval test, but the amount should be higher than 20 % before any correlation occurs (Figure 4.21g).

Micro-cracks

It is reasonable to believe that incidence of micro-cracks should influence rocks' mechanical strength. A micro crack represents a weak point in a particle and an increasing appearance of micro-cracks should decrease the strength (e.g. resistance to crushing). This study showed that micro-cracks within certain limits do not affect either resistance to crushing or resistance to abrasion. The Los Angeles abrasion loss for both fraction 10/14 mm (dry) and 31.5/50 mm (dry) did not correlate with luminescence (Paper IV). Wet Los Angeles abrasion test exerts hydraulic splitting forces on the ballast particles, but neither this effect was visible (Figure 4.43). Replacing luminescence with absorption on fraction 40/50 mm did not improve the correlation (not displayed). The lack of correlation between micro-cracks and micro-Deval (resistance to abrasion) is shown in Figure 4.21b)
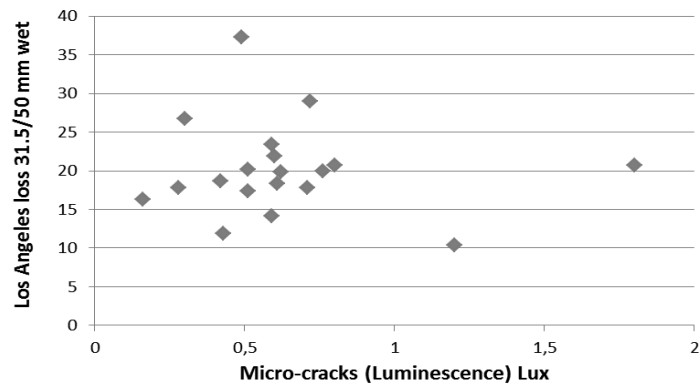
Figure 4.43 Influence of luminescense (micro-cracks) on mechanical strength (Los Angeles abrasion loss, wet state).

Average mineral grain size

Several investigations have shown that the grain size is an important parameter for understanding differences in mechanical properties of rock types of the same composition (e.g., Lounsbery and West (1965) on limestone, Onodera and Asoka-Kumara (1980) on granite, Ballivy and Dayre (1984) on limestone, Singh (1988) on greywacke, Liu et al. (2005) on granite and Åkesson et al. (2001) on granite and granodiorite. They all observed that decreasing mineral grain size increases both the resistance to fragmentation and abrasion. Kazi and Al-Mansour (1980) came to the same conclusion despite their investigation included 14 different types of igneous rocks of a wide variety. It should be pointed out that it appears as if this conclusion is valid for both crystalline and sedimentary non-foliated rocks despite quite different origin. Brattli (1992) investigated mafic rocks and found that the impact from mineral grain size overruled the effect from all other parameters when the average mineral grain diameter was about 1 mm or less. However, contrary conclusions exist. Haraldsson (1984), found no significant difference in mechanical strength properties between fine- and coarse-grained basalts.

The rock samples in this study make up a wide variety of igneous rocks, metamorphic rocks and consolidated/metamorphosed sedimentary rocks. This means that many of the samples contain very fine mineral grains to varying degrees. The most conventional way to express mean grain size is investigation of thin sections with optical microscopy using one-dimensional measurements along a line of traverse (number of grain boundaries per length unit e.g. 30 mm (Chayes 1956) or individual recording of each grain (frequency) respectively) expressed with arithmetic or median values. It is believed that this technique would overestimate the significance of the finest mineral grains regarding mechanical strength (Figure 4.44). One coarse grain is more important (in a negative way owing to the fact that coarser grains introduce longer micro-cracks) for the strength than a fine one and needs to be recognized as more influential.
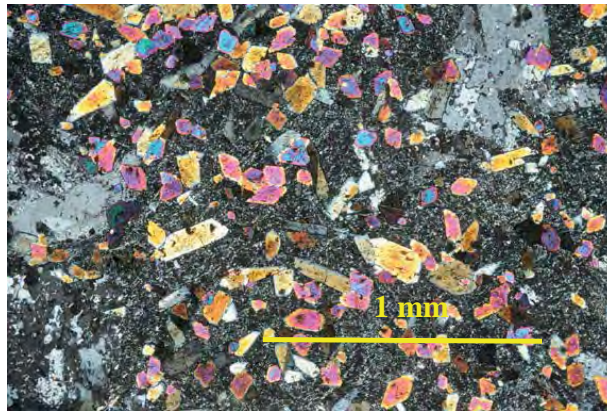
Figure 4.44   Micro image from thin section of a very fine grained greenstone (Meraftåsen 08115-2B) in X-polarised light.

Thus it was necessary to create a new technique to enhance the influence of coarse grains at the sacrifice of smaller grains by making a new grain size distribution curve, similar to the conventional sieving or grading curve for aggregate characteristics, where each fraction is measured by weight and not by the total number of grains (Paper IV). For converting thin section data to their sieve equivalents, the approach that each grain's cross-section area displayed in thin section was equal to a circle area calculated on the basis of each grain's measured "diameter" was used. The cumulative grain size distribution curve could now be drawn by summing up every mineral grain's area within each fraction (Figure 4.45). The point D_{50} on the curve was used to represent the sample's average grain size. The dimension means that 50 % of the area in the thin section consists of mineral grains with diameter greater than 49 micro meter.
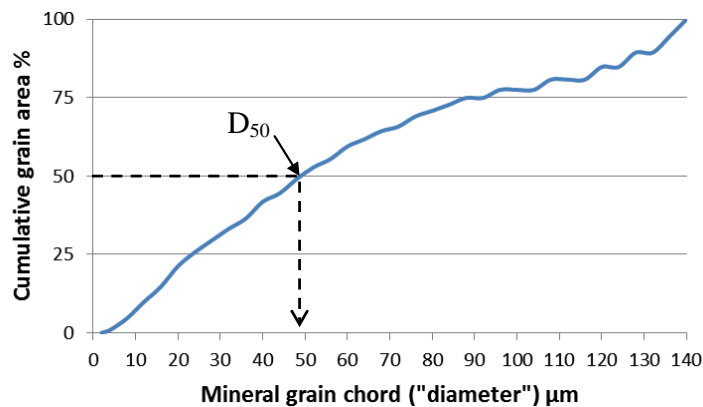
Figure 4.45   An instance of cumulative mineral grain size distribution curve based on calculated mineral grain area (Greenstone, Meraftåsen quarry). The curve is technically comparable with that of sieving of aggregates. D_{50} is about 49 micro meter.

This technique enables the correlation of mechanical strength with "average" mineral grain size where the largest mineral grains are most important. The result is shown in Figure 4.46. Despite most of the samples in the diagram belonging to fine grained rocks, the corresponding LAA values vary from 9 to 25 and the conclusion is that this study did not find any correlation between

strength and mineral grain size. We did not get any improved relationship when D_{50} was replaced by frequency based average mineral grain size (Paper IV).
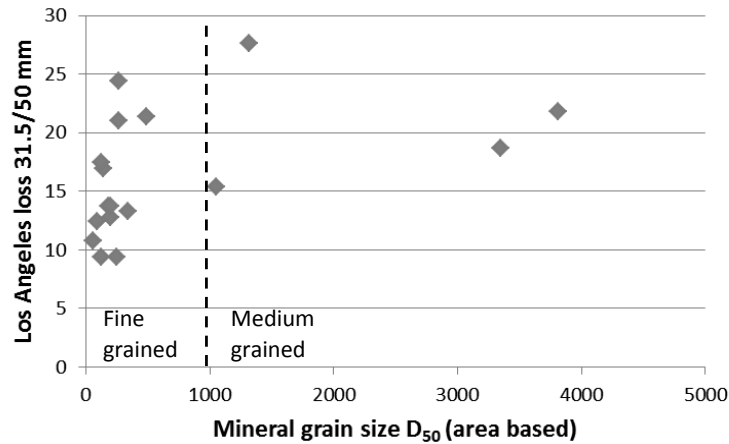
Figure 4.46   The significance of variation in average mineral grain size D_{50} on Los Angeles abrasion loss (mechanical strength).

This does not imply that there is no correlation. It rather implies that measuring mineral grain size suitable for this use is very difficult and that the topic rock's mechanical strength is quit complex. Many of the intrinsic properties that can influence the result are difficult to quantify and can be time consuming (e.g. (1) the mineral grain size, (2) mineral grain size distribution (single graded or well graded), (3) shape or grain boundary relations (more or less complex perimeter e.g. suturing), (4) spatial orientation (foliation) of mineral grains, (5) configuration of mineral grains, (6) mineral distribution (even or uneven E-modulus), (7) the amount of micro-cracks, (8) mineral deformation and (9) degree of alteration (e.g. sericite in feldspar)).

Mineral grain size distribution

Another of the properties mentioned in the paragraph above (2) was also investigated. This concerns whether the mineral grain size distribution curve has any influence on mechanical strength or not (even graded or broadly graded which means the slope of the curve). The symbol D_{50} makes it possible to quantify the incline of the grading curve (Paper IV). Johansson (2011) demonstrated that uneven graded granitoid rocks obtained poorer results from the mechanical analyses (Los Angeles abrasion and micro-Deval) than even grained ones. This study did not find any association between mineral grain size distribution curve and mechanical strength. A weakness of this investigation was that the selection of samples was not adapted to this comparison and the range of slopes was probably too narrow to get any correlation.

4.2.2 The effect of pre-treatment of test samples on ballast's mechanical strength.

Standard procedure requires air dried test material. This study wanted to investigate if pre-moistening of test samples would have any negative effect on the resistance to wear according to the knowledge that water usually reduces rocks' mechanical strength (Kessler et al. 1940). Micro-Deval is already a wet test and pre-moistening could improve the method further.

Micro-Deval test

<u>Water saturation of test samples in advance</u>

A survey on pre-moistening of test samples performed by Woodside and Woodward (1998) on three different rock types did not find any effect of this additional handling of the aggregates. The correlation between wet and soaked micro-Deval loss was very good as shown in Figure 4.47.
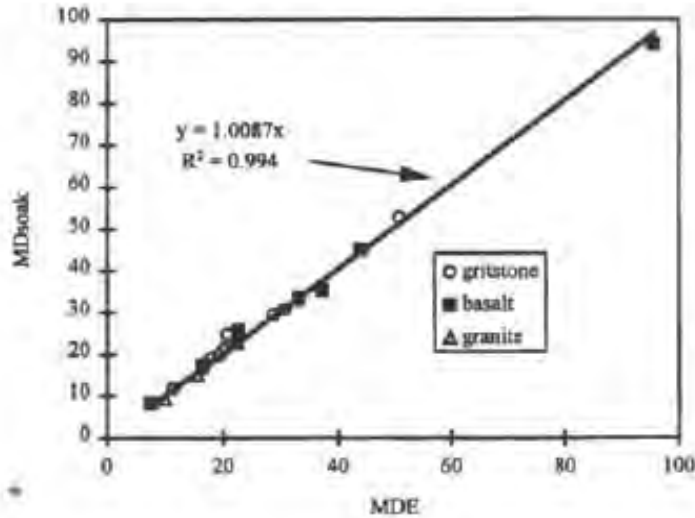
Figure 4.47 Correlation between wet and soaked micro-Deval loss (Woodside and Woodward 1998).

The micro-Deval results with pre-moistening of test samples from this study are displayed in Figure 4.48. None of the 18 samples can reveal any significant decrease in abrasion resistance. Five samples like Sefrivatn, Hello quarry, Vassfjell, Meraftåsen and Lauvåsen showed a slight increase in MD value but this is probably within normal variation. This means that pre-moistening of test sample does not have any influence on mechanical strength. The result is limited to the investigated rocks and rock types.

<u>Saturation of test sample with salt water in advance</u>

This study replaced pure water with salt solution (1 % NaCl) due to the fact that a greater part of the Norwegian Nordland Line runs along the coast and is subjected to salty rain during stormy weather. As shown in Figure 4.48 neither did salt water have any effect on abrasion resistance. There is no difference in sensibility between the strongest and the weakest rocks.
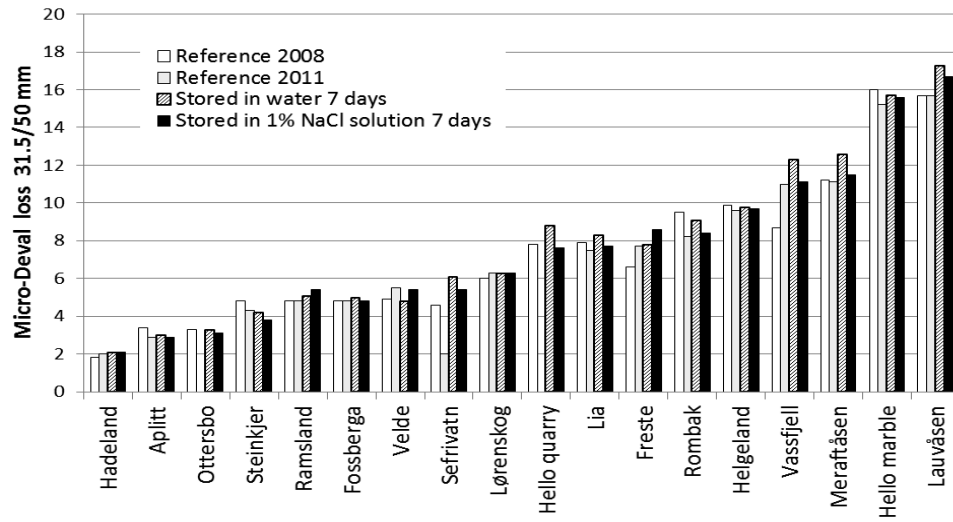
Figure 4.48   The effect from pre-treatment of test samples on micro-Deval values (fraction 31.5/50 mm).

5.   CONCLUSIONS

Conclusions that can be drawn from this research are:

Mineral grain size and mechanical strength

- A new and simple technique for determination of average mineral grain size (D_{50}) derived from a grain size distribution curve similar to a sieving curve is demonstrated.

- The conventional average mineral grain size ("diameter") based on frequency did not show any correlation with LAA loss (resistance to crushing) neither with $LAA_{10-14mm}$ nor $LAA_{31.5-50mm}$.

- The conventional average grain size (chord length) based on frequency did not show any correlation with micro-Deval$_{31.5-50mm}$.

- The average mineral grain size D_{50} derived from the "sieving curve" did not show any correlation with neither LAA nor micro-Deval, independent of the test fraction.

- Contrary to the literature review findings, a change from dry to wet triaxial testing procedure did not reduce the mechanical strength of ballast materials.

- No correlation was found between the slope of the grading curve (Cu) and $LAA_{10-14mm}$ loss.

Correlations between laboratory tests

- There is a fair correlation between the Los Angeles abrasion test and the Point Load test under wet condition testing.

What affects the micro-Deval value?

- Particle angularity, surface texture index (particle surface roughness) and the amount of soft minerals have a pronounced effect on the micro-Deval value.
  - The resistance to abrasion increases (lower MD-value) with increasing angularity, increasing Surface Texture Index and decreasing content of soft minerals. A slight relationship may occur between the micro-Deval value and the rock's specific density. No correlation was observed for mineral grain size (D_{50}), water absorption, amount of micro-cracks and content of hard minerals (% quartz).

Freeze-thaw resistance and frost effects on mechanical strength

- Comparing average luminescence with freeze-thaw loss and water absorption with freeze-thaw loss, no correlation could be found for railway ballast with water absorption less than 1 % (measured on 8/16 mm fraction). However, when the water absorption is higher than approximately 1 %, correlation between water absorption and freeze-thaw loss might occur, but more testing is needed to confirm this.

- The mineralogy is affecting the freeze-thaw resistance, e.g. aggregate with high amount of quartz and feldspar is likely to be more resistant than aggregate consisting of high amount of amphibole.

- Norwegian rocks suitable for construction purposes show generally high resistance to frost impact.

- The rest material after the freeze-thaw test (fraction 8/16 mm and 150 cycles) performed with water did not show any reduction in abrasion resistance when subjected to the micro-Deval$_{8/16 \text{ mm}}$ test. The rest material after the freeze-thaw test (150 cycles) performed with 1 % NaCl showed nearly the same result regarding abrasion. However, this series demonstrated that some of the weaker rock types were affected by the frost impact.

- The rest material after the freeze-thaw test (fraction 31.5/50 mm and 60 cycles) performed with water did not show any reduction in resistance to crushing when subjected to the Los Angeles abrasion test.

Effect of water and sodium-chloride (NaCl) on mechanical strength

- Many rocks lost mechanical strength when they were tested under wet conditions (Los Angeles abrasion test and Point Load test). On the other hand, some rocks mainly composed of quartz and feldspar achieved higher mechanical strength.

- The ballast breakage during cyclic triaxial testing was not affected by change in the procedure from dry to wet condition.

- Use of 1 % NaCl solution had no effect on rocks' micro-Deval$_{31.5/50 \text{ mm}}$ value even though the materials were stored in the NaCl solution for 7 days.

Effect of mineralogy on mechanical strength and ballast performance

- Some relations between ballast performance and mineralogy have been found:
Rocks with a high total content of the minerals quartz and feldspar (40–50 %) showed the greatest frost resistance (almost no weathering at all), did not lose mechanical strength when they were humidified, and did not change the elastic properties when they were soaked in water and subjected to cyclic loading. A high content of the mineral amphibole, i.e. approximately more than 40 %, gave the opposite results: the frost resistance was weakened, the mechanical strength under wet conditions could be greatly reduced, and the resilient modulus could be reduced with about 10 % when tested wet.
- The total content of soft minerals correlated well with the ballast layer's permanent vertical strain. The higher the content of soft minerals, the larger the strain.

Resilient modulus

- Ballast' resilient modulus, measured on a medium strong meta-sandstone, increased with increasing average particle size (D_{50}), but the differences were small.

- The ballast's resilient modulus increased with increasing specific density.

- The modulus decreased with about 10 % when the ballast was stored in water.

Laboratory tests vs "field" measurements.

- Dry Los Angeles Abrasion$_{31.5-50\text{mm}}$ (LAA) results correlated fairly well with cumulative wet triaxial test breakage (0-22.4 mm). An increase in regression coefficient from 0.83 to 0.97 was obtained when LAA$_{31.5-50}$ was replaced with LAA$_{10-14\text{mm}}$. This suggests that LAA$_{10-14\text{mm}}$ can be a more suitable test for assessing ballast durability than LAA$_{31.5-50\text{mm.}}$

- The correlation between the full scale model test and LAA$_{31.5-50\text{mm}}$ dry state was poor. Consequently, the LAA test did not predict ballast degradation in a reliable way, assuming that the full scale model test simulated the field condition taking properly into account applied rail track stresses. Replacing LAA$_{31.5-50\text{mm}}$ with LAA$_{10-14\text{mm}}$ had no improving effect.

- A fair correlation was obtained between the full scale model test and $LAA_{31.5-50mm}$ wet state.

Permanent vertical deformation
- A change in particle grain size distribution to a denser grading (reduced D_{50}) will lower the permanent axial deformation. The grading Arema 4 obtained 33% less deformation than grading Ecoarse.

- Micro-Deval values correlated well with the ballast's permanent strain under cyclic triaxial loading. Decreasing micro-Deval values gave reduced permanent strain. This correlation is probably caused by the rocks' surface roughness (Surface texture Index).

- Los Angeles abrasion value did not show any correlation with permanent axial strain from cyclic triaxial loading.

Ballast breakage
- Change in ballast grading by increasing average particle size D_{50} resulted in increasing ballast breakage.

- With reference to the triaxial test, seven out of totally nine rock samples did not change their resistance to fragmentation during impact from repeated compaction, both in dry and wet state.

- Two rock samples improved their resistance to crushing during impact from repeated compaction as a consequence of repeated crushing.

- Micro-Deval values did not correlate well with the amount of ballast breakage by triaxial testing. Hence, in this study, abrasion seemed to be less important or had no effect on ballast degradation for fine grained rocks.

Water absorption
- Average luminescence (amount of micro-cracks) has been compared with water absorption. Best correlation was obtained from drilled cores with a correlation coefficient (R^2) on 0.73.

Micro-cracks
- The amount of luminescence (micro-cracks) did not correlate with $LAA_{10-14mm}$ loss.

- Lack of correlation between luminescence and freeze-thaw loss and other mechanical tests suggests that micro-cracks are not important for the freeze-thaw processes and the mechanical properties.

- Micro-cracks are surprisingly abundant and common in Norwegian railway ballast, and 5 types of micro-cracking have been identified and classified, namely 1) inter granular, 2) intra granular, 3) trans granular (or "long" micro-cracks), 4) massive-porosity and 5) isolated holes or cracks.

- A method to measure amount of micro-cracks using luminescence measurements in fluorescent impregnated thin sections has been developed and tested on 71 thin sections from 22 quarries. The method uses inexpensive equipment and can be performed relatively quickly. Results have been given as average luminescence values.

- The lack of correlation between luminescence (micro-cracks) and $LAA_{10\text{-}14mm}$ loss (resistance to crushing) can indicate that micro-cracks have minor influence on mechanical strength when fine grained rocks are concerned.

6.   FIELDS OF APPLICATION

6.1   Taylor ballast

This study has shown that a lot of means can be performed to affect ballast and track performance like ballast breakage, ballast or track settlement, track stiffness and rail buckling. Cause and effect can be seen in Figure 6.1.
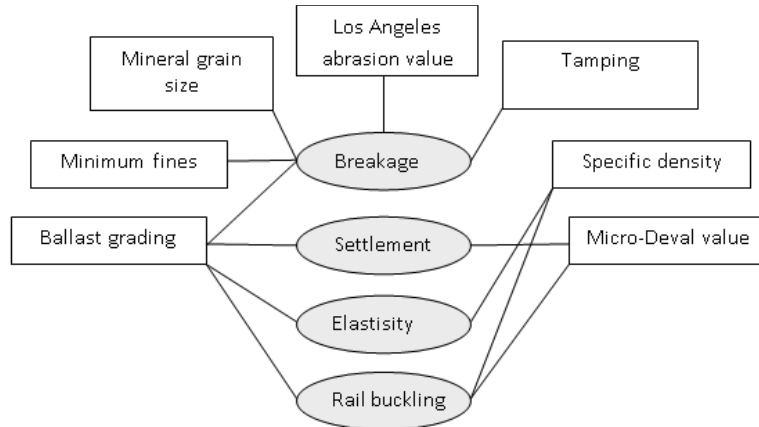
Figure 6.1. Impact from different variables on ballast breakage, track settlement, track stiffness and rail buckling

It is almost possible to tailor not only the ballast but also the track according to construction requirements for the achievement of best possible performance.

6.1.1 How to reduce ballast degradation?

The degradation of ballast can be lowered by
  a) using a finer grading (reduced D_{50}),
  b) choosing a ballast with as low production of fines as possible if there are options,
  c) avoiding coarse grained rocks,
  d) always using the ballast that has the lowest Los Angeles abrasion value if there are options and
  e) not using tamping more than absolutely necessary.

6.1.2 How to get the tamping to last longer?

The effect of tamping can last longer if we can reduce the settlement in the ballast layer by
  a) using a finer grading (reduced D_{50}) and
  b) choosing a ballast with a low micro-Deval value.

The effect of these measures is explained below:
Permanent vertical deformation results displayed in Figure 4.24 and Figure 4.25 provide information regarding future maintenance costs for new railway tracks. It makes it possible to optimize the ballast grading in such a way that the rail alignment after tamping operation (Figure 6.2) will last longer.
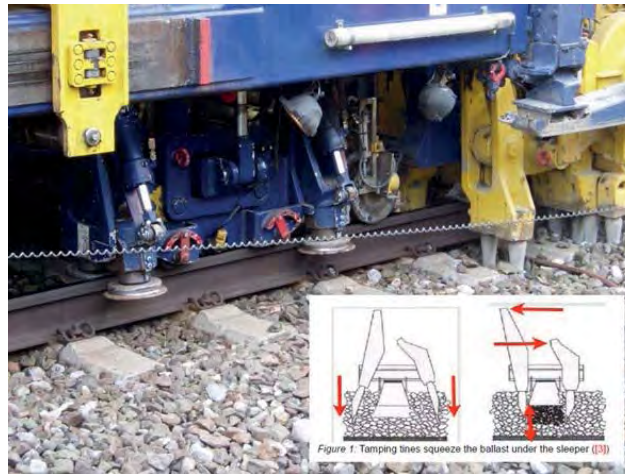
Figure 6.2   Maintenance of track alignment by tamping: 1) lifting track, 2) penetrating tines and 3) squeezing ballast (Selig and Waters 1994).

Shenton (1975) has shown that compacted ballast more or less will return to previous track level after tamping including some traffic in normal running lines. Consequently, the new vertical profile will look like the old one from before tamping after a year in service, and has negligible long-run effect on the alignment quality. However, the tamping effect gradually gets better if the track lift given by tamper exceeds about 20 mm (Figure 6.3). The settlement can be reduced and partly replaced by a permanent track lift by use of a finer grading, even though the tamping lift is less than 20 mm. The effect can further be improved if we in addition choose a ballast material with the right micro-Deval value (the relationship between permanent ballast settlement and both micro-Deval value and the content of soft minerals is discussed in Chapter 4.1.9 and Figure 4.32.).
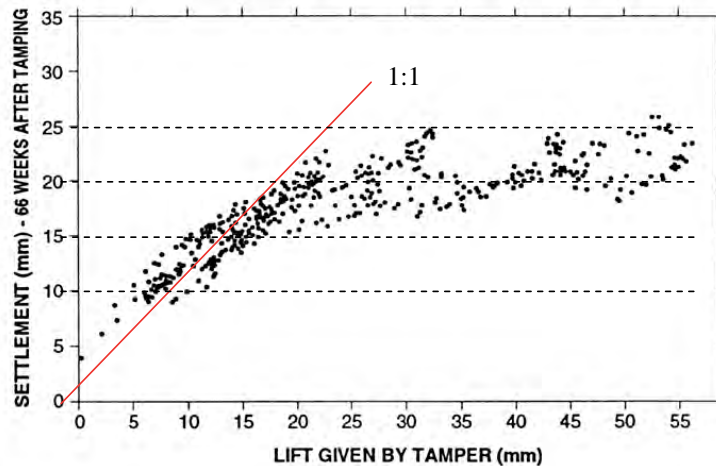
Figure 6.3   Measurement of sleeper settlements 66 weeks after tamping as a function of tamping lift (modified after Selig and Waters 1994).

Many Norwegian railway lines suffer economically due to tamping work with minimal long-term effect. The time between each tamping will shorten and this will result, as a consequence, in an

accidental and negative increase in ballast breakage. Optimization of ballast gradation can partly increase the positive effect of tamping and save maintenance work. But the real size of the amount is not investigated in this study.

6.1.3 How to build railway with desired stiffness?

Following factors are influencing the ballast layers resilient modulus
   a. the grading kurve of the ballast material (4.1.1)
   b. the specific density of the ballast (4.1.1)

The resilient modulus increases both with increasing average particle size (D_{50}) and increasing specific density. This is also valid for subballast materials (see below)

The stiffness of the track affects both the annual maintenance costs (tamping and alignment operations) and driving costs (enrgy dissipated in the track) (Lopez Pita et al.(2004). With reference to the high speed line between Paris and Lyon, Lopez Pita et al. (2004) showed that a high-speed track has an economical optimum value of the vertical stiffness (Figure 6.4).
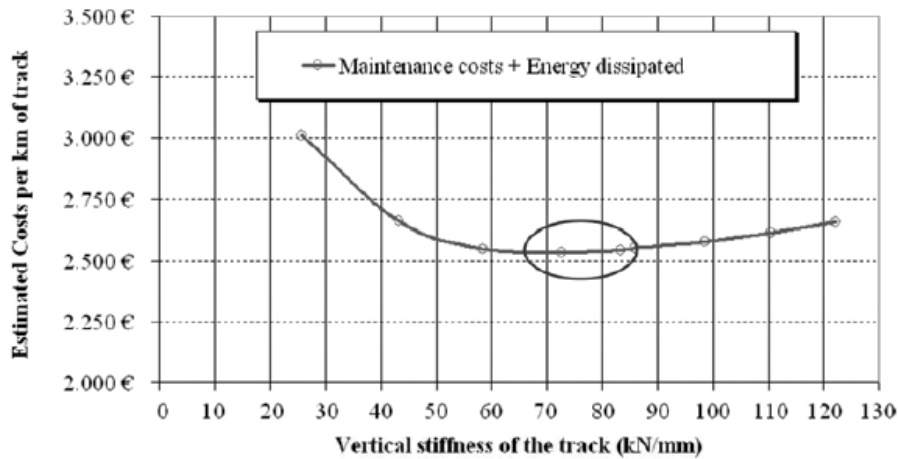
Figure 6.4   Relationship between track stiffness and total costs (Lopez Pita et al. 2004)

The railway line owner can benefit from building new railway lines with vertical stiffness close to the optimum value. This can be done by choosing ballast materials with suitable grading and suitable density. The knowledge is linked to tests with the ballast gradation 22.4/63 mm. Is it also valid for coarser materials used in the subballast layer?
A field investigation (Nålsund 1989) from higway construction suggested that it may have a more general validity. The road structure in this case was buildt with a subballast layer and a frost protection layer overlaying subgrade of glacial clay (Figure 6.5).
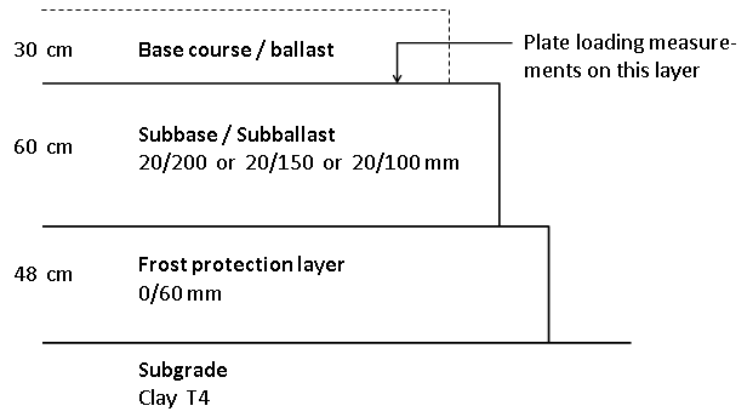
Figure 6.5   Vertical cross section of the design of Highway E6 between Trondheim and Stjørdal.

Due to access to different quarries, road sections of subballast were filled with materials from different rock types and different gradings. To control the required level of compaction, a plate-loading test was used and the processed data for the road stiffness modulus are shown in Figure 6.6.
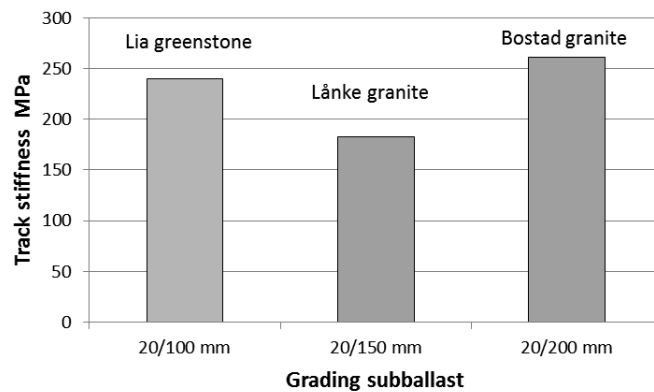
Figure 6.6   Calculated values of the road stiffness modulus based on deflection measurements from the construction of Highway E6 between Trondheim and Stjørdal. Use of different fractions and different rock types as subballast material caused different road stiffness. (Nålsund 1989).

The diagram in Figure 6.6 displays E-values valid for the construction as a hole and not for a single layer. The two different rocks in the subballast layer have specific density about 3.02 for Lia greenstone and about 2.65 for Bostad granite. According to the diagram in Figure 4.2 Lia is expected to get a higher modulus than Bostad due to higher specific density which also is in accordance with the data in Figure 6.6. The diagram suggests firstly that the stiffness of the construction increases when the fraction range increases from 20/100 mm to 20/200 mm (increasing D_{50}), and secondly that resilient modulus increases with increasing specific density (Lia greenstone). These findings correspond with results in this study, but now linked to coarser materials employed as subballast material.

6.1.4 How to increase the track's lateral resistance?

Rail buckling constitutes a potential danger to train services when the rail's neutral-temperature is beyond recommended value. The track's lateral resistance can be improved in different ways to prevent rail buckling such as:

    a. rising the weight of rail (kg/m),
    b. utilizing different design of sleepers such as increased area of end cross section,
    c. replacing existing shoulder ballast with one with higher specific density if possible,
    d. performing compaction of the shoulder ballast, and
    e. increasing ballast shoulder's width and height.

These factors do not give great contributions alone to increased lateral resistance, but all together can contribute significantly. The latter (e) is shown in Figure 6.7 including expected magnitude of a possible improvement of the lateral resistance.
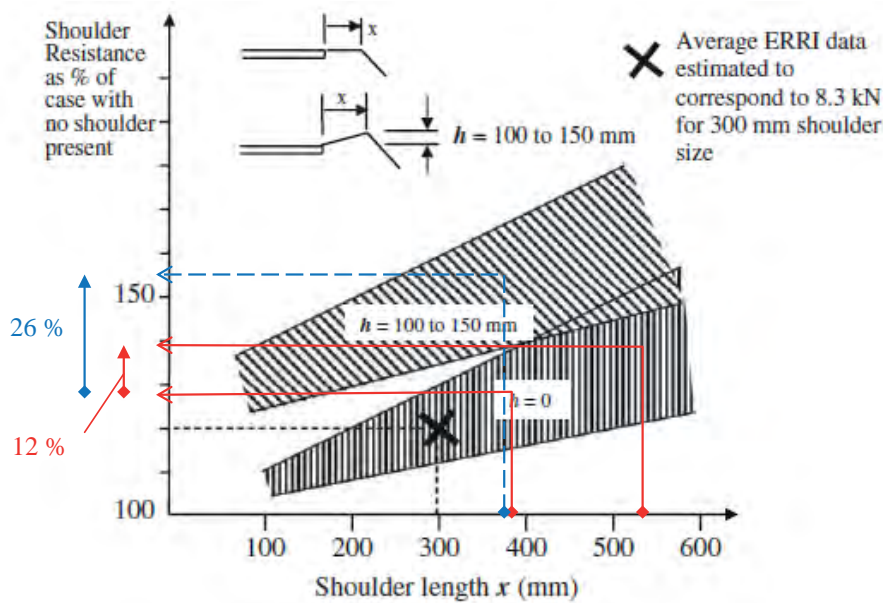
Figure 6.7   Track's lateral resistance depending on the design of the ballast shoulder (modified after ERRI 1995).

This sketch from ERRI (1995) estimates the track's lateral resistance depending on different shape of the ballast shoulder. It shows that it is more effective to increase the height of the shoulder from zero to 15 cm than expanding the shoulder width with 15 cm from 40 to 55 cm. The resistance increased twice as much, from 12 % to 26 %.

Particle surface texture
The final mean which has not been documented previously is to use a type of ballast that has the largest particle surface roughness expressed by the Surface Texture Index, see Figure 2.12. It is supposed that increasing roughness leads to increasing friction between particles and, consequently, larger lateral resistance. Few laboratories in the world offer this analysis, but due to the correlation between Surface Texture Index and the micro-Deval value (Figure 4.21 f), the latter gives largely a good estimation of the Index or surface roughness. The higher Index the

better. This means that ballast materials with low micro-Deval values probably give the highest shoulder ballast resistance. It remains to investigate how large the increase in the lateral resistance can be achieved by means of an increase in internal friction.

6.2   Ballast specification improvements

This study does not end in proposals to improve ballast specifications or requirements, but suggests that further work on the following three tasks has the potential to lead to improvements.

1. On the basis that ballast breakage is very important for maintenance costs, one should evaluate the use of finer materials (decreased D_{50}) than allowed today, and at the same time consider making the grading envelope narrower. This may also have a positive effect on longer lasting tamping.

2. Production of fines is a core question regarding ballast performance. Additional works on rocks' potential to produce fines can be fruitful. This study suggests that it is possible to make a further quality differentiation among rocks that are supposed to have similar mechanical strength according to the Los Angeles abrasion test, but a relevant test method is needed.

3. To identify rocks that recover mechanical strength as a consequence of repeated crushing can be the third task to improve specifications, but a relevant test method is needed.

6.3   Concept of railway ballast life model

Clifton et al. (1987) introduced a ballast life model which took into account the ballast's mechanical strength (abrasion number), ballast grading and cumulative tons of rail traffic (Figure 6.8). Thus it is possible to calculate the ballast's service life time. However, this thesis suggests that number of tampings is more important than cumulative tons of rail traffic. An alternative model should considerate the ballast crushing experience from the triaxial and full scale rail track model testing (Figure 4.13), rocks ability to recover strength, number of tampings, and a climate factor. The train traffic should also be represented where the heaviest axle loads are emphasized.
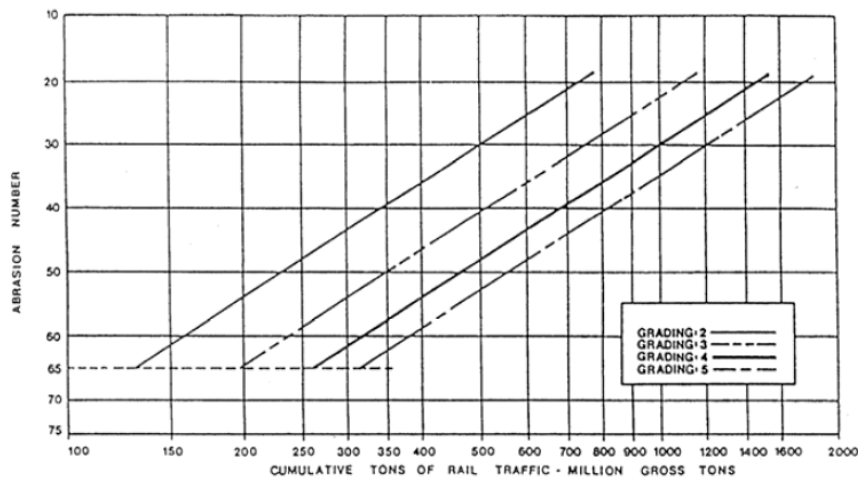
Figure 6.8   Cumulative tons of rail traffic versus ballast's mechanical strength (Clifton et al. 1987).

7. RECOMMENDATIONS FOR FUTURE RESEARCH

Here is a list of some suggestions for further research work in order of priority.

PRIORITY 1:

1. Los Angeles abrasion test improvements

Two additional rock properties should be considered:

- *The property to recover mechanical strength after repeated crushing*
  It is revealed that some rocks recover strength when they are subjected to repeated crushing (e.g. compaction after tamping in a railway line or use of an additional crushing stage in the quarry). To redo one Los Angeles abrasion test with the same material will probably not provide the result we are looking for. Thus, the LAA test needs to be supplemented with a new test that can measure this property. It will make it possible to reveal that some rocks perform better than their reputation. Some quarries will take advantage of this. A test similar to the Falling Weight test used by the Norwegian Public Road Administration until about 2004 is a possible solution.

- *Production of fines due to crushing*
  Rocks with similar resistance to crushing can produce different amount of fines. This was the result when the crushing product (0/1.6 mm) after a LAA test was examined. The Norwegian railway ballast specification does not include a test for assessing the potential for production of fines. Too much fines in a degraded ballast layer is the core issue regarding track alignment problems and leads to accelerating track maintenance costs. A 0.125 mm sieve can easily be added to the LAA procedure in addition to sieve 1.6 mm when the LAA value is determined. This will reveal differences in fines production between rocks. The challenge is to control that this way of measuring the amount of fines corresponds with the production of fines in the track in service due to train loadings.

2. Triaxial testing

Future development of repeated triaxial testing of ballast degradation:

- *Reduced specimen compaction*
  The ballast degradation from the triaxial tests was about five to six times greater compared with ballast breakage from the full scale tests measured on fraction 0/22.4 mm. A strong pre-compaction by means of a vibrating device with weight of 30 kg with 48 Hz for 30 seconds is probably the main reason for the differences in degradation. The compaction energy should be significantly reduced so that the ballast breakage is on the same level as that from full scale test/ field performance.

- *Reduced specimen height*
  Measurements of accumulated ballast breakage material were based on a test specimen height of 60 cm. Normal height of the ballast bed is 30 to 35 cm. This difference originates from the field of triaxial testing of cohesive soils like clay where friction between the sample and loading plate can affect the result. This matter can be questioned when coarse ballast particles are tested. It should be relevant to examine if 30 cm sample height gives results closer to the in situ performance compared with 60 cm height.

3. **What is the maximum deviator stress level to avoid fatigue of the ballast and corresponding accelerated ballast breakage?**
   - Interesting tests remain after this study. When the Iron Ore Line (Ofotbanen) between Narvik and Kiruna in Northern Norway wants to rise the axle load limit from 30 to 40 tons, it would be interesting to explore the consequences for the ballast maintenance. When the axle load is beyond the fatigue level, the ballast breakage will accelerate as well as the maintenance costs. What is the stress limit for ballast fatigue and what happens with the ballast breakage when the axle load increases from 25 to 50 tons? Where is the nearest quarry that can provide a ballast material with sufficient durability (transportation costs)? These questions are closely linked to Paragraph 5 in this chapter: Is there a linear correlation between increasing axle load and ballast breakage?

4. **A tool to improve the track's lateral resistance to prevent rail buckling**
   - Rail buckling is a question of the size of lateral resistance provided by the shoulder ballast material. It is now possible to quantify the surface texture of a ballast particle by a Surface Texture Index. Increasing index value can increase the internal friction to the ballast. This should be confirmed and quantified with laboratory tests. There is a good correlation between the micro-Deval value and Surface Texture Index. A rock's potential to increase the internal friction can be predicted by the micro-Deval value.

PRIORITY 2:

5. **Improving the ballast life model**
   - A model for calculating the ballast service life must in some way contain a factor describing the impact from axle loadings, e.g. accumulate number of axles passing a cross section multiplied with measured real axle load. It can be questioned if all axle-passing, light or heavy, contribute to the total ballast degradation. On the other hand, might the contributions from light axles be so small compared with an overloaded freight train that they are to be ignored? It may in practice mean that passenger trains can be skipped, or more generally, axle loads less than for instance 9 tons are not taken into account in the calculation. Triaxial testing should be performed to give an answer to this question.

6. **Are LAA tests on fraction 10/14 mm more reliable than fraction 31.5/50 mm in terms of ballast durability ranking?**
   - Caution should be exercised in comparing LAA values obtained from fraction 10/14 mm and 31.5/50 mm. They give different results for apparently similar materials. The Figure 7.1 shows a selection of rocks that are tested on both fraction 10/14 mm and fraction 31.5/50 mm. It was supposed that the LAA value would decrease when going from small particles to larger ones. This is correct for about half of the rocks tested. But some showed indifferent results and others increased their LAA values. It is not obvious that the ranking of one ballast material is more reliable than another in terms of durability. It would be interesting to investigate the case.
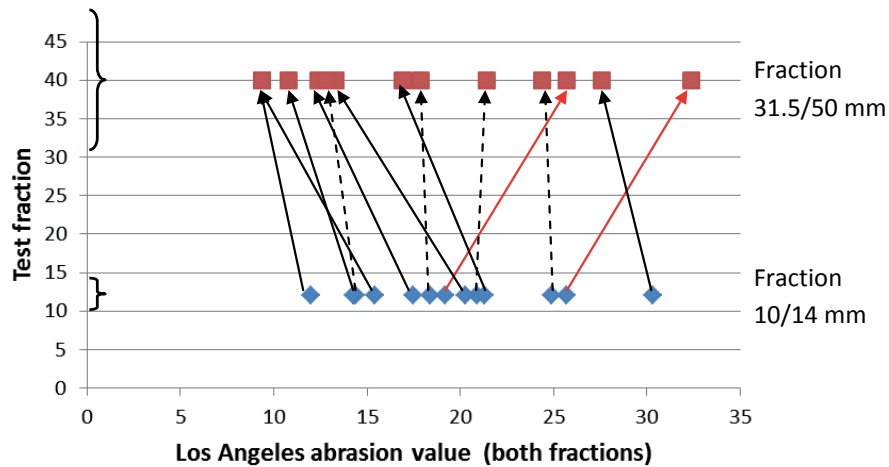
Figure 7.1   Los Angeles abrasion loss for a selection of rocks tested on fraction 10/14 mm and fraction 31.5/50 mm. Black lines marks decreasing values, dotted lines mark indifferent values and red lines mark increasing values when going from fraction 10/14 mm to fraction 31.5/50 mm

7. Effect of variable concentrations of sodium-chloride on frost resistance and abrasion resistance

- Water has little weathering effect on rocks with low water absorption. The Norwegian standard for frost resistance requires as an alternative procedure use of 1 % NaCl. Experience abroad suggests that the NaCl concentration with maximum impact on rock weathering can vary from 2 to 6 % with a maximum average value around 3 %. Some rocks respond to low concentrations of sodium chloride, others to higher concentrations. It would be useful to investigate whether this result is valid for Norwegian rocks. In that case the Norwegian standard on frost resistance is not necessarily totally reliable.

- Use of 1 % NaCl solution had no effect on rocks' micro-Deval$_{31.5/50 \text{ mm}}$ value even though the test materials were stored in the NaCl solution for 7 days. Further investigations can reveal if sodium chloride may have a stronger impact at higher concentrations.

8. Impact from micro-cracks on resilient modulus and ballast breakage

- This study did not find a correlation between the amount of micro-cracks in the rock and the ballast's resilient modulus. It was neither found any association with ballast breakage. But the same study suggests a possible relationship. Lørenskog mylonite with absolute lowest amount of micro-cracks achieved both highest resilient modulus of all tested rocks and the lowest amount of breakage material. Further work is needed but the task is probably quite complicated. The new and easy method for indirect determination of cracks by measuring transmitting light through thin section is not necessarily the right tool in this case.

9.   Some advice related to future research on rocks' mechanical strength

- Apparently homogeneous rocks are not always that after a careful inspection. They can be composed of different rock types. It is necessary to examine several thin sections to cover all variants.

- Some rocks which appear to be weak recover mechanical strength when they are subjected to repeated crushing. This property can cause unintended scattering in diagrams regarding

correlations when they are mixed together with rocks without this property. They should be kept apart.

- Rocks with different mechanical strength can respond to physical impact in different ways. Correlations between to parameters (e.g. relation between breakage and ballast grading) can be more clearly expressed in weak rocks and responds with higher magnitude.

- The lack of correlation between grain size (fine grained rocks) and mechanical strength in this study can indicate that the amount of alteration minerals (very fine grained) affect the strength. They are supposed to have a positive effect on mechanical strength and need to be quantified.

- The ballast's resilient modulus, measured on a medium strong meta-sandstone, increased with increasing average particle size (D_{50}), but the differences were small. It is expected that the differences would have been more evident if the test had been conducted on a weaker rock. Similar tests should contain at least one weak and one strong rock in order to do obtain a more nuanced result.

REFERENCES

Ballivy, G. and Dayre, M. (1984): *The mechanical behaviour of aggregates related to the physico-mechanical properties of rocks* (in French). Bulletin of Engineering Geology and the Environment. Vol.29, 339-342.

Bjerga, T.R. (2011): *Investigation of mechanical degradation and accompanying production of fines from crushed aggregates for road and railway purposes (In Norwegian).* Master Thesis, Norwegian University of Science and Technology, Trondheim, pp.115.

Bosserman, B. N. (1981): *Ballast experiments at FAST*. In: Proceedings of FAST Engineering Conference, Denver, Colorado, p. 45-54. US Department of Transportation, Federal Railroad Administration,

Brattli, B. (1992): *The influence of geological factors on the mechanical properties of igneous rocks used as road surface aggregates. Engineering Geology.* Vol. 33, 31-44.

Broch, E. & Franklin, J.A. (1972): *The point load strength test.* International Journal of Rock Mechanics and Mining Science, Vol. 9, p. 669 - 697.

Broch, E. (1974): *The influence of water on some rock properties*. Proceedings of the 3th Congress of the International Society for Rock Mechanics, Vol. 2, p. 33-37, Denver, Colorado.
.
Broch, E. (1979): *Changes in rock strength caused by water.* Proceedings of the 4th Congress of the International Society for Rock Mechanics, Vol. 1, p. 1-5. Montreaux. Balkema.

Chayes, F. (1956): *Petrographic Modal Analysis*. Johan Wiley & Sons, New York.

Chrismer, S.M. (1986): *Considerations of factors affecting ballast performance*. AREA Proceedings of the Annual Meeting, Vol.87, Bulletin 704, p.118-150.

Clifton, A.W., Klassen, M.J. and Watters, B.R. (1987). *Production and testing of ballast.* Transportation research record **1131**: 26-34.

Cuelho, E., Mokwa, R. and Obert, K. (2007): *Comparative analysis of coarse surfacing aggregate using micro-Deval, L.A. abrasion and sodium sulfate soundness test*. Department of Transportation, State of Montana, U.S. Final Project Report FHWA/MT-06-016/8117-27, pp.50.

Erichsen, E., Ulvik, A. and Sævik, K., 2011. *Mechanical degradation of aggregate by the Los Angeles-, the micro-Deval- and the Nordic test methods.* Rock Mechanics and Rock Engineering, **44**: 333-337.

Esveld, C. (1989): *Modern Railway Track*. MRT-Productions, The Netherlands.

European Rail Research Institute (1994): *Unified assessment criteria for ballast quality and methods for assessing the ballast condition in the track. Determining the criteria for ballast durability using triaxial tests*. ERRI D182/RP3, Utrecht, Holland.

FAST (1981): *Report No FRA/TTC-82/01*. FAST Engineering Conference 1981, Denver, Colorado, US Department of Transportation, Federal Railroad Administration, pp. 283.

Führer, G. (1978): *Oberbauberechnung*. Transpress, VEB Verlag Verkehrswesen, Berlin.

Fowler, D.W., Allen, J.J., Lange, A. and Range, P. (2006): *The Prediction of Coarse Aggregate Performance by Micro-Deval and Other Aggregate Tests. Application and Significance of the Micro-Deval Test.* International Center for Aggregates Research, Austin, Texas. Report No. ICAR 507-1F, pp.616.

Heikkila, P. (1991): *Improving the quality of crushed rock aggregate*. PhD thesis, Helsinki University of Technology, Finland. Acta Polytechnica Scandinavica, Ci 96, pp.191.

Haraldsson, H. (1984): *Relation between petrography and the aggregate properties of Icelandic rocks*. Bulletin of the International Association of Engineering Geology **30** (1), p.73-76.

Heydinger, A.G., Xie, Q., Randolpf, B.W. and Gupta, J.D. (1996): *Analysis of Resilient Modulus of Dense- and Open-Graded Aggregates.* Transportation Research Record **1547**: 1-6.

Hoang, T.M.P., Saussine, G., Dureisseix, D. and Alart, P. (2011): *Behaviour of a portion of railway track under maintenance operation.* Proceedings of 9th World Congress on Railway Research. Lille, France, pp.8.

Hudec, P.P. (1983): *Aggregate tests-their relationship and significance*. Durability of building materials, **1**: 275-300. Elsevier, Amsterdam.

Indraratna, B., Ionescue, D. and Christie, H.D. (1998): *Shear behavior of railway ballast based on large scale triaxial tests.* Journal of Geotechnical and Geoenvironmental Engineering, **124** (5): 439-449.

Indraratna, B., Lackenby, J. and Christie, H.D. (2005): *Effect of confining pressure on the degradation of ballast under cyclic loading.* Geotechnique, **55** (4), 325-328.

Johansson, E., Lukschová, Š. and Miškovský, K. (2011): "*Petrographic characteristics of granitoid and gabbroid intrusive rocks as a tool for evaluation of mechanical properties*". In E. Johansson (2011): Technological properties of rock aggregates. PhD Thesis, Luleå University of Technology, Luleå, Sweden.

Kazi, A., and Al-Mansour, Z.R. (1980): *Influence of geological factors on abrasion and soundness characteristics of aggregates.* Engineering Geology. **15** : 195-203.

Kessler, D. W., Insley, H. and Sligh, W.H. (1940): *"Physical, mineralogical and durability studies of the building and monumental granites of the United States."* Journal of Research of the National Bureau of Standards **25**: 161-206.

Klassen, M.J., Clifton, A.W. and Watters, B.R. (1987): *Track evaluation and ballast performance specifications.* Transportation Research Record **1131**: 35-44.

Knutson, R. M. and Thompson, M.R. (1978): *Permanent-deformation behavior of railway ballast.* Transportation Research Record, **694**: 47-53.

Lichtberger, B. (2003): *Handbuch Gleis. Unterbau, Oberbau, Instandhaltung, Wirtschaftichkeit.* Tetzlaff Verlag, Berlin.

Lim, W.L. (2004): *Mechanics of railway ballast behaviour.* PhD thesis, University of Nottingham, UK, pp.215.

Liu, H., Kou, S., Lindqvist, P-A., Lindqvist, J.E. and Åkesson, U. (2005): *Microscope Rock Texture Characterization and Simulation of Rock Aggregate Properties.* SGU project 60-1362/2004 (Geological Survey of Sweden).

López Pita, A., Teixeira, P.F. and Robusté, F. (2004): *High speed and track deterioration: the role of vertical stiffness of the track.* Proceedings of the Institution of Mechanical Engineers, Part F: Journal of Rail and Rapid Transit **218**: 31-40.

Lounsbery, R.W. and West, T.R. (1965): *Petrography of some Indiana aggregates in relation to their engineering properties.* University of Kentucky Engineering Experiment Station Bulletin Series. Vol. **20** (2): 24-41.

Lynch, J.K. (1978): *Factors which affect the stability, testing, selection and performance of suitable aggregates for railway ballast.* AREA Proceedings of the Annual Meeting **79**, Bulletin 668: 368-377.

Meininger, R.C. (1994): *Degradation Resistance, Strength, and Related Properties.* Proceedings of a conference on Significance of Tests and Properties of Concrete and Concrete Making Materials. American Society for Testing and Materials, Special Publication, **STP 169C**, p.388-400.

Monismith, C.L., Seed, H.B., Mitry, F.G. and Chan, C.K. (1967): *Prediction of pavement deflections from laboratory tests.* Proceedings of The Second International Conference on Structural Design of Asphalt Pavements, University of Michigan, Ann Arbor, Michigan, USA.

Norwegian Railway Company (NSB) (2000): *Catalogue of rolling stock.* NSB' Management System, Document No.G-72.

Nålsund, R. (1989): Field measurements of road stiffness from construction of Highway E6 between Trondheim and Stjørdal, Norway. Unpublished work.

Nålsund, R. and Jensen, V. (2011): "*Classification of micro-cracks, luminescence measurement, water absorption and frost resistance in Norwegian produced railway ballast.*" 13th Euroseminar on Microscopy Applied to Building Materials. Ljubljana, Slovenia, pp.10.

Obert, L., Windes, S.L.and Duvall, W.I. (1946): *Standardized test for determining the physical properties of mine rock.* United States Department of the Interior – Bureau of Mines, Report of investigations no.3891, pp84.

Onodera, T.F., and Asoka-Kumara, H.M. (1980): *Relation between texture and mechanical properties of crystalline rocks.* Bulletin of Engineering Geology and the Environment **22**: 173-177.

Pan, T. and Tutumluer, E. (2005): *Imaging Based Evaluation of Coarse Aggregate Size and Shape Properties Affecting Pavement Performance*. In: ASCE Geotechnical Special Publication **130** "Advances in Pavement Engineering":1-15, Austin, Texas.

Profillidis, V.A. (2006): *Railway Management and Engineering* (Third Edition). Ashgate Publishing Group.

Rao, C., Pan, T. and Tutumluer, E. (2003): *Determination of Coarse Aggregate Surface Texture Using Image Analysis.* In: Proceedings of the Pavement Mechanics Symposium at the 16th ASCE Engineering Mechanics Division Conference (EM2003), Seattle, Washington, pp.6.

Raymond, G.P., Gaskin, P.N. and Svec, O. (1975): *Selection and performance of railroad ballast.* In A.D. Kerr (editor): Railroad track mechanics and technology. Proceedings of a Symposium held at Princeton University April 21-23, 1975. New Jersey, Pergamon Press.

Raymond, G.P. (1977a): *Improvement in Rail Support.* Transportation Research Record **653**: 11-21.

Raymond, G.P., Lake, R.W. and Boon, C.J. (1977b): *Stresses and deformations in railway track.* Canadian Institute of Guided Ground Transport, Report 77-15, pp.110. Queen's University at Kingston, Ontario.

Raymond, G.P. and Davies (1998): *Triaxial tests on dolomite railroad ballast.* Proceedings of the American Society of Civil Engineers, Journal of the Geotechnical Engineering Division, Vol.4, No. GT6, p.737-751, June 1998.

Raymond, G.P., Lamson, S.T. and Law, J.E. (1983): *A review of current track structure design and future track research requirements.* Canadian Institute of Guided Ground Transport, CIGGT Report 83-6, pp.58. Queen's University at Kingston, Ontario.

Raymond, G.P. and Bathurst, R.J. (1987): *Performance of large-scale model single tie-ballast systems.* Transportation Research Record **1131**:7-14.

Rogers, C.A. (1998): *Canadian experience with the micro-Deval test for aggregates.* In J.P. Latham (editor): The Geological Society, Engineering Geology Special Publication **13**: 139-147, London.

Rogers, C.A. (2010): Oral communication.

Selig. E.T. and Alva-Hurtado, J.E. (1982): *Predicting effects of repeated wheel loading on track settlement*. Proceedings of the second International Heavy Haul Railway Conference, Colodado Springs, p.476-487.

Selig, E.T. and Roner, C.J. (1987): *Effects of particle characteristics on behavior of granular material*. Transportation Research Record **1131**: 1-6.

Selig, E.T. and Boucher, D.L. (1990): *Abrasion Tests for Railroad Ballast*. American Society for Testing and Materials, Geotechnical Testing Journal **13** (4): 301-311.

Selig, E. T., and Waters, J. M. (1994): *Track Geotechnology and Substructure Management*. Thomas Telford, London.

Selig, E.T. (1998): *Ballast deformation: Its causes and cures*. Railway Track and Structure. May Issue, p.25-31, Simmons-Boardman, New York.

Shenton, M. J. (1975): *Deformation of railway ballast under repeated loading conditions*. In A.D. Kerr (editor): Symposium on Railway Track Mechanics, Princeton University, New Jersey, Pergamon Press.

Shenton, M.J. (1984): *Ballast deformation and track deterioration*. Proceedings of a conference on Track Technology, p.253-265, Nottingham, UK. Telford.

Simpson, D.R. and Fergus, J.H. (1968): *The effect of water on the compressive strength of diabase*. Journal of Geophysical Research **73** (20): 6591-6594.

Singh, S.K. (1988): *Relationship Among Fatigue Strength, Mean Grain Size and Compressive Strength of a Rock*. Rock mechanics and rock engineering **21**: 271-276.

Skoglund, K.A. (2002): *A study of some factors in mechanistic railway track design*. PhD thesis, Norwegian University of Science and Technology, Trondheim, pp.210.

Suiker, A.S.J. (2002): *The mechanical behavior of ballasted railway tracks*. PhD thesis, Delft University of Technology, Netherlands, pp.248.

Thom, N.H. and Brown, S.F. (1988): *The effect of grading and specific density on the mechanical properties of a crushed dolomitic limestone*. Proceedings of the Australian Road Research Board **14** (7), p.94-100.

Thom, N.H. and Brown, S.F. (1989): *The mechanical-properties of unbound aggregates from various sources*. In R.H. Jones and A.R. Dawson: Proceedings of the Third International Conference on Unbound Aggregates in Roads, p.130-142. Nottingham, UK.

Verbeck, G.J. and Klieger, P. (1957): *Studies of "salt" scaling of concrete*. Highway research Board, Washington D.C., Bulletin **150**: 1-13.

West, T.R., Johnson, R.B. and Smith, N.M. (1970): *Tests for evaluating degradation of base course aggregates*. National Cooperative Highway Research Program, Report **98**, pp.94. Washington DC.

Woodside, A.R. and Woodward, W.D.H. (1998): *Assessing the Wear Characteristics of Aggregate Exposed at the Road Surface*. In J.P. Latham (editor): The Geological Society, Engineering Geology Special Publication **13**: 149-157.

Woolf, D.O. (1936): *Results of cooperative tests using the Los Angeles abrasion machine*. Highway Research Record **16**: 174-180.

Wright: S.E. (1983): *Damage caused to ballast by mechanical maintenance techniques*. British Rail Research, Technical Memorandum TMTD **15**.

Åkesson, U., Lindqvist, J, E., Göransson, M., Stigh, J. (2001): "*Relationship between texture and mechanical properties of granites, Central Sweden, by use of image-analyzing techniques*. Bulletin of Engineering Geology and the Environment **60**: 277-284.

APPENDIX I   Papers

APPENDIX II Petrographic description of rock aggregates

Effect of grading on degradation
of crushed-rock railway ballast
and on permanent axial
deformation.

Presented at Transportation
Research Board's 89th Annual
Meeting, Washington DC,
in 2010. Published in the
Journal Transportation Research
Record 2154 in 2010.

Paper I

Effect of Grading on Degradation of Crushed-Rock Railway Ballast and on Permanent Axial Deformation.

Roar Nålsund

ABSTRACT

A series of large scale repeated load triaxial tests on crushed meta-sandstone railway ballast are described. The effects of different gradings on degradation and accumulation of permanent strain are investigated. The material tested was a mechanically strong ballast aggregate with grading curves similar to the envelope curves in the Norwegian railway ballast specification (EN13450, category E) and the finer grading Arema 4, commonly used in the US on railway mainline tracks.

   The scope of the research was to assess the influence of grading on ballast breakage and permanent vertical deformation. Breakage and production of fines are influencing the ballast service life, and permanent strain is affecting the duration of track alignment due to tamping. As an approach to simulate the impact from ballast tamping, each test specimen was loaded totally with 4 million load repetitions but dismantled and rebuilt after each 1 million load application. The results of the study indicate that an increase in average grain size to a single-graded ballast material gives more permanent strain, more ballast breakage as well as slightly more production of fines less than 0.063 mm. The recompaction after each tamping operation is the main cause to ballast breakage.

INTRODUCTION

Railway ballast specifications generally call for uniformly graded aggregates mainly due to drainage requirement. However, the influence of the ballast grading (i.e. single-sized) on degradation and permanent deformation has not been a major concern for many researchers. Raymond (1) states that single-sized ballasts have larger void volumes than broadly graded ballasts. Thus, where production of fines from aggregate breakdown under train loads is a major source of contamination, they are generally to be preferred.

   On the other hand, Raymond and Diyaljee (2) stated that a more well-graded ballast has proved to perform, in terms of minimizing permanent deformations, as well as or better than uniformly sized ballast within the same size range. He tested three different gradings shown in Figure 1.
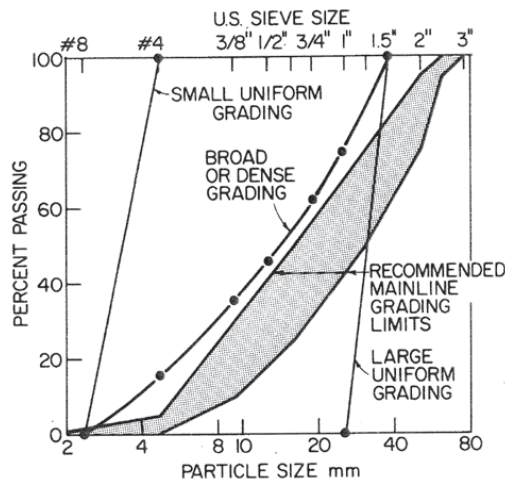
Figure 1   Three ballast gradings investigated by Raymond and Diyaljee (2).

1

In order to optimize the distribution of particles Skoglund (3) compared a railway ballast material (gabbro) with a typical grading according to the Norwegian requirements with another specimen made with a slightly more dense gradation where the amount of smaller grains exceeded the current specification. He found that the more dense grading did not significantly change the permanent deformation. There was however a need for more testing in this case to investigate the influence of grading over a broader span of grading variations. The objective of this investigation is to examine if it is possible to both reduce the permanent strain in fresh railway ballast and to reduce the ballast breakage (extension of ballast life) by optimization of the grain size distribution.

LARGE SCALE TRIAXIAL TEST

The triaxial testing unit
The equipment used in the present study is a large scale triaxial cell for repeated loading. The cell is earlier described by Skoglund et al. (4) and the triaxial unit has the capability of cycling both the deviatoric and the confining stress. It is primarily designed for testing of railway ballast, thus requiring large specimens typically 300 mm in diameter and 600 mm in height (Figure 2). The test unit comprises three main parts, a triaxial cell with two hydraulic loading actuators, a load control unit, and a data logger.

Figure 2   Instrumentation of a sample in the triaxial test rig

Preparation of specimens
The quarried ballast material was washed, sieved and blended into three predetermined grading curves. The specimens were built of five equal layers in a cylindrical steel mould. Each layer was compacted in a dry state for 30 sec using a vibrating plate compactor equipped with two vibrating motors. A maximum centripetal force of 12 kN and 48 Hz was used. A change in grading will influence the ballast density and the sample height. Each specimen should have a height of approximately 600 mm at the beginning of the test. In order to obtain this, a certain amount of material was added according to TABLE 1.

TABLE 1   Weight of samples and other properties.

	Grain size distributions tested			
	E coarse	E fine	E fine	Arema 4
Weight of sample step 1	67022g	68540g	68495g	69992 g
Height of specimen after compaction step 1	618 mm	602 mm	607 mm	602 mm
Density after compaction step 1	1.535 kg/dm^3	1.612 kg/dm^3	1,596 kg/dm^3	1.646kg/dm^3
Loading procedure	4 mill cycles in four steps	4 mill cycles in four steps	4 mill cycles in **one** step	4 mill cycles in four steps

After compaction the specimen was dressed with an inner rubber membrane while a hydraulic piston pushed the sample out of the cylinder. Suction is used under this process in order to avoid collapse. After demoulding the specimen is placed in the triaxial rig, the outer rubber membrane is mounted and instrumented with four LVDTs for axial and radial strain monitoring. Then the specimen is moistened by adding water through the drainage system from the bottom pedestal and then drained immediately.
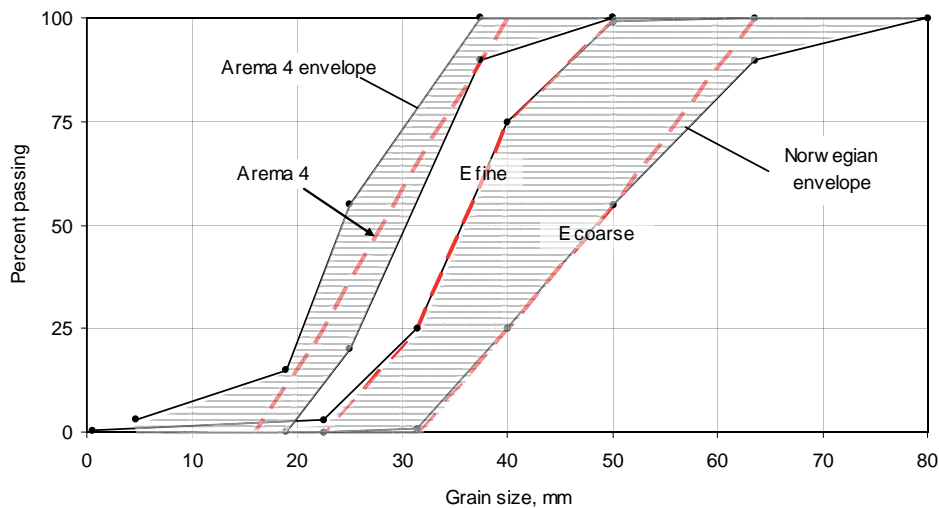
Figure 3   Grain size distribution curves for the three single-graded railway ballast samples used in this project (broken line).

Materials tested

The ballast used in this investigation was taken from Steinkjer quarry. The rock type contains of a great amount of very small mineral grains and appears to be a very fine-grained quartzite or meta sandstone. The main minerals are quartz (60%), feldspar (15%) and mica (20%), determined with petrographic analysis by use of a thin section microscopy (average of three thin sections). The quantifications are approximately. The mica minerals are very small due to recrystallization.

Three different grain size distribution curves were tested, all single-graded. Two are similar to the envelope curves of the current Norwegian specification represented by the gradings E fine (22.4/50 mm) and E coarse (31.5/63 mm) in Figure 3. The third is called Arema 4 (16/40 mm), an even finer grading very commonly used in the US on railway mainline tracks with good results (5). The average grain size diameter (D_{50}) was 28, 36 and 48 mm.

Roar Nålsund

TABLE 2   Material properties for railway ballast from Steinkjer quarry in North Trondelag county.

Properties	Measured values	Requirement	Standard
Density	2,71 kg/dm^3		
Los Angeles $_{31,5-50mm}$	LA_{RB}= 16,9	Less than 24	EN 13450/EN 1097-2
Micro Deval $_{31,5-50mm}$	M_{DE} RB = 4,8	Less than 15	EN 13450/EN 1097-1
Shape index	SI=18	Less than 20	EN 13450 / EN 933-4
Los Angeles$_{19-37,5mm}$	23,6	Less than 30	ASTM C535
Grading		Category E	EN 13450 / EN 933-1

The testing procedure
The single-graded railway ballast specimens as described above were subjected to long term cyclic loading to simulate railway traffic. All triaxial tests were performed in drained condition and with a maximum dynamic axial stress of 250 kPa corresponding to about 250 kN axle load given a stiff foundation, and a cycle rate of 5 Hz. The static confining (air) pressure was 60 kPa for all samples. Each test is conducted in four steps. To simulate the tamping operation the load application (step 1) was stopped after 1 million cycles. The test specimen got dismantled, recompacted with the same material used in step 1 and subjected for another 1 million load applications (step 2). This loading procedure was followed by similar steps 3 and 4 until a total of 4 million dynamic loads or 110 million gross tons. After each dismantling and before rebuilding, the tested ballast was sieved to remove breakage material with grain size less then the original grading. This material was accumulated and sieved after the end of step 4 to show the total amount of breakage after 4 million load applications. This loss of material was not compensated with fresh material and a lower sample was accepted (and a lower density).

To compare this result with a non tamping situation a new ballast sample with the same grading curve labelled E fine (see Figure 3) was subjected to 4 million cyclic loadings continuously in one step with the same testing procedure.

TEST RESULTS

The 4 steps test conducted in order to simulate the impact from tamping on uniformly graded railway ballast with three different grain size distributions has provided information about the ballast behaviour in terms of permanent strain, ballast breakage, resilient modulus and density.

Plastic behaviour
The effect of repeated tamping and subsequent recompaction (train loads) of ballast simulated in this project should mainly be crushing of particle edges and change in grain shape from angular to less angular material during years of service.
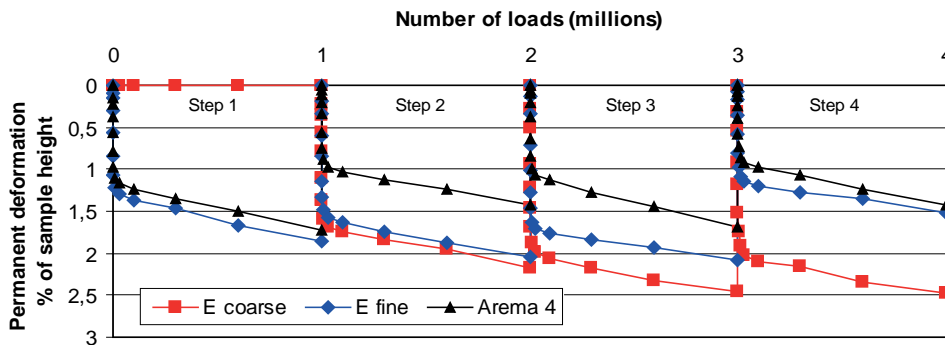
Figure 4   Permanent deformation against number of loads. Each of the three different gradings (E coarse, etc) was divided into four steps and totally subjected to 4 million load applications. Data from step 1 for grading E coarse was unintentionally not recorded.

4

This gives the material a permanent vertical deformation (i.e. less volume) which increases with number of loads as seen in Figure 4. Generally, it is expected as a hypothesis that this deformation in the ballast layer will gradually decrease from one loading sequence between two tamping operations to the next. Instead, the measurements of permanent strain from three test specimens shown in Figure 4, do not show any clear tendency to reduced accumulated strain from step 1 to step 4.

However, the connection between permanent strain and number of load repetitions are quite linear after a certain number of loads within all four steps. It can be seen in Figure 5 that the permanent strain rate measured between load number 100 000 and one million, within each step are decreasing from step 1 to step 4 for grading E coarse and E fine, but not for Arema 4 which shows no such decreasing tendency. Nevertheless, the rate development in Figure 5 can be an indication of the hypothesis on decreasing permanent deformation due to accrued edge abrasion.
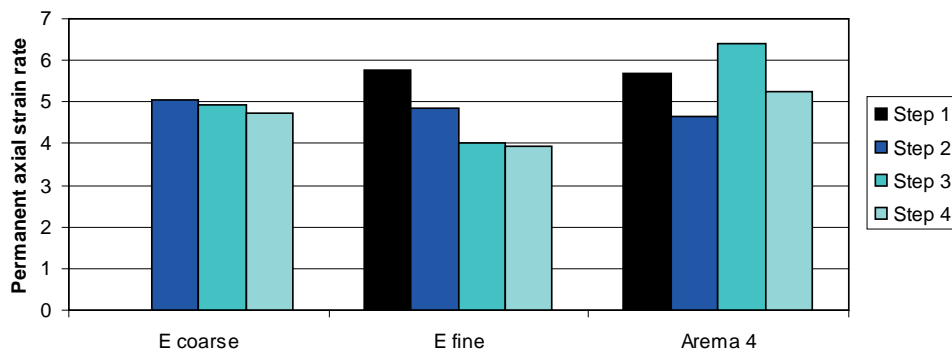
Figure 5   The correlation between permanent axial strain rate and number of test steps. Data from E coarse step 1 was not recorded.

Furthermore, it can be seen in Figure 6 that the three gradings tested are clearly ranked in terms of accumulated permanent vertical strain. Grading E coarse obtains about 50% more permanent deformation (average of four steps) compared with grading Arema 4. This means that a change to a more dense grain size distribution curve (single-graded) according to Figure 7 for measured specimen densities has great advantages with reduced permanent strain.
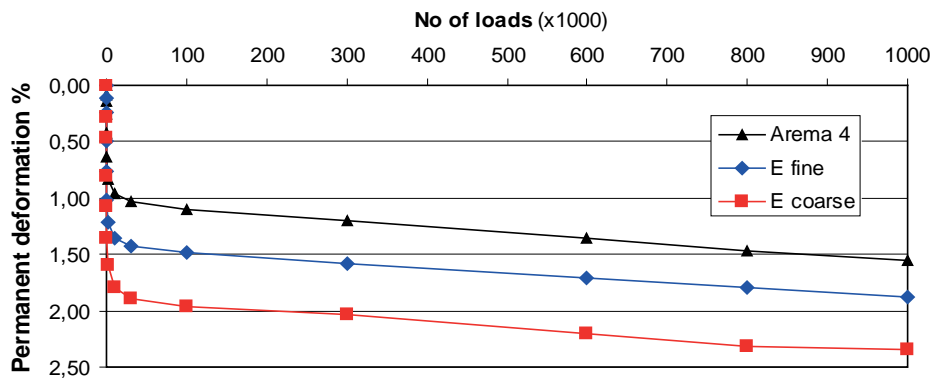
Figure 6   Permanent vertical deformation against number of loads. Each curve represents the average of four steps, totally 4 x 1 million loadings (average of three steps for grading E coarse).

Elastic properties

The resilient modulus changes during a loading sequence but reaches a stabile level in the last half of the sequence. The values used in Figure 8 represent the elastic ballast behaviour at the end of each loading sequence for all specimens. After step 4 the ranking between the three gradings is quite rational as the most dense grading (Arema 4) has the lowest resilient modulus. This corresponds with findings by Kamal et al. (6) who conducted a series of repeated load triaxial tests on 50 mm maximum-sized broad-graded unbound granular roadbase material as well as Thom and Brown (7) who investigated both well-graded and single-graded road base materials with maximum particle size of 10 mm.
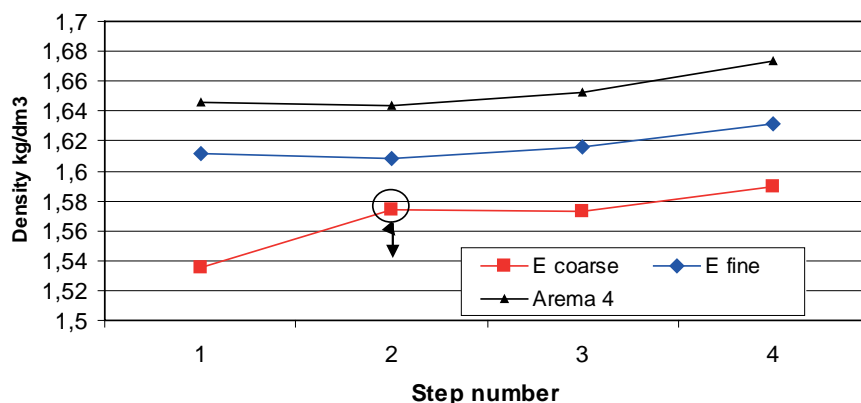
Figure 7   Change in the specimen density from step 1 to step 4. The measures are taken after each preconditioning (compaction in the steel mould) but before the loading sequence.

On the other hand, the situation after step 1 and 2 are almost converse. This means that there is no unambiguous correlation between resilient modulus and the tested gradings (density) within this span of variation.
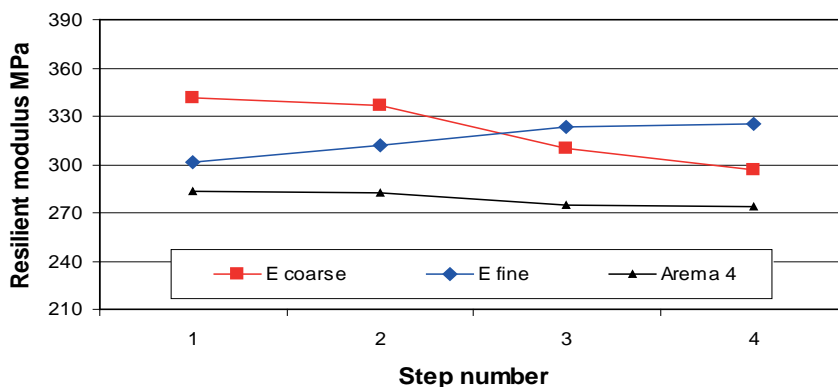
Figure 8   Change in resilient modulus from step 1 to step 4 for three different gradings. Each value is recorded at the end of each step (1 million loads). The average value for each grading is: E coarse 321 kPa, E fine 315 kPa, and Arema 4 is 278 kPa.

6

Ballast breakage and simulated effect of tamping

The grain size distribution for the breakage materials from E coarse, E fine and Arema 4 is shown in Figure 9. The production of breakage particles are accumulated sum from all four steps. After 4 million "train" loads and four "tamping operations" the quantity of broken particles less than 31.5 mm (Dmin) has risen to 7.6% of the original sample E coarse. Corresponding Figures for E fine is 6.3% and Arema 4 is 5.8%. The portion of fines less than 0,063 mm is respectively 0.26, 0.25 and 0.23%. This demonstrates that the ballast breakage decreases with increasing material density or decreasing average grain size for single-graded ballast.
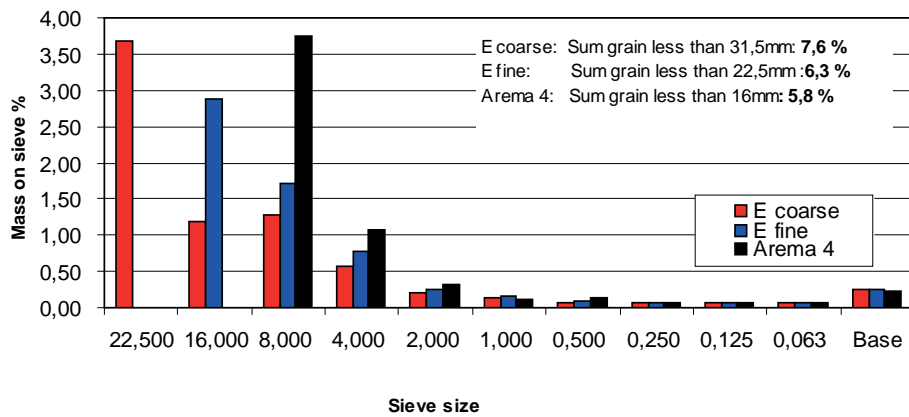
Figure 9   Amount of breakage material after the triaxial test (sum of four steps) less than Dmin in the original samples. Grading E coarse less than 31.5 mm, grading E fine less than 22.4 mm and Arema 4 less than 16.0 mm.

Consequently, the grading E coarse has 31% more breakage than the finer grading Arema 4. The relationship between permanent axial strain and ballast particle breakage in
cyclic triaxial tests after 4 million cycles and "tamping" impact is shown in Figure 10 where the particle breakage increases with increasing permanent deformation. This is in accordance with Shi and Thom (8) who investigated a single-graded material similar with sample E fine.
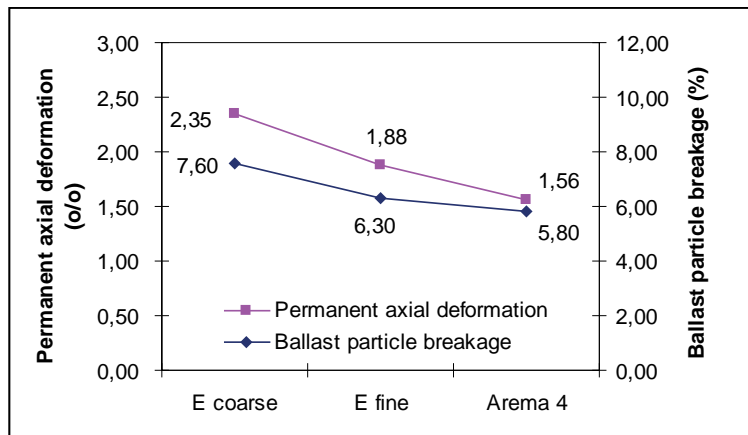
Figure 10   Permanent axial deformation compared to amount of ballast particle breakage smaller than Dmin in test specimen.

In order to assess the influence of no tamping a specimen designated E fine (22.4-50 mm) was subjected to 4 million cyclic loadings without interruption (the particles were not disturbed). This effect is demonstrated in Figure 11 where "Fine breakage" represents particles less than 8.0 mm in size while "Coarse breakage" represents particles between than 8.0 and 22,4mm in size. The bar designated With "tamping" shows the results from one of the three different gradings used (E fine). It can be seen that the recompaction after each tamping operation is the main source to ballast breakage (voids filled). The degradation from the tamping action itself is not included. Selig and Waters (9) came to a similar conclusion when they used a ballast box arrangement with a wooden sleeper segment to simulate in situ condition.
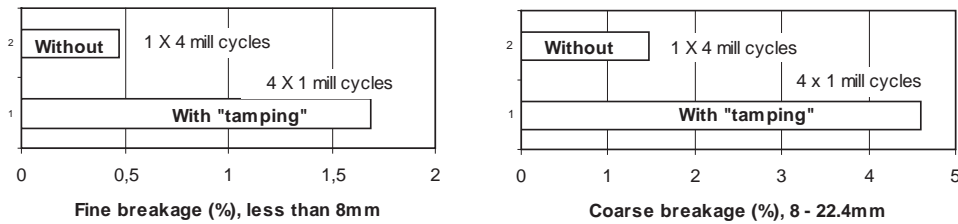
Figure 11   Effect of tamping simulation (particle rearrangement) on ballast breakage. The comparison between With and Without "tamping" is done with the grading E fine.

DISCUSSION OF RESULTS

Content of mica minerals
It is commonly known that a high content of mica minerals normally reduce the mechanical strength of a rock. The rock type investigated in this project contains about 20 % mica which is a very high amount. In this case it seems to have no significant negative effect on the mechanical strength as the Micro Deval value of 4.8 is very good, and an LA value of 16.9 (EN13450) is fairly good compared with other Norwegian hardrock ballast materials. The mica minerals appear in the rock as very fine grains. This may explain the unusually small influence of the mica content on the mechanical properties in this project.

Plastic strain
As appears in Figure 4, the permanent vertical strain from one step to the other goes up and down and does not show any clear tendency to reduced deformation. This may be explained by the fact that the stone skeleton, after each remoulding, will change more randomly so the transformation of stress from top to bottom of every step will be different each time. On the other hand, it can be seen that the large quantity of deformation during the first 10 000 of loads also changes from step to step. A probable cause is that the specimen was not prestressed in the triaxial rig before the loading sequence. The ballast material could have been slightly loosened in different extent when the specimen was moved from the steel mould to the test rig. Use of a static force of 10 kN in 30 seconds could perhaps give less scattering in the results.

Specimen density
The specimens' densities were measured after each preconditioning (compaction in the steel mould) but before the loading sequence. To obtain test samples with equal composition with respect to homogeneity, the breakage material less than D_{min} was generally taken away from the sample by sieving between each loading step without adding fresh material. This will give a higher density. As shown in Figure 7, this was forgotten with grading E coarse between loading step 1 and step 2 and the measured value (in diagram) of 1.574 should have been just about 1.55-1.56 (showed with an arrow).

CONCLUSIONS

The following may be concluded from the laboratory tests of single-graded ballast:

1. The permanent axial deformation increases with increasing number of loads, but the deformation rate can be decreasing with increasing numbers of tamping operations due to accumulating edge abrasion.
2. A change in grain size distribution to a more dense grading will reduce the permanent axial deformation. The grading Arema 4 obtained 33% less deformation than grading E coarse.
3. Ballast tamping which includes particle rearrangement is the main cause of ballast breakage
4. It was expected that the ballast resilient modulus should increase with decreasing density, but this correlation was only slightly achieved.
5. Ballast breakage increases with increasing permanent deformation. The grading E coarse obtained 31% more breakage than the finer grading Arema 4.

Limitation:
These conclusions are based on a test program that depends solely on the results of a single repetition and the test values will vary to some extent. But the main results are in accordance with relevant literature.

RECOMMENDATIONS

According to the conclusions a change in railway ballast grading (single-graded) from coarse to finer grain size (more dense grain size distribution curve) will lead to both less permanent deformation and less particle breakage. This can increase the ballast service life and bring down the maintenance cost in the long run.

ACKNOWLEDGEMENT

REFERENCES

1. Raymond, G.P. Research on railroad ballast specification and evaluation. In *Transportation Research Record: Journal of the Transportation Research Board*, No. 1006, Transportation Research Board of the National Academies, Washington, D.C., 1985, pp. 1-8.

2. Raymond, G.P., and V.A.Diyaljee. Railroad ballast sizing and grading. *Journal of the Geotechnical Engineering Division*, ASCE, Vol.105, No. GT5, 1979, pp. 676-681.

3. Skoglund, K.A. A study of some factors in mechanistic railway track design. PhD thesis, Norwegian University of Science and Technology, Trondheim, 2002.

4. Skoglund, K.A., S. Hoseth, and E. Vaernes. Development of a large triaxial cell apparatus with variable deviatoric and confining stresses. *Proceedings of the 5th international symposium on unbound aggregates in roads (UNBAR 5),* Nottingham, UK, 21-23. June 2002.

5. AREMA. Manual for Railway Engineering. American Railroad Engineering and Maintenance of Way Association, Washington D.C. 2009.

6. Kamal, M.A., A.R.Dawson, O.T. Farouki, D.A.B. Hughes, and A.A. Sha'at. Field and laboratory Evaluation of the Mechanical Behaviour of Unbound granular materials in Pavement. In *Transportation Research Record: Journal of the Transportation Research Board*, No. 1406, Transportation Research Board of the National Academies, Washington, D.C., 1993, pp. 88-97.

7. Thom, N.H. and S.F. Brown. Effect of Moisture on the Structural Performance of a cruched-Limestone Road Base. In *Transportation Research Record: Journal of the Transportation Research Board*, No. 1121, Transportation Research Board of the National Academies, Washington, D.C., 1987, pp. 50-56

8. Shi, X, and Thom, N.H. A laboratory study of railway ballast deformation behaviour. In *Proceedings of the 10th International Railway Engineering Conference*, London, 24-25. June 2009.

9. Selig, E.T., and J.M. Waters. *Track Geotechnology and Substructure Management*. Thomas Telford, London, 1994.

Classification of micro-cracks, luminescence measurement, water absorption and frost resistance in Norwegian produced railway ballast.

Presented at the 13th Euroseminar on Microscopy Applied to Building Materials. Ljubljana, Slovenia, in 2011.

Paper II

CLASSIFICATION OF MICRO CRACKS, LUMINESCENCE MEASUREMENT, WATER ABSORPTION AND FROST RESISTANCE IN NORWEGIAN PRODUCED RAILWAY BALLAST

R. Nålsund[a.] and V. Jensen[b.]

a. Norwegian University of Science and Technology, Department of Civil and Transport Engineering, 7491 Trondheim Norway. *roar.nalsund@ntnu.no*, www.ntnu.no

b. Norwegian Concrete and Aggregate Laboratory LTD, Sorgenfriveien 11, 7037 Trondheim Norway, *viggo.jensen@nbtl.no*, www.nbtl.no

Abstract

This paper demonstrates a new method using luminescence to quantify micro cracks and porosities in fluorescent impregnated thin section. Micro cracking is common and abundant in Norwegian aggregates and 5 types of micro cracks have been identified and classified. Luminescence measurements have been carried out on a wide range of commercially produced Norwegian railway ballast as well as detailed petrographic analyses. The results suggest correlation between luminescence and water absorption measurements indicating that micro cracks causes ingress of water into the aggregate. This is not the case from freeze-thaw tests and other mechanical tests where correlation not occurred suggesting that other micro textural parameters than micro cracks are the influencing parameter.

Keywords: Railway ballast, water absorption, frost resistance, micro cracks, fluorescence.

Introduction

From the mechanical point of view the relationship between micro textural parameters and mechanical properties of rock aggregates are quite complex (Liu 2005). According to Spry (1969) micro texture is defined as particle size, size distribution, shape and spatial orientation of mineral grains. In addition, other parameters like mineral distribution, grain-crystal contact, micro cracks, mineral deformation and degree of alteration will have influence on the mechanical strength and other properties of the aggregate. A majority of these parameters can be verified through microscopic examination in thin sections. However, micro texture by microscopic examination is difficult and often uncertain to quantify into absolute figures.

Micro cracks are important for the mechanical and physical properties of aggregates. This because micro cracks cause mechanically weak planar discontinuities on a micro or nano size scale. Micro cracks also make access channels for ingress of water into the aggregate. Kranz (1983) subdivides micro cracks into (i) Inter granular, which are associated with grain boundaries, (ii) intra granular, which are confined to the interior of a single grain, and (iii) trans granular, which cross more than one grain. Strength properties change drastically as the characteristics and quantity of micro cracks are modified under stress. In most cases grain boundaries are preferred sites for tiny flaws and cracks, which may develop to penetrative fractures (Brattli 1992).

A technique for quantifying micro cracks was introduced by Nishiyama et al. (1990) by combining microscopy with image analysis. They saturated pore spaces and micro cracks in the aggregate sample with synthetic resins mixed with fluorescent paint and dye before microscopy. In this way, pore spaces and micro cracks could be visualized under ultraviolet (UV) light due to a great difference in displayed brightness. Using image analysis it was possible to characteristics and measure porosity and total length of micro cracks per unit area (Nishiyama and Kusuda, 1994). Other researchers have since then used this technique to detect micro cracks in aggregates. Nishiyama and Kusuda (1996) showed how different stages in the weathering process could be quantified by introducing the term image brightness to describe the increase in number of micro cracks. However, they did not give any closer description.

This study is part of an ongoing PhD mainly investigating the reliability of standard tests for rating railway ballast with regard to mechanical strength, e.g. resistance to crushing. One of the goals is to assess the influence of petrography, mineralogy and micro texture on the mechanical and physical property of commercially produced railway ballast in Norway.

The present work use the intensity of light in fluorescent impregnated thin sections assessed by luminescence measurements for indirectly quantifying micro cracks and porosities in the aggregates. Average measurement results have been assessed and "correlated" with water absorption and freeze-thaw loss from the same aggregate deposit.

Test materials

The selection of rock samples was focused on representing a wide variation in the mechanical properties, i.e. Los Angeles value, as well as to be sufficient representative for Norwegian rock types. It was requested that samples should be taken from quarries supporting The National Railway Administration (Jernbaneverket) with railway ballast, if possible. Most samples meet the Norwegian requirements for mechanical strength, including one of Norway's strongest rocks. The rock samples make up a wide variety of igneous rocks, metamorphic rocks and consolidated/metamorphosed sedimentary rocks. A list of rock samples is presented in Table 1.

Representative rock samples were sampled from stockpiles inside the quarries (commercial products). All samples were required to have passed two crushing stages, no more or less, with a jaw and a cone crusher. Each sample consisted of about 800 to1600 kg. In addition two types of rock, i.e. mica schist and carbonate rock, with documented low frost resistance were included in the investigation.

Petrographic description of aggregates

As mentioned, first step in the investigation was to select representative rock samples from commercial railway ballast deposits. From each deposit "suitable" rock fragments were selected and visual examined. With aim to reveal a possible geological variation in the deposit, rock fragments that "looked" different were selected for further investigation. About 3-6 samples were selected from each deposit and polished slabs and fluorescent vacuum impregnated thin sections were prepared. The polished slaps were first investigated by use of stereo microscope and a macroscopic examination was carried out. Fluorescent impregnated thin sections were investigated under the petrographic microscope of type Olympus BX 51 mounted with polarizing filters and fluorescence equipment. For each thin section the following was investigated: mineralogy estimated by use of measurement grid, crystal-grain size, micro texture, crystal-grain contact, micro cracking (fluorescence light) and sign of recrystallization, deformation and alteration. The observations give basis for a correct classification and naming of the rock types. In addition, micro-graphs were taken from each thin section. Examples of "petrographic description of rock aggregates" are given in appendix to this paper.

Table 1 shows aggregates from 22 deposits (quarries) where the rock type have been classified according to correct geological name as well as major minerals and the dominating grain-crystal sizes in the rocks. Note that several of the quarries produce aggregates from different rock types. One of the commercial aggregate producers was marketing/selling the aggregate type as "rhyolite" but our petrographic investigation showed the aggregate to be meta greywacke.

Table 1: Aggregate deposit with geologic names, mineralogy and particle sizes.

Deposit no. 08115-	Geological name	Major minerals	Particle size (mm)
1	Meta sandstone, meta greywacke, quartzite	Quartz, felspar, mica	0.1-1.5
2	Greenstone	Plagioclase, actinolite, epidote	0.01-0.2
3	Meta greywacke-argillite, pebble conglomerate	Felspar chlorite, sericite, quartz	0.05-0.5
4	Meta gabbro, cataclasite	Felspar, amphibole, epidote	0.1-5
6	Cataclasite, crush breccia, granite	Plagioclase, quartz, felspar	0.05-2.5
7	Mylonite, cataclasite	Quartz, felspar, epidote	0.01-0.1
9	Marble	Carbonate	0.05-0.3
10	Greenstone, meta gabbro-basalt	Amphibole, plagioclase, epidote	0.1-0.5
11	Mylonite, gneiss, gabbro	Quartz, felspar, biotite	0.05-1
12	Monzonite	Plagioclase, felspar	7-10
13	Syenite, monzonite, gneiss	Felspar, amphibole, quartz	0.3-10
14	Sandstone, siltstone, greywacke	Quartz, felspar, mica	0.1-2
15	Porphyric trachyte	Felspar, opaque phases, pyroxene	0.01-5
16	Granite	Felspar, quartz, mica	0.2-7
17	Mylonite, cataclasite	Felspar, quartz, mica	0.2-3
19	Anorthosite	Felspar, sericite, epidote	1-8
20	Anorthosite	Felspar, epidote, sericite	3-8
21	Greywacke	Felspar, quartz, mica, carbonate	0.1-2
22	Greenstone, schist, slate	Amphibole, epidote, quartz	0.1-2
23	Gneiss	Quartz, felspar, mica	0.01-0.4
24	Sandstone	Quartz, felspar	0.2-1.5
26	Gneiss	Felspar, quartz, mica	0.1-0.5

Testing of aggregates

The testing includes microscopic examination, luminescence measurements, water absorption and frost resistance.

Microscopy of thin section and classification of micro cracks

By use of fluorescence technique a surprising variation and significant "amount" of micro cracking could be revealed in all the aggregates. By use of traditionally petrographic analyses, in "normal" thin sections that have not been fluorescent impregnated, micro cracking is not visible and therefore not observed. It has to be noted that micro cracks are important for the durability and possible also for the mechanical properties of the aggregate and will not be detected without use of fluorescence technique. In the present investigation 71 fluorescence impregnated thin sections from 22 commercial railway aggregate deposits in Norway have been investigated and the types of micro cracking have been classified as described in the following and shown in Figure 1.

- Inter granular micro cracks: *the crack follows the outer boundary of crystals or grain particles (perimeter) sometimes showing a mesh like pattern.*
- Intra granular micro cracks: *the crack is located internally in the crystal or grain particle often caused by mineral lattices.*
- Trans granular cracks or "long" micro cracks: *inter granular and/or intra granular micro cracks or a combination of inter granular and intra granular cracks located around or internally in more than one crystal or grain particle.*
- Massive-porosity: *very fine inter-grown cracks where individual cracks are difficult to distinguish and/or inter-grown sub microscopic small voids.*
- Holes*: Individual small isolated holes occasionally isolating small cracks.*

Polarized light   Fluorescence light
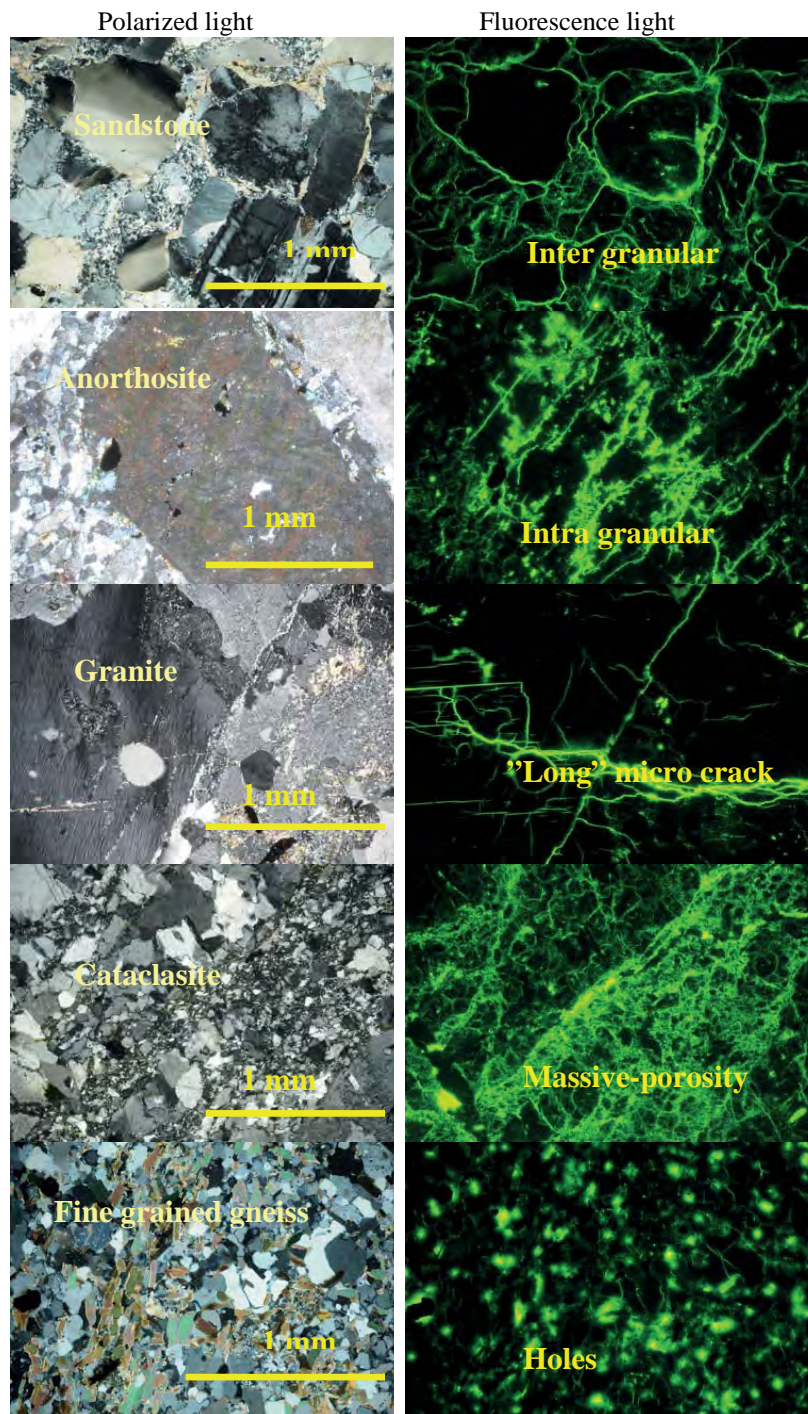
Figure 1: Micro graph of thin sections with 5 types of "micro cracks".

In most cases more than one type of micro crack is observed in the aggregate, as shown in Table 2 where a visual quantification of micro cracks in thin sections has been given as "none", "few", "some" or "many", as well as an average (arithmetic) luminescence (Lux) and standard deviation (se later). Note that several to all types of micro cracks have been observed in the aggregate samples but also that more than one thin section has been investigated and therefore more than one rock type can be represented.

Table 2: Average Lux (luminescence), standard deviation and semi quantitative amount of crack types.

Deposit no. 08115-	Thin section.	Lux	Std.	Inter granular	Intra granular	"Long" micro crack	Massive-porosity	Holes
1	3	0.59	0.07	+++	+	+	+++	+
2	3	0.60	0.19	+++	+	+	+++	-
3	4	0.30	0.12	+	+	++	++	+
4	3	0.67	0.35	-	++	+	+++	-
6	3	1.68	0.62	++	+	++	+++	+
7	4	0.44	0.11	+	+	+	+++	-
9	3	0.49	0.23	-	++	++	++	+
10	3	0.29	0.06	+	+	-	++	-
11	4	0.17	0.07	++	+	+	-	-
12	3	0.60	0.30	-	+	+	+	+
13	3	0.73	0.21	+	+++	++	+	-
14	3	0.27	0.04	++	+	+	+	+
15	3	1.22	0.25	+	+++	-	+++	-
16	3	0.75	0.32	++	++	++	-	+
17	4	0.28	0.07	+	-	+	+	++
19	3	0.89	0.37	-	++	++	+++	+
20	3	0.52	0.23	-	++	++	+	++
21	3	0.80	0.20	+	++	++	+++	-
22	5	0.62	0.11	+++	+	+	+++	+
23	3	0.47	0.18	++	-	++	-	++
24	3	0,43	0.14	++	++	++	-	+
26	2	0.47	0.16	+	++	+	++	-

- none	+ few	++ some	+++ many

Luminescence measurement

Different types of micro cracks occur in different amounts in thin sections and are therefore difficult to quantify. Moreover, quantification of micro cracks is not a standard procedure and the few published papers dealing with this subject have not given a "standardized" way to do it. Image analysis is one method being used for quantification of micro cracks in fluorescent impregnated thin sections but the results up till now are not promising. Image analysis may have problems quantifying distinct micro cracks in combination with more massive-porosity cracking and "holes" as observed in most of the aggregate samples in this study. Therefore a new measurement method was developed and used in the present doctoral project, namely luminescence measurement. The term "luminescence" has been used because light intensity has been measured in fluorescence light by use of UV filters in the microscope. Luminescence has been detected by use of a Mavolux Digital Luxmeter 5032B with the luminance attachment sensor mounted in one of the eyepieces of the microscope, se Figure 2. The Mavolux 5032B is suitable for measurement of extremely low light intensities with initial sensitivity of 0.01 lx (Lux).

Figure 2: Microscope with Mavolux luminance sensor mounted in one eyepiece.

The following procedure has been used for all the measurements. First all unnecessary filters were removed from the microscope to obtain maximum light intensity. Fluorescence light was obtained by using a primary filter (SWP 490) and a secondary filter (LP 520). By use of an object stage, the same coordinate system with 5 x 5 measurements point covering an area on 10 mm x 15 mm of the thin section was used by all the measurements. The used objective was 10 x magnified covering an area on 3.5 mm^2, hereby the total measurement area was 25 x 3.5 mm^2 = 87.5 mm^2. Measurements with defects or larger holes were excluded and therefore, the total numbers of measurements in some cases are less than 25. To detect possible drift or errors, measurements were checked by a standard with known Lux value before and after measurements. Measurement results from the Mavolux were transferred via an USB port to a data program in a PC and Excel spread sheets. The average luminescence in Lux was calculated and has been presented as average arithmetic values from all thin sections representing the aggregate deposit as shown in Table 2. In some of the aggregate deposit a rather large variation in luminescence has been detected between the thin sections explaining the rather large standard deviation shown in Table 2. This is probably caused by different aggregate types or variation in alteration in many of the aggregate deposits.

Water absorption

Water absorption has been carried out on different fractions. Aggregate fraction used for freeze-thaw tests were 8-16 mm and the same fraction was tested according to EN 1097-6. In addition to water absorption, the water saturated surface dry density, apparent density and oven dry density was measured. For the fraction 32-50 mm water absorption was measured according to EN 1097-6 Annex B on 10 pieces of aggregate. For drilled cores, water absorption was measured according to EN 1097-6 Annex B on 6 pieces (from each deposit) with 50mm diameter and length varying between 139 and 204 mm. The defined geometrical surface gives the possibility to measure water absorption with a high level of accuracy.

Freeze-thaw test

Freeze-thaw test on 12 different types of quarried aggregates was carried out according to EN 1367-1 (pure water) and EN 1367-6 (1% salt solution). More samples are at present time under testing. The standard testing has been modified by using one container with 1 kg 8-16 mm aggregates (one with pure water and another with 1% NaCl solution) due to the freezing capacity in the freeze-thaw chambers. The testing time was also prolonged (cycles from + 20 °C to -15 °C per day) from 10 cycles to 150 cycles with measurements of material change after 10, 20, 30, 60, 90, 120 and 150 days. The frost resistance was recorded as weight loss in percent of original dry sample weight. Frost resistance from 150 cycles is probably more representative for the climatic conditions in Norway instead of 10 cycles required in the standards and has therefore been used for further assessments in the project.

Results

Results and correlations from the luminescence measurements, water absorption tests and frost resistance tests are shown in Table 3 and the following clauses.

Table 3: Results from luminescence measurements, water absorption and freeze-thaw analyses.

Deposit no. 08115-	Luminescence Lux	Water absorption			Freeze-thaw (150 cycles)	
		8-16 mm water abs. %	32-50 mm water abs. %	Drilled cores water abs. %	Water % weight loss	1% salt solution % weight loss
1	0.59	0.48	0.27	-	0.66	0.53
2	0.60	0.49	0.24	0.22	0.62	2.98
3	0.30	0.42	0.22	0.14	0.98	4.31
4	0.67	0.46	0.27	0.19	0.81	13.11
6	1.68	0.59	0.47	0.53	0.39	0.48
7	0.44	0.34	0.20	0.25	0.27	4.16
9	0.49	0.30	0.10	-	-	-
10	0.29	0.41	0.21	0.15	0.62	2.88
11	0.17	0.26	0.12	0.10	0.42	0.39
12	0.60	0.67	0.38	0.28	1.09	3.61
13	0.73	0.43	0.29	-	-	-
14	0.27	-	0.14	-	-	-
15	1.22	0.94	0.66	0.52	-	-
16	0.75	0.34	0.22	-	-	-
17	0.28	-	0.09	-	-	-
19	0.89	-	0.28	-	-	-
20	0.52	0.31	0.13	-	-	-
21	0.80	0.47	0.32	0.22	-	-
22	0.62	0.50	0.31	-	0.70	10.28
23	0.47	0.39	0.17	-	0.59	0.46
24	0.43	-	-	0.16	-	-
26	0.47	0.59	0.31	0.32	0.48	1.03
Mica schist	-	1.59	-	-	44.3	49.89
Carbonate rock	-	0.97	-	-	20.63	24.37

Luminescence

Table 2 and 3 show results from luminescense measurements given as arithmetic average (Lux) including standard deviation. Luminescense values vary from 0.17 to 1.68 Lux. Note that the results are averages of 2 to 5 thin sections from the same deposit. In some deposits the standard deviation is rather large probably because the thin sections represent different aggregate types from the deposit or varying degree of alterations.

Water absorption

Table 3 shows results from the water absorption tests on three different size fractions. Note that the water absorption is reduced by increased particle size on same aggregate type as expected. Water absorption is less than 1 % in all samples except in the carbonate rock samples. Figures 3, 4 and 5 present scatter plots of luminescence (Lux) and water absorption as well as correlation. Figure 3 on size fraction 8-16 mm, Figure 4 on size fraction 32-50 mm and Figure 5 on drilled cores. Note that a more or less significant correlation between luminescence and water absorption exist and that correlation increases with increased particle sizes, Best correlation is from drilled cores with a correlation factor (R^2) on 0.73
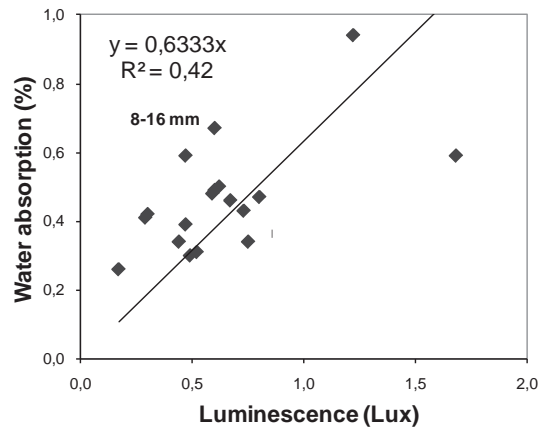
Figure 3: Graphical plot between luminescence and water absorption from fraction 8-16 mm.
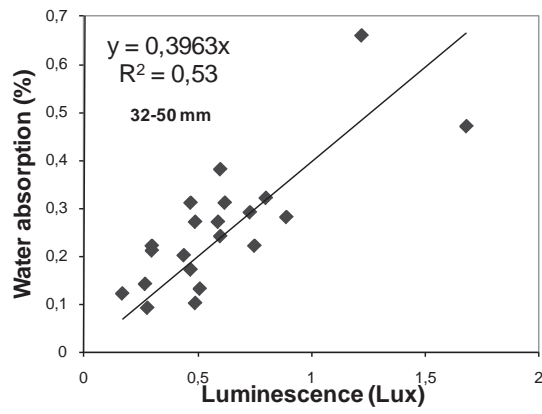
Figure 4: Graphical plot between luminescence and water absorption from fraction 32-50 mm.
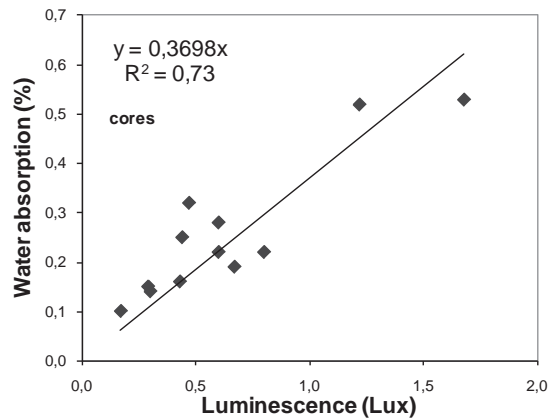
Figure 5: Graphical plot between luminescence and water absorption from drilled cores.

Freeze-thaw test.

Table 3 shows results from freeze-thaw test in pure water and in 1% salt solution after 150 cycles. Note that in most aggregate samples, but not all, the weight loss is larger in 1% salt solution compared with in pure water. In some aggregate types the loss is 14-16 times higher in 1% salt solution than in pure water. Figure 6 show a graphical plot between luminescence (lux) and freeze-thaw loss after 150 cycles in 1% salt solution and in pure water. Figure 7 show a graphical plot between water absorption and freeze-thaw loss after 150 cycles in 1% salt solution and in pure water. Note the lack of correlation (not calculated) in Figure 6 between luminescence and freeze-thaw and in Figure 7 between water absorption and freeze-thaw.
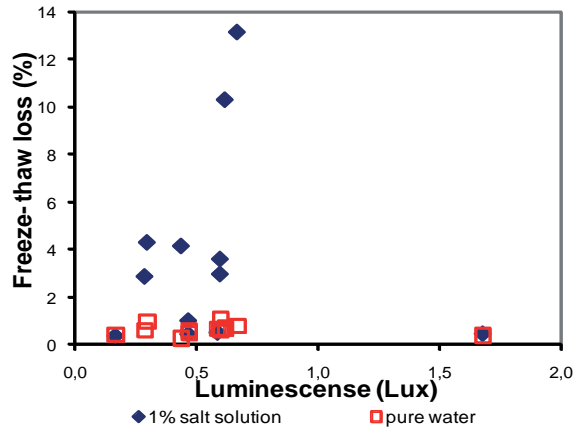
Figure 6: Graphical plot between freeze-thaw loss and luminescence.
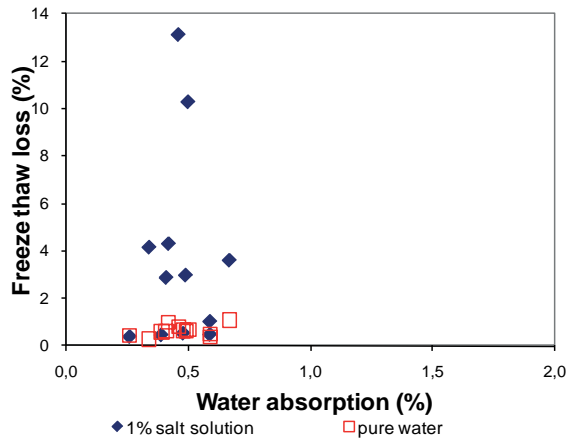
Figure 7: Graphical plot between freeze-thaw loss and water absorption from 8-16mm.

In this part of the investigation two extra rock samples (mica schist and carbonate rock) which were proven not to be frost resisting were added to the investigation. The rock samples have been used as erosion protection in a hydro power water supply dam in Nordland County over a period of 40 years but are now replaced because the aggregates disintegrated. Both rock samples have water absorption (8-16 mm) from 1 to 2 %. Figure 8 show a graphical plot between water absorption from the 8-16 mm fraction and freeze-thaw loss after 150 cycles in 1% salt solution and in pure water including the mica schist and carbonate rock. Note that correlation (not calculated) probably exist between water absorption and freeze-thaw loss for the samples with water absorption higher than 1 %, both for freeze-thaw in 1 % salt solution and in pure water.
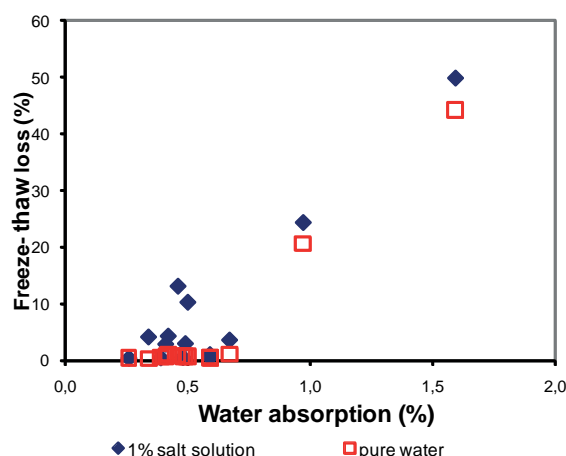
Figure 8: Graphical plot between freeze-thaw loss and water absorption from 8-16 mm fractions including mica schist and carbonate rock.

Summary and discussion

The rock samples in the doctoral prosject are selected to be representative for railway ballast used by the Norwegian National Railway Administration (Jernbaneverket) and represent a wide selection of Norwegian rock types. Petrographic analyses have been carried out on the railway ballast samples by use of polished slabs and fluorescent impregnated thin sections and has revealed the occurrences of different rock types in several of the quarried deposits. For the entire number of investigated quarries detailed petrographic descriptions have been made and examples included this paper in annex.

The petrographic investigations are focusing on several issues namely classifying micro cracks; quantify micro cracks indirectly by use of luminescence measurements and compare luminescence measurements with water absorption and freeze-thaw loss from the same quarry. The microscopic examinations in fluorescence light have revealed that micro cracks are surprisingly common and often abundant. 5 types of micro cracking have been identified and classified, namely 1) inter granular, 2) intra granular, 3) trans granular (or "long" micro cracks), 4) massive-porosity and 5) isolated holes or cracks. The different types and varying concentration of micro cracks identified in the aggregates do it difficult to make quantitative analyses of micro cracks and a new method using luminescence measurements has been developed. The method, which is inexpencive and rather fast to carry out, measure luminescence in fluorescence light in 25 measurements points located in a regular grid in the thin sections. Average (arithmetic) values have been calculated from the 2-5 thin sections from each deposit and used for further comparison with water absorption and freeze-thaw loss (median value and arithmetic average gives more or less same result). In some of the quarries a rather large standard deviation has been measured which probably is caused by the different rock types identified in most of the quarries or varying degree of alteration in the rock e.g. saussuritization and seritization which causes porosities.

Water absorption according to EN 1097-6 has been carried out on samples from most of the quarries on 3 different fractions, 8-16 mm, 32-50 mm and drilled cores. As expected the water absorption decreases with increased particle sizes. Most reliable results is supposed to come from drilled cores (largest "particle" size and lowest water absorption) because of a more "smooth surface" which do it easier to obtain more even conditions for the testing compared with a more uneven grain surface in crushed samples. Water absorption in the railway ballast samples varies from 0.14 to 0.97 in all the fractions and 0.97 to 1.59 in mica schist and carbonate rock which were added to the investigation because of documented low frost resistance.

Freeze-thaw test have been carried out on 12 different types of quarried aggregates according to EN 1367-1 (pure water) and EN 1367-6 (1% salt solution). The procedures have been modified and testing time prolonged to 150 cycles. In most of the aggregate samples, but not all, the weight loss is larger in 1% salt solution compared with in pure water. In some aggregate types the loss is 14-16 times higher in 1% salt solution than in pure water. Very high weigh loss up to 50 % was found in carbonate rock and the mica schist. Frost resistance from 150 cycles is probably more representative for the climatic conditions in Norway instead of 10 cycles required in the standards and therefore been used for further assessments in the project.

Luminescence has been compared with water absorption from the 3 different size fractions and it has been shown that a more or less significant correlation exist between luminescence and water absorption. Best correlation was obtained from drilled cores with a correlation coefficient (R^2) on 0.73. Comparing water absorption with freeze-thaw loss from pure water and 1 % salt solution did not show any sign of correlating on

railway ballast samples with water absorption less than 1 %. However, it seems that correlation exist when water absorption is higher than 1 % as for mica schist and carbonate rock but more results are needed to confirm this.

The mineralogical composition of the aggregates is probably important for the frost resistance as shown in Figure 9.
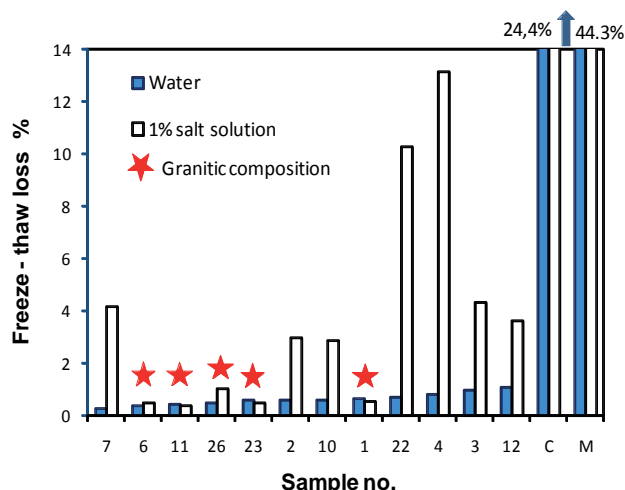
Figure 9: Freeze-thaw results for 14 different rock types (fraction 8-16 mm) after 150 freeze-thaw cycles. C = carbonate rock and M = mica amphibole schist.

In Figure 9 the five samples with lowest freeze-thaw loss, both in pure water and 1 % salt solution, all have granitic composition dominated by quartz and feldspar. For some rock types the 1 % salt solution causes significant higher freeze-thaw loss compared with in pure water which could be caused by a high content of amphibole minerals in the aggregates but this has do be further confirmed (sample no. 4 and 22).

The investigation has shown that correlation exist between luminescence and water absorption probably because micro cracking makes access channels for ingress of water into the aggregate. Best correlation has been found on drilled cores which probably also have the most correct water absorption. It is supposed that the correlation coefficient can be improved in case luminescence measurements and water absorption is carried out on the same rock aggregate type with same degree of alteration. This is not the case for all the quarries which produce aggregates from several rock types and possible different degree of alterations.

Comparing luminescence with freeze-thaw loss and water absorption with freeze-thaw loss, correlation between the methods could not be found in railway ballast with water absorption less than 1 %. However, in mica schist and carbonate rock with higher water absorption it seems that correlation exist but more results are needed to confirm this. The lack of correlation both between luminescence and freeze-thaw loss and water absorption and freeze-thaw loss suggest that micro cracks do not have the same influence on the freeze-thaw processes as for water absorption (except when the water absorption is higher than 1 %). Probably is the mineral composition more important for the freeze-thaw processes than micro cracking and quartz and feldspar more resistant than amphibole as shown in Figure 9.

In the investigation several mechanical tests have been carried out on samples from the same aggregate quarries as described in the paper (will be published elsewhere). The lack of correlation for luminescence (and water absorption) compared with both Los Angeles crushing test, Micro Deval abrasion test and Point load test suggest that micro fracturing not is an important parameter for the mechanical properties of railway ballast.

Conclusion

1. Norwegian produced railway ballast is not always homogeneous and can be composed by different rock types which can explain variations in the properties sometimes observed.
2. Micro cracks are surprisingly abundant and common in Norwegian railway ballast and 5 types of micro cracking have been identified and classified, namely 1) inter granular, 2) intra granular, 3) trans granular (or "long" micro cracks), 4) massive-porosity and 5) isolated holes or cracks.

3. A new method using luminescence measurements in fluorescent impregnated thin sections has been developed and tested on 71 thin sections from 22 quarries. The method uses inexpensive equipment and is rather fast to carry out. Results have been given as average luminescence values.

4. Average luminescence has been compared with water absorption and it has been shown that a more or less significant correlation exists between luminescence and water absorption depending on aggregate fraction. Best correlation was from drilled cores with a correlation coefficient (R^2) on 0.73.

5. Comparing average luminescence with freeze-thaw loss and water absorption with freeze-thaw loss correlation could not be found in railway ballast with water absorption less than 1 %. However, when the water absorption is higher than 1 % correlation between water absorption and freeze-thaw loss might occur but more testing is needed to confirm this.

6. The correlation between luminescence and water absorption suggest that micro cracks are the most important micro textural parameter for ingress of water into the aggregate.

7. Lack of correlation between luminescence and freeze-thaw loss and other mechanical tests suggest that micro cracks are not important for the freeze-thaw processes and the mechanical properties. Regarding to freeze-thaw the mineralogy is probably more important e.g. quartz and feldspar is likely more resistant than amphibole.

Acknowledgement

References

Brattli, B. (1992): "The influence of geological factors on the mechanical properties of igneous rocks used as road surface aggregates." *Engineering Geology*. Vol. 33, 31-44.

European Committee for Standardization (2000): EN 1097-6 Tests for mechanical and physical properties of aggregates. Part 6: Determination of particle density and water absorption.

European Committee for Standardization (2007): EN 1367-1 Tests for thermal and weathering properties of aggregates. Part 1: Determination of resistance to freezing and thawing.

European Committee for Standardization (2007): EN 1367-6 Tests for thermal and weathering properties of aggregates. Part 1: Determination of resistance to freezing and thawing in the presence of salt (NaCl).

Kranz, R.L. (1983): " Microcracks in rocks: a review." *Tectonophysics*. Vol. 100, 449–480.

Liu, H., Kou, S., Lindqvist, P-A., Lindqvist, J.E. and Åkesson, U. (2005): Microscope Rock Texture Characterization and Simulation of Rock Aggregate Properties. *Geological Survey of Sweden (SGU)*. Project 60-1362/2004.

Nishiyama, T., Kusuda, H. and Kitagawa, M. (1990): "A new method of visualization and image analysis of microcracks" (in Japanese with English abstract). *Journal of the Mining and Materials Processing Institute of Japan*. Vol. 106, 573-579.

Nishiyama, T. and Kusuda, H. (1994): "Identification of pore spaces and microcracks using fluorescent resins." *International Journal of Rock Mechanics and Mining Sciences & Geomechanics Abstracts*. Vol. 31, No. 4, 369-375.

Nishiyama, T. and Kusuda, H. (1996): "Application of a fluorescent technique to the study of the weathering process." *Engineering Geology*. Vol. 43, 247-253.

Spry, A. (1969): "Metamorphic Textures." Pergamon, London, 350 pp.

Degradation of railway
ballast through large scale
triaxial and full scale rail
track model tests
- Comparison with
mechanical laboratory tests.

Presented at the 9th
International Conference
on the Bearing Capacity of
Roads, Railways and Airfields.
Trondheim, Norway, in 2013.

Paper III

Degradation of railway ballast through large scale triaxial and full scale rail track model tests - Comparison with mechanical laboratory tests.

R. Nålsund
Department of Civil and Transport Engineering, Norwegian University of Science and Technology, 7491 Trondheim, Norway

E. Tutumluer
Department of Civil and Environmental Engineering, University of Illinois, Urbana, Illinois, USA 61801

I.Horvli
Norwegian Public Roads Administration, Trondheim, Norway

ABSTRACT: The aim of the research was to assess if the standard tests provided a reliable ranking of nine ballast aggregate materials with respect to mechanical strength. Standard tests were compared with the results from large scale triaxial and full scale model tests employed to simulate in-service stress and environment. Four different mechanical strength tests were conducted on nine crushed rock railway ballast types with fixed grading (22.4 - 63 mm) to investigate degradation with respect to breakage and production of fines. The equipment used are the standard tests: Los Angeles Abrasion (31.5-50 mm (dry and wet)/10-14 mm (only dry)) and micro-Deval (31.5-50 mm (wet)), large scale repeated load triaxial test (dry and wet), and a full scale rail track model test (only dry) for cyclic loading, all performed in the laboratory environment. The test procedure also included simulation of the impact loading from tamping and the effect from water. Aggregate petrographic tests were used to reveal whether there was any possible rating weakness associated with the mechanical strength. The rock samples were three igneous rocks, four metamorphic rocks and two consolidated/ metamorphosed sedimentary rocks, all fine and medium grained. The results of the study indicate that the three types of mechanical tests rank the ballast samples in three different ways.

KEY WORDS: Railway ballast degradation, triaxial test, Los Angeles Abrasion test, full scale railway track model test, micro-Deval test.

1   INTRODUCTION

In railway track, repeated wheel loads transferred from sleepers to the ballast layer cause abrasion and degradation of ballast aggregates over time which contributes to the fouled content in the ballast layer and alter the gradation (Boler et al. 2012). These changes weaken the bearing capacity of the ballast layer and eventually cause track geometry problems. To maintain the optimal track alignment, tamping is commonly applied. Tamping, on the other hand, contributes to degradation of aggregates in ballast layer. Tamping loosens ballast, rearranges particles and produces new particle contact points which fracture under contact stress. When this degradation is added to degradation caused by traffic loading, fouling content of ballast layer can increase to a level that prevents free drainage of water after some years in service.
Both Selig and Waters (1994) and Lim (2004) showed that tamping speeds up the fouling of ballast when they used ballast box tests to investigate the effect of particle rearrangement on particle breakage. This finding was recently confirmed by Nålsund (2010) from triaxial tests.

Lims (2004) investigation of four granitic rocks simulating the effects of both train loading and ballast tamping provided only a slight correlation between Los Angeles Abrasion (LAA) test and ballast degradation, but this conclusion was quite uncertain mostly due to few results in the commercial area (LAA less than 20%) of the diagram. The main crushing process realized in both LAA test and in the field under the sleepers is that rock particles lose weight due to loss of fracturing and chipping off the sharp corners and therefore, the angularity decreases (Boler et al. 2012). This fragmentation depends on the rock's tensile strength which in turn depends on, to some extend, the frequency of micro-cracks (Johansson et al. 2011). Ugur (2010) and Kahraman and Gunaydin (2007) have revealed that LAA results corresponded well with Point Load Index, which indirectly expressed rock core tensile strength properties of 14 different rock types. Hence, the magnitude of breakage under train loads might be predicted by the LAA value.

In a considerable study by Raymond and Diyaljee (1979) ballast aggregate breakdown on eight different rock types tested under repeated triaxial loading were related to mechanical tests and showed high correlation with Mill Abrasion tests. This result suggested a grinding mechanism and the importance of mineral hardness. The Mill Abrasion test used requires an aggregate charge of 3 kg with 20 - 30 mm particles together with 3 liter of water and no steel balls. Lower correlation was obtained with LAA suggesting toughness as a secondary factor for breakdown. The ballast materials were subjected to a repeated deviator stress of 210 kPa and a confining stress of 35 kPa.

It is of great interest that the selection of ballast material for construction purposes is based on sufficient resistance to load associated degradation. The most common way of predicting ballast degradation under train loads is through the use of LAA test which celebrated its 100 year anniversary in utilization in 2016 (Woolf and Crandell 1936). It is a quick and easy test that mainly measures coarse aggregate resistance to crushing. Many rock properties contribute to the mechanical strength, e.g. the average mineral grain size, grain size distribution (uniformly graded or well graded), shape (perimeter) and spatial orientation (foliation) of mineral grains. In addition, other petrological properties like mineral hardness, modulus (E), grain boundary relations (suturing), amount of micro-cracks, mineral deformation and degree of alteration (sericite in feldspar) make the situation quite complicated. Hence, it is quite difficult to predict a rock´s mechanical strength and corresponding functional properties. It can be suggested that it is too good to be true that such a simple test can separate in all aspects good performing ballast materials from the poor performance ones in a reliable way.

The purpose of the current study described in this paper has been to assess if the standard tests for mechanical strength provide a reliable ranking of the ballast materials in comparison with results from the triaxial and the full scale model tests. The two latter are employed to simulate in-service loading and environmental aspects in laboratory condition and to improve our understanding of ballast behaviour through petrographic characteristics. In addition, evaluating to what extent the parameters average grain size, amount of micro-cracks and mineral composition govern the mechanical strength has also been an essential task.

2 TEST MATERIALS AND ROCK CHARACTERISTICS

The selection of rock samples was based on representing a wide variation in the mechanical properties, i.e. LAA and micro-Deval (MD) values. All samples are taken from quarries, and most of them are supplying The Norwegian National Railway Administration with railway ballast (nominal 31.5-63 mm). All samples were required to have passed two crushing stages, first, with a jaw crusher and secondly with a cone crusher. The ballast samples represented both igneous rocks, metamorphic rocks and consolidated /metamorphosed sedimentary rocks.

Tables 1 and 2 list all investigated aggregates from 9 deposits (quarries) where the rock types have been classified according to their geological names, and the following features have been taken into account: Mineralogy, mineral grain size, mineral grain size interval (from D_{min} to D_{max}), specific density, grain shape, and mechanical properties such as LAA and MD values. Note that several of the quarries produced aggregates naturally "blended" with different rock types (heterogeneous).

Table 1: Aggregate deposits with geologic names and mineralogical compositions . Minerals: Q(quartz), F (plagioclase), K (k-feldspar), B (biotite), M (muscovite), A (amphibole), E (epidote), Chl (chlorite), Car (carbonate).

Deposit no. 08115-	Quarry	Geological name	Minerals									Grain size mm interval
			Q	F	K	B	M	A	E	Chl	Car	
1	Steinkjer	Meta sandstone, meta greywacke, quartzite	48	18	15		18					0.1-1.5
2	Meraftåsen	Greenstone	5	32	5		6	8	9	29	6	0.01-0.2
3	Lauvåsen	Meta greywacke-argillite	14	23	3		26			25	9	0.05-0.5
4	Vassfjell	Meta gabbro, cataclasite	1	18	6			41	12	18	4	0.1-5
6	Aplitt	Cataclasite, crush breccia, granite	54	15	29					2		0.05-2.5
11	Lørenskog	Mylonite, gneiss, gabbro	28	48	6	4		14				0.05-1
12	Freste	Monzonite	7	59	23			7		2	1	7-10
23	Rombak	Mica gneiss	46	21	2	10	17			3	1	0.01-0.4
26	Sefrivatn	Gneiss granitic	24	42	27	2		2		2	1	0.1-0.5

The mineralogy has been estimated by means of both microscopic examination of thin sections (measurement grid, 363 points) and semi-quantitative X-ray diffraction (XRD) analyses.

Table 2: Aggregate deposits with mechanical strength, shape, rock density and roughness.

Deposit nr	Quarry name	LAA_{dry}	LAA_{wet}	Micro Deval	SI20	Specific density	Surface Texture Index	$LAA_{10-14mm}$	Mineral grain size D_{50} mm
1	Steinkjer	16.9	14.1	4.8	18.2	2.71	2.00	20.9	0.138
2	Meraftåsen	12.4	18.3	11.2	7.1	2.95	0.88	17.5	0.088
3	Lauvåsen	25.7	26.7	15.7	13.5	2.77	0.90	19.2	0.119
4	Vassfjell	13.3	23.4	8.7	7.3	3.08	1.33	14.4	0.333
6	Aplitt	21.4	20.7	3.4	13.4	2.67	1.89	21.3	0.487
11	Lørenskog	12.8	16.3	6.0	14.7	2.91	1.56	20.3	0.203
12	Freste	21.8	21.9	6.6	13.9	2.73	1.10	22.5	3.815
23	Rombak	13.7	20.2	9.5	11.7	2.78	1.40	18.1	0.180
26	Sefrivatn	24.4	19.3	4.6	11.2	2.67	2.27	24.9	0.263

The rock characterisation is performed on fraction 31.5-50 mm.

In addition, a quantitative aggregate surface texture (ST) index was also investigated to reveal a possible impact on crushing and abrasion resistance. To calculate the ST, an image analysis technique, known as "erosion and dilation" integrated in the University of Illinois Aggregate Image Analyzer system for analysing coarse aggregate particles, was used (see Figure 1). Determination of ST is further described in Rao et al. (2003).
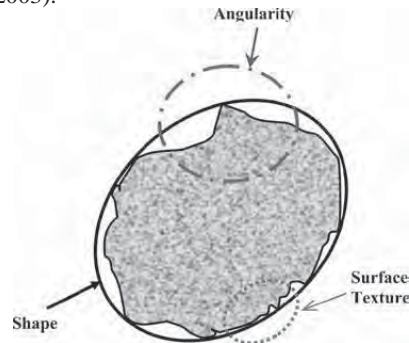
Figure 1: Key morphological properties of an aggregate particle (Pan and Tutumluer 2005).

3   TEST METHODS

It is assumed that the standard ballast testing methods consistently provide results reflecting the performances of different ballast materials in situ in the railway trackbed. In this research, extensive laboratory tests were conducted to investigate the correlation regarding degradation between two standard simple ballast index tests (i.e. Los Angeles abrasion and micro-Deval), a large scale cyclic loading triaxial test with constant confining pressure and a full scale rail track model test with pulsating jack simulating field conditions. A total of nine different ballast materials were investigated. The first two tests mentioned above were conducted in accordance with EN-NS1097-1, EN-NS1097-2 and EN-NS13450. The sample fractions used were 31.5 to 50.0 mm in sizes, partly 10-14 mm. The last two tests were non-standard. The large triaxial equipment was described in detail by Skoglund (2002) and Skoglund et al. (2002) and the sample fraction used was 22.4 to 63.0 mm in accordance with Norwegian requirements for railway ballast. The grading curves used for both the triaxial and the full scale model tests were identical (Table 3), and the weight of the samples for the triaxial testing varied between 67 to 72 kg to achieve a sample height of approximately 600 mm and allow for differences in specific densities. The corresponding sample weight for the full scale model test was 240kg.

Table 3: Similar grading curve used for both triaxial and full scale rail track model tests.

Fraction	22.4-31.5 mm	31.5-40.0 mm	40.0-50.0 mm	50.0-63.0 mm
Per-cent by weight	10	30	35	25

The two large-scale tests were both performed in such a manner that the test specimens were subjected to the same stress level as expected in railway tracks in service. The stress level is equivalent to 25 tonnes axle load. Hence, the degradation results from the two types of tests are comparable. The axle load limit on most railway lines in Norway is 22.5 tonnes.

3.1   Triaxial test procedure

The quarried ballast material was washed, sieved, air dried and blended into one fixed predetermined grading curve (Table 3). The specimens were built with five equal layers in a cylindrical steel mould. Each layer was compacted in a dry state for 30 seconds using vibration. Each specimen had to be at a height of approximately 600 mm in the beginning of the loading. After compaction, the specimen was dressed with two rubber membranes. After preparation, the specimen was placed in the triaxial rig and instrumented with four LVDTs for axial and radial deformation measurements. Then, the specimen was moistened by adding water through the drainage system from the bottom pedestal and then drained immediately.

The single-graded railway ballast specimens as described above were subjected to long term cyclic loading to simulate railway traffic. All triaxial tests were performed with a maximum dynamic axial stress of 250 kPa corresponding to about 250 kN axle load given a stiff foundation, and a cyclic loading rate of 5 Hz. The static confining (air) pressure was 60 kPa for all samples.

3.2   Tamping simulation

Each test is conducted in four steps. To simulate the tamping operation the load application (step 1) was stopped after 1 million cycles. The test specimen got dismantled, re-compacted with the same material used in step 1 and subjected for another 1 million load applications (step 2). This loading procedure was followed by two additional similar steps (3 and 4) until a total of 4 million dynamic loads or approximately 100 million gross tons. After each dismantling and before rebuilding, the tested ballast was sieved to remove breakage material with grain size less than the original grading (22.4-63 mm). This material was accumulated and weighed at the end of the test to show the total amount of breakage after 4 million load applications (inclusive tamping). The removed crushed material was not compensated with fresh material and a lower sample height (and lower sample weight as well as lower bulk density) was accepted.

3.3   Water influence

Another four triaxial tests (4x1million loadings) were accomplished to investigate water influence (also an attempt to simulate wet climate). In this case the material was soaked in water for 7 days before testing, drained during compaction, and subsequently soaked during the cyclic loading.

3.4   Full scale rail track model test procedure

The general test setup is shown in Figure 2. A railway track section was built with ballast, sub-ballast and subgrade of crushed rock and confined within a rigid test box 3m long by 1.5m wide, all resting on a concrete floor. The support layers under the upper layer of ballast were neither changed nor removed during the complete test.

Figure 2: Full scale rail track model test setup for cyclic loading.

A standard concrete sleeper 2400 mm long, 260 mm wide and 200 mm deep (at rail seat) was placed in the middle directly on the ballast floor with another sleeper on each side with 500 mm spacing to simulate typical track structure but without any ballast in the cradle in an attempt to run a less time consuming test. Limited with a steel frame with inside dimensions of 400 mm width and 1000 mm length, a test sample weighing 240 kg was placed within the ballast layer under each end of the middle sleeper (see Figure 3). The ballast degradation for each tested rock (9 in total) was calculated as average of the two test samples. No under-sleeper-pads were used.
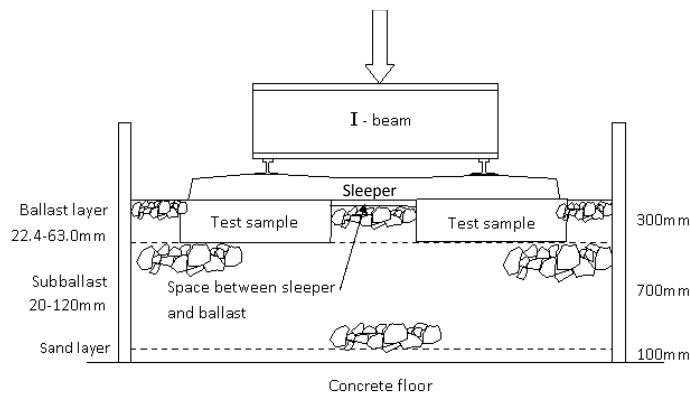
Figure 3: Cross-section of the full scale rail track model test setup.

To differ test sample from surrounding ballast and avoid loss of degraded fines, a geotextile was used which also enabled lifting by crane. Having backfilled the surrounding ballast material and removed the steel frame, the area was leveled by hand and compacted with a vibrating device "LOPPE" with ten passages for each sample. Under the middle of the sleeper, some ballast was removed to avoid riding during the test due to experience from Raymond (1977). The area of interface between sleeper and ballast at each end of the sleeper was 260 mm by 950 mm.

3.5   Tamping simulation

The wheel load was assumed to be distributed equally with 50% to the main sleeper and 25% to each of the neighboring sleepers according to Selig and Waters (1994). A computer-controlled closed-loop electrohydraulic actuator applied a 5 kN to 125 kN repeated load to the I-beam and distributed 62.5 kN load to each rail seat for a duration of totally 4 million load repetitions interrupted after each 1 million to perform a "tamping operation." After having temporarily moved the hydraulic jack, the I-bar and the middle sleeper, the samples were penetrated with a crowbar "in situ" on ten different points to loosen the ballast with the intention to re-orientate each rock particle to get new contact points. Then, the next step that followed was a new compaction and a new sequence with 1 million loadings until 4 million was reached. The degraded material was recovered <u>after</u> test completion as distinct from the triaxial test. The test samples were finally sieved (finer than 22.4 mm) and the material breakdown was assessed as an average of the two test samples.

4   TEST RESULTS AND ANALYSES

4.1   Ballast breakage under triaxial testing

The results of the cyclic triaxial tests on dry and wet ballast are displayed in Figures 4 and 5.
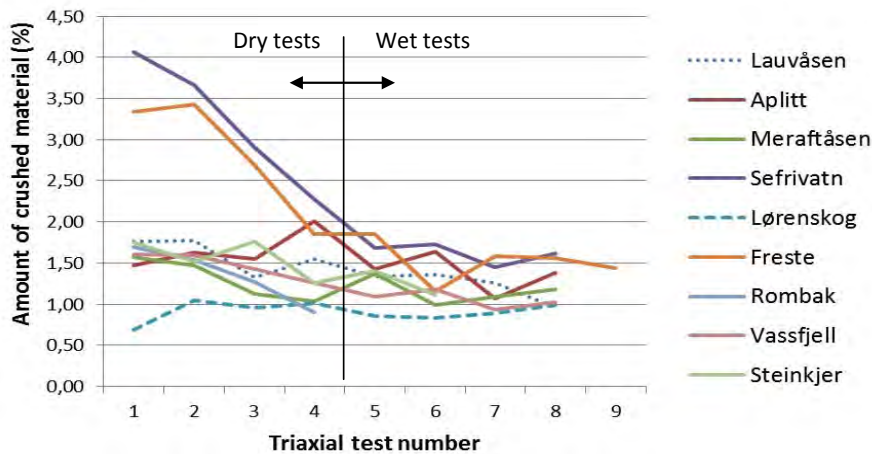
Figure 4: Amount of crushed material 0-22.4 mm after each triaxial test. The test fraction at the beginning of each test was 22.4- 63.0 mm. Number 1 to 4 represent dry state, and 5 to 8 represent wet state. Mica gneiss from Rombak was tested only in dry state.

There are several methods to characterize breakage (Anderson and Fair 2008, p 323. Indraratna 2011), but the reason why the fraction 0-22.4 mm is being used in this study, is that it corresponds with one of the recommendations in European Rail Research Institute's report (ERRI 1994) on ballast durability and fouling characterization.

Overall, the resistance to crushing does not seem to change significantly during eight test repetitions conducted on seven out of the total of nine ballast materials (Figure 4). The last two (Sefrivatn and Freste) however show an increase in strength during the first part of the test series. This is previously documented by Heikkila (1991) for medium to coarse grained rocks in Finland by using full scale crushing tests in quarries, which suggested that mineral grain size can influence rock's ability to recover mechanical strength when there is repeated crushing. As opposed to Heikkila's rock materials, Sefrivatn is fine grained and should behave in accordance with the other seven tested ballasts with no strength improvements, since they are fine to very fine grained with D_{50} within range 90 to 490 μm ($D_{50} = 90$ means that half the area of the thin section consists of mineral grains with diameter greater than 90 μm). Freste (monzonite) is the only one that is coarser than fine grained with D_{50} equal to 3815 μm (medium grained).

It has been known for a long time that moisture has in general a negative influence on rock strength (Kessler et al. 1940). Among the nine test materials in this project, four specimens (Lauvåsen, Rombak, Meraftåsen and Vassfjell) have a pronounced drop in mechanical strength when measured by wet $LAA_{31.5-50mm}$ test with an increase in LAA value from 27% to 75%. This phenomenon is not observed from the triaxial tests as shown in Figure 4. Surprisingly, there is no increase in ballast breakage in tests 5 to 8 (wet state) compared with the dry state tests.
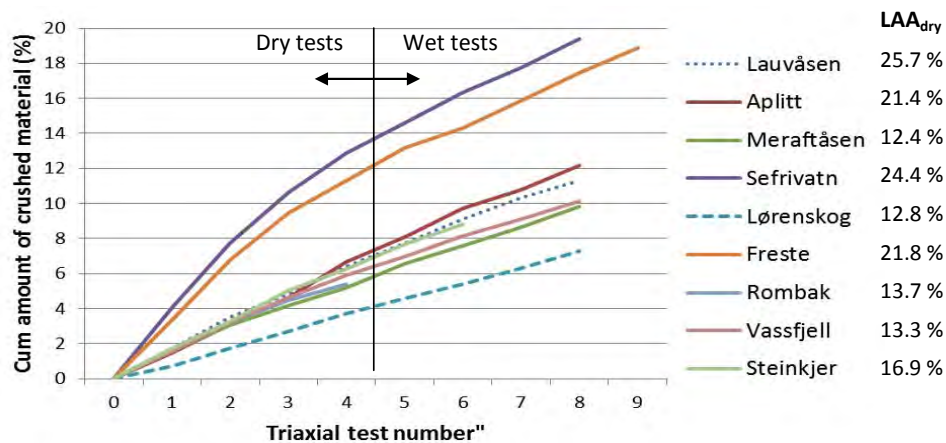
Figure 5: Cumulative amounts of crushed material 0-22.4 mm after 8 triaxial tests. Freste was tested 9 times. Test number 1 to 4 represents dry state, and number 5 to 8 represent wet state. Mica gneiss from Rombak was tested only under dry conditions. All rocks are fine to very fine grained except Freste.

The total amounts of material breakdown from all the test series are shown in Figure 5, and indicate a ranking of the ballast's durability under simulated field conditions with train loading, tamping (sample compaction between each test) and climate (wet state). The diagram shows a fair correlation between crushing and the results from LAA tests (fraction 31.5-50 mm). However, there are three interesting deviations that attract attention. Sefrivatn (granitic gneiss) should perform better than shown in the diagram due to this rock's average mineral grain size. But presence of a great amount of inter and intra granular micro-cracks may have a negative effect on the strength. Aplitt (cataclasite) and Lauvåsen (meta-greywacke) had slightly more breakage than Vassfjell and Meraftåsen despite its almost twice as high LAA value. An explanation is hard to find, but Lauvåsen consists of nearly 60% soft minerals, which should be a drawback in this context. Thus, it is regarded as an outlier in this study. According to LAA results, Lørenskog was equally durable with Vassfjell and Meraftåsen but performed 20% better than the other two. A possible explanation is that Lørenskog is almost without micro-cracks and appears

7

somewhat solid which can contribute to high strength. Micro-Deval values do not correlate at all with the amount of breakage material after triaxial testing, neither plotted against fraction 0-22.4 mm nor 0-0.125 mm. Hence, in this study, abrasion seems to be less important for ballast degradation compared with resistance to crushing when the rocks are fine grained.

The rate of strength improvement for ballasts Sefrivatn and Freste shown in Figure 4 levels out after four triaxial tests performed in the dry state. The rest of the test samples do not have any change in mechanical strength, which makes it difficult to create reliable correlations between mechanical strength and other parameters. Most of the fine grained rock materials had strengths unaffected (resistance to crushing) through all eight triaxial tests. This implies that the breakage results from wet stage (step 5 to 8) are representative for the long term performance. A plot of LAA results against cumulative wet triaxial test breakage is shown in Figure 6. The correlation is fair but there is some scattering. The triaxial test performs mainly a dynamic impact (only crushing) while the LAA method uses shock (strokes) and abrasive impact (Erichsen et al. 2011). Hence, their rates of degradation are different for the different rocks as shown in Figure 6.
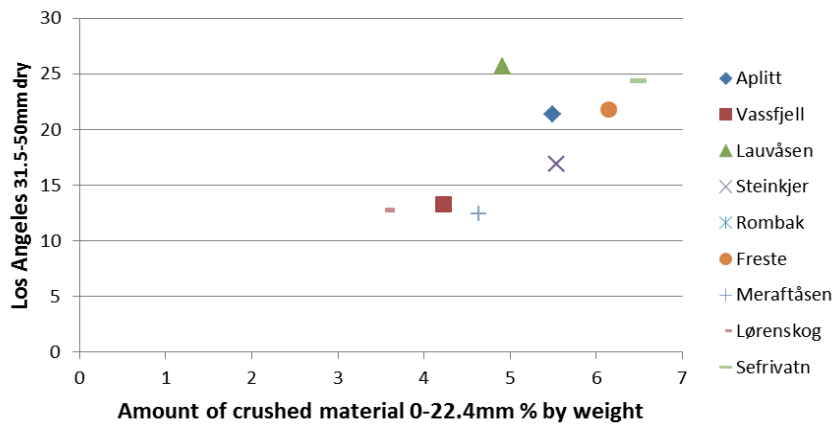
Figure 6: Correlation of LAA (dry) against cumulative wet triaxial test breakage (four repetitions and totally 4 million loadings). Ballast test fraction 22.4-63 mm. R^2 without Lauvåsen is 0.83.

However, if we replace $LAA_{31.5-50}$ with $LAA_{10-14mm}$ which causes a more uniform crushing impact on the test material (Erichsen et al. 2011), a better correlation can be obtained, as will appear from Figure 7. This suggests that $LAA_{10-14mm}$ can be a more suitable test for assessing durability of ballast materials when compared to $LAA_{31.5-50mm}$.
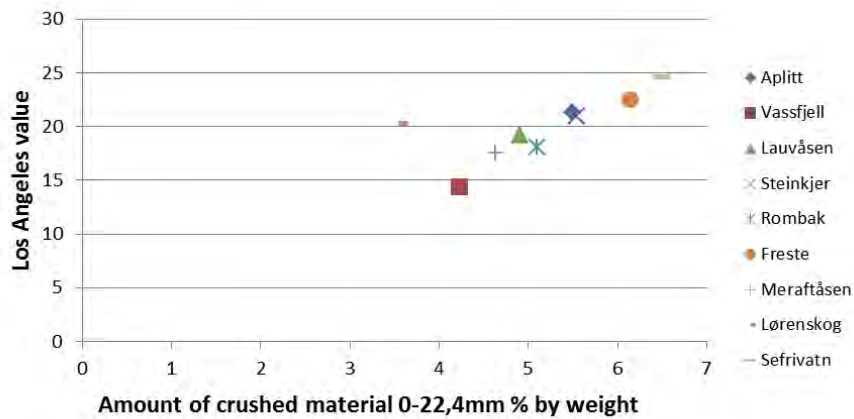
Figure 7: LAA values (10-14 mm) plotted against breakage from triaxial tests performed in wet state (4 million loadings). R^2 without Lørenskog is 0.97.

4.2   Permanent deformation

As mentioned above, abrasion seems to be less important for ballast degradation in this study. But on the other hand, micro-Deval values correlate well with the ballast's permanent settlement under cyclic triaxial loading as shown in Figure 8. This was first discovered by Raymond and Diyaljee (1979). This correlation depends in turn on the material's surface texture (test results displayed in Table 2). The lower the micro-Deval value is, the higher is the surface texture index, which means that the surface friction decreases when the micro-Deval value increases. The ballast settlement during cyclic triaxial loadings is therefore probably mainly caused by rotation of aggregate grains causing a higher density of the ballast. Some crushing may occur during the cyclic loading, but the recorded correlation between settlements and LAA values is poor in this study. The major part of the aggregate's crushing takes place during compaction under sample preparation.
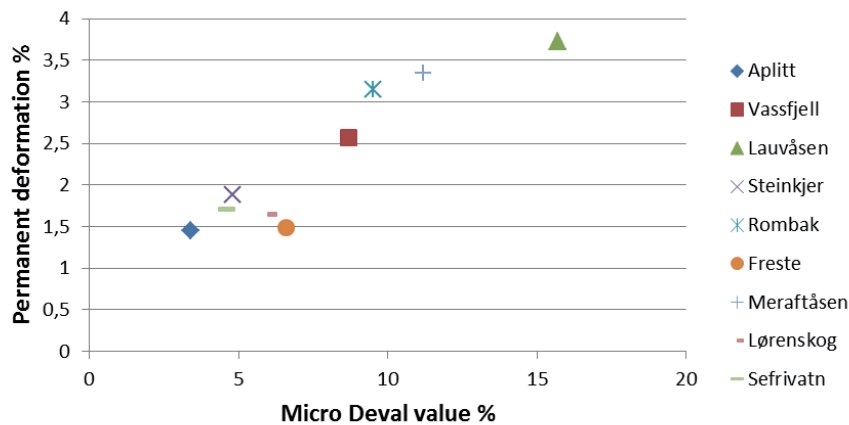
Figure 8: Ballast permanent deformation from dry triaxial tests (4x1mill loadings) plotted against micro-Deval values (31.5-50 mm). R^2 is 0.86 with Lauvåsen included.

4.3   Ballast breakage under full scale model testing.

Full scale model tests were conducted on all nine materials tested. It was supposed that the full scale model test would simulate field condition very well and therefore provide more reliable results. Figure 9 shows the relationship between LAA loss and ballast degradation from the full scale model test (totally 4 mill loadings with ballast loosening after each million). The correlation is far from as good as in Figure 6 (LAA vs. triaxial cyclic impact). If we replace $LAA_{31.5-50mm}$ with $LAA_{10-14mm}$, no correlation occurs in contrast to what was expected with reference to Figure 7. A possible explanation can be that the LAA test does not simulate the materials' field performance in a reliable manner, and the triaxial test also is a bit away from the reality in situ.
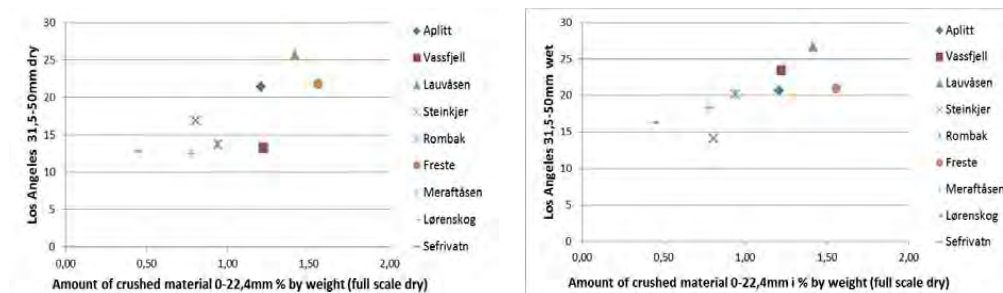
Figure 9: Total amount of crushed material from full scale model test (4x1 million loadings /only dry state) plotted against $LAA_{31.5-50mm}$. Left: dry state with $R^2 = 0.56$. Right: wet state with $R^2 = 0.58$, but increase to 0.73 when Freste (medium grained) is removed.

Neither crushed material from the triaxial test nor from the full scale model test shows any correlation with micro-Deval values (not shown). Hence, it is likely to believe that abrasion does not occur or is of secondary importance for ballast degradation in this study. According to Figure 9 (left), the LAA method dry state does not rank the aggregate materials in a proper way compared to the full scale model test. The judgment of the four samples all with LAA loss around 13% (Lørenskog, Meraftåsen, Rombak and Vassfjell), says that they are equal in mechanical strength. But the full scale model test (supposed to be the most reliable test) separates the four samples clearly based on ballast breakage. Lørenskog is more than twice as good as Vassfjell. A replacement with data from $LAA_{10-14mm}$ did not improve the correlation.

If we compare the breakage material 0-22.4 mm with $LAA_{31.5-50mm}$ wet state (see Figure 9 right), the regression coefficient increases from 0.58 to 0.73 if sample Freste leaves out. This can be done due to the fact that the nine test samples consists of two groups, one that recover improved mechanical strength during repeated crushing, and one that does not recover any change in mechanical strength (see Figure 4). The four test samples mentioned above, Lørenskog, Meraftåsen, Rombak and Vassfjell, are not equal any longer according to $LAA_{31.5-50mm}$ wet state. The ranking now comply with the results from the full scale model test. But it looks strange that the strongest correlation is obtained when comparing a dry test with a wet test.

5   DISCUSSION

5.1   Improved ranking of ballast materials

This study suggests that ballast breakage in situ is mainly governed by the resistance to crushing, and that the process of abrasion contributes in a minor degree, provided that the rock is fine grained, crystalline and is composed of mainly hard minerals. An interesting phenomenon appears when the crushed material from the full scale model test was sieved on 0.125 mm grain diameter as illustrated in Table 4.

Table 4: Amount of fines (0-0.125 mm) in the crushed material after the full scale test compared with respective values from fraction 0-22.4 mm (ref. Figure 9). Per cent refers to sample's total weight.

Quarry	Aplitt	Vass-fjell	Lauv-åsen	Stein-kjer	Rom-bak	Freste	Meraft-åsen	Løren-skog	Sefri-vatn
0-22.4 mm (%) after sieving	1.21	1.22	1.41	0.80	0.94	1.56	0.78	0.44	1.59
0-0.125 mm (%) after sieving	0,13	0,12	0,37	0,09	0,14	0,11	0,12	0,07	0.17
0-0.040 mm (%) after Coulter test	0.075	0.087	0.263	0.059	0.079	0.067	0.088	0.039	n.d.

Graywacke from Lauvåsen is an outlier within the present rock suite, since it consists of about 60% soft minerals (mica, chlorite and carbonate) but performs apparently as an ordinary hard rock. An extraordinary production of fines (three times more than expected) was revealed when sieved on 0.125 mm sieve after strained in the full scale model test. This was also confirmed by Coulter test (Table 4). The poor quality (Lauvåsen) was not detected neither by LAA, micro-Deval, triaxial test nor full scale model test when sieved on 22.4 mm sieve. In general, rocks with equal mechanical strength do not produce the same amount of fines (less than 0.125 mm) when they get crushed (West et al. (1970). West analysed the amount of fines after LAA tests. This is an important property because the content of fines in the fouling material is the main reason for the loss of performance of the ballast bed (Han and Selig (1997), This can be developed to a simple technique to discriminate rocks in a more reliable manner based on LAA method, but more investigations are necessary to document the correlation between laboratory work and in situ performance.

5.2   Improving the triaxial test procedure

The amount of crushed material (0-22.4 mm) from the triaxial test run on one sample, compared with the corresponding amount of crushed material from the full scale model test (after four parallel tests and four million load applications) is quite different. Due to the selected procedure for the triaxial test in this study, it produced up to 8 times more breakage material than the full scale model test on the same type of material. The difference in impact of stress under the two test methods can cause a difference in response from the materials which may give two different ballast durability rankings. Less crushing under compaction of the triaxial test samples can be an improved approach to simulating field stress conditions. The triaxial test samples were compacted in 30 seconds in the steel mould. Duration of 10-15 seconds could probably have been a more proper practice.

6   CONCLUSIONS AND RECOMMENDATIONS

It is difficult to obtain good correlations between mechanical tests and rock parameters particularly when many different rock types are involved. Hence, this introduces many variables which can influence the mechanical strength in different magnitudes. Specific conclusions are as follows.

On the basis of triaxial testing:
1. With reference to the triaxial test, seven out of totally nine rock samples did not change their resistance to fragmentation during impact from repeated compaction, both in dry and wet state.

2. Two rock samples improved their crushing resistance during impact from repeated compaction.

3. It is not clear why some rocks developed higher mechanical strength as a consequence of repeated crushing while others did not. A possible explanation may consider linkages to average mineral grain size and amount of micro-cracks.

4. Contrary to the literature review findings, a change from dry to wet triaxial testing procedure did not reduce the mechanical strength of ballast materials.

5. Micro-Deval values did not correlate well with the amount of material breakdown after triaxial testing without regard to use of fraction 0-22.4 mm or 0-0.125 mm. Hence, in this study, abrasion seemed to be less important or had no effect on ballast degradation regarding resistance to crushing for fine grained rocks.

6. Dry Los Angeles Abrasion$_{31.5-50mm}$ (LAA) results correlated fairly well with cumulative wet triaxial test breakage (0-22.4 mm). An increase in regression coefficient from 0.83 to 0.97 was obtained when LAA$_{31.5-50}$ was replaced with LAA$_{10-14mm}$. This suggests that LAA$_{10-14mm}$ can be a more suitable test for assessing ballast durability than LAA$_{31.5-50mm.}$

7. Micro-Deval values correlated well with the ballast's permanent settlement under cyclic triaxial loading. Decreasing micro-Deval values gave reduced permanent settlements. This correlation is probably caused by the rocks' surface roughness (Surface texture Index). No good correlation could be established between permanent deformation and LAA results.

On the basis of full scale rail track model test:
8. The correlation between the full scale model test and LAA$_{31.5-50mm}$ dry state was poor. Consequently, the LAA test did not predict ballast degradation in a reliable way, assuming that the full scale model test simulated the field condition taking properly into account applied rail track stresses. Replacing LAA$_{31.5-50mm}$ with LAA$_{10-14mm}$ had no improving effect.

9. A fair correlation war obtained between the full scale model test and LAA$_{31.5-50mm}$ wet state.

Comparison of results from the triaxial testing and the full scale testing:

10. The amount of crushed material (0-22.4 mm) from the triaxial test was four to eight times more compared with the corresponding amount of crushed material from the full scale model test.

11. Less compaction in the triaxial test conditioning phase can be an improved approach. Reduced vibration from 30 seconds to 10-15 seconds could probably have been a more proper practice to avoid initial crushing.

ACKNOWLEDGEMENTS

REFERENCES

Anderson, W. F. and Fair, P., 2008. *Behavior of Railroad Ballast under Monotonic and Cyclic Loading.* Journal of Geotechnical and Geoenvironmental Engineering (ASCE) 134(3): 316-327.

Aursudkij, B., 2007. *A laboratory study of railway ballast behaviour under traffic loading and tamping maintenance*. PhD thesis, The University of Nottingham, UK, pp.215.

Boler, H., Wnek, M. and Tutumluer, E., 2012. *Establishing Linkages between Ballast Degradation and Imaging Based Aggregate Particle Shape, Texture and Angularity Indices.* In: N. Abe (Ed.) Advances in Transportation Geotechnics 2: 186-191. ISBN: 978-0-415-62135-9. CRC Press.

Erichsen, E., Ulvik, A. and Sævik, K., 2011. *Mechanical degradation of aggregate by the Los Angeles-, the micro-Deval- and the Nordic test methods.* Rock Mechanics and Rock Engineering, 44: 333-337.

European Rail Research Institute, 1994. *Unified assessment criteria for ballast quality and methods for assessing the ballast condition in the track. Determining the criteria for ballast durability using triaxial tests.* ERRI D182/RP3, Utrecht, Holland.

Han, Xiangdong and Selig, E.T., 1997. *Effects of fouling on ballast settlement.* Proceedings of the 6th International heavy haul conference: 257-268, Cape Town, South Africa.

Han, Xu, 2012. *The role of particle breakage on the permanent deformation of ballast*. PhD thesis, University of Wollongong, Australia.

Heikkila, P., 1991. *Improving the quality of crushed rock aggregate*. PhD thesis, Helsinki University of Technology, Finland. Acta Polytechnica Scandinavica, Ci 96, pp.191.

Indraratna, B., Saliam, W. and Rujikiatkamjorn, C., 2011. *Advanced Rail Geotechnology –Ballasted Track, pp.411. T*aylor & Francis Group, London, UK.

Johansson, E., Lukschova, S. and Miskovsky, K., 2011. *Petrographic characteristics of granitoid and gabbroid intrusive rocks as a tool for evaluation of mechanical properties*. In Johanssen (2011): Technological properties of rock aggregates. PhD Thesis, Luleå University of Technology, Luleå, Sweden.

Kahraman, S. and Gunaydin, O., 2007. *Empirical methods to predict the abrasion resistance of rock aggregates.* Bulletin of Engineering Geology and the Environment 66: 449-455.

Kessler, D.W. Insley, H. and Sligh, W. H., 1940. *Physical, mineralogical and durability studies of the building and monumental granites of the United States.* Journal of Research of the National Bureau of Standards 25: 161-206.

9th International Conference on the Bearing Capacity of Roads, Railways and Airfields. Trondheim, Norway, 2013.

Lim, W. L., 2004. *Mechanics of railway ballast behaviour*. PhD thesis, The University of Nottingham, UK, pp.195.

McDowell, G. R., Lim, W. L., Collop, A. C., Armitage, R. and Thom, N. H., 2005. *Laboratory simulation of train loading and tamping on ballast.* Proceedings of the Institution of Civil Engineers-Transport 158(2): 89-95.

Nålsund, R., 2010. *The Effect of Grading on Crushed Rock Railway Ballast Degradation and Permanent Axial Deformation.* Transportation Research Record 2154: 149-155.

Pan, T. and Tutumluer, E., 2005. *Imaging Based Evaluation of Coarse Aggregate Size and Shape Properties Affecting Pavement Performance*. In: ASCE Geotechnical Special Publication 130 "Advances in Pavement Engineering": 1-15, Austin, Texas.

Rao, C., Pan, T. and Tutumluer, E., 2003. *Determination of coarse aggregate surface texture using image analysis.* Proceedings of the Pavement Mechanics Symposium at the 16th ASCE Engineering Mechanics Division Conference (EM2003), Seattle, US.

Raymond, G. P., 1977. *Improvement in Rail Support*. Transportation Research Record 653: 11-21.

Raymond, G. P. and Diyaljee, V. A., 1979. *Railroad ballast load ranking classification.* Journal of the Geotechnical Engineering Division (ASCE) 105(GT10): 1133-1153.

Selig, E. T., and Waters, J. M., 1994. *Track Geotechnology and Substructure Management*. Thomas Telford, London.

Skoglund, K. A., 2002. *A study of some factors in mechanistic railway track design*. PhD thesis, Norwegian University of Science and Technology, Trondheim, Norway.

Skoglund, K. A. et al., 2002. *Development of a large triaxial cell apparatus with variable deviatoric and confining stresses*. Proceedings of the 5th International symposium on unbound aggregates in roads (UNBAR 5), Nottingham, UK.

Thom, N. H. and Brown, S. F., 1989. The mechanical properties of unbound aggregates from various sources. In: R. H. Jones and A. R. Dawson (Ed) Unbound Aggregates in Roads: 130-142. Proceedings of the 3rd International symposium on unbound aggregates in roads (UNBAR 3), Nottingham, UK.

Ugur, I., Demirdag, S. and Yavuz, H., 2010. *Effect of rock properties on the Los Angeles abrasion and impact test characteristics of the aggregates.* Materials Characterization 61(1): 90-96.

West, T.R., Johnson, R.B. and Smith, N.M., 1970. *Tests for evaluating degradation of base course aggregates*. National Cooperative Highway Research Program 98, pp.94.

Influence of mineral grain size, grain size distribution and micro-cracks on rocks' mechanical strength.

Presented at the 14th Euroseminar on Microscopy Applied to Building Materials. Helsingør, Denmark, in 2013

Paper IV

INFLUENCE OF MINERAL GRAIN SIZE, GRAIN SIZE DISTRIBUTION AND MICRO-CRACKS ON ROCKS' MECHANICAL STRENGTH.

R. Nålsund[a], V, Jensen[b]

a.   *Norwegian University of Science and Technology, Department of Civil and Transport Engineering, 7491 Trondheim Norway. roar.nalsund@jbv.no*

b.   *Norwegian Concrete and Aggregate Laboratory LTD, Sorgenfriveien 11, 7037 Trondheim Norway. viggo.jensen@nbtl.no*

Abstract

Previous investigations have shown that the mineral grain size is an important parameter for understanding differences in mechanical properties of rock types of the same composition. Different techniques for measuring the grain size (diameter) and grain size distribution quantification have not been of great concern in the literature. The objective for this study is to show how the mineral grain size and grain size distribution can be quantified in order to find the most suitable correlation with mechanical strength (aggregate crushing resistance). Rock samples from 16 different railway ballast quarries make up a wide variety of igneous, metamorphic and consolidated/ metamorphosed sedimentary rocks, some of them subjected to extensive alteration. Most of them are fine to very fine grained. All the tested rock types are composed of combinations of principal rock-forming silicate minerals with few exceptions. The mineral grain size is measured manually by optical microscopy due to the occurrence of very fine grained minerals. A simple technique for measurement of mineral grain size (D_{50}) from a grain size distribution curve similar to a sieving curve is demonstrated. One of the intentions of the investigation was to avoid overestimation of the significance for mechanical strength of very fine mineral grains when they are numerous, and to enable a quantitative classification of the slope of the grain size distribution curve (from well-graded to single-graded). Textural parameters like grain size, grain size distribution curve and micro-cracks are compared with Los Angeles abrasion test (LAA) and micro-Deval test and poor correlations were found.

Keywords: Mechanical strength, microscopy, mineral grain size distribution, railway ballast, Los Angeles abrasion test, micro-Deval test.

Introduction

Background

The relationship between the textural and mechanical parameters of rock aggregates from the mechanics point of view is quite complicated (Liu et al. 2005 abstract). Texture is, according to Spry (1969), defined as (1) the mineral grain size, (2) mineral grain size distribution (single graded or well graded), (3) shape (more or less complex perimeter) and (4) spatial orientation (foliation) of mineral grains. In addition, other petrological parameters like (5) mineral distribution (even or uneven E-modulus), (6) grain boundary relations (suturering), (7) the amount of micro-cracks, (8) mineral deformation and (9) degree of alteration (sericite in feldspar) are also affecting the mechanical strength. A majority of these properties can be quantified with high accuracy mainly through microscopic examination of thin section in case the rock has kept its primary texture. However these investigations are still difficult to translate into absolute figures exactly revealing the functional properties, e.g. unbound base course resistance to fragmentation and abrasion. Examining different rock samples, all these parameters mentioned above may be present at the same time but with varying magnitude from sample to sample. Thus it is obvious that it can be difficult to document the degree of correlation between a texture or petrologic parameter on the one hand, and a mechanical parameter on the other hand. This is why many researchers examine one rock at a time to minimize the number of variables.

Grain size and shape

Several investigations have shown that the grain size is an important parameter for understanding differences in mechanical properties of rock types of the same composition (e.g., Lounsbery and West (1965) on limestone; Onodera and Asoka-Kumara (1980) on granite; Ballivy (1984) on limestone; Singh (1988) on greywacke; Brattli (1992) on mafic rocks; and Liu et al. (2005) on granite). They all observed that decreasing grain size increases both the resistance to fragmentation and abrasion. Brattli (1992) also proved that the influence of mineral grain size overruled the effect from all the other parameters when the average diameter was about 1 mm or less (arithmetic average). Kazi and Al-Mansour (1980) came to the same conclusion in spite of their investigation included 14 different types of igneous rocks of a wide variety. It should be pointed out that it appears as if this conclusion is valid for both crystalline and sedimentary non foliated rocks despite quite different origin. Åkesson et al. (2001) investigated granite and granodiorite and used the term perimeter (mm/mm^2), i.e. the circumference of minerals and mineral phases, which provides information on the complexity of grain boundaries based on image analysis and this reflects the strength of the rock. He revealed that rocks with high perimeter values also had the highest resistance to fragmentation (LAA) and abrasion (Nordic ball mill). The perimeter can also express the mineral grain size where increasing perimeter values correspond with decreasing grain size (increasing mechanical strength).

Based on Griffiths theories (Griffith1921), Wills and Atkinson (1993) gives an explanation of why this correspondence is reasonable. All rocks contain inherent micro-cracks derived from many sources due to the appreciable mechanical, thermal and chemical actions during many millions of years. The measurable tensile stress of a rock is much less than that can be predicted theoretically. This is due to the presence of small cracks or flaws. The extremities of these cracks acting as stress raisers. Griffith assumed that the theoretical stress was obtained at the end of the crack (Figure 1), even though the average stress was still far below the theoretical strength. Fracture occurs when the stress at the ends of the cracks exceeds the theoretical strength (critical crack length). As the mineral particle size decreases the portion of cracks above the critical crack length decreases and the tensile strength increases.
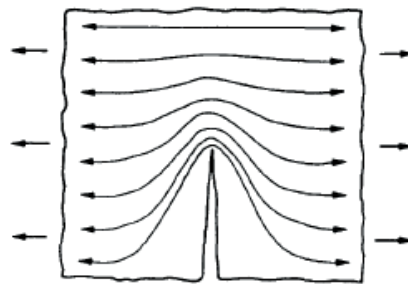
Figure 1: Stress concentration at a crack tip. After Wills and Atkinson (1993).

This is in accordance with Eberhardt et al. (1999) which suggests that longer grain boundaries and larger inter granular cracks, resulting from increased grain size, provide longer paths of weakness for growing cracks to propagate along. This promoted degradation of material strength once the longer cracks began to coalesce and interact.

Micro-cracks

Micro-cracks are an important parameter because they create mechanically weak planar discontinuities in rocks on the grain scale or smaller, commonly with some dilation but with negligible displacement. Kranz (1983) subdivides micro-cracks into (i) grain-boundary, which are associated and perhaps coincide with boundaries of grains, (ii) intra granular, which are confined to the interior of a single grain, and (iii) trans granular or "long" micro-cracks, which cross more than one grain. In addition two other types of discontinuities have been launched (Nålsund and Jensen 2011), namely massive porosity and holes. Strength property change drastically as the characteristics and quantity of micro-cracks are modified under stress. In most cases grain boundaries are preferred sites for tiny flaws and cracks, which may develop to penetrative fractures (Brattli 1992).

A technique for quantifying micro-cracks was introduced by Nishiyama et al. in 1990 by combining microscopy with image analysis. They described the results of saturating pore spaces and micro-cracks with synthetic resins mixed with fluorescent paint and dye before microscopy. In this way, pore spaces and micro-cracks could be visualized under ultraviolet (uv) light due to a great difference in displayed brightness, and, using image analysis, their characteristics including porosity, and total length of micro-cracks per unit area, could easily be measured (Nishiyama and Kusuma 1990/1994). Since then several investigators have used this technique. Later on Nishiyama and Kusuda (1996) showed how different stages in the weathering process could be quantified by launching the term image brightness to describe the increase in number of micro-cracks. But they did not give any closer description of the term.

Different types of micro-cracks occur in different amounts in thin sections and are therefore difficult to quantify. Moreover, quantification of micro-cracks is not a standard procedure and the few published papers dealing with this subject have not given a "standardized" way to do it. Image analysis is one method being used for quantification of micro-cracks in fluorescent impregnated thin sections but the results up till now are not promising for all types of rocks. Image analysis may have problems quantifying distinct micro-cracks in combination with more massive-porosity cracking and "holes". Both porosity and holes as observed in most of the aggregate samples in this study. Therefore a new measurement method has been developed and used in the present doctoral project, namely luminescence measurement in order to quantify the amount of micro-cracks and which is more closely described elsewhere in Nålsund and Jensen (2011). The present work uses the intensity of light in fluorescent impregnated thin sections assessed by luminescence measurements for indirectly quantifying micro-cracks and porosities in the aggregates.

Test materials

The selection of rock samples was focused on representing a wide variation in the mechanical properties, i.e. LAA value, as well as to be sufficient representative for Norwegian rock types. It was requested that samples should be taken from quarries supporting The National Railway Administration with railway ballast, if possible. Most samples meet the Norwegian requirements for mechanical strength. The rock samples make up a wide variety of igneous rocks, metamorphic rocks and consolidated/metamorphosed sedimentary rocks. Most rocks are fine to very fine grained. All the tested rock types are composed of combinations of principal rock-forming silicate minerals with few exceptions. Representative rock samples were sampled from stockpiles inside the quarries (commercial products). All samples were required to have passed two crushing stages, no more or less, with a jaw and a cone crusher. The ballast samples from different quarries were assumed to be homogeneous and representative of each source. No matter how random the selection process may be, it is difficult to avoid differences between samples from the same source. This was clearly documented during the microscopic inspection of thin sections to provide texture characteristics. With aim to reveal a possible geological variation in the deposit, rock fragments that "looked" different were selected for further investigation. Three thin sections from each deposit in average were prepared to cover "all" variations.

Method

Looking for correlations between rock texture and mechanical strength the challenge is to express the textural property in the most suitable way for the purpose. The purpose of the current study described in this paper has been to create a simple technique to quantify the mineral grain size distribution to each rock type through thin section analysis using optical microscopy. It is necessary to decide how to count the mineral grains and how to express the grain size. In the present work the grain size was not recorded as that conventionally used as coarse, medium and fine grained rock. Generally all grains were counted with following specification. (i) An altered crystal was counted as one grain unless the alteration products were visually dominating. (ii) In grains inter grown or otherwise combined to make a unit of fine grained matrix all grains were counted. (iii) Inter-grown mineral faces which occur in same crystal were counted as one. (iv) Small inclusions in grains were not counted. In practice, the results obtained were typically given in micro meters.

There are several ways of quantifying the grain size on the basis of examination of thin section with optical microscopy. The most conventional way is to express mean grain size with

arithmetic or median value based on one-dimensional measurements along a line of traverse (number of grain boundaries per length unit e.g. 30mm (Chayes 1956) or individual recording of each grain (frequency) respectively. A sufficiently reliable estimate (total traverse length is divided by total number of grain chords) is obtained when the magnitude of the continuously calculated average chord length (by use of Excel spread sheet) appears almost stable (Figure 2). In this example the recording could have been terminated after grain number 250 approx and not 1000 without any change in the conclusion. A closure after 160 is an alternativ, but that would have been too early.
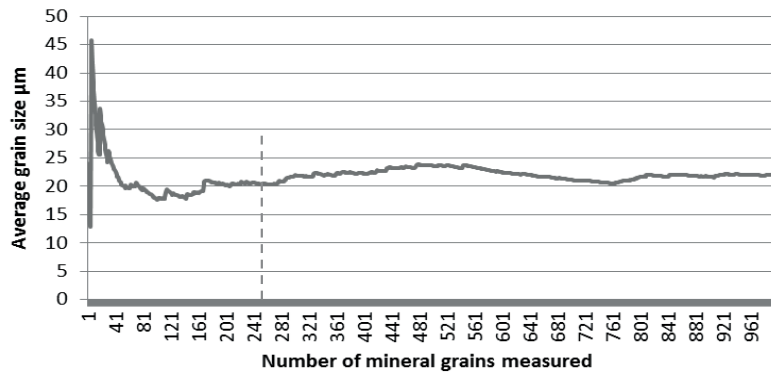
Figure 2: The plot shows the relation between calculated average mineral grain size (arithmetic) and the number of grains counted (Steinkjer quarry). Note that average grain size is stable after approximately 250 measurements.

This can avoid oversized measurements and will usually occur between 200 and 1000 counts, dependent on how inhomogeneous, well graded or porphyritic the rock is. However, the thin section represents a two-dimensional plane that cuts the rock minerals randomly (cross section) and the recorded average chord length will therefore always be an underestimation (Johnson 1994) of the real grain size. French et al. (2001) found out experimentally that the mean grain size (in mm) could be more correct determined by multiplying the average chord length by 1.75. This factor was employed in this paper. An example on grain size frequency or the relative values of the different grain-size categories are shown in Figure 3. 50% on right vertical axis represents the mean grain size (median). In case of any possible foliation the line of traverse was oriented in two directions perpendicular to each other.
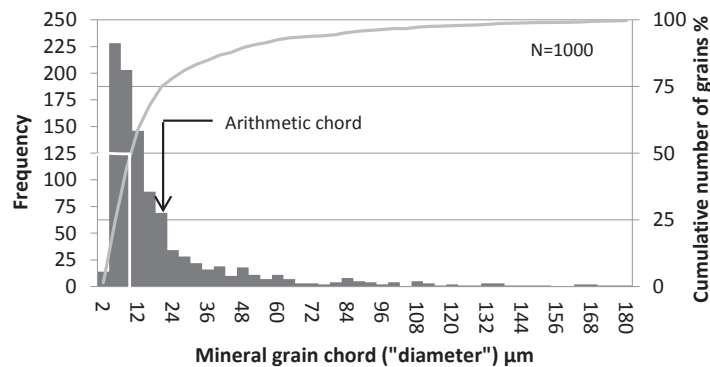
Figure 3: Mineral grain size frequency (the relative values of the different grain-size categories) and cumulative grain size distribution curve for a meta sandstone (Steinkjer quarry) based on measurements of grain "diameter". Average (median) grain size is 10 micro meter (marked on the plot (50%)), arithmetic average (calculated) is 22 micro meter (not multiplied with French factor 1.75)

Further, in the present study the grain size was calculated by transforming measured diameter D (chord length) to a corresponding grain cross-section area (circle area with $A=\Pi*(D/2)^2$)). As can be seen all the grains in the grain size distribution curve in Figure 3 have the same importance which means that the coarsest grains are underestimated in terms of influence on the mechanical strength. This is based on the hypothesis that one coarse grain is more important (in a negative way owing to the fact that coarser grains introduce longer micro-cracks) for the strength than a fine one and needs to be given more weight. An example: mineral grains coarser than 0.1mm constitute about 51% of the total thin section area (Figure 4), but account to 3% of the total number of measured grains (Figure 3). Hence, we need to increase the influence of coarse grains at the sacrifice of smaller grains by creating a new grain size distribution curve (Figure 4) similar to the conventional sieving or grading curve for aggregate characteristics where each fraction is measured by weight and not by total number of grains.
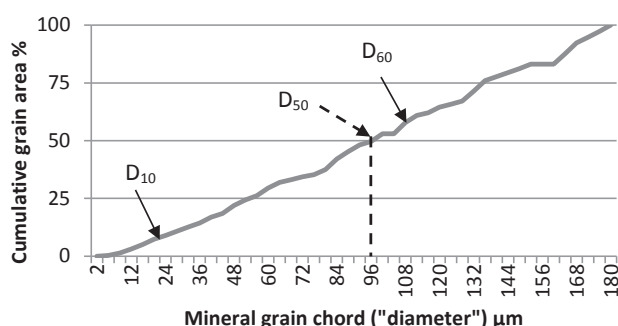
Figure 4: An instance of cumulative mineral grain size distribution curve based on calculated grain area (meta sandstone /Steinkjer quarry. The curve is comparable with that of sieving of aggregates. D_{50} is about 95 micro meter.

For converting thin section data to their sieve equivalents we assume that each grain's cross-section area displayed in thin section is equal to a circle calculated on the basis of the measured "diameter". This is an approximation that is supposed to be sufficiently accurate, taken into consideration all the other influencing textural parameters that appear without control. Instead of measuring the total weight within each fraction, the amount of calculated grain area was measured and a similar "sieving curve" was created. The mineral grain size in Figure 4 labeled D_{50} means, in this context, that 50% of the area in the corresponding thin section is constituted of mineral grains larger than the actual grain size (0,096mm) as shown in Figure 4. The image of the corresponding thin section (Steinkjer quarry) can be seen in Figure 5.

This model enables to classify quantitatively whether the mineral grain size distribution is well-graded or single graded or something in between. Correlating the grain size distribution curve (i.e. the slope of the grading curve) with mechanical strength is now possible by the ratio of the values for the parameters D_{10} and D_{60} taken from Figure 4 (Coefficient of uniformity $C_u=D_{60}/D_{10}$). This is a well-known technique among geotechnical engineers (Hazen 1892) used to describe coarse grained soil. In the literature no proposal has been found on how to classify a well graded or a uniformly graded grain size distribution in terms of C_u by microscopic analysis. The challenge is to express the slope of the grading curve in the most suitable way for the purpose which is to find out how the rock's grain size distribution influences the mechanical strength (LAA).

If we want to increase the influence of coarse grains even more, the grain cross-section area can be converted to a ball with volume $V=4/3*\Pi*(D/2)^3$ based on the same measured grain "diameter". This variant will be carried out elsewhere. The technique with calculated spherical grains was proposed by Lindqvist et al. (1999).
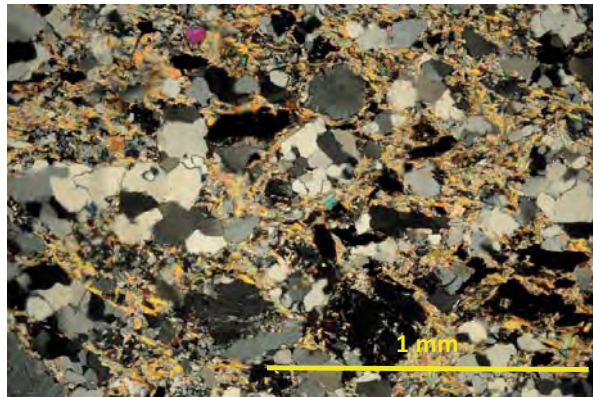
Figure 5: Thin section image of a very fine grained meta sandstone (Steinkjer quarry), X-polarised light.

Results

The average mineral grain size has for a long time been associated with rocks' mechanical strength. Conventionally understood the average mineral grain size means the arithmetic average of individual measurements of chord length for each mineral grain (diameter) along a line of traverse from inspection of two-dimensional thin sections. This technique is also used in the present paper. The results of this part of the investigation are shown in Figure 6 and Figure 7. The first plot indicates a rather poor correlation between mineral grain size and mechanical strength expressed as $LAA_{10/14\ mm}$ loss.
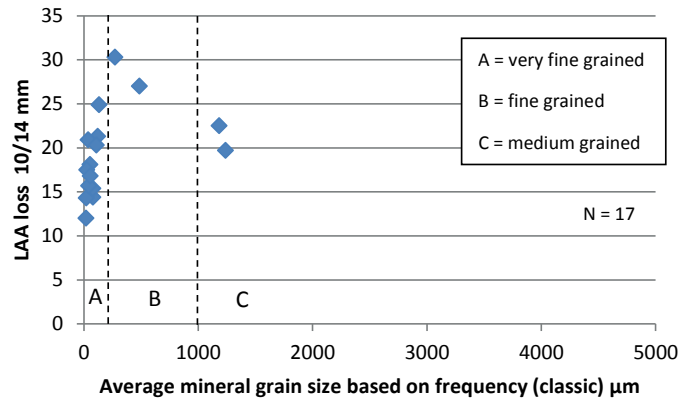
Figure 6: Average mineral grain size (arithmetic) based on grain frequency (classic calculation) plotted against $LAA_{10-14mm}$. Most samples were crystalline rocks and constituted of mainly hard minerals.

The 13 samples within sector A "Very fine grained" reveal a very scattering resistance to fragmentation with recorded LAA values from 12 to 30. It was expected that they should be situated in the lower part of the actual strength range. A possible explanation is that other rock texture properties have an obvious influence on the mechanical strength, which does not comply fully with Brattli (1992). He stated that the impact from mineral grain size overrules the effect from all the other parameters when the average diameter (based on frequency) is about 1mm or less. $LAA_{10/14\ mm}$ was chosen because this LAA procedure causes a more uniform crushing impact on the test material

(Erichsen et al. 2011) and can be a more suitable test for assessing ballast materials' durability compared with $LAA_{31,5/50\ mm}$ which has a lot of abrasion impact in addition. The plot with $LAA_{31.5/50\ mm}$ against average grain size shows no correlation either (not displayed).
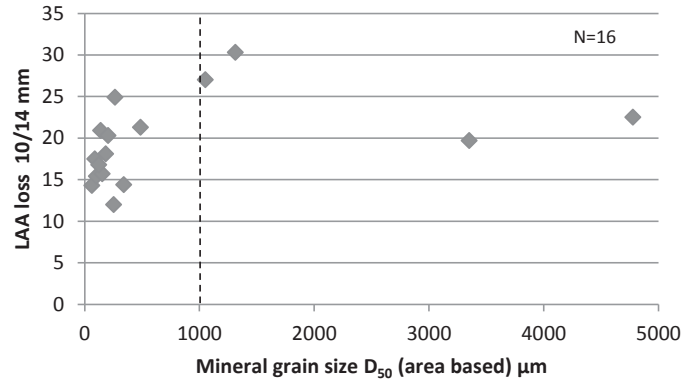
Figure 7: Mineral grain size D_{50} based on grain area plotted against $LAA_{10/14mm}$ (mechanical strength) loss. Most samples were crystalline rocks and are constituted of mainly hard minerals.

The use of arithmetic (or median) value as a measure for mean mineral grain size can overestimate the significance of the smallest grains because they are most numerous as seen in Figure 3. The use of parameter D_{50} will emphasize the importance of the more coarse grains. The plot in Figure 7 shows measured $LAA_{10/14mm}$ loss with mineral grain size D_{50} (area based). In Figure 8 the LAA test is replaced with micro-Deval test but none of them can show any association with mineral grain size.
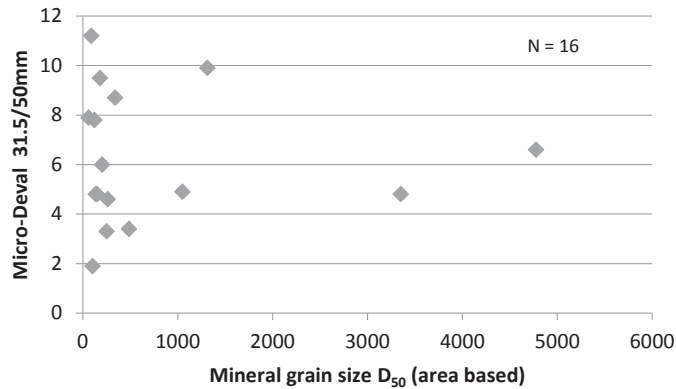
Figure 8: Mineral grain size D_{50} based on grain area plotted against micro-Deval (mechanical strength). Test results from alternative fraction Micro-Deval $_{10/14mm}$ gave fairly the same correlation.

Another central textural variable that influences mechanical properties is the presence of micro-cracks. This was pointed out by Johansson (2011) who investigated granitic and gabbroid rocks. In present study micro-cracks, measured in terms as luminescence, were taken into account in an attempt to reduce the scattering in Figure 6 and to try to associate the amount of cracks with the mechanical strength. As can be seen in Figure 9 there is no significant correlation between luminescence and $LAA_{10/14mm}$. Use of alternative fraction 31.5/50 mm gave the same result (not displayed). In order to eliminate the effect of micro-cracks, a selection of samples (7 in total) with almost equal occurrence concerning luminescence (Lux values from 0.51 to 0.61) were compared with accompanying values for LAA loss, but unfortunately very low correlation did occur (not displayed).

This suggests that other geological parameters in addition to mineral grain size and micro-cracks can be influencing the ballast's respond to impact such as grain size distribution and alteration products. On the other hand luminescence obtained good correlation with water absorption on the same samples (Nålsund and Jensen 2011).
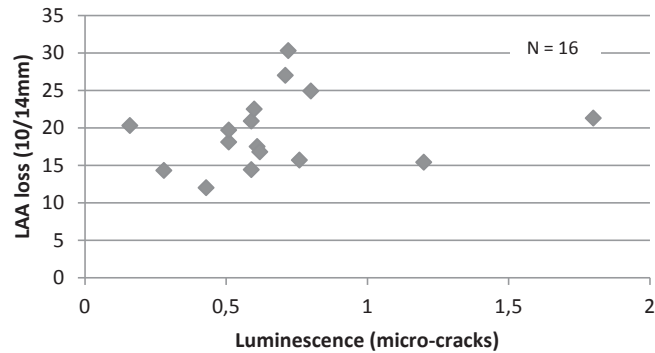
Figure 9: Luminescence against $LAA_{10/14mm}$ loss (mechanical strength). Test results from alternative fraction $LAA_{31.5/50\,mm}$ gave fairly the same correlation.

The slope of the grading curve based on microscopic measurements of chord lengths of mineral grains in thin section is correlated with $LAA_{10/14\,mm}$ in Figure 10. As can be seen no correlation occurs in this case. This topic has not been of great concern in the literature, but positive correlations exist. Johansson (2011) investigated granitic and gabbroid rocks and found that uneven-grained granitoid rocks obtained poorer results from the mechanical analyses ($LAA_{10/14mm}$ and micro-Deval (both 10/14mm and 31.5/50 mm) than even-graded ones.
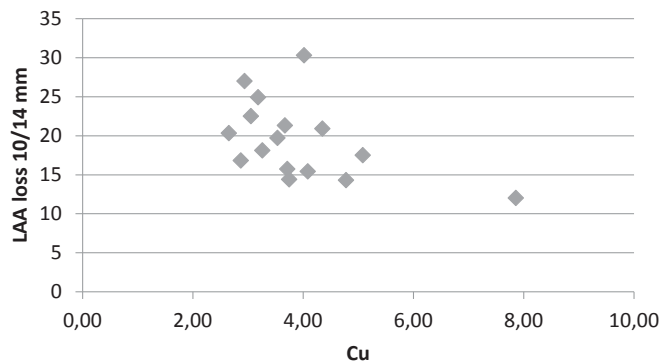
Figure 10: Correlation between slope of grading curve ($Cu = D_{60}/D_{10}$) and $LAA_{10/14\,mm}$ loss (mechanical strength)

Discussion

Reliable data

According to the literature a more evident association between texture and mechanical strength should have appeared in the results from present investigation. The scattering and absent correlations in the displayed plots are most probably due to large random errors in measurement of various petrographic parameters. There are several causes of this. The primary reason can be that too many different rocks in the test material will introduce too many uncontrollable parameters (Liu et al. 2005). However, exceptions to the "rule" exist. Kazi and Al-Mansour's investigation (1980) came up

with good correlations in spite of 14 different types of igneous rock samples of a wide variety, from basic till acidic in composition.

Another obvious uncertainty is the difficulty with achieving reproducible counting of average mineral grain size. The ballast samples from different quarries were assumed to be homogeneous and representative of each source. No matter how random the selection process may be, it is difficult to avoid differences between samples from the same source. This was clearly documented during the microscopic inspection of thin sections to provide texture characteristics (Nålsund and Jensen 2011). With aim to reveal a possible geological variation in the deposit, rock fragments that "looked" different were selected for further investigation. Three thin sections from each deposit in average were prepared to cover "all" variations. I addition it is necessary to find out how large part of the rock source each thin section represents in such a way that the respective average grain size can be weighted. This has not been taken into account in this investigation.
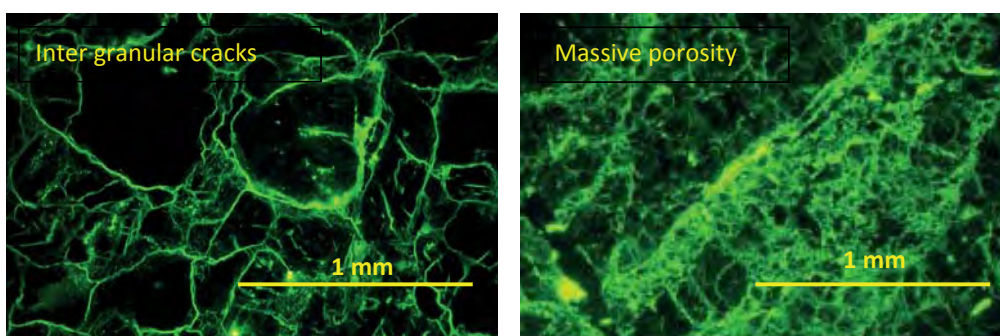
Figure 11: Examples of thin section (meta sandstone (left) and cataclasite (right)) in fluorescence light. Transmitted light was measured in Lux to express the average amount of both micro-cracks, porosity and holes.

The third uncertainty is connected to the measuring of micro-cracks which in this study is based on fluorescent light intensity in thin section (Figure 11). Several of the investigated rocks contain both cracks and porosity and holes. However, the light passing through the thin section does not differentiate between the three types of voids and is an average measurement. It is unknown, also in the literature, whether porosity and holes in crystalline rocks can decrease the strength. According to Figure 11 it can be a likely conclusion that porosity and holes do not contribute to any weakening of the rock but rather lead to increased scattering in the plot.

Grain size distribution curve

The advantage in reproducing the grain size distribution curve obtained through sieving is that average mineral grain size can be expressed in an alternative way (D_{50}) and enable a technique for numerical description of the qualitative term "well graded" and "uniformly graded" by Coefficient of conformity C_u. The three basic problems here are to choose the right parameters to be measured in the thin section, the recalculation of results from a 1-D measurement (chords along a line of traverse) to give a 2-D (area) or a 3-D (spherical) grain size distribution curve and to determine gradient intervals for different degrees of the term "graded". The gradient intervals valid for a coarse grained rock do not need to be the same as for a fine grained rock. The microscopic examination of thin section in this paper did not provide suitable data for making a proposal to gradient intervals.

This project has not controlled the reliability of the grain size distribution curve which means the relation between thin section data and true size data. Lindqvist et al. (1999) used thin sections of even-graded sand cast in epoxy to investigate the relationship between the grain size distribution curve and the true sieving curve, and the conformity was good.

Lack of correlations between textural properties and mechanical strength

This study shows poor correlations between rocks' textural properties and mechanical properties when fine grained rocks are concerned. Only linear-regression analyses have been used in this study. In efforts to explain partial cooperation of several petrographic agents on the one mechanical property, multiple-regression analyses have to be performed. Several possible causes to the lack of correlations can be mentioned: (i) Most probable cause is statistical error. The different rocks are not homogeneous and several of the associated thin sections used are not representative (too few). (ii) It is difficult to know what type of mineral grain that contributes most or less to the mechanical strength in metamorphic rocks, the original grain or the alternation product. (iii) The luminescence measurements include passing light from both cracks and porosity and holes. It is not sure that the two last contribute to the weakening of the rock. (iv) Finally it can be suggested that different rocks respond with different magnitude towards the same textural parameter, such as mineral grain size, grain size distribution and micro-cracks. Searching for correlations, many different rocks involved make it difficult to obtain good results.

Conclusions and summary

The influence of some textural properties of 16 different rocks (most fine grained) on the mechanical properties of railway ballast aggregates can be summarized as follows:

1. A simple technique for determination of average mineral grain size (D_{50}) derived from a grain size distribution curve similar to a sieving curve is demonstrated. The intention was to avoid overestimation of the significance of very fine mineral grains in terms of mechanical strength when they are numerous.
2. The conventional average mineral grain size ("diameter") based on frequency did not show any correlation with LAA loss (resistance to crushing) neither with $LAA_{10/14mm}$ nor $LAA_{31.5/50 mm.}$
3. The conventional average grain size (chord length) based on frequency did not show any correlation with micro-$Deval_{31.5/50 mm.}$
4. The mineral grain size D_{50} derived from the "sieving curve" did not show any correlation with neither LAA nor micro-Deval, independent of the test fraction. It is not proved that it is more correct to use D_{50} instead of average diameter (arithmetic).
5. The amount of luminescence (micro-cracks) did not correlate with $LAA_{10/14mm}$ loss. Separate plotting of seven samples with quite equal occurrence of luminescence did not improve the correlation.
6. It can be suggested that different rocks respond with different magnitude towards the same textural parameter, such as mineral grain size, grain size distribution and micro-cracks.
7. The lack of correlations between grain size (fine grained rocks) and mechanical strength can indicate that the amount of alteration minerals can matter.
8. There is no correlation between the slope of the grading curve (Cu) and $LAA_{10/14mm}$ loss.
9. The lack of correlation between luminescence (micro-cracks) and $LAA_{10/14mm}$ loss (resistance to crushing) can indicate that micro-cracks have minor influence on mechanical strength when fine grained rocks are concerned.

One experience from this project comply with Johansson (2011) who stated that *"The result of the present study show the complex pattern of associations between the granitoid and gabbroid intrusive rocks' mechanical properties tested with methods used in the aggregate industry and their petrographic variables"*.

Acknowledgement

References

Brattli, B. (1992): "The influence of geological factors on the mechanical properties of igneous rocks used as road surface aggregates." *Engineering Geology,* Vol. 33, 31-44.

Ballivy, G. and Dayre, M. (1984): "The mechanical behavior of aggregates related to the physico-mechanical properties of rocks" (in French). *Bulletin of Engineering Geology and the Environment*, Vol.29, 339-342.

Chayes, F., 1956: "Petrographic Modal Analysis". Johan Wiley & Sons, New York.

Erichsen, E., Ulvik, A. and Sævik, K. (2011): "Mechanical Degradation of Aggregate by the Los Angeles-, the Micro-Deval- and the Nordic Test Methods." *Rock Mechanics and Rock Engineering*, Vol. 44, 333-337.

Eberhardt, E., Stimpson, B. and Stead, D. (1999): "Effects of grain size on the initiation and propagation thresholds of stress-induced brittle fractures". *Rock Mechanics and Rock Engineering.* Vol. 32, No. 2, 81-99.

French, W. J., Kermani, S. and Mole, C. F. (2001): "Petrographic evaluation of aggregate parameters". *8th Euroseminar on Microscopy Applied to Building Materials.* Athen, Greece.

Griffith, A. A. (1921). "The phenomena of rupture and flow in solids." *Transactions of the Royal Society of London,* Series A **221**, 163-198.

Hazen, A. (1892): "Experiments Upon the Purification of Sewage and Water at the Lawrence Experimental Station, No. 1." *Massachusetts State Board Health Publication*, No. 34 (Twenty-Third Annual Report, for 1891, p. 428-434).

Johansson, E., Lukschová, Š. and Miškovský, K. (2011): "Petrographic characteristics of granitoid and gabbroid intrusive rocks as a tool for evaluation of mechanical properties". In E. Johansen (2011): Technological properties of rock aggregates. PhD Thesis, Luleå University of Technology, Luleå, Sweden.

Johnson, M. R. (1994): "The thin section grain size analysis revisited". *Sedimentology*, Vol. 41(5), 985-999.

Lindqvist, J-E. and Sandström, M. (1999): Determination of the size distribution, sieve curve, for aggregates using optical microscopy. *7th Euroseminar on Microscopy Applied to Building Materials,* Delft, Netherlands.

Liu, H., Kou, S., Lindqvist, P-A., Lindqvist, J.E. and Åkesson, U. (2005). "Microscope Rock Texture Characterization and Simulation of Rock Aggregate Properties." SGU project 60-1362/2004 (Geological Survey of Sweden).

Kazi, A. and Al-Mansour, Z.R. (1980): "Influence of geological factors on abrasion and soundness characteristics of aggregates." *Engineering Geology*. Vol. 15, 195-203.

Kranz, R.L. (1983): " Micro-cracks in rocks: a review." *Tectonophysics*. Vol. 100, 449–480.

Lounsbery, R.W. and West, T.R. (1965): "Petrography of some Indiana aggregates in relation to their engineering properties." *University of Kentucky, Engineering Experiment Station Bulletin Series.* Vol. 20, No. 2, 24-41.

Nishiyama, T., Kusuda, H., and Kitagawa, M. (1990): "A new method of visualization and image analysis of micro-cracks (in Japanese with English abstract)". *Journal of the Mining and Materials Processing Institute of Japan.* Vol. 106, 573-579.

Nishiyama, T. and Kusuda, H. (1994): "Identification of pore spaces and micro-cracks using fluorescent resins." *International Journal of Rock Mechanics and Mining Sciences & Geomechanics Abstracts*. Vol. 31, No. 4, 369-375.

Nishiyama, T. and Kusuda, H. (1996): "Application of a fluorescent technique to the study of the weathering process." *Engineering Geology*. Vol. 43, 247-253.

Nålsund, R. and Jensen, V. (2011): "Classification of micro-cracks, luminescence measurement, water absorption and frost resistance in Norwegian produced railway ballast." *13th Euroseminar on Microscopy Applied to Building Materials.* Ljubljana, Slovenia.

Onodera, T.F., and Asoka-Kumara, H.M. (1980): "Relation between texture and mechanical properties of crystalline rocks." *Bulletin of Engineering Geology and the Environment.* Vol. 22, 173-177.

Singh, S.K. (1988): " Relationship Among Fatigue Strength, Mean Grain Size and Compressive Strength of a Rock." *Rock mechanics and rock engineering.* Vol. 21, 271-276.

Spry, A. (1969): "Metamorphic Textures." Pergamon, London, 350 pp.

Wills, B. A. and Atkinson, K. (1993): "Some observations on the fracture and liberation of mineral assemblies." *Materials Engineering.* Vol.6. No. 7, 697-706.

Åkesson, U., Lindqvist, J, E., Göransson, M., Stigh, J. (2001): "Relationship between texture and mechanical properties of granites, central Sweden, by use of image-analysing techniques. *Bulletin of Engineering Geology and the Environment*. Vol. 60, 277-284.

Petrographic description
of rock aggregates

Appendix II

Petrographic description of rock aggregate

Sample no.08115A **Location: Steinkjer pukkverk**

Macroscopic description. Fine grained grey coloured granoblastic - granular rock

Mineralogy: estimated by use of measurement grid (363 points)

quartz	mica*	k-feldspar	plagioclase	opaque	epidote	carbonate	titanite
60	22	15	1	2	<1	<1	<1

* Muscovite (sericite)

Crystal/grain size: average 0.1-0.2 mm, max 1 mm (feldspar)
Micro texture: granoblastic - granular, indistinct lamination by bands with higher content of opaque phases, epidote and carbonate
Crystal/grain contact: straight and curved (polycrystalline quartz), concave/convex (feldspar/quartz particles)
Recrystallization: polycrystalline quartz, sericite
Deformation: strained quartz and feldspar, recrystallized quartz
Alteration: sericite , epidote, carbonate (saussuritization)
Micro cracking (UV light): intergranular
Classification: diagenetic/low metamorphosed sedimentary rock
Naming: meta sandstone, meta siltstone, alternatively quartzite

Micro photos:
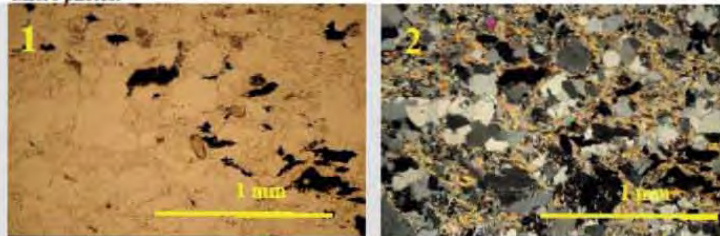
Micro photos of selected area in thin section

1 Ordinary light. Note opaque phases

2 Polarized light. Note high content of sericite

3 Fluorescence light. Note micro cracks

Viggo Jensen 17 September 2008

Petrographic description of rock aggregate

Sample no.08115B **Location: Steinkjer pukkverk**

Macroscopic description. Fine grained grey coloured granoblastic-granular rock

Mineralogy: estimated by use of measurement grid (363 points)

quartz	k-feldspar**	mica*	epidote	opaque	chlorite	carbonate	fluorite
69	24	4	2	1	<1	<1	<1

* Muscovite (sericite)** most feldspar occur in "matrix"

Crystal/grain size: average 0.1 mm, max 1 mm (feldspar), "matrix" 0.02 mm
Micro texture: granoblastic - granular, interconnected elongated lenticules and veins of polycrystalline quartz, "matrix" consisting mainly of inter grown 0.02 mm feldspar and quartz crystals
Crystal/grain contact: straight and curved (polycrystalline quartz), floating and concave/convex (feldspar/quartz particles)
Recrystallization: polycrystalline quartz, "matrix", sericite
Deformation: strained quartz and feldspar, recrystallized quartz
Alteration: chlorite (chloritization), epidote and carbonate vein (saussuritization)
Micro cracking (UV light): intergranular
Classification: diagenetic/low metamorphosed sedimentary rock
Naming: quartzite, alternatively meta sandstone, meta siltstone
Micro photos:
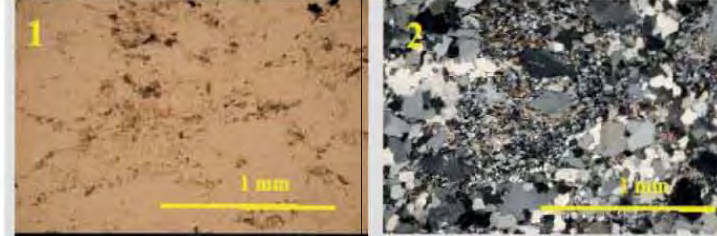
Micro photos of selected area in thin section

1 Ordinary light. Note opaque phases

2 Polarized light. Note interconnected polycrystalline quartz lenticules and veins

3 Fluorescence light. Note micro cracks

Viggo Jensen 18 September 2008

Petrographic description of rock aggregate
Sample no.08115F **Location: Steinkjer pukkverk**

Macroscopic description. Fine grained dark-grey coloured laminated rock|

Mineralogy: estimated by use of measurement grid (< 500 points)

quartz	mica*	k-feldspar	opaque	chlorite	epidote	fluorite	titanite
50	37	6	7	<1	<1	<1	<1

* Biotite, muscovite (sericite)

Crystal/grain size: average 0.1 mm, max 1.5 mm (feldspar)
Micro texture: laminated by thin parallel bands with higher concentration of opaque phases and biotite
Crystal/grain contact: straight and curved (polycrystalline quartz), floating and grain contact (feldspar/quartz particles)
Recrystallization: few polycrystalline quartz, biotite and sericite
Deformation: strained quartz and feldspar, recrystallized quartz
Alteration: chlorite in thin late phase cracks (crossing lamina)
Micro cracking (UV light): intergranular and in lamina
Classification: diagenetic/low metamorphosed sedimentary rock
Naming: meta graywacke

Micro photos:
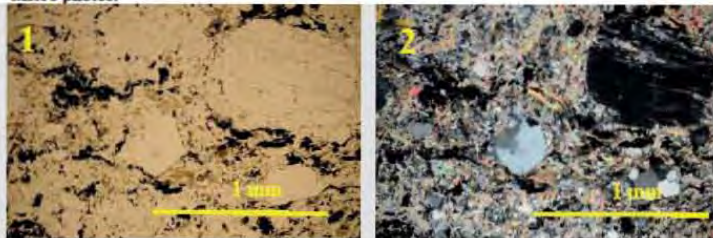
Micro photos of selected area in thin section

1 Ordinary light. Note opaque phases and biotite

2 Polarized light. Note high content of biotite and sericite

3 Fluorescence light. Note micro cracks

Viggo Jensen 17 September 2008

Petrographic description of rock aggregate
Sample no. 08115-2A **Location: Meraftåsen (Kvål)**

Macroscopic description. Green fine grained porphyric rock

Mineralogy: estimated by use of measurement grid (363 points)

plagioclase	epidote	chlorite	actinolite	carbonate	cryptocrystalline*	opake
45	18	12	11	4	10	<1

* Possible carbonate/ titanite

Crystal/grain size: matrix 0.01-0.2 mm, phenocrysts 1-2 mm
Micro texture: seriate texture with relict porphyric texture
Crystal form: anhedral plagioclase phenocrysts
Recrystallization: epidote, chlorite, actinolite, carbonate, albite? and quartz. Pseudomorphs and amygdales with carbonate, actinolite and chlorite
Deformation: not observed
Alteration: saussuritization, chloritization, carbonatization
Micro cracking (UV light): intergranular
Classification: low grade metamorphosed basalt (greenschist facies)
Naming: greenstone
Micro photos:
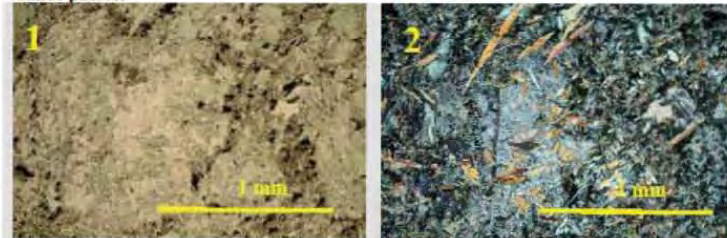
Micro photos of selected area in thin section

1 Ordinary light. Note plagioclase phenocryst

2 Polarized light. Note fibrous actinolite

3 Fluorescence light. Note micro cracks

Viggo Jensen 27 oktober 2008

Petrographic description of rock aggregate
Sample no. 08115-2B   **Location: Meraftåsen (Kvål)**

Macroscopic description. Yellow-green fine grained porphyric rock

Mineralogy: estimated by use of measurement grid (363 points)

matrix*	epidote	plagioclase	quartz	cryptocrystalline**	carbonate	opake	
46	33	9	8	4	< 1	< 1	

* chlorite/actionolite/sericite   **Possible carbonate/ titanite

Crystal/grain size: matrix 0.01-0.1 mm, phenocrysts 0.5 - 5 mm
Micro texture: glomeroporphyric texture
Crystal form: subhedral plagioclase phenocrysts and clusters, euhedral epidote
Recrystallization: epidote, chlorite, actinolite, carbonate, pseudomorphs with albite? and quartz,
Deformation: not observed
Alteration: saussuritization, chloritization, carbonatization
Micro cracking (UV light): intergranular, high porosity in epidote enriched areas
Classification: low grade metamorphosed basalt (greenschist facies)
Naming: greenstone
Micro photos:

Micro photos of selected area in thin section

1 Ordinary light. Note plagioclase porphyres

2 Polarized light. Note euhedral epidote crystals

3 Fluorescence light. Note micro cracks

Viggo Jensen 27 oktober 2008

Petrographic description of rock aggregate
Sample no. 08115-2C   **Location: Meraftåsen (Kvål)**

Macroscopic description. Yellow-green fine grained porphyric rock with white and yellow veins

Mineralogy: estimated by use of measurement grid (363 points)

plagioclase	actinolite	epidote	chlorite	cryptocrystalline*	carbonate	opake	
41	26	17	10	5	1	< 1	

* possible carbonate/ titanite

Crystal/grain size: matrix 0.01-0.1 mm, phenocrysts 0.5 - 5 mm
Micro texture: porphyric texture, matrix with serate texture
Crystal form: anhedral plagioclase phenocrysts, euhedral epidote
Recrystallization: epidote, chlorite, actinolite, carbonate, pseudomorphs with albite? and quartz
Deformation: strained quartz
Alteration: saussuritization, chloritization, carbonatization. Veins and amygdales with epidote, carbonate, chlorite and quartz
Micro cracking (UV light): intergranular
Classification: low grade metamorphosed basalt (greenschist facies)
Naming: greenstone
Micro photos:
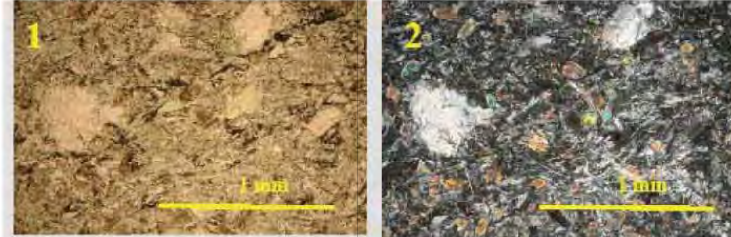
Micro photos of selected area in thin section

1 Ordinary light. Note anhedral porphyres

2 Polarized light. Note euhedral epidote crystals and fibrous actinolite

3 Fluorescence light. Note micro cracks and porosities

Viggo Jensen 27 oktober 2008

Petrographic description of rock aggregate
Sample no. 08115-3B   **Location: Lauvåsen (Lånke)**

Macroscopic description. Dark green fine grained granular rock

Mineralogy: estimated by use of measurement grid (363 points)

chlorite	feldspar	sericite	carbonate	quartz	epidote	cryptocrystalline*	
37	16	16	16	15	< 1	< 1	

    * possible carbonate/ titanite

Clast: detrital quartz particles, feldspar particles and relicts of aggregates.
Matrix. Intergrown chlorite and sericite with epidote and cryptocrystalline phases
Grain size: 0.05 – 0.3 mm, secondary carbonate up to 0.8 mm
Micro texture: clasts surrounded by matrix of chlorite and sericite, weak orientation by lenticulare particles and sericite "lines", bands with carbonate
Grain shape: angular and irregular formed clasts, recrystallized quartz with straight grain boundaries
Recrystallization: chlorite, carbonate and quartz
Deformation: strained quartz
Alteration: chloritization, carbonatization
Micro cracking (UV light): intergranular and along some sericite "lines"
Classification: diagenetic/low metamorphosed siltstone-claystone, meta sediment
Naming: meta greywacke, meta argillite
Micro photos:

Micro photos of selected area in thin section

1 Ordinary light. Green phases is chlorite

2 Polarized light. Note carbonate

3 Fluorescence light. Note micro cracks

Viggo Jensen 4. November 2008

NBTL' Norwegian Concrete and Aggregate Laboratory Ltd

Petrographic description of rock aggregate
Sample no. 08115-3C   **Location: Lauvåsen (Lånke)**

Macroscopic description. Dark green fine grained laminated rock

Mineralogy: estimated by use of measurement grid (363 points)

quartz/feldspar	chlorite	sericite	carbonate	opake	cryptocrystalline*		
42	28	22	8	< 1	< 1		

    * possible carbonate/ titanite

Clast: detrital quartz particles, feldspar particles and relicts of aggregates.
Matrix. Chlorite, sericite and cryptocrystalline phases
Grain size: 0.01 – 0.1 mm, secondary carbonate up to 0.8 mm
Micro texture: clasts intermixed with chlorite and sericite, orientation shown by thin dark "lines" with chlorite, sericite and cryptocrystalline phases, beginning crenulation foliation (phyllite), veins and bands with carbonate
Grain shape: angular and irregular formed clasts, recrystallized quartz with straight grain boundaries
Recrystallization: chlorite, carbonate and quartz
Deformation: strained quartz
Alteration: chloritization, carbonatization
Micro cracking (UV light): intergranular and along some sericite "lines"
Classification: diagenetic/low metamorphosed siltstone-claystone, meta sediment
Naming: meta greywacke, meta argillite
Micro photos:

Micro photos of selected area in thin section

1 Ordinary light. Lines with opake, chlorite, sericite and cryptocrystalline phases

2 Polarized light. Note carbonate

3 Fluorescence light. Note micro cracks

Viggo Jensen 4. November 2008

NBTL' Norwegian Concrete and Aggregate Laboratory Ltd

Petrographic description of rock aggregate
Sample no. 08115-4A   **Location: Vassfjellet Pukkverk**

Macroscopic description.   White - dark-green spotted fine grained rock

Mineralogy: estimated by use of measurement grid (363 points)

feldspar/ plagioclase	ampibole/ actinolite	zoisite/ epidote	carbonate	quartz	chlorite	accessory*	opake
45	32	10	5	4	2	1	1

* possible titanite, apatite

Grain size:	1-2 mm, epidote and quartz 0,1-0,05 mm
Micro texture:	poikilitic actinolite, pseudomorph of feldspar
Grain shape:	anhedral, consertal
Recrystallization:	zoisite/epidote, carbonate, chlorite, quartz
Deformation:	veining
Alteration:	saussuritization, chloritization, carbonatization. Veins and replacements of feldspar with quartz and zoisite/epidote. Pseudomorph of feldspar.
Micro cracking (UV light):	intergranular, in veins/cracks
Classification:	retrograde metamorphosed mafic rock
Naming:	metagabbro

Micro photos:

Micro photos of selected area in thin section

1 Ordinary light. Note relicts of feldspar (brown)

2 Polarized light. Note poikilitic actinolite (yellow-red coloured)

3 Fluorescence light. Note micro cracks
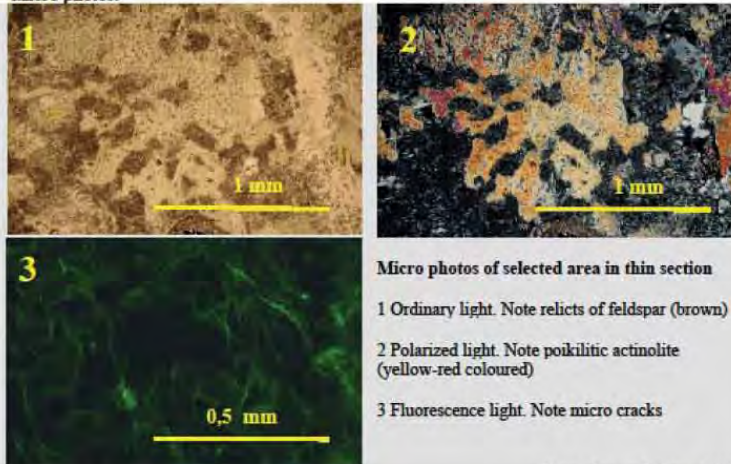
Viggo Jensen 9. Mars 2009

Petrographic description of rock aggregate
Sample no. 08115-4B   **Location: Vassfjellet Pukkverk**

Macroscopic description.   Dark gray dense-fine grained rock

Mineralogy: estimated by use of measurement grid (363 points)

zoisite/ epidote	ampibole/ actinolite	chlorite	accessory*/ opake	feldspar/ plagioclase	carbonate	quartz	
63	22	5	3	3	3	1	

* sulphides and possible titanite, apatite

Grain size:	0.1-0.2 mm, actinolite max. 0.8 mm
Micro texture:	cataclastic
Grain shape:	anhedral, consertal, curved
Recrystallization:	zoisite/epidote, carbonate, chlorite. Sulphides in veins/cracks
Deformation:	cataclase, strained feldspar, veining
Alteration:	saussuritization, chloritization, carbonatization, quartz
Micro cracking (UV light):	intergranular, in veins/cracks
Classification:	dynamic metamorphosed mafic rock
Naming:	cataclasite, breccia

Micro photos:

Micro photos of selected area in thin section

1 Ordinary light. Note cataclastic texture

2 Polarized light. Note actinolite (yellow-red coloured)

3 Fluorescence light. Note micro cracks
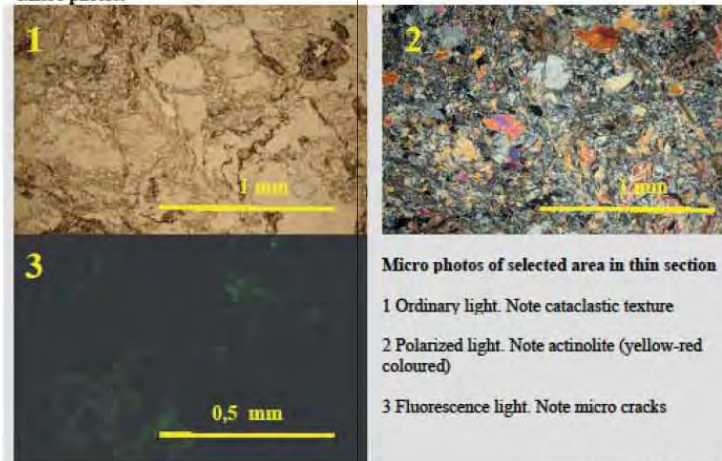
Viggo Jensen 9. Mars 2009

Petrographic description of rock aggregate

Sample no. 08115-4C **Location: Vassfjellet Pukkverk**

Macroscopic description. Dark gray medium grained granular rock with veins

Mineralogy: estimated by use of measurement grid (363 points)

ampibole/ actinolite	feldspar/ plagioclase	zoisite/ epidote	carbonate	accessory*/ opake	chlorite		
61	17	12	5	4	1		

* possible titanite, apatite

Grain size:	1-5 mm
Micro texture:	granular
Grain shape:	anhedral (actinolite), subhedral (plagioclase), consertal,
Recrystallization:	zoisite/epidote, carbonate, chlorite
Deformation:	veining
Alteration:	saussuritization, chloritization, carbonatization. Carbonate replaces relict twinned crystals of pyroxene?

Micro cracking (UV light): intergranular, in veins/cracks
Classification: retrograde metamorphosed mafic rock
Naming: metagabbro
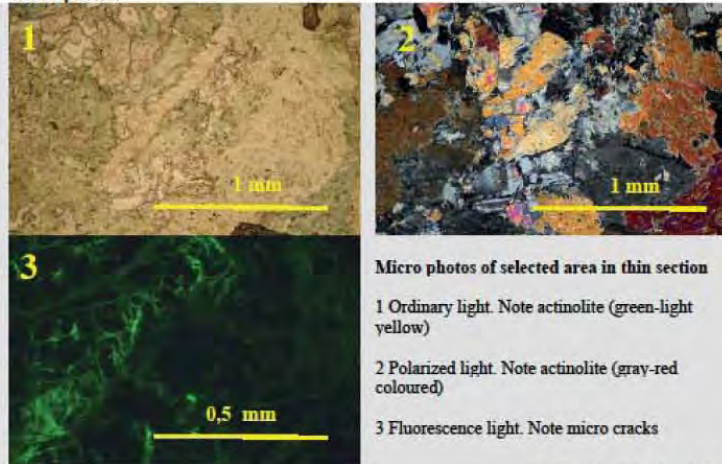
Micro photos:

Micro photos of selected area in thin section

1 Ordinary light. Note actinolite (green-light yellow)

2 Polarized light. Note actinolite (gray-red coloured)

3 Fluorescence light. Note micro cracks

Viggo Jensen 9. Mars 2009

NBTL' Norwegian Concrete and Aggregate Laboratory Ltd

Petrographic description of rock aggregate

Sample no. 08115-6A **Location: Namskogan Aplitt**

Macroscopic description. White and gray coloured fine-medium grained rock with many irregular thin veins

Mineralogy: estimated by use of measurement grid (363 points)

quartz	feldspar/ microcline	plagioclase	chlorite	epidote	antigorite?		
20	20	54	2	1	1		

Crystal/grain size: 0.05-2.5 mm, cataclasite vein < 0.1 mm
Micro texture: inequigranular with long thin cataclasite veins/areas
Crystal/grain form: anhedral, consertal, quartz crystals subhedral
Recrystallization: quartz, epidote, chlorite, antigorite? (in veins)
Deformation: cataclase, strained quartz, deformed and "broken" feldspar
Alteration: minor saussuritization, chloritization
Micro cracking (UV light): intergranular, in veins/cracks, significant in cataclasite areas
Classification: dynamically metamorphosed and crushed granite
Naming: cataclasite, protocataclasite
Micro photos:
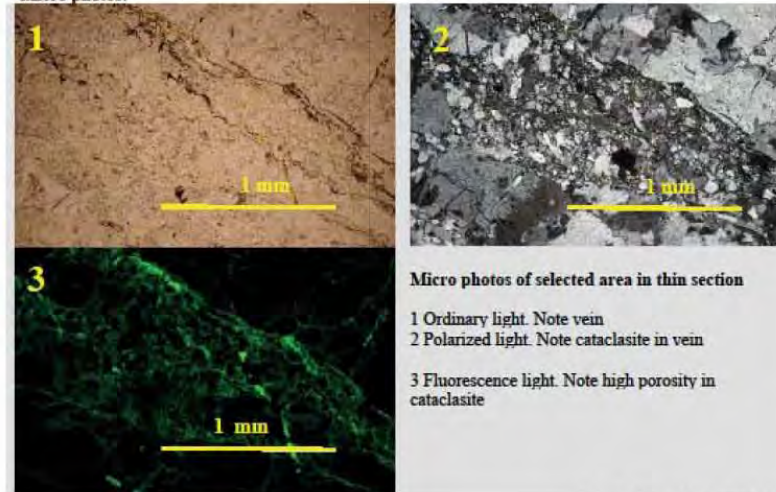
Micro photos of selected area in thin section

1 Ordinary light. Note vein
2 Polarized light. Note cataclasite in vein

3 Fluorescence light. Note high porosity in cataclasite

Viggo Jensen 23. Mars 2009

NBTL' Norwegian Concrete and Aggregate Laboratory Ltd

Petrographic description of rock aggregate
Sample no. 08115-6B　　　　　**Location: Namskogan Aplitt**

Macroscopic description. White and gray coloured fine-medium grained rock with thin veins

Mineralogy: estimated by use of measurement grid (363 points)

quartz	feldspar/ microcline	plagioclase	chlorite	epidote			
47	22	29	1	1			

Crystal/grain size: 0.25-2.5 mm, quartz in veins 0.25-2.5 mm, cataclasite veins < 0.1 mm
Micro texture: inequigranular with quartz and cataclasite veins/areas
Crystal/grain form: anhedral, consertal, subhedral quartz crystals
Recrystallization: quartz, epidote, chlorite
Deformation: cataclase, strained quartz, deformed and "broken" feldspar
Alteration: minor saussuritization, chloritization
Micro cracking (UV light): intergranular, in veins/cracks, higher in cataclasite areas
Classification: dynamically metamorphosed and crushed granite
Naming: protocataclasite
Micro photos:

Micro photos of selected area in thin section

1 Ordinary light. Note the quartz vein

2 Polarized light. Note varying crystal sizes

3 Fluorescence light. Note a relative high porosity
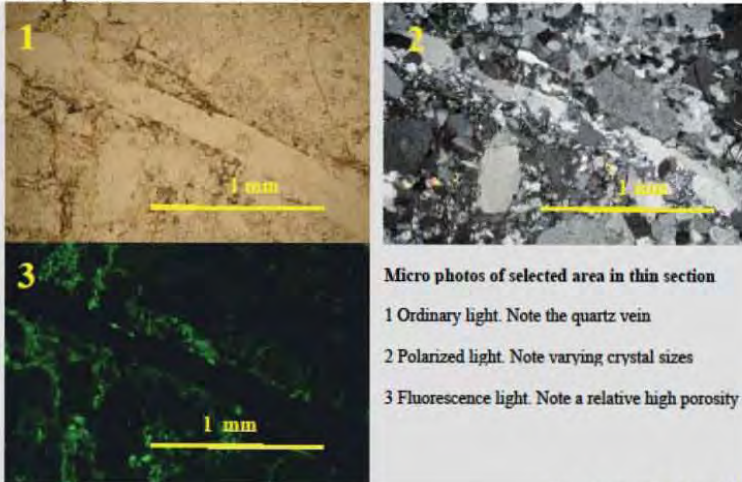
Viggo Jensen 23. Mars 2009

Petrographic description of rock aggregate
Sample no. 08115-6C　　　　　**Location: Namskogan Aplitt**

Macroscopic description. White and gray coloured fine-medium grained rock with few thin veins

Mineralogy: estimated by use of measurement grid (363 points)

plagioclase	feldspar/ microcline	quartz	chlorite	epidote	antigorite?		
38	36	23	1	1	< 1		

Crystal/grain size: 0.25-2.5 mm , cataclasite veins < 0.1 mm
Micro texture: inequigranular with cataclasite veins, weak orientation by elongation of quartz and feldspar/plagioclase
Crystal/grain form: anhedral, consertal
Recrystallization: quartz, epidote, chlorite, antigorite? (in veins)
Deformation: cataclase, strained quartz
Alteration: minor saussuritization, chloritization
Micro cracking (UV light): intergranular, in veins/cracks, higher in cataclasite areas
Classification: dynamically metamorphosed and crushed granite
Naming: crush breccia, fine-medium grained granite
Micro photos:

Micro photos of selected area in thin section

1 Ordinary light. Note the vein

2 Polarized light. Note varying crystal sizes

3 Fluorescence light. Note a relative high porosity in cracks
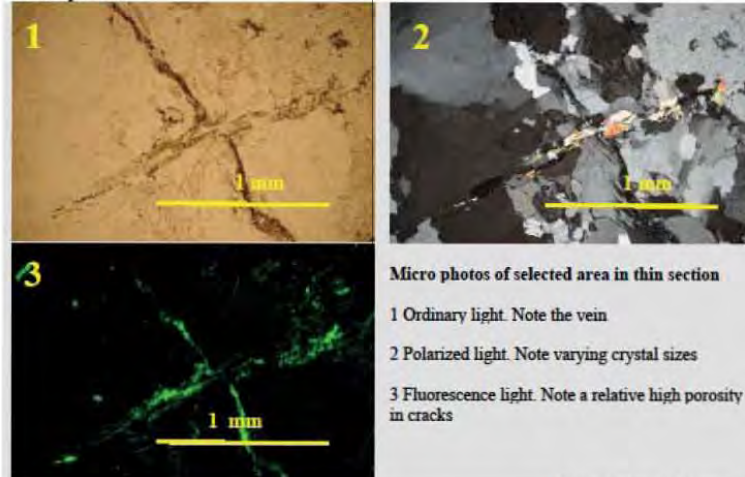
Viggo Jensen 23. Mars 2009

Petrographic description of rock aggregate
Sample no. 08115-7A   **Location: Ottersbo**

Macroscopic description. Grey-green fine grained foliated rock

Mineralogy: estimated by use of measurement grid (363 points)

matrix*	quartz	feldspar	epidote	carbonate	chlorite	plagioclase	accessory
40	25	13	10	5	4	3	< 1

* matrix (groundmass) consisting of crushed quartz and feldspar?
Crystal/grain size: matrix 0.01-0.1 mm, porphyroclast up to 1 mm
Micro texture: foliated, bands with elongated strained quartz and feldspar/plagioclase porphyroclast. Feldspar/plagioclase is often broken and lenticular. Thin veins filled with quartz and chlorite.
Crystal/grain form: anhedral, curved and sutured in some quartz crystal
Recrystallization: quartz, epidote, chlorite, carbonate
Deformation: cataclase, foliation, tectonic crushing, subgrain and straining in feldspar/plagioclase and quartz.
Alteration: saussuritization, chloritization, carbonatization
Micro cracking (UV light): intergranular, higher porosity in some epidote enriched areas
Classification: Dynamically metamorphosed rock
Naming: Mylonite
Micro photos:

Micro photos of selected area in thin section

1 Ordinary light. Note irregular foliation

2 Polarized light. Note elongate and lenticular quartz

3 Fluorescence light. Note micro cracks and higher porosity (holes) in some relict minerals
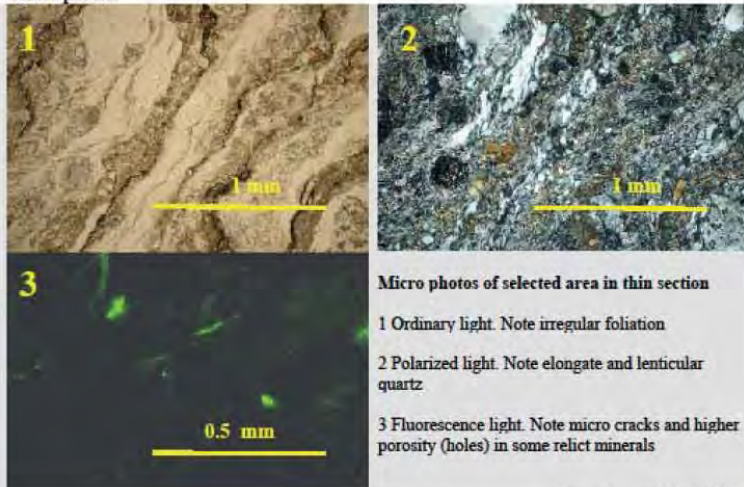
Viggo Jensen 22 May 2009

Petrographic description of rock aggregate
Sample no. 08115-7C   **Location: Ottersbo**

Macroscopic description. Grey-green fine grained granular rock

Mineralogy: estimated by use of measurement grid (363 points)

matrix*	quartz	feldspar	plagioclase	epidote	chlorite	carbonate	accessory
35	32	9	9	7	4	4	< 1

* matrix (groundmass) consisting of crushed quartz and feldspar?
Crystal/grain size: matrix 0.01-0.1 mm, porphyroclast up to 1 mm
Micro texture: unfoliated, crush texture, porphyroclast of quartz and feldspar/plagioclase. Feldspar/plagioclase is broken and bended. Thin veins filled with quartz, carbonate and chlorite.
Crystal/grain form: anhedral, curved
Recrystallization: epidote, chlorite, carbonate, minor quartz,
Deformation: cataclase, tectonic crushing, subgrain and straining in feldspar/plagioclase and quartz.
Alteration: saussuritization, chloritization, carbonatization
Micro cracking (UV light): intergranular, higher porosity in some porphyroclast
Classification: Dynamically metamorphosed rock
Naming: Cataclasite
Micro photos:

Micro photos of selected area in thin section

1 Ordinary light. Note lack of orientation (foliation)

2 Polarized light. Note tectonic crush texture

3 Fluorescence light. Note micro cracks and higher porosity in some porphyroclast
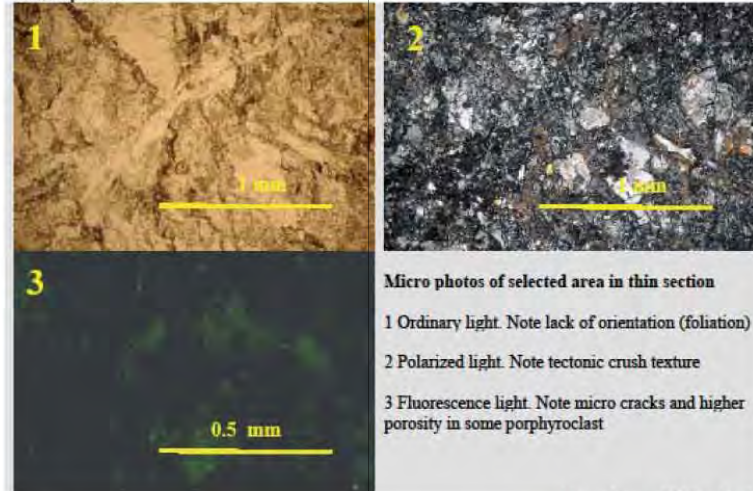
Viggo Jensen 22 May 2009

Petrographic description of rock aggregate

Sample no. 08115-9B   **Location: Hello**

Macroscopic description. Dark grey fine grained weakly laminated rock with a cm thick layer of white coarse grained carbonate (not described in the following)

Mineralogy: estimated (%)

Carbonate minerals*	Assesory**	** opaque phases, mica, relict minerals (quartz and feldspar)
98-100	< 2	

calcite, possibly with some anhydrite
Crystal/grain size: 0.05 – 0.3 mm
Micro texture: eguigranular, twinned carbonate minerals, weak orientation by thin bands of opaque phases and relict minerals and elongated carbonate minerals
Crystal/grain form: anhedral, curved
Recrystallization: carbonate
Deformation: not observed.
Alteration: not observed
Micro cracking (UV light): intergranular and in relict minerals (holes)
Classification: carbonate rock
Naming: marble
Micro photos:

Micro photos of selected area in thin section

1 Ordinary light. Note relict minerals

2 Polarized light. Note twinned carbonate minerals

3 Fluorescence light. Note porosity in relict minerals

Viggo Jensen 22 May 2009

Petrographic description of rock aggregate

Sample no. 08115-9C   **Location: Hello**

Macroscopic description. Dark grey fine grained laminated rock with irregular bands of white coarse grained carbonate

Mineralogy: estimated (%)

Carbonate minerals*	Assesory**	** opaque phases, mica, relict minerals (quartz and feldspar)
95-100	< 5	

calcite, possibly with some anhydrite
Crystal/grain size: dark layer: 0.05 – 0.3 mm, white layer up to 6 mm
Micro texture: ineguigranular, twinned carbonate minerals, orientation by thin layers of opaque phases and relict minerals and elongated carbonate minerals, "floating" relict minerals
Crystal/grain form: anhedral - subhedral, straight and curved grain contact
Recrystallization: carbonate
Deformation: not observed.
Alteration: not observed
Micro cracking (UV light): intergranular and in relict minerals (holes)
Classification: carbonate rock
Naming: marble
Micro photos:

Micro photos of selected area in thin section

1 Ordinary light. Note lamination by opaque phases

2 Polarized light. Note "floating" relict minerals (feldspar)

3 Fluorescence light. Note porosity in relict minerals
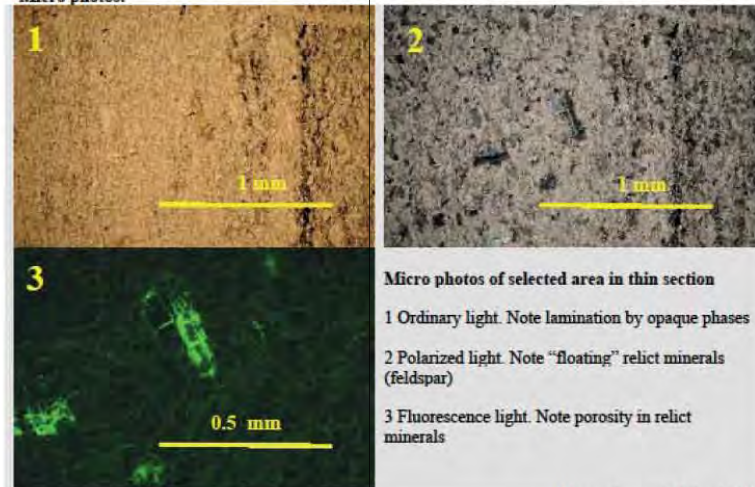
Viggo Jensen 22 May 2009

Petrographic description of rock aggregate

Sample no. 08115-10B　　　　　　　**Location: Lia Pukkverk**

Macroscopic description.　Dark grey fine grained granular rock with few scattered phenocrysts and thin green coloured veins.

Mineralogy: estimated by use of measurement grid (363 points)

hornblende	plagioclase	zoisite/epidote	chlorite	carbonate	opaque
38	34	12	9	6	< 1

Grain size:	0.1 – 0.5 mm phenocrysts up to 3 mm
Micro texture:	equigranular, poikilitic plagioclase, thin veins filled with epidote
Grain shape:	anhedral plagioclase and euhedral hornblende
Recrystallization:	hornblende, zoisite/epidote, carbonate, chlorite
Deformation:	not observed
Alteration:	saussuritization, chloritization, carbonatization.
Micro cracking (UV light):	intergranular, holes in some minerals
Classification:	retrograde metamorphosed mafic rock
Naming:	greenstone, metabasalt/gabbro

Micro photos:

Micro photos of selected area in thin section

1 Ordinary light. Note hornblende (green - brown)

2 Polarized light. Note poikilitic plagioclase

3 Fluorescence light. Note micro cracks and "holes"
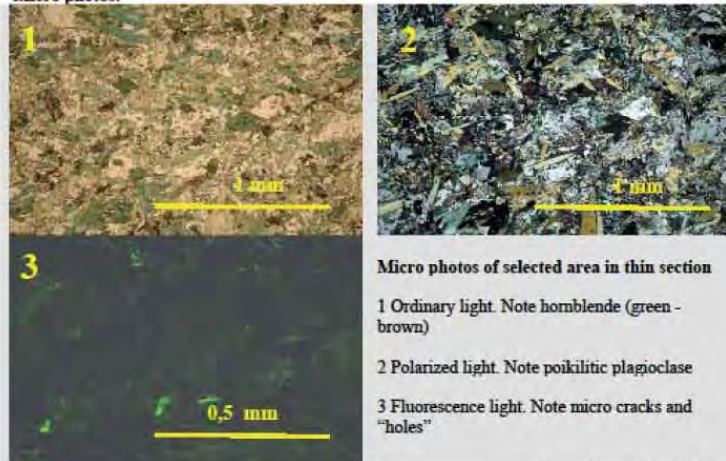
Viggo Jensen 26 May 2009

Petrographic description of rock aggregate

Sample no. 08115-10C　　　　　　　**Location: Lia Pukkverk**

Macroscopic description.　Dark grey fine grained granular rock with thin green coloured veins.

Mineralogy: estimated by use of measurement grid (363 points)

plagioclase	hornblende/actinolite	zoisite/epidote	carbonate	chlorite	quartz	opaque
37	23	12	10	9	8	1

Grain size:	0.1 – 0.5 mm carbonate minerals up to 2 mm
Micro texture:	equigranular, poikilitic plagioclase, fibrous actinolite, irregulare thin veins and "pseudomorps" filled with epidote, chlorite, carbonate and quartz
Grain shape:	anhedral plagioclase, subhedral - euhedral hornblende/actinolite
Recrystallization:	hornblende/actinolite, zoisite/epidote, carbonate, chlorite, quartz
Deformation:	not observed
Alteration:	saussuritization, chloritization, carbonatization
Micro cracking (UV light):	intergranular, holes in some minerals
Classification:	retrograde metamorphosed mafic rock
Naming:	greenstone, metabasalt/gabbro

Micro photos:

Micro photos of selected area in thin section

1 Ordinary light. Note hornblende/actinolite and chlorite (green - brown)

2 Polarized light. Note veins with chlorite (deep purple)

3 Fluorescence light. Note micro cracks and "holes"

Viggo Jensen 26 May 2009

Petrographic description of rock aggregate
Sample no. 08115-11A   **Location: Lørenskog**

Macroscopic description. Grey-green fine grained foliated rock with up to 1 mm porphyroclasts

Mineralogy: estimated by use of measurement grid (363 points)

quartz	feldspar	chlorite	biotite	epidote	accessory: opaque, plagioclase
62	30	4	3	1	< 1

Crystal/grain size: groundmass (matrix) 0.05-0.3 mm, porphyroclast up to 1 mm
Micro texture: foliated, elongated strained quartz and lenticular feldspar porphyroclast.
Crystal/grain form: anhedral, curved and embayed, straight in some quartz crystal
Recrystallization: quartz, chlorite, epidote, biotite
Deformation: cataclase, foliation, subgrain and straining in feldspar and quartz.
Alteration: saussuritization, chloritization,
Micro cracking (UV light): intergranular, holes in some minerals
Classification: dynamically metamorphosed rock
Naming: mylonite
Micro photos:

Micro photos of selected area in thin section

1 Ordinary light. Note orientation by biotite and chlorite (green-brown)

2 Polarized light. Note elongated quartz and lenticular feldspar

3 Fluorescence light. Note micro cracks and holes in some minerals
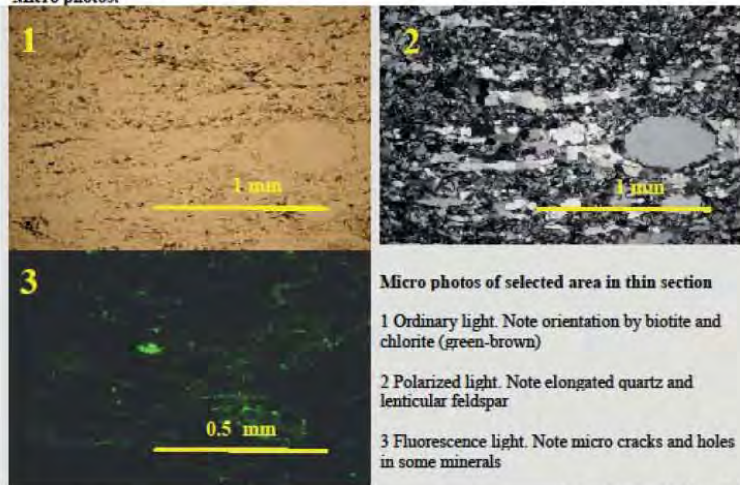
Viggo Jensen 25 May 2009

Petrographic description of rock aggregate
Sample no. 08115-11B   **Location: Lørenskog**

Macroscopic description. Dark grey fine grained foliated rock with alternate light coloured layers with porphyroclasts and lensoids

Mineralogy: estimated by use of measurement grid (363 points)

quartz	biotite/muscovite	hornblende	plagioclase	feldspar	garnet	accessory*
48	13	12	11	8	7	1

* *opaque phases, epidote, titanite*

Crystal/grain size: groundmass 0.1-0.5 mm, porphyroclast of plagioclase up to 4 mm
Micro texture: ineguigranular, foliated, lenticular banding, augen of feldspar, elongated strained quartz. Dark layer with high content of biotite, hornblende and garnet. Light layer with high content of elongated quartz
Crystal/grain form: anhedral, curved and embayed, straight in some quartz crystal, subhedral- euhedral quartz, biotite, hornblende, garnet
Recrystallization: quartz, biotite/muscovite, hornblende, garnet
Deformation: foliation, sub grain and straining in feldspar and quartz.
Alteration: seritication of feldspar
Micro cracking (UV light): intergranular, holes in some minerals
Classification: high grade metamorphic rock
Naming: eye gneiss, banded gneiss
Micro photos:

Micro photos of selected area in thin section

1 Ordinary light. Note foliation by biotite (light brown-red brown)

2 Polarized light. Note "snow ball" structure of feldspar

3 Fluorescence light. Note few micro cracks
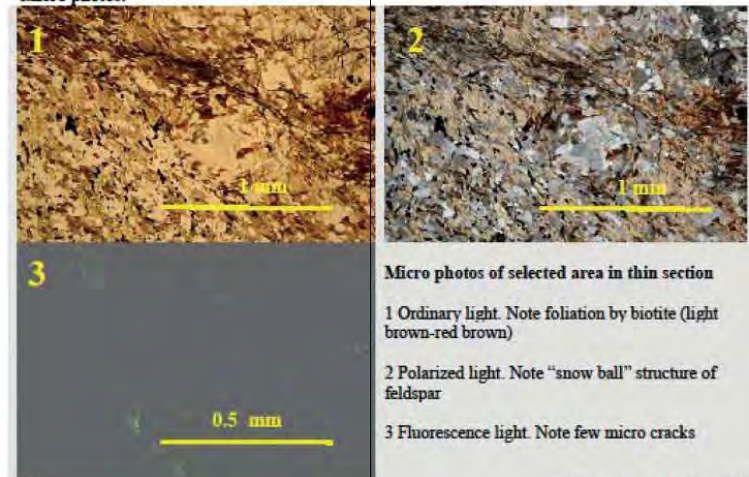
Viggo Jensen 25 May 2009

Petrographic description of rock aggregate
Sample no. 08115-11C   **Location: Lørenskog**

Macroscopic description. Dark grey porphyritic rock with up to 5 mm light and red coloured phenocrysts

Mineralogy: estimated by use of measurement grid (363 points)

quartz	plagioclase	biotite	feldspar	opaque	accessory: clinozoizite, apatite
44	30	14	9	2	1

Crystal/grain size: groundmass 0.1-0.4 mm, phenocrysts (or porphyroclasts) of plagioclase/feldpar up to 5 mm

Micro texture: porphyritic with granular groundmass, some elongated quartz and lenticular feldspar suggesting some foliation

Crystal/grain form: anhedral, curved and embayed, elongated quartz crystals, subhedral-euhedral in some quartz and biotite crystals

Recrystallization: quartz

Deformation: strained quartz, bended plagioclase

Alteration: sericitation in some feldspar

Micro cracking (UV light): intergranular, micro cracks, holes in some minerals

Classification: plutonic igneous rock, alternatively high grade metamorphic rock

Naming: porphyritic granite, alternatively eye gneiss

Micro photos: *(only granular part of groundmass)*
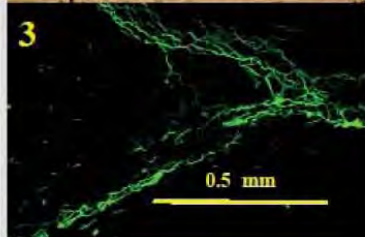
Micro photos of selected area in thin section

1 Ordinary light. Note biotite (light brown-red brown)

2 Polarized light. Note granular texture

3 Fluorescence light. Note micro cracks

Viggo Jensen 25 May 2009

Petrographic description of rock aggregate
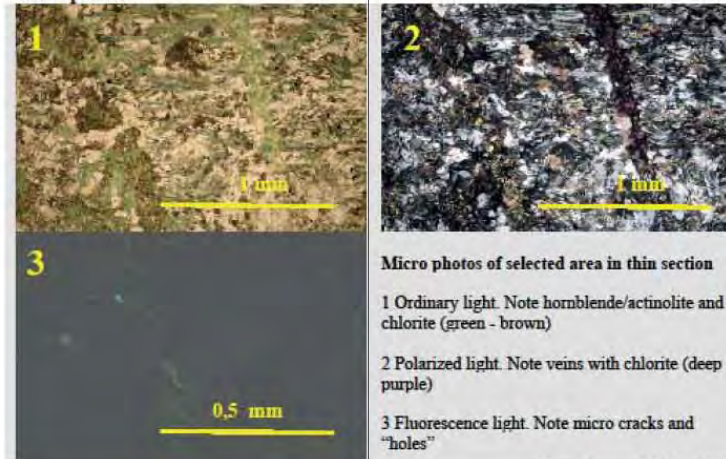Sample no. 08115-11D   **Location: Lørenskog**

Macroscopic description.   Dark grey fine grained granular rock.

Mineralogy: estimated by use of measurement grid (363 points)

plagioclase	pyroxene (augite)	alteration corona*	opaque
62	23	12	3

chlorite/hornblende/iron hydroxide

Grain size: 0.1 – 1 mm

Micro texture: intergranular, (pyroxene enclosed by plagioclase), alteration corona on pyroxene and opaque phases

Grain shape: anhedral pyroxene, subhedral - euhedral plagioclase

Recrystallization: alteration coronas of hornblende, chlorite and iron hydroxide

Deformation: not observed

Alteration: internal in pyroxene, corona on pyroxene and opaque phases

Micro cracking (UV light): intergranular

Classification: plutonic rock

Naming: gabbro

Micro photos:
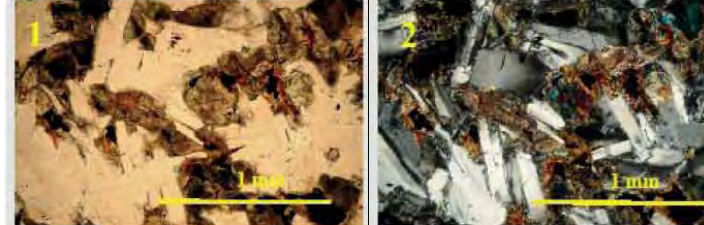
Micro photos of selected area in thin section

1 Ordinary light. Note pyroxene

2 Polarized light. Note altered pyroxene

3 Fluorescence light. Note few micro cracks

Viggo Jensen 26 May 2009

Petrographic description of rock aggregate
Sample no. 08115-12A   **Location: Freste Pukkverk**

Macroscopic description. Coarse grained red and grey coloured spotted granular rock with black veins containing "floating" euhedral phenocrysts

Mineralogy: estimated

plagioclase	feldspar	chlorite	carbonate	opaque	accessory: iron hydroxide, epidote, sericite
45	40	5	5	5	< 1

Crystal/grain size: plagioclase/feldspar up to 7 mm, altered pyroxene 0.2-1 mm
Micro texture: granular, pseudomorph (pyroxene?) with carbonate, chlorite and opaque phases, some poikilitic feldspar/plagioclase, veins with opaque phases and feldspar
Crystal/grain form: anhedral (plagioclase and feldspar), euhedral "floating" feldspar
Recrystallization: carbonate, chlorite, epidote
Deformation: strained feldspar/plagioclase
Alteration: carbonatization, chloritization, seritization in feldspar/plagioclase
Micro cracking (UV light): intergranular, some micro cracks
Classification: magmatic rock (plutonic)
Naming: monzonite
Micro photos:
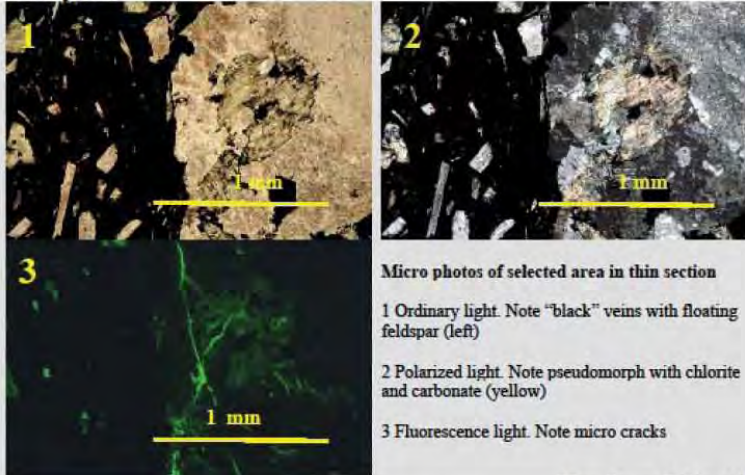
Micro photos of selected area in thin section

1 Ordinary light. Note "black" veins with floating feldspar (left)

2 Polarized light. Note pseudomorph with chlorite and carbonate (yellow)

3 Fluorescence light. Note micro cracks

Viggo Jensen 26 May 2009

Petrographic description of rock aggregate
Sample no. 08115-12C   **Location: Freste Pukkverk**

Macroscopic description. Coarse grained red and grey coloured spotted granular rock

Mineralogy: estimated

plagioclase	feldspar	amphibole	pyroxene	opaque	quartz	accessory*
45	45	3	3	2	2	< 2

* biotite, chlorite, apatite, iron hydroxide, epidote
Crystal/grain size: plagioclase/feldspar up to 10 mm, amphibole and pyroxene 0.2-1 mm
Micro texture: granular, interstitial amphibole, pyroxene, opaque phases and quartz, some poikilitic feldspar/plagioclase
Crystal/grain form: anhedral – subhedral plagioclase and feldspar, some euhedral amphibole and pyroxene
Recrystallization: biotite, chlorite, quartz
Deformation: not observed
Alteration: chloritization
Micro cracking (UV light): intergranular, some micro cracks
Classification: magmatic rock (plutonic)
Naming: monzonite
Micro photos:
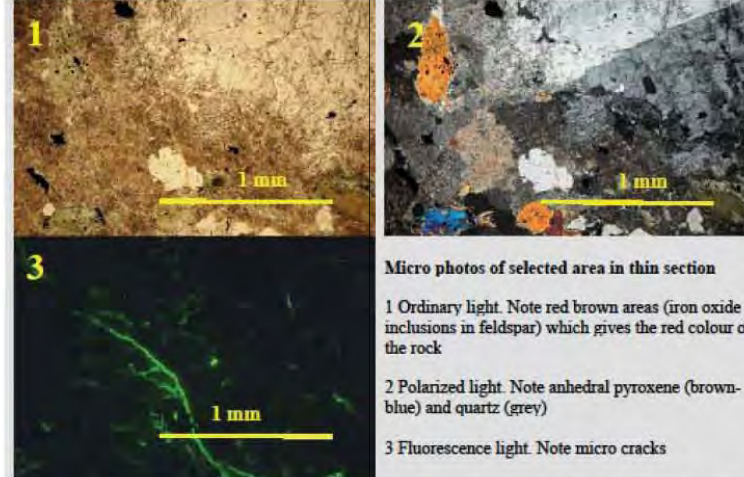
Micro photos of selected area in thin section

1 Ordinary light. Note red brown areas (iron oxide inclusions in feldspar) which gives the red colour of the rock

2 Polarized light. Note anhedral pyroxene (brown-blue) and quartz (grey)

3 Fluorescence light. Note micro cracks

Viggo Jensen 26 May 2009

Petrographic description of rock aggregate
Sample no. 08115-13A   **Location: Helgeland Pukkverk**

Macroscopic description. Coarse grained black and white spotted porphyritic rock

Mineralogy: estimated

feldspar	plagioclase	hornblende	biotite	quartz	titanite	epidote	accessory*
40	20	20	15	3	1	1	< 1

* carbonate, chlorite, apatite, opaque phases

Crystal/grain size:	plagioclase/feldspar up to 8 mm, hornblende, biotite, quartz 0.2-2 mm
Micro texture:	inequigranular, interstitial intergrown of hornblende and biotite (between coarser feldspar/plagioclase), some granophyric texture
Crystal/grain form:	anhedral, curved and embayed contact, some subhedral biotite
Recrystallization:	minor quartz
Deformation:	strained feldspar/plagioclase and quartz
Alteration:	insignificant carbonatization, chloritization
Micro cracking (UV light):	intergranular
Classification:	magmatic rock (plutonic)
Naming:	syenite/monzonite
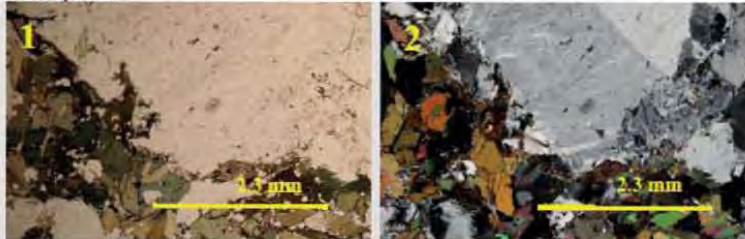
Micro photos:

Micro photos of selected area in thin section

1 Ordinary light. Note intergrown hornblende and biotite (brown – green)

2 Polarized light. Note large feldspar with Carlsbad twins and below granophyric texture

3 Fluorescence light. Note few micro cracks

Viggo Jensen 28 May 2009

Petrographic description of rock aggregate
Sample no. 08115-13B   **Location: Helgeland Pukkverk**

Macroscopic description. Coarse grained black - white and light red spotted porphyritic and foliated rock containing lenticular phenocrysts (blasts)

Mineralogy: estimated

feldspar	plagioclase	hornblende	biotite	quartz	titanite	epidote	accessory*
40	20	20	10	8	1	1	< 1

* carbonate, chlorite, apatite, opaque phases

Crystal/grain size:	plagioclase/feldspar up to 10 mm, hornblende, biotite, quartz 0.2-2 mm
Micro texture:	inequigranular, interstitial intergrown hornblende and biotite (between coarser feldspar/plagioclase), some granophyric texture, tectonic deformation (cataclase)
Crystal/grain form:	anhedral, curved and embayed contact, some subhedral biotite
Recrystallization:	quartz
Deformation:	strained feldspar/plagioclase and quartz, elongated and recrystallized quartz
Alteration:	insignificant carbonatization, chloritization
Micro cracking (UV light):	intergranular
Classification:	tectonic foliated magmatic rock (plutonic)
Naming:	gneiss, metamorphosed syenite/monzonite

Micro photos:

Micro photos of selected area in thin section

1 Ordinary light. Note intergrown hornblende and biotite (brown – green)

2 Polarized light. Note strained feldspar and tectonic deformation with elongated and recrystallized quartz

3 Fluorescence light. Note few micro cracks

Viggo Jensen 28 May 2009

Petrographic description of rock aggregate
Sample no. 08115-14A **Location: Lillehammer**

Macroscopic description. Medium grained grey coloured rock

Mineralogy: estimated by use of measurement grid (363 points)

quartz	feldspar	plagioclase	muscovite/sericite	carbonate	accessory*		
51	36	7	2	2	< 2		

epidote ,chlorite, titanite, organic matter, opaque phases

Crystal/grain size: 0,3 mm – 2 mm
Micro texture: grain – grain contact, dustlines and voids filled with matter, no preferred orientation
Grain shape: subrounded – subangular, curved and embayed contact
Recrystallization: some secondary epitaxic quartz on particles
Deformation: compaction and strained quartz
Alteration: insignificant carbonatization, chloritization
Micro cracking (UV light): significant, cleavage, interfaces, higher in altered particles
Classification: terrigenous clastic sediment
Naming: medium grained sandstone
Micro photos:

Micro photos of selected area in thin section

1 Ordinary light. Note red brown dustlines on some particles and as pore filling (intergranular)

2 Polarized light. Note strained quartz

3 Fluorescence light. Note micro cracks

Viggo Jensen 11 June 2010

NBTL Norwegian Concrete and Aggregate Laboratory Ltd
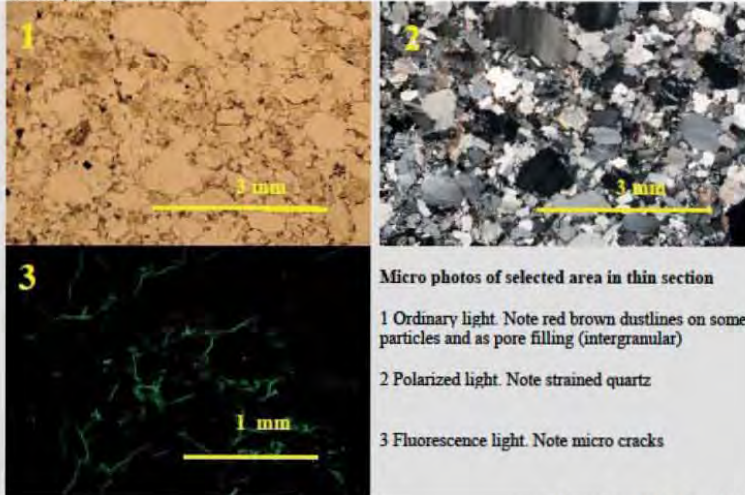
Petrographic description of rock aggregate
Sample no. 08115-14B **Location: Lillehammer**

Macroscopic description. Fine grained dark and grey coloured rock

Mineralogy: estimated by use of measurement grid (363 points)

quartz	feldspar	chlorite	muscovite/sericite	opaque/organic	plagioclase	accessory*	
55	26	8	5	4	2	< 1	

carbonate, epidote, titanite

Crystal/grain size: 0,1 mm – 0,5mm
Micro texture: grain – grain contact, lamination shown by thin "lines" of organic matter/ clay minerals.
Grain shape: subrounded – subangular, some curved and embayed contact
Recrystallization: sericite
Deformation: compaction
Alteration: chloritization, seritization
Micro cracking (UV light): insignificant
Classification: terrigenous clastic sediment
Naming: siltstone/greywacke
Micro photos:

Micro photos of selected area in thin section

1 Ordinary light. Note orientation by thin lines with organic matter/clay minerals

2 Polarized light. Note sericite in "lines" and interfaces on some particles

3 Fluorescence light. Note few micro cracks and voids

Viggo Jensen 11 June 2010

NBTL Norwegian Concrete and Aggregate Laboratory Ltd
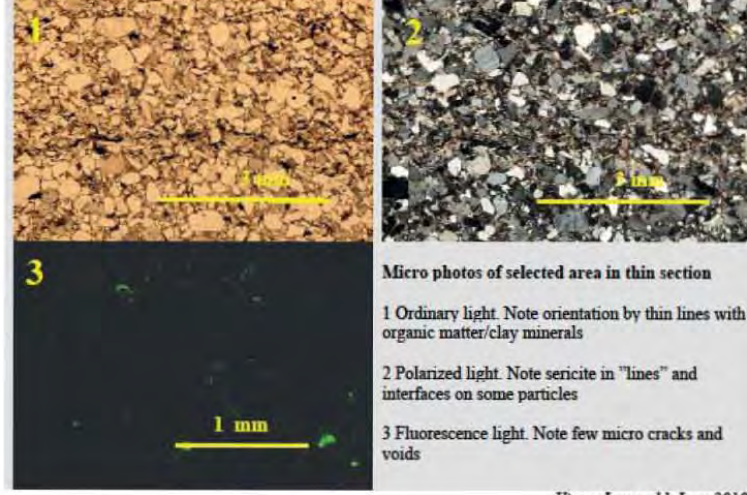
Petrographic description of rock aggregate
Sample no. 08115-15C   **Location: Hadeland pukkverk**

Macroscopic description. Fine grained dark grey porphyric rock with feldspar phenocrysts

Mineralogy: estimated by use of measurement grid (363 points)

feldspar	opaque	pyroxene	plagioclase	quartz	accessory*		
91	4	3	1	1	< 1		

carbonate, chlorite, sericite

Crystal/grain size:	groundmass 0,01 – 0,1 mm, phenocrysts up to 5 mm
Micro texture:	seriate texture with intergrown feldspar, feldspar phenocrysts
Crystal/grain form:	euhedral-subhedral feldspar phenocrysts
Recrystallization:	secondary quartz in matrix
Deformation:	none
Alteration:	hematite in feldspar, insignificant saussuritization, seritization, carbonatization

Micro cracking (UV light): cleavage in feldspar, porosity in groundmass and altered feldspar

Classification:	magmatic rock (volcanic)
Naming:	porphyric trachyte

Micro photos:
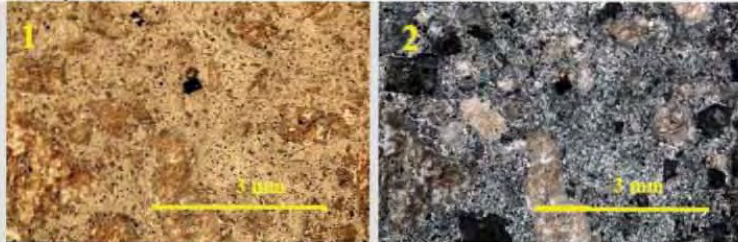
Micro photos of selected area in thin section

1 Ordinary light. Note feldspar phenocrysts

2 Polarized light. Note size of groundmass and altered feldspar phenocrysts (with hematite)

3 Fluorescence light. Note micro cracks in feldspar and higher porosity in groundmass

Viggo Jensen 11 June 2010

NBTL Norwegian Concrete and Aggregate Laboratory Ltd

Petrographic description of rock aggregate
Sample no. 08115-16A   **Location: Velde Pukk**

Macroscopic description. Fine to medium grained grey granular rock

Mineralogy: estimated

feldspar	quartz	plagioclase	garnet	muscovite/sericite	biotite	accessory*	
66	17	13	2	1	1	< 1	

chlorite, epidote ,opaque phases

Crystal/grain size:	0,2 – 2 mm
Micro texture:	granular, feldspar with micro perthitic texture and epitaxial owergrowth
Crystal/form:	anhedral, curved and embayed contact
Recrystallization:	sericite
Deformation:	none
Alteration:	insignificant chloritization, sericitization, saussuritization

Micro cracking (UV light): significant in cleavage, interface, higher in altered feldspar, voids in garnet

Classification:	magmatic rock (plutonic)
Naming:	fine to medium grained syenite/granite

Micro photos:
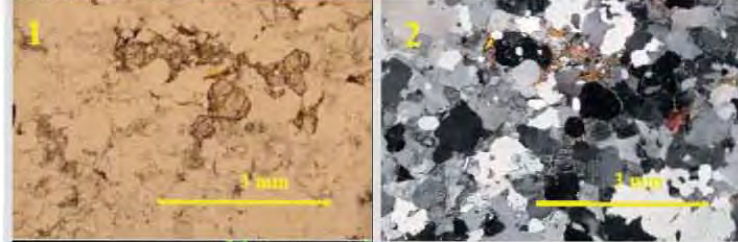
Micro photos of selected area in thin section

1 Ordinary light. Note garnet (light brown)

2 Polarized light. Note large feldspar with pertithic texture

3 Fluorescence light. Note voids in garnet

Viggo Jensen 14 June 2010

NBTL Norwegian Concrete and Aggregate Laboratory Ltd

Petrographic description of rock aggregate
Sample no. 08115-16B   **Location: Velde Pukk**

Macroscopic description. Medium to coarse grained light- and dark grey granular rock

Mineralogy: estimated

feldspar	quartz	plagioclase	muscovite/sericite	amphibole	biotite	accessory*	
43	36	16	2	1	1	< 1	

* chlorite, epidote ,opaque phases

Crystal/grain size:	1-7 mm
Micro texture:	granular, feldspar with micro perthitic texture and epitaxial overgrowth, larger irregular quartz
Crystal/form:	anhedral, curved and embayed contact
Recrystallization:	sericite
Deformation:	breccia (observed in small part of thin section)
Alteration:	insignificant chloritization, sericitization, saussuritization

Micro cracking (UV light): significant in cleavage, interfaces, higher in altered feldspar, voids in garnet

Classification:	magmatic rock (plutonic)
Naming:	medium to coarse grained granite

Micro photos:

Micro photos of selected area in thin section

1 Ordinary light.

2 Polarized light. Note "large" irregular formed quartz

3 Fluorescence light. Note micro cracks

Viggo Jensen 14 June 2010

Petrographic description of rock aggregate
Sample no. 08115-17A   **Location: Tau**

Macroscopic description. Dark grey medium grained white spotted rock

Mineralogy: estimated by use of measurement grid (363 points)

plagioclase	quartz	muscovite/sericite	chlorite	carbonate	epidote	accessory*	
58	22	10	5	3	1	< 1	

* opake minerals and apatite

Crystal/grain size:	plagioclase 0.5-3 mm, recrystallized quartz, muscovite, chlorite 0.1 mm
Micro texture:	unfoliated, subhedral granular plagioclase (altered), strained quartz with subgrains and recrystallized quartz, crush texture (little)
Crystal contact:	curved and embayed
Recrystallization:	quartz, epidote, chlorite, carbonate
Deformation:	cataclase, tectonic crushing, strained quartz, subgrain, recrystallized quartz
Alteration:	seritization, saussuritization, chloritization, carbonatization

Micro cracking (UV light): few micro cracks

Classification:	Dynamically metamorphosed rock (quartz diorite)
Naming:	Cataclasite

Micro photos:

Micro photos of selected area in thin section

1 Ordinary light. Note lack of orientation (foliation)

2 Polarized light. Note altered plagioclase

3 Fluorescence light. Note micro cracks

Viggo Jensen 3 September 2010

Petrographic description of rock aggregate
Sample no. 08115-17B   Location: Tau

Macroscopic description. Dark and green coloured fine grained rock

Mineralogy: estimated by use of measurement grid (363 points)

plagioclase	quartz	epidote	muscovite/sericite	chlorite	carbonate	accessory*	
62	29	5	3	< 1	< 1	< 1	

* opake minerals and apatite

Crystal/grain size: plagioclase, strained quartz, epidote 0.2-1 mm, recrystallized quartz, muscovite, chlorite 0.1 mm

Micro texture: some foliation/orientation by elongated quartz, subhedral granular plagioclase (altered), some elongated plagioclase, strained quartz with subgrains and recrystallized quartz

Crystal contact: curved and embayed

Recrystallization: quartz, epidote, chlorite, carbonate

Deformation: cataclase, strained quartz, subgrain, recrystallized quartz

Alteration: saussuritization, little seritization, chloritization, carbonatization

Micro cracking (UV light): microcracks, intergranular

Classification: dynamically metamorphosed rock (quartz diorite)

Naming: mylonite/cataclasite

Micro photos:
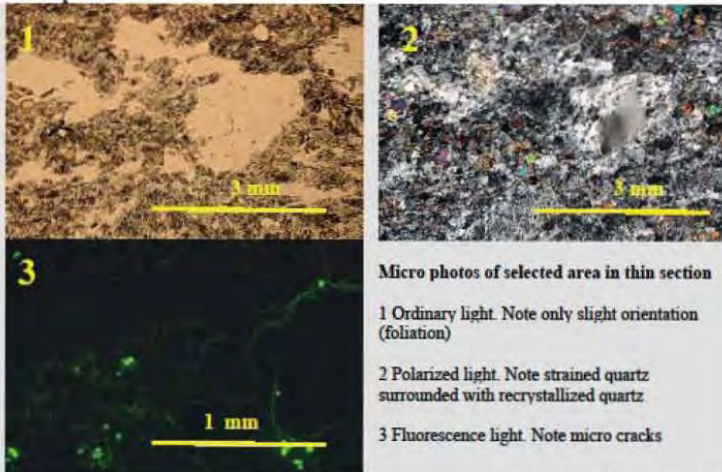
Micro photos of selected area in thin section

1 Ordinary light. Note only slight orientation (foliation)

2 Polarized light. Note strained quartz surrounded with recrystallized quartz

3 Fluorescence light. Note micro cracks

Viggo Jensen 3 September 2010

Petrographic description of rock aggregate
Sample no. 08115-17D   Location: Tau

Macroscopic description. Dark grey dense - fine grained rock

Mineralogy: estimated by use of measurement grid (363 points)

plagioclase	quartz	muscovite/sericite	carbonate	chlorite	epidote	Accessory*	
44	39	9	7	1	< 1	< 1	

* opake minerals and apatite

Crystal/grain size: few plagioclase up to 1 mm, recrystallized quartz, muscovite-sericite 0.1 mm

Micro texture: foliation/orientation by elongated quartz and quartz- muscovite bands, subhedral granular plagioclase (altered), elongated plagioclase, strained quartz with subgrains and recrystallized quartz

Crystal contact: curved and embayed

Recrystallization: quartz, epidote, chlorite, carbonate

Deformation: cataclase and recrystallizatied quartz, very few strained quartz particles

Alteration: seritization, carbonatization, little chloritization and saussuritization

Micro cracking (UV light): microcracks

Classification: dynamically metamorphosed rock

Naming: mylonite

Micro photos:

Micro photos of selected area in thin section

1 Ordinary light. Note significant orientation (foliation)

2 Polarized light. Note bands of recrystallized quartz and muscovite

3 Fluorescence light. Note micro cracks

Viggo Jensen 3 September 2010

Petrographic description of rock aggregate
Sample no. 08115-19A   Location: Hellvik Vest "Lysitt"

Macroscopic description.   White medium grained granular rock

Mineralogy: estimated by use of measurement grid (363 points)

plagioclase	sericite*	zoisite	quartz	pyroxene	accessory		
66	27	4	3	< 1	< 1		

* possible intermixed with zeolite minerals

Crystal/grain size:	1-4 mm (plagioclase)
Micro texture:	subhedral granular, veins with zoisite and pyroxene
Crystal/grain form:	subhedral plagioclase, straight and bowed
Recrystallization:	sericite (with possible zeolite minerals), quartz
Deformation:	some veining
Alteration:	significant seritization of plagioclase, saussuritization

Micro cracking (UV light): high porosity in altered plagioclase, micro cracks

Classification:	plutonic rock
Naming:	anorthosite
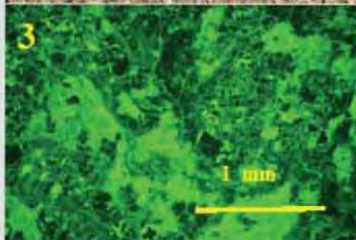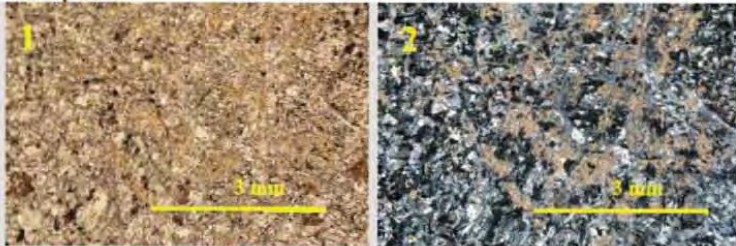
Micro photos:

Micro photos of selected area in thin section

1 Ordinary light. Note altered plagioclase (brownish colour)

2 Polarized light. Note sericite in altered plagioclase

3 Fluorescence light. Note high porosity (in altered plagioclase)

Viggo Jensen 7 September 2010

Petrographic description of rock aggregate
Sample no. 08115-19B   Location: Hellvik Vest "Lysitt"

Macroscopic description.   White medium grained granular rock with veins

Mineralogy: estimated by use of measurement grid (363 points)

plagioclase	sericite	zoisite	pyroxene	quartz	accessory		
80	8	7	5	< 1	< 1		

Crystal/grain size:	1-4 mm (plagioclase), pyroxene, zoizite 0.1-1 mm
Micro texture:	subhedral granular, veins with zoisite and pyroxene
Crystal/grain form:	subhedral plagioclase, straight and bowed
Recrystallization:	sericite (with possible zeolite minerals), quartz
Deformation:	some veining and cataclase
Alteration:	seritization of plagioclase, saussuritization

Micro cracking (UV light): high porosity in altered plagioclase, micro cracks

Classification:	plutonic rock
Naming:	anorthosite
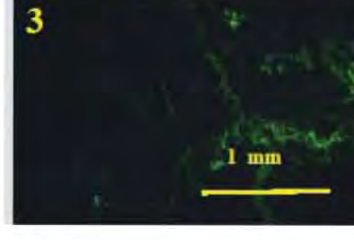
Micro photos:

Micro photos of selected area in thin section

1 Ordinary light. Note veins

2 Polarized light. Note pyroxene and zoisite in veins

3 Fluorescence light. Note micro cracks

Viggo Jensen 7 September 2010

Petrographic description of rock aggregate
Sample no. 08115-19D **Location: Hellvik Vest "Lysitt"**

Macroscopic description. White and greyish medium to coarse grained granular rock

Mineralogy: estimated by use of measurement grid (363 points)

plagioclase	sericite	opaque	pyroxene	quartz	zoisite	accessory	
84	9	6	1	< 1	< 1	< 1	

Crystal/grain size: 1-8 mm (plagioclase)
Micro texture: subhedral granular, some thin veins
Crystal/grain form: subhedral plagioclase, straight and bowed
Recrystallization: sericite (with possible zeolite minerals)
**Deformation:** some veining
Alteration: seritization of plagioclase, saussuritization
Micro cracking (UV light): "long" micro cracks
Classification: plutonic rock
Naming: anorthosite
Micro photos:
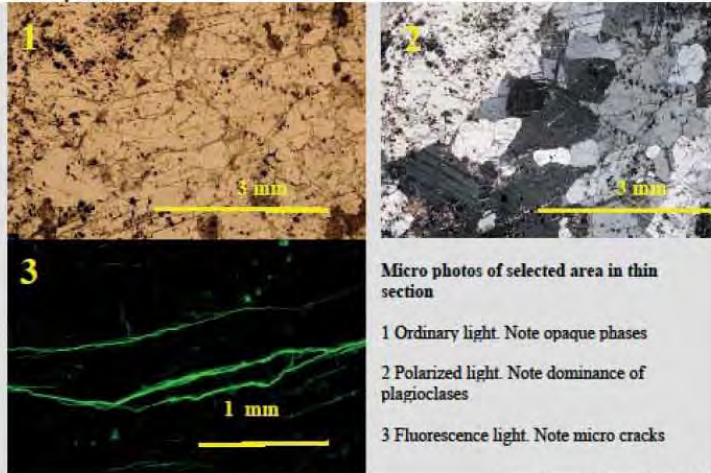
Micro photos of selected area in thin section

1 Ordinary light. Note opaque phases

2 Polarized light. Note dominance of plagioclases

3 Fluorescence light. Note micro cracks

Viggo Jensen 7 September 2010

Petrographic description of rock aggregate
Sample no. 08115-20A **Location: Ramsland Pukkverk**

Macroscopic description. White greenish medium to coarse grained granular rock

Mineralogy: estimated by use of measurement grid (363 points)

plagioclase	zoisite	alteration product*	sericite	accessory			
69	15	9	7	< 1			

* sub microscopic products

Crystal/grain size: 3-8 mm (plagioclase), 0.1-0.2 mm zoizite
Micro texture: subhedral granular, scattered zoisite crystals and sericite in altered plagioclase
Crystal form: subhedral plagioclase, curved and embayed contacts
Recrystallization: zoizite and sericite
Deformation: not observed
Alteration: significant saussuritization and seritization
Micro cracking (UV light): higher porosity in altered plagioclase, micro cracks
Classification: plutonic rock
Naming: anorthosite (altered)
Micro photos:

Micro photos of selected area in thin section

1 Ordinary light. Note altered plagioclase (brownish colour)

2 Polarized light. Note zoisite and sericite in altered plagioclase

3 Fluorescence light. Note high porosity (in altered plagioclase) and voids
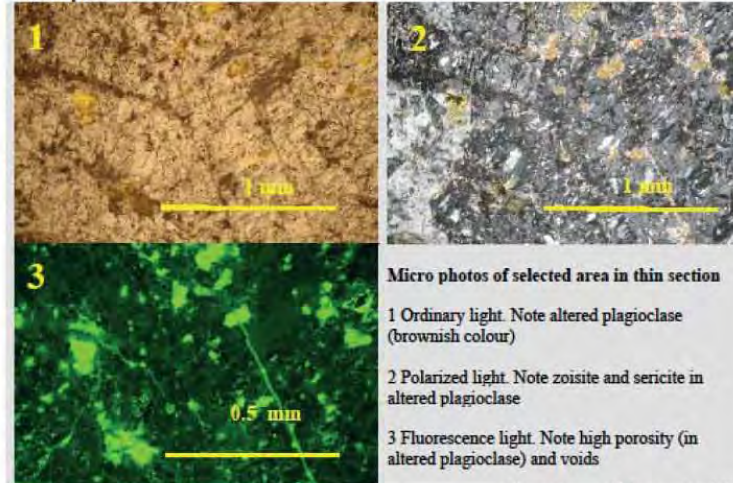
Viggo Jensen 24 September 2010

Petrographic description of rock aggregate

Sample no. 08115-20C   **Location: Ramsland Pukkverk**

Macroscopic description.   White greyish partly spotted medium to coarse grained granular rock with thin veins

Mineralogy: estimated by use of measurement grid (363 points)

plagioclase	sericite-muscovite	zoisite- epidote	chlorite	alteration product*	accessory
75	16	8	1	<1	< 1

* sub microscopic products

Crystal/grain size:	3-8 mm (plagioclase), 0.1-0.2 mm zoisite - epidote
Micro texture:	subhedral granular, scattered zoisite – epidote crystals and sericite – muscovite in altered plagioclase, sericite and chlorite in veins
Crystal form:	subhedral plagioclase, curved and embayed contacts
Recrystallization:	sericite, muscovite, zoisite-epidote, chlorite
Deformation:	not observed
Alteration:	significant seritization and saussuritization, chlorite
Micro cracking (UV light):	higher porosity in altered plagioclase, micro cracks
Classification:	plutonic rock
Naming:	anorthosite (altered)
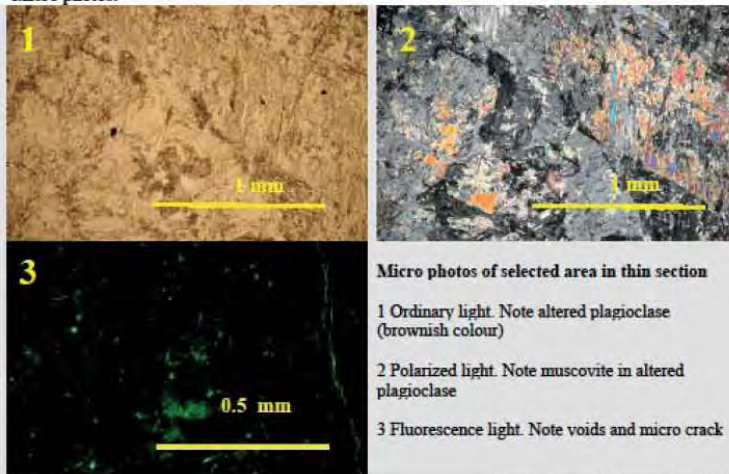
Micro photos:

Micro photos of selected area in thin section

1 Ordinary light. Note altered plagioclase (brownish colour)

2 Polarized light. Note muscovite in altered plagioclase

3 Fluorescence light. Note voids and micro crack

Viggo Jensen 24 September 2010

Petrographic description of rock aggregate

Sample no. 08115-20D   **Location: Ramsland Pukkverk**

Macroscopic description.   White and brownish spotted medium to coarse grained granular rock

Mineralogy: estimated by use of measurement grid (363 points)

plagioclase	alteration product*	sericite	opaque	accessory
94	3	2	1	<1

* sub microscopic products

Crystal/grain size:	0.5-6 mm (plagioclase)
Micro texture:	subhedral unevenly sized plagioclase, sericite in grain contacts, some pseudo morphs with alteration products
Crystal form:	subhedral plagioclase, curved and embayed contacts
Recrystallization:	sericite
Deformation:	not observed
Alteration:	some seritization
Micro cracking (UV light):	micro cracks
Classification:	plutonic rock
Naming:	anorthosite (unaltered)

Micro photos:

Micro photos of selected area in thin section

1 Ordinary light. Note pseudo morph with alteration products (brownish colour)

2 Polarized light. Note unaltered plagioclase and sericite in grain contacts and pseudo morph

3 Fluorescence light. Note micro cracks

Viggo Jensen 24 September 2010

Petrographic description of rock aggregate
Sample no. 08115-21A   **Location: Fossberga**

Macroscopic description. Light grey spotted fine grained rock with thin veins

Mineralogy: estimated by use of measurement grid (363 points)

groundmass*	quartz	carbonate	feldspar	sericite	biotite/chlorite	opaque	epidote
72	8	8	4	3	2	2	1

* crypto-microcrystalline possible re-crystallized clay minerals and lumps

Crystal/grain size:	0,1 mm – 1.5 mm
Micro texture:	floating clasts in crypto-micro crystalline groundmass, dust lines on some clasts, carbonate filled veins, orientation by elongated particles
Grain shape:	subrounded particles
Recrystallization:	biotite, carbonate, some re-crystallized quartz, re-crystallized groundmass,
Deformation:	compaction of clasts (of possible clay lumps), veining
Alteration:	carbonatization, sericite, chloritization of biotite
Micro cracking (UV light):	micro cracks, higher porosity in groundmass
Classification:	terrigenous clastic sediment
Naming:	greywacke

Micro photos:

Micro photos of selected area in thin section

1 Ordinary light. Note biotite/chlorite (brown), opaque phases and some orientation in the sample

2 Polarized light. Note clasts of quartz, feldspar and scattered carbonate

3 Fluorescence light. Note micro cracks

Viggo Jensen 24 September 2010

Petrographic description of rock aggregate
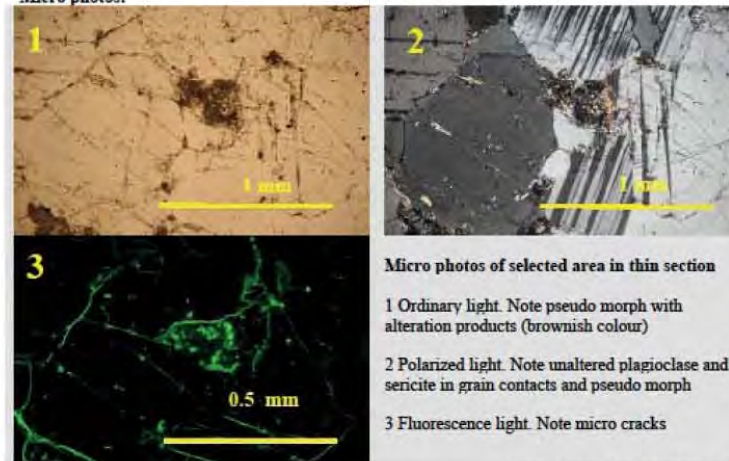Sample no. 08115-21B   **Location: Fossberga**

Macroscopic description. Dark grey dense- to fine grained rock

Mineralogy: estimated by use of measurement grid (363 points)

groundmass*	quartz	biotite/chlorite	carbonate	sericite	opaque	feldspar	titanite	epidote
52	22	9	7	3	3	2	1	1

* crypto-microcrystalline possible re-crystallized clay minerals and lumps

Crystal/grain size:	0,1 mm – 2 mm
Micro texture:	floating clasts in crypto-micro crystalline groundmass, dust lines on some clasts, orientation by elongated particles
Grain shape:	subrounded angulare particles, some grain-grain contacts
Recrystallization:	biotite, carbonate, sericite, some re-crystallized quartz, re-crystallized groundmass,
Deformation:	compaction of clasts (of possible clay lumps)
Alteration:	carbonatization, sericite, chloritization of biotite
Micro cracking (UV light):	micro cracks, higher porosity in groundmass
Classification:	terrigenous clastic sediment
Naming:	greywacke

Micro photos:

Micro photos of selected area in thin section

1 Ordinary light. Note biotite/chlorite (brown), opaque phases

2 Polarized light. Note higher content of quartz, felspar clasts

3 Fluorescence light. Note micro cracks

Viggo Jensen 24 September 2010

Petrographic description of rock aggregate
Sample no. 08115-21C   Location: Fossberga

Macroscopic description. Dark grey fine grained rock with vein

Mineralogy: estimated by use of measurement grid (363 points)

groundmass*	quartz	feldspar	biotite/chlorite	sericite	opaque	titanite	epidote
70	7	7	6	6	2	1	1

* crypto-microcrystalline possible re-crystallized clay minerals and lumps

Crystal/grain size:	0,5 mm – 2 mm
Micro texture:	floating clasts in crypto-micro crystalline groundmass, dust lines on some clasts, orientation by elongated particles
Grain shape:	subrounded angulare clasts
Recrystallization:	biotite, sericite, some re-crystallized quartz, re-crystallized groundmass,
Deformation:	compaction of clasts (of possible clay lumps)
Alteration:	sericitization, chloritization of biotite
Micro cracking (UV light):	micro cracks, higher porosity in groundmass
Classification:	terrigenous clastic sediment
Naming:	greywacke

Micro photos:

Micro photos of selected area in thin section

1 Ordinary light. Note biotite/chlorite (brown), opaque phases

2 Polarized light. Note outlines of clay lumps, and scattered quartz clasts

3 Fluorescence light. Note micro cracks

Viggo Jensen 24 September 2010

Petrographic description of rock aggregate
Sample no. 08115-22A   Location: Hello

Macroscopic description. Dark grey dense- fine grained foliated rock

Mineralogy: estimated by use of measurement grid (363 points)

quartz	feldspar	hornblende	biotite	epidote	garnet	opaque	
74	8	6	5	3	3	1	

|	
Crystal/grain size:	0,1 mm – 0.3 mm
Micro texture:	orientation (foliation) by elongated particles of quartz, hornblende and biotite
Grain contact:	straight and curved
Recrystallization:	possible quartz
Deformation:	not observed
Alteration:	little saussuritization
Micro cracking (UV light):	micro cracks around crystals
Classification:	metamorphic rock
Naming:	hornblende biotite quartz schist/slate

Micro photos:

Micro photos of selected area in thin section

1 Ordinary light. Note hornblende and biotite (green-brown) and some orientation in the sample

2 Polarized light. Note elongated quartz

3 Fluorescence light. Note micro cracks
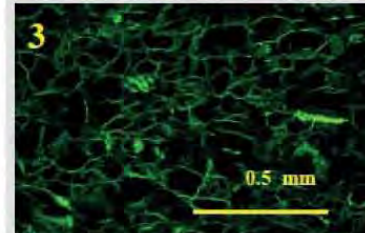
Viggo Jensen 22 October 2010

Petrographic description of rock aggregate

Sample no. 08115-22B   Location: Hello

Macroscopic description. Dark grey white spotted medium grained granular rock

Mineralogy: estimated by use of measurement grid (363 points)

zoizite-epidote	hornblende	feldspar	titanite/opaque	chlorite		
47	35	15	2	1		

Crystal/grain size:	0,1 mm – 0.8 mm, pseudo morph 1-2 mm
Micro texture:	meshlike pattern of inter grown hornblende and more or less "isolated" mm large pseudo morph of feldspar? with zoizite-epidote and relict feldspar (plagioclase). Fine cracks with chlorite
Grain form:	subhedral granular, euhedral zoizite
Recrystallization:	zoizite-epidote
Deformation:	few thin veins
Alteration:	significant saussuritization
Micro cracking (UV light):	micro cracks around crystals
Classification:	magmatic (plutonic) rock
Naming:	saussuritizated gabbro/greenstone
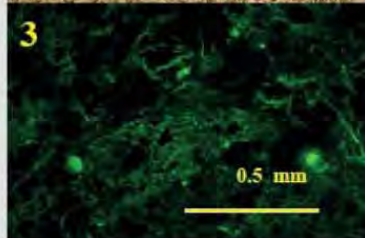
Micro photos:

Micro photos of selected area in thin section

1 Ordinary light. Note hornblende (green) and pseudo morph (lighter areas)

2 Polarized light. Note crystal sizes of hornblende and epidote (blue-red)

3 Fluorescence light. Note higher porosity in zoizite-epidote areas and micro cracks

Viggo Jensen 22 October 2010

Petrographic description of rock aggregate

Sample no. 08115-22C   Location: Hello

Macroscopic description. Dark grey white spotted medium grained rock

Mineralogy: estimated by use of measurement grid (363 points)

hornblende	zoizite-epidote	feldspar	chlorite	titanite/opaque		
57	28	10	4	1		

Crystal/grain size:	hornblende 1 - 2 mm, zoizite-epidote and feldspar 0.1 mm
Micro texture:	porphyric hornblende (some inter grown), matrix with intergrown zoizite-epidote and feldspar. Some larger relict feldspar
Grain form:	subhedral hornblende, euhedral zoizite-epidote and some hornblende
Recrystallization:	zoizite-epidote
Deformation:	not observed
Alteration:	significant saussuritization
Micro cracking (UV light):	micro cracks, higher porosity in matrix
Classification:	magmatic rock
Naming:	saussuritizated gabbro/greenstone
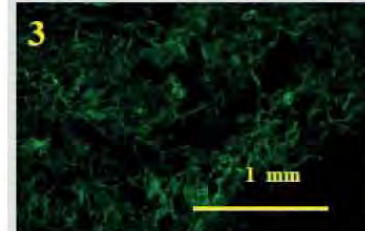
Micro photos:

Micro photos of selected area in thin section

1 Ordinary light. Note hornblende (green)

2 Polarized light. Note matrix with zoizite-epidote and feldspar, some larger relict feldspar

3 Fluorescence light. Note higher porosity in matrix and micro cracks

Viggo Jensen 22 October 2010

Petrographic description of rock aggregate
Sample no. 08115-22D   Location: Hello

Macroscopic description. Dark grey dense rock

Mineralogy: estimated by use of measurement grid (363 points)

hornblende	quartz	garnet	opaque	epidote		
53	38	4	3	2		

Crystal/grain size: 0,1 mm, garnet 0.3 mm
Micro texture: equigranular, slight orientation by elongated hornblende and quartz, porphyric euhedral garnet
Grain form/contact: subhedral, straight and curved
Recrystallization: epidote
Deformation: not observed
Alteration: little saussuritization
Micro cracking (UV light): micro cracks around crystals
Classification: metamorphic rock
Naming: hornblende quartz schist/slate
Micro photos:

Micro photos of selected area in thin section

1 Ordinary light. Note hornblende (green) and euhedral garnet

2 Polarized light. Note elongated hornblende

3 Fluorescence light. Note micro cracks

Viggo Jensen 22 October 2010

Petrographic description of rock aggregate
Sample no. 08115-22E   Location: Hello

Macroscopic description. Dark grey dense rock (description of hornblendite part of sample)

Mineralogy: estimated by use of measurement grid (363 points)

hornblende	epidote	opaque	feldspar	chlorite	
87	7	4	1	1	

Crystal/grain size: 0.1-0.3 mm
Micro texture: subhedral equigranular hornblende (some inter grown)
Grain contact: curved mostly
Recrystallization: epidote
Deformation: not observed
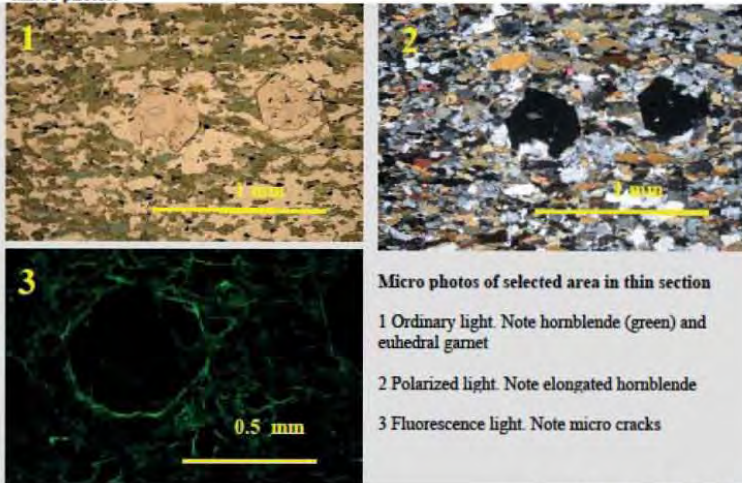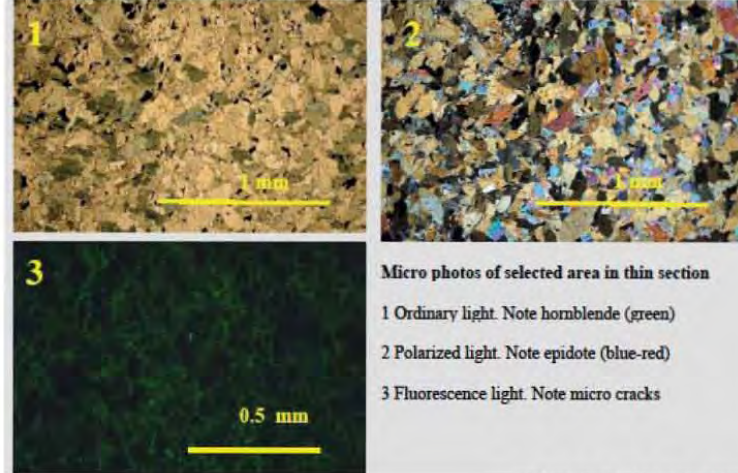Alteration: saussuritization
Micro cracking (UV light): micro cracks
Classification: magmatic rock
Naming: hornblendite
Micro photos:

Micro photos of selected area in thin section

1 Ordinary light. Note hornblende (green)

2 Polarized light. Note epidote (blue-red)

3 Fluorescence light. Note micro cracks

Viggo Jensen 22 October 2010

Petrographic description of rock aggregate

Sample no. 08115-23A   **Location: Rombakk Pukkverk**

Macroscopic description. Dark grey dense- to fine grained foliated rock

Mineralogy: estimated

quartz	biotite	feldspar	muscovite/sericite	opaque	chlorite	accessory*	
57	17	16	5	3	2	< 1	

* *epidote carbonate*

Crystal/grain size: 0.1 – 0.3 mm, quartz up to 0.8 mm
Micro texture: granoblastic with irregular oriented biotite, pseudomorph with sericite and chlorite
Crystal form/contact: anhedral, curved and embayed contact
Recrystallization: sericite, chlorite
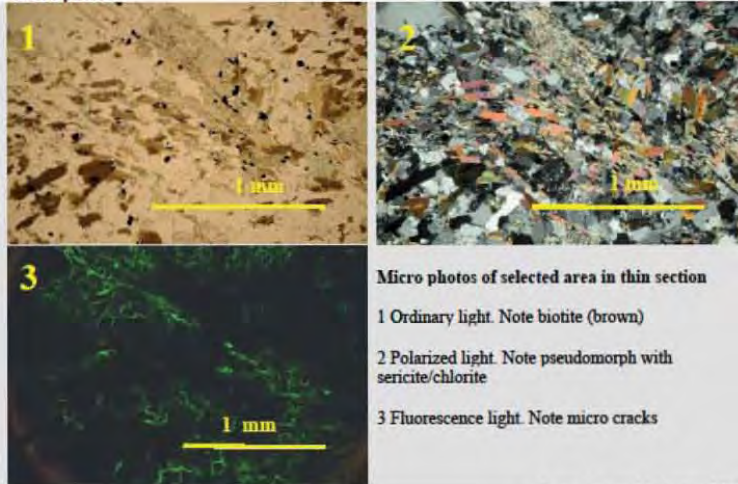**Deformation:**   strained quartz
Alteration: chloritization, sericitization
Micro cracking (UV light) intergranular, few long micro cracks
Classification: metamorphic rock
Naming: fine grained biotite gneiss
Micro photos:

Micro photos of selected area in thin section

1 Ordinary light. Note biotite (brown)

2 Polarized light. Note pseudomorph with sericite/chlorite

3 Fluorescence light. Note micro cracks

Viggo Jensen 11 August 2011

Petrographic description of rock aggregate

Sample no. 08115-23B   **Location: Rombakk Pukkverk**

Macroscopic description. Dark grey dense- to fine grained foliated rock

Mineralogy: estimated

quartz	biotite	feldspar	muscovite/sericite	chlorite	epidote	accessory*	
45	24	17	10	2	2	< 1	

* *opaque phases, carbonate*

Crystal/grain size: 0.05 – 0.1 mm, quartz up to 1 mm
Micro texture: granoblastic with irregular oriented biotite, some linsoides and band with quartz, pseudomorph of felspar
Crystal form/contact: subhedral-anhedral, straight, curved and embayed contact
Recrystallization: sericite, chlorite, epidote
Deformation: strained quartz
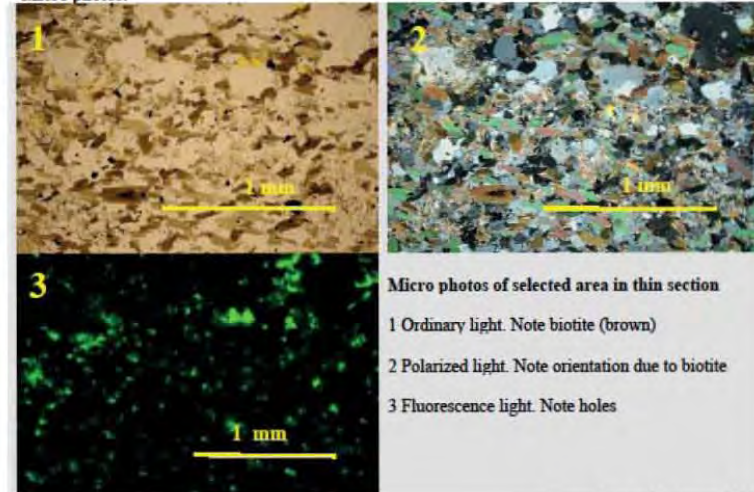**Alteration:**   chloritization, sericitization, saussuritization
Micro cracking (UV light) intergranular, holes
Classification: metamorphic rock
Naming: fine grained biotite gneiss
Micro photos:

Micro photos of selected area in thin section

1 Ordinary light. Note biotite (brown)

2 Polarized light. Note orientation due to biotite

3 Fluorescence light. Note holes

Viggo Jensen 12 August 2011

Petrographic description of rock aggregate
Sample no. 08115-23C   Location: Rombakk Pukkverk

Macroscopic description. Dark grey dense laminated-foliated rock

Mineralogy: estimated

quartz	biotite	feldspar	muscovite/sericite	chlorite	epidote	accessory*	
74	17	9	< 1	< 1	< 1	< 1	

* opaque phases, carbonate

Crystal/grain size: 0.05 – 0.1 mm, some quartz up to 0.3 mm
Micro texture: granoblastic with oriented bands of biotite, linsoides and band with polycrystalline quartz
Crystal form/contact: subhedral-anhedral, straight, curved and embayed contact
Recrystallization: quartz
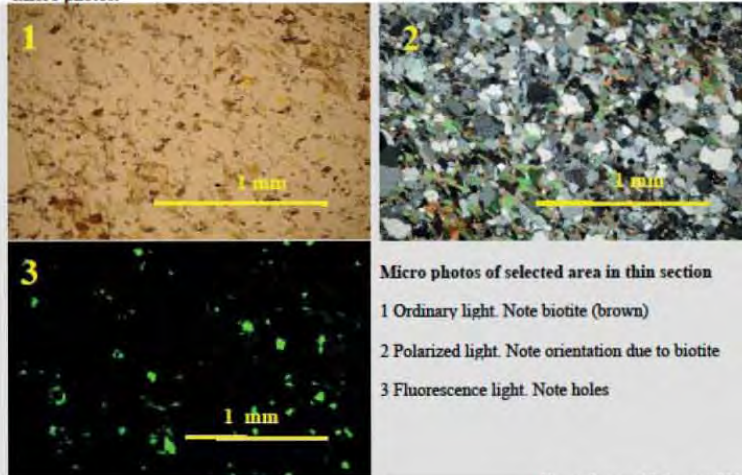**Deformation:** strained quartz
Alteration: insignificant sericitization
Micro cracking (UV light) intergranular, holes
Classification: metamorphic rock
Naming: fine grained quartz biotite gneiss/quartz biotite schiest
Micro photos:

Micro photos of selected area in thin section

1 Ordinary light. Note biotite (brown)

2 Polarized light. Note orientation due to biotite

3 Fluorescence light. Note holes

Viggo Jensen 12 August 2011

Petrographic description of rock aggregate
Sample no. 08115-24A   Location: Kleivaberget

Macroscopic description. Light grey fine to medium grained rock

Mineralogy: estimated

quartz	feldspar **	sericite	accessory*				
57	37	6	< 1				

* opaque phases, carbonate ** and few plagioclase

Crystal/grain size: 0.5 - 3 mm
Micro texture: Subangular – subrounded, poorly sorted
Grain form/contact: curved and embayed contact, concave/convex, sutured
Recrystallization: polycrystalline quartz, sericite
Deformation: strained quartz, subgrain development, recrystallization, mortar texture, cataclase (slight)
Alteration: none
Micro cracking (UV light) intergranular, intra granulare, long micro cracks, porosity
Classification: sedimentary rock (clastic)
Naming: fine to medium grained sandstone
Micro photos:

Micro photos of selected area in thin section

1 Ordinary light. Note clastic grains

2 Polarized light. Note grain forms and recrystallization

3 Fluorescence light. Note micro cracks

Viggo Jensen 12 August 2011

Petrographic description of rock aggregate

Sample no. 08115-24B   **Location: Kleivaberget**

Macroscopic description. Light grey fine to medium grained rock

Mineralogy: estimated

quartz	feldspar **	sericite	accessory*				
83	11	6	<1				

* opaque phases, carbonate ** and few plagioclase

Crystal/grain size: 0.2 – 1.5 mm
Micro texture: subrounded, well sorted
Grain form/contact: curved and embayed contact, concave/convex, sutured
Recrystallization: polycrystalline quartz, sericite
Deformation: strained quartz, subgrain development, recrystallization, mortar texture, cataclase (slight)
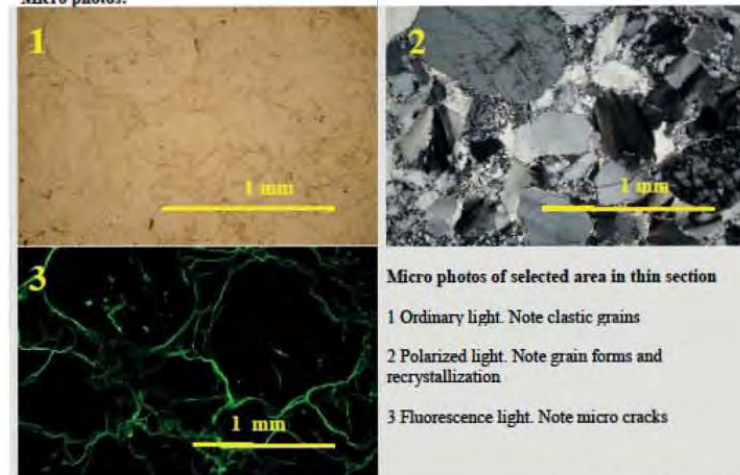**Alteration:** none
Micro cracking (UV light) intergranular, intra granulare, long micro cracks, porosity
Classification: sedimentary rock (clastic)
Naming: fine to medium grained sandstone/quartzite
Micro photos:

Micro photos of selected area in thin section

1 Ordinary light. Note clastic grains

2 Polarized light. Note grain forms and recrystallization

3 Fluorescence light. Note micro cracks

Viggo Jensen 12 August 2011

Petrographic description of rock aggregate

Sample no. 08115-26A   **Location: Sefrivatn**

Macroscopic description. Red coloured fine grained granular rock with irregular black bands/lines

Mineralogy: estimated

quartz	feldspar	plagioclase	biotite	accessory*			
45	44	10	1	<1			

* hematite, chlorite, epidote ,carbonate, opaque phases, titanite

Crystal/grain size: 0.1 – 1 mm
Micro texture: granular
Crystal/form: anhedral, straight, curved and embayed contact
Recrystallization: quartz?
Deformation: strained quartz and feldspar
Alteration: insignificant. Hematite gives the red colouring
Micro cracking (UV light): inter granular, long micro crack, holes
Classification: magmatic rock (plutonic)
Naming: fine grained granite
Micro photos:

Micro photos of selected area in thin section

1 Ordinary light. Note red coloured hematite

2 Polarized light. Note feldspar with hematite

3 Fluorescence light. Note holes and inter granular micro cracks

Viggo Jensen 15 august 2011

Petrographic description of rock aggregate
Sample no. 08115-26B   **Location: Sefrivatn**

Macroscopic description. Grey coloured fine grained foliated rock with darker striations

Mineralogy: estimated

quartz	feldspar	plagioclase	biotite	muscovite	carbonate	accessory*		
67	22	6	2	2	1	<1		

hematite, chlorite, opaque phase

Crystal/grain size: 0.1 – 1 mm
Micro texture: granular, orientation by biotite/muscovite
Crystal/form: anhedral, straight, curved and embayed contact
Recrystallization: quartz
Deformation: strained quartz and feldspar
Alteration: insignificant.
Micro cracking (UV light): inter- intra granular, long micro crack
Classification: magmatic rock (plutonic)/ metamorphosed
Naming: fine grained granite/granitic gneiss
Micro photos:

Micro photos of selected area in thin section

1 Ordinary light. Note few orientated biotite

2 Polarized light. Note "large" irregular formed feldspar

3 Fluorescence light. Note inter- og intragranular micro cracks

Viggo Jensen 15 august 2011

Petrographic description of rock aggregate
Sample no. 08115-26C   **Location: Sefrivatn**

Macroscopic description. Grey coloured fine –medium grained foliated rock with darker striations

Mineralogy: estimated

quartz	feldspar	plagioclase	biotite	accessory*			
56	23	17	4	<1			

hematite, chlorite, opaque phase, carbonate, sericite, titanite

Crystal/grain size: 0.1 – 3 mm
Micro texture: granular, orientation by biotite
Crystal/form: anhedral, curved and embayed contact, sutured
Recrystallization: none
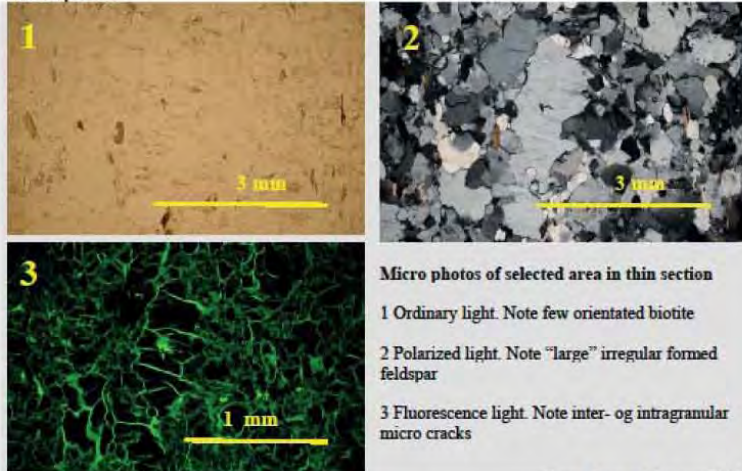**Deformation:** strained quartz and feldspar
Alteration: insignificant.
Micro cracking (UV light): inter- intra granular, long micro crack
Classification: magmatic rock (plutonic)/ metamorphosed
Naming: fine grained granite/granitic gneiss
Micro photos:

Micro photos of selected area in thin section

1 Ordinary light. Note holes (yellow)

2 Polarized light. Note feldspar

3 Fluorescence light. Note inter granular micro cracks and holes
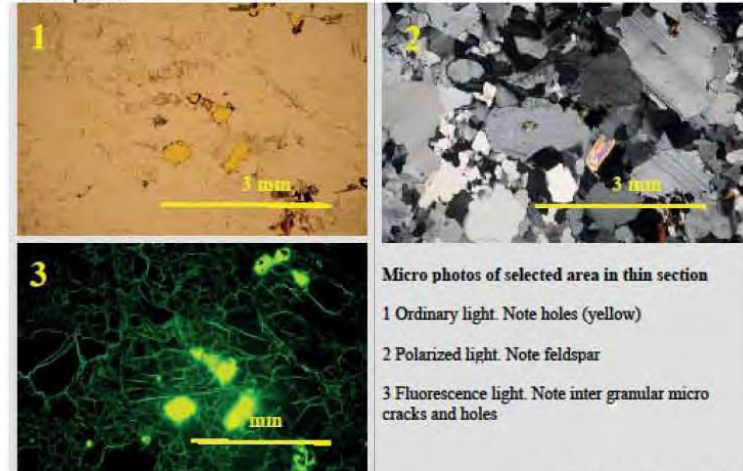
Viggo Jensen 15 august 2011
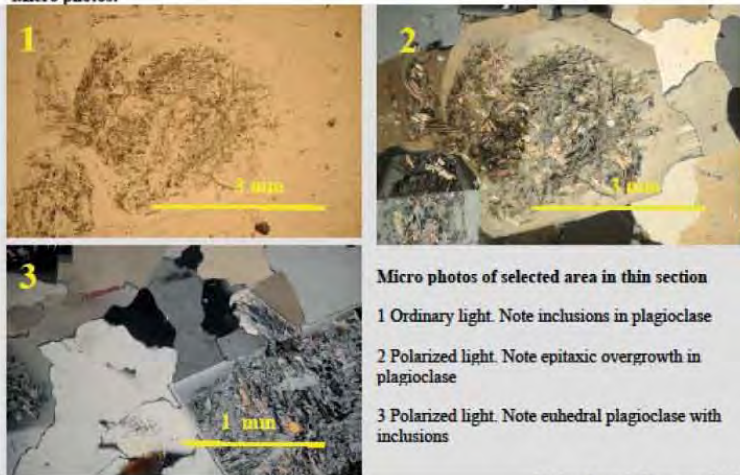
Petrographic description of rock aggregate

Sample no. 08115-27A   **Location: Follstad steinbrud**

Rock sample and thin section from NTNU (forekomst nr. 1648-501)

Macroscopic description. White dark spotted medium grained granular rock

Mineralogy: estimated

plagioclase	quartz	epidote	muscovite/sericite	biotite	accessory		
62	29	4	3	2	<1		

Crystal/grain size: 0.5 – 2 mm
Micro texture: granular, epitaxic owergrowth of plagioclase
Crystal/form: euhedral, straight contact, bowed
Recrystallization: plagioclase (late magmatic ?) and quartz
Deformation: none
Alteration: secondary plagioclase, saussuritization, seritization
Micro cracking (UV light): not visible. Thin section is not fluorescents impregnated
Classification: magmatic rock (plutonic)
Naming: quartz diorite/tonalite/*trondhjemitt*
Micro photos:

Micro photos of selected area in thin section

1 Ordinary light. Note inclusions in plagioclase

2 Polarized light. Note epitaxic overgrowth in plagioclase

3 Polarized light. Note euhedral plagioclase with inclusions

Viggo Jensen 15 august 2011

Petrographic description of rock aggregate

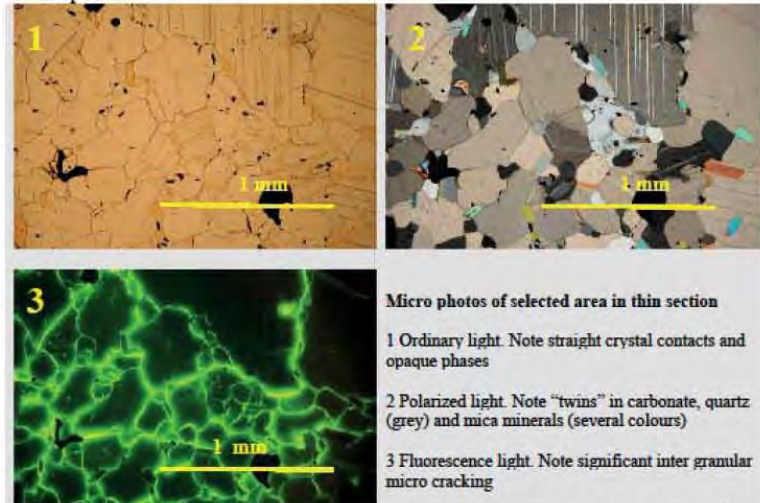**Sample no. 08115-28A**   **Location: Beiarn**

Macroscopic description. Grey coloured fine grained slightly spotted granular carbonate rock with bands/lenticular bodies of coarser carbonate crystals. The rock contains sulphide and is friable.

Mineralogy: estimated (%)

Carbonate minerals	Biotite	Quartz	Opaque *	Muscovite	Pyroxene	Feldspar
89	4	3	2	1	1	<1

* *inclusive iron hydroxide (rust)*

Crystal/grain size: 0.1 – 1 mm, coarser carbonate crystals op to 3 mm
Micro texture: eguigranular, twinned carbonate minerals, inclusions and inter granular quartz, mica, opaque phases and pyroxene
Crystal form/contact: euhedral, straight contact, reduced contact by micro cracks
Recrystallization: not observed
Deformation: not observed.
Alteration: some altered opaque phases and iron hydroxide (rust) in cracks
Micro cracking (UV light): significant inter granular, some "long" micro cracks
Classification: metamorphosed carbonate rock
Naming: marble
Micro photos:

Micro photos of selected area in thin section

1 Ordinary light. Note straight crystal contacts and opaque phases

2 Polarized light. Note "twins" in carbonate, quartz (grey) and mica minerals (several colours)

3 Fluorescence light. Note significant inter granular micro cracking

Viggo Jensen 12. April 2012

Petrographic description of rock aggregate

Sample no. 08115-28B   **Location: Beiarn**

Macroscopic description. Grey –yellow coloured fine- to medium grained weakly foliated granular carbonate rock with bands of coarser carbonate crystals. The rock contains sulphide, rust and is friable.

Mineralogy: estimated (%)

Carbonate minerals	Quartz	Muscovite	Opaque*	Pyroxene	Feldspar
85	5	4	3	3	<1

* inclusive iron hydroxide (rust)

|	
Crystal/grain size:	0.2 – 2 mm
Micro texture:	eguigranular, twinned carbonate minerals, slightly orientation of mica minerals, inclusions and inter granular quartz, mica, opaque phases and pyroxene
Crystal form/contact:	euhedral, straight contact, reduced contact by micro cracks
Recrystallization:	not observed
Deformation:	not observed.
Alteration:	altered opaque phases (sulphide) and iron hydroxide in cracks
Micro cracking (UV light):	significant inter granular, "long" micro cracks
Classification:	metamorphosed carbonate rock
Naming:	marble
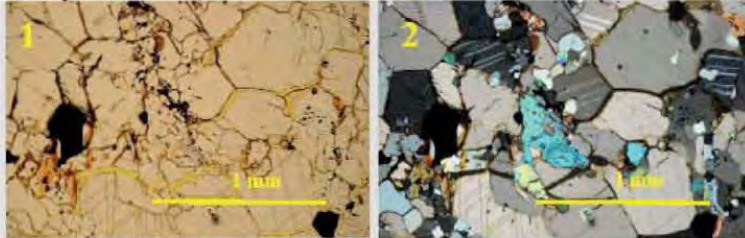
Micro photos:

Micro photos of selected area in thin section

1 Ordinary light. Note opaque phases and "rust" (iron hydroxide) in micro cracks

2 Polarized light. Note "twins" in carbonate, quartz (grey) and pyroxene (blue)

3 Fluorescence light. Note significant inter granular micro cracking

Viggo Jensen 12. April 2012

Petrographic description of rock aggregate

Sample no. 08115-29A   **Location: Beiarn**

Macroscopic description. Dark grey dense rock with thin fissures, some lineation

Mineralogy: estimated by use of measurement grid (363 points)

amphibole	quartz/feldspar*	opaque/sulphides	titanite?	biotite
70	23	5	2	<1

* In thin section it is difficult to distinguish between quartz and feldspar

Crystal/grain size:	0.05 – 0.2 mm
Micro texture:	equigranulare, thin veins with quartz and opaque (sulphides)
Grain form/contact:	subhedral, straight and curved
Recrystallization:	not observed
Deformation:	not observed
Alteration:	not observed
Micro cracking (UV light):	holes, inter granular
Classification:	metamorphic rock
Naming:	amphibole schist/amphibole rock

Micro photos:
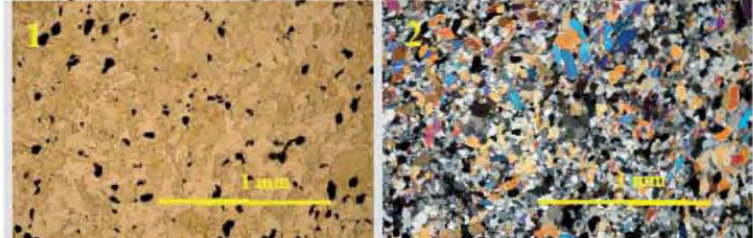
Micro photos of selected area in thin section

1 Ordinary light. Note amphibole (green) and opaque phases

2 Polarized light. Note inter grown quarts (feldspar)

3 Fluorescence light. Note holes

Viggo Jensen 13. April 2012

Petrographic description of rock aggregate

Sample no. 08115-29B   **Location: Beiarn**

Macroscopic description. Dark grey dense foliated rock

Mineralogy: estimated by use of measurement grid (363 points)

amphibole	quartz/feldspar*	biotite	opaque/sulphides	titanite?
66	19	9	4	2

* In thin section it is difficult to distinguish between quartz and feldspar

|	
Crystal/grain size:	0.05 – 0.5 mm
Micro texture:	equigranulare, slightly orientation by biotite and elongated opaque
Grain form/contact:	subhedral, straight and curved
Recrystallization:	not observed
Deformation:	not observed
Alteration:	not observed
Micro cracking (UV light):	holes, "long"micro cracks
Classification:	metamorphic rock
Naming:	biotite amphibole schist

Micro photos:
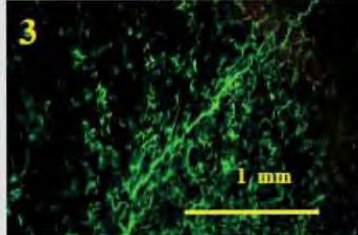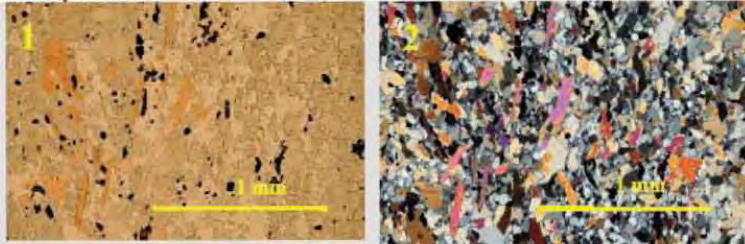
Micro photos of selected area in thin section

1 Ordinary light. Note amphibole (green), biotite (brown) and opaque phases

2 Polarized light. Note inter grown quarts (feldspar)

3 Fluorescence light. Note holes and "long" micro crack

Viggo Jensen 13. April 2012

NTNU – Trondheim
Norwegian University of
Science and Technology